



Al-Azhar University
Faculty of Science (boys)
Chemistry department



**Synthesis and spectral measurements of some new
heterocyclic compounds with expected
pharmacological importance.**

Thesis Presented by

Mohammed mohammed saed wassel

Assistant Researcher - Veterinary Serum and Vaccine Research Institute
M. Sc. 2015 Organic chemistry
Cairo University

TO

Faculty of Science-Chemistry Department
Al-Azhar University (Cairo)

For the fulfillment of
Ph.D. Degree in Organic Chemistry

Under the Supervision of

Prof.Dr. Yousry A.Ammar

Prof. of Organic Chemistry -Chemistry Department,
Faculty of Science (Boys), Al-Azhar University.

Prof.Dr. Gameel Ahmed Mohamed

Prof. of Organic Chemistry, Chemistry Department,
Faculty of Science (Boys), Al-Azhar University.

(2020)

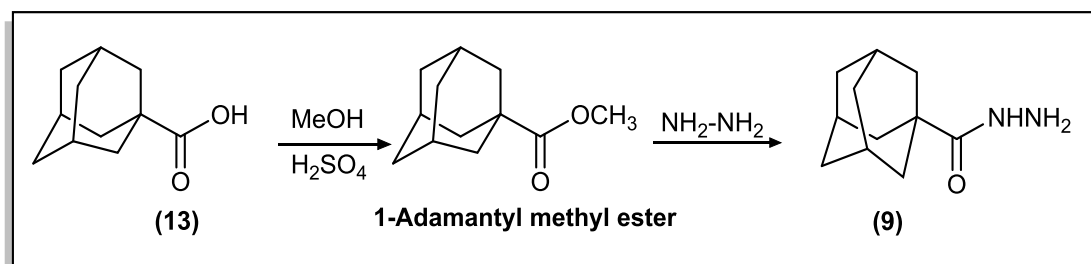
Table of contents

	page
Summary	i-xi
Introduction.....	1
Results and discussion.....	44
Antiviral activity.....	111
Experimental methods.....	136
References.....	180
Arabic summary.....	1-6

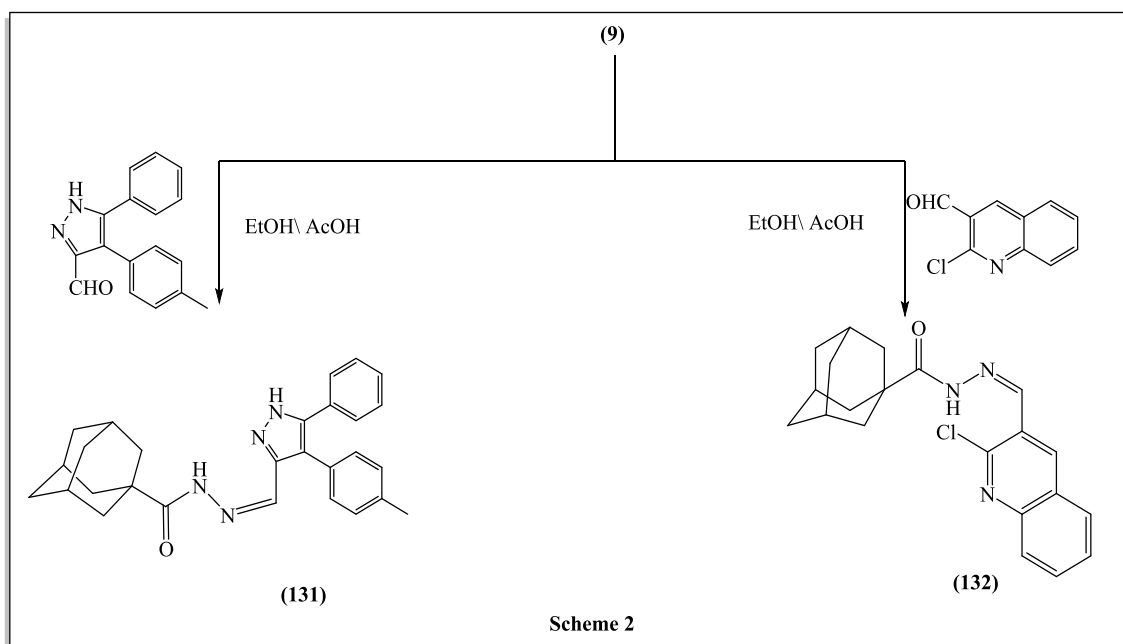
Synthesis and spectral measurements of some new heterocyclic compounds with expected pharmacological importance

In the present study was designed to synthesize new adamantane pyrazole, hydrazone and thiadiazole derivatives and evaluate their biological activities. various functional groups were introduced into the target compounds to investigate their preliminary structure activity relationships (SAR).

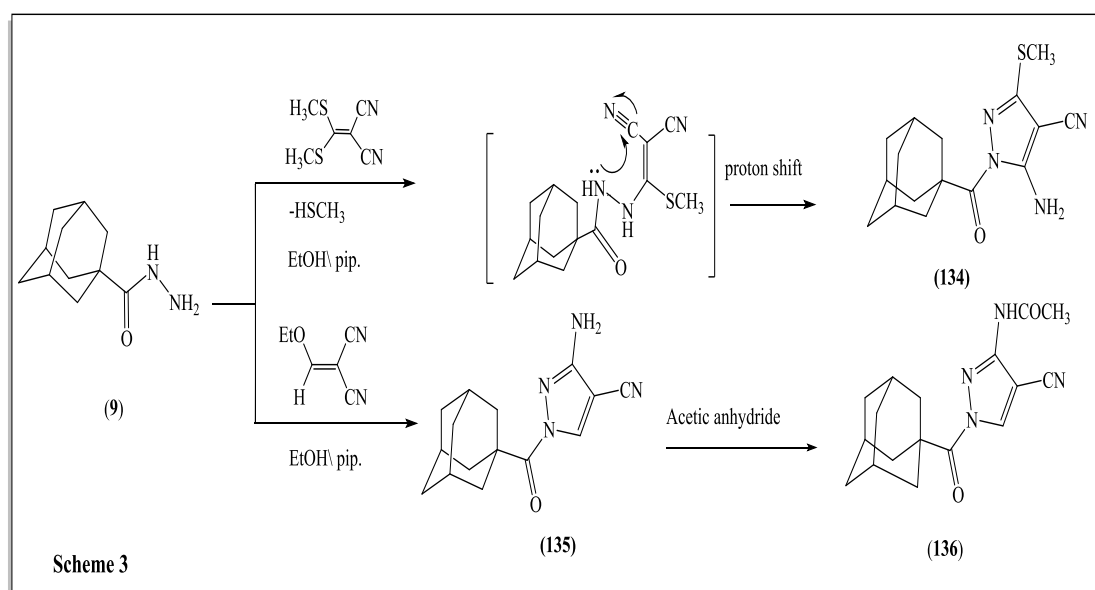
Adamanatan-1-carbohyrazide (**9**) that used as key starting material was prepared as in (**Scheme 1**).



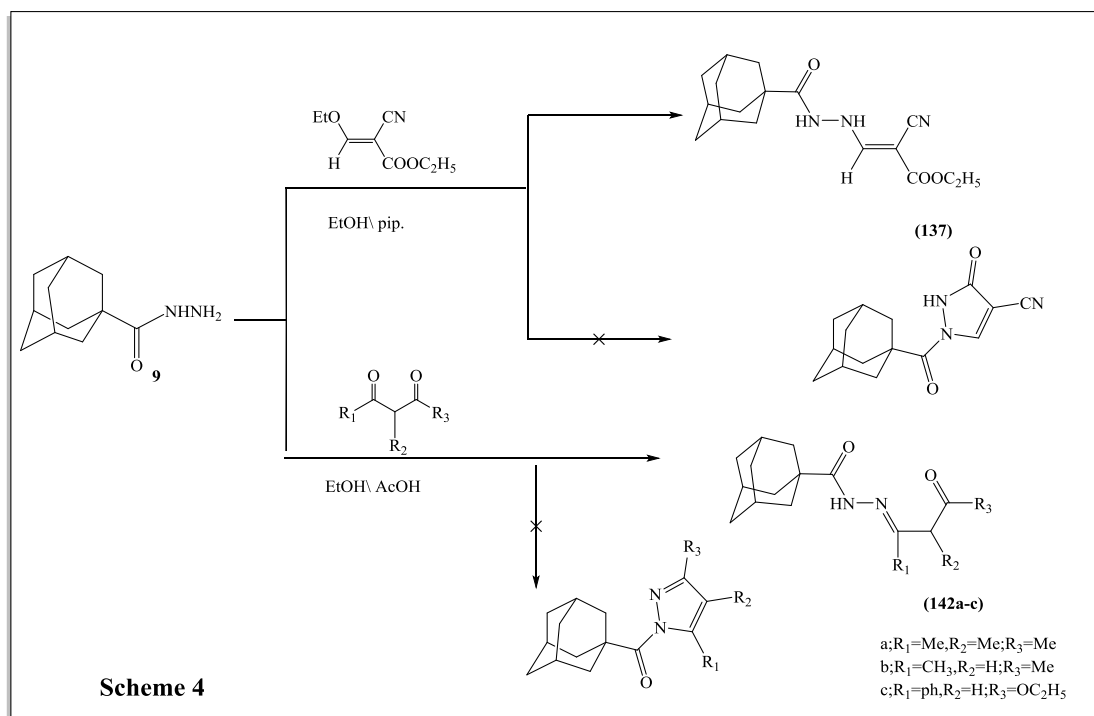
Condensation of adamanatan-1-carbohyrazide (**9**) with 5-phenyl-4-(*p*-tolyl)-1*H*-pyrazole-3-carbaldehyde afforded the corresponding hydrazone derivative (**131**), In the same way, interaction of compound (**9**) with 2-chloro-3-formylquinoline give hydrazone derivative (**132**) in (**Scheme2**).



The reaction of adamantane-1-carbohydrazide (**9**) with bis(thiomethyl) methylene malononitrile afforded 2-amino pyrazole derivative (**134**). Similarly, interaction of the hydrazide derivative (**9**) with ethoxy methylene malononitrile afforded the corresponding 2-amino pyrazole derivative (**135**) and also underwent acetylation when heated with acetic anhydride for one hour under reflux condition to obtain N-acetyl amino pyrazole derivative containing adamantane moiety (**136**) in (Scheme 3).

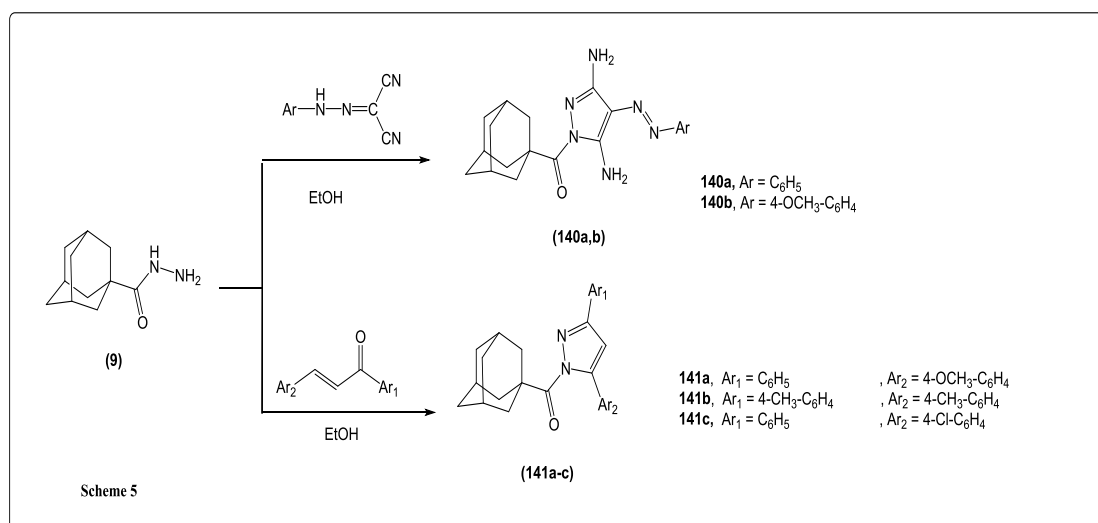


On the other hand, the reaction of hydrazide derivative (9) with ethyl ethoxy methylene cyanoacetate not demonstrate pyrazole derivatives as previous compounds (134) but the reaction stop at the addition elimination step. and not underwent to form compound 137 and also the reactivity of hydrazide derivative 9 toward some electrophiles was checked as 1,3-dicarbonyl derivatives do not undergo cyclization and produce acyclic hydrazone derivatives 142a-c appeared in (Scheme 4).



Compound (**140**) as in (**Scheme 5**) having an azo moiety were afforded by the reaction of hydrazide derivatives (**9**) that coupled with Arylidene azo-malononitrile in the presence of ethanol and produced the corresponding pyrazole **140a, b**

Finally, Pyrazole derivatives (**141**) containing two aryl groups at position three and five positions were obtained through the reaction of adamantane-1-carbohydrazide with α , β -unsaturated carbonyl derivatives (chalcones).

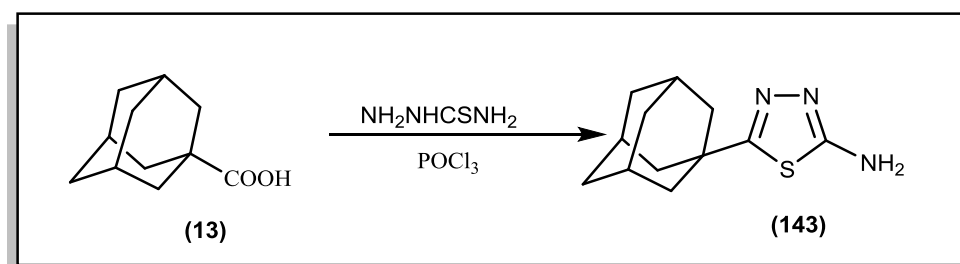


Generally, we successfully designed and synthesized a small library of adamantane nucleus (lipophilic part) bearing pyrazole **131**, **134**, **135**, **136**, **140**, **141**, and hydrazone **137**, **142**, **132** derivatives at position 1 and all the chemical reaction involve an only one-step reaction to obtain the desired products. The cytotoxic activity against three cell line MCF-7, HepG-2 and A549 were evaluated and displayed good to moderated activity with IC₅₀ values (1.55-42.17 μ M). The newly synthesized derivatives revealed sensitive and selectivity to lung cancer cells (A549) with IC₅₀ values ranged between 1.55 ± 0.08 to 15.42 ± 1.4 μ M, with eight compounds (**134**, **135**, **142a**, **142b**, **142c**, **131**, **140a** and **141c**) having IC₅₀ less than or equal ten micromole except for compound **141a** that showed IC₅₀ (27.18 ± 1.95 μ M). The most promising three adamantane derivatives **131**, **140a** and **142a** with IC₅₀ values less than 5 μ M were elected to evaluate their inhibitory action against isoenzyme hCAIX and hCAXII for the first time. Superiorly, 3,5-diamino-pyrazole core **140a** showed higher IC₅₀ values than hydrazo-pyrazole **131** and hydrazone derivatives **142a** that hybrid with adamantane and exhibited inhibitory effect with submicromolar between (0.107-0.695 μ M), in comparison to Dorzolamide HCl (0.052-0.086 μ M). Among them, compound **140a** is considered the most

promising derivatives with anti-proliferative (A549) ($IC_{50} = 1.55 \pm 0.08 \mu M$) and CAIX/XII inhibitors ($IC_{50} = 0.11$ and $0.18 \mu M$), respectively. Finally, some drug-likeness model as Lipinski and Verber were predicted. Molecular docking simulation was performed inside the active site of CA IX (PDB: 3IAI) and CA XII (PDB: 1JD0) to evaluate the binding modes of the adamantane derivatives as well as Dorzolamide HCl. Docking score of the promising compounds showed lower values (-9.94 to -19.81 Kcal/mol) in comparison to Dorzolamide HCl (-13.23 to -14.55 Kcal/mol) and different type of interaction as H-bond, arene-arene and arene-cation interaction were present beside in some cases ligand coordinated to Zn ion.

Finally, the present study is viable to demonstrate that adamantane pyrazole derivatives **141a**, **141b** and **141c** can suppress FMDV replication in vitro as well as prolong the survival of mice in vivo, suggesting the potential applications of this drug as an antiviral regiment for FMD treatment. Of the end, it is necessary to test the antiviral effect of pyrazole containing two arylidene groups at position three and five in natural hosts such as swine, cattle, and goats, and against more FMDV strains.

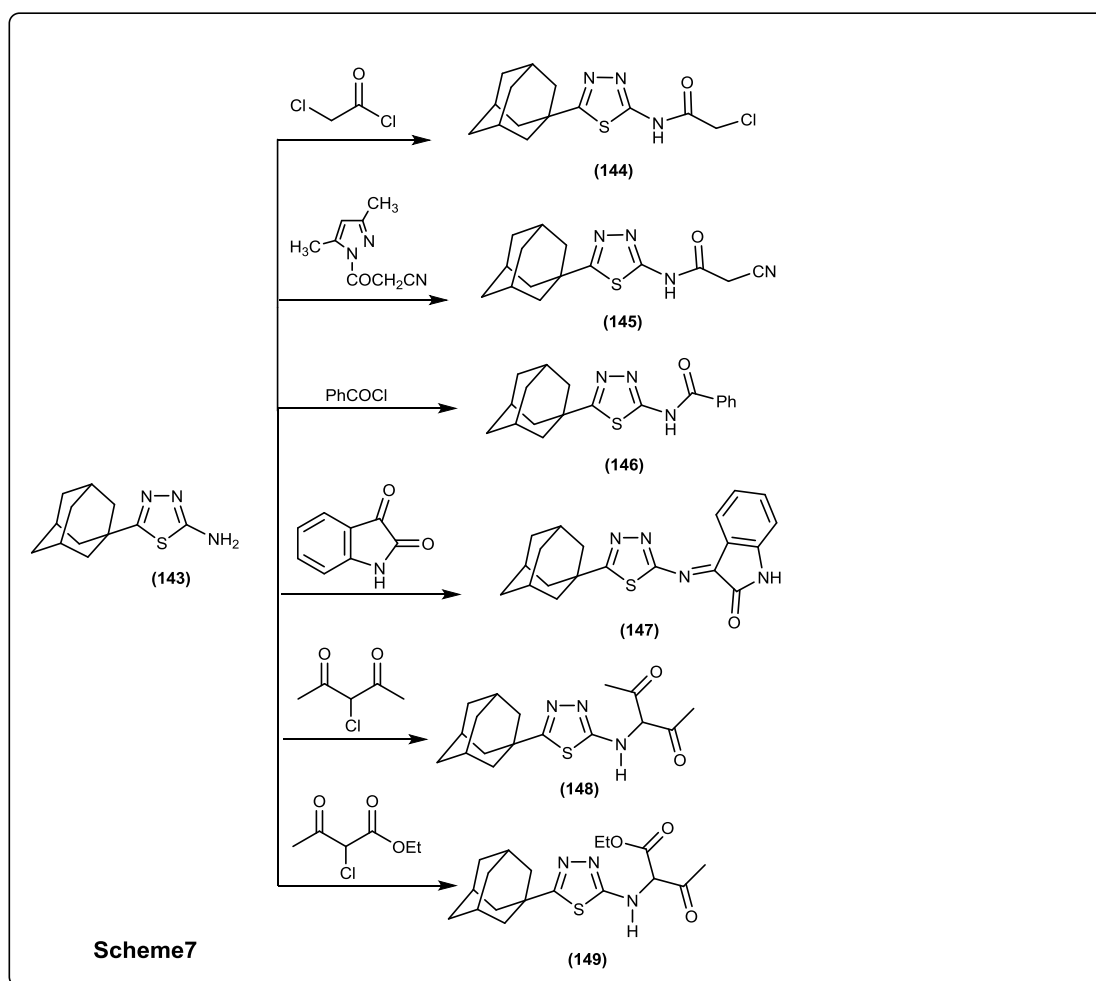
The starting compound, 5-(adamantan-1-yl)-1,3,4-thiadiazol-2-amine (**143**) was prepared to produce adamantyl thiadiazole derivative which are derived from reaction of adamantyl carboxylic acid with thiosemicarbazide and phosphorous oxychloride as in (Scheme 6).



Thus, 2-aminothiadiazole derivative **143** was subjected to chloroacetylation through its reaction with chloroacetyl chloride in the presence of trimethylamine as a catalyst to afford the corresponding 2-chloro acetamide derivative **144**. In addition, *N*-(5-(adamantan-1-yl)-1,3,4-thiadiazol-2-yl)-2-cyanoacetamide (**145**) was obtained through cyanoacetylation of compound **143** with 3-(3,5-dimethyl-1*H*-pyrazol-1-yl)-3-oxopropane-nitrile in toluene.

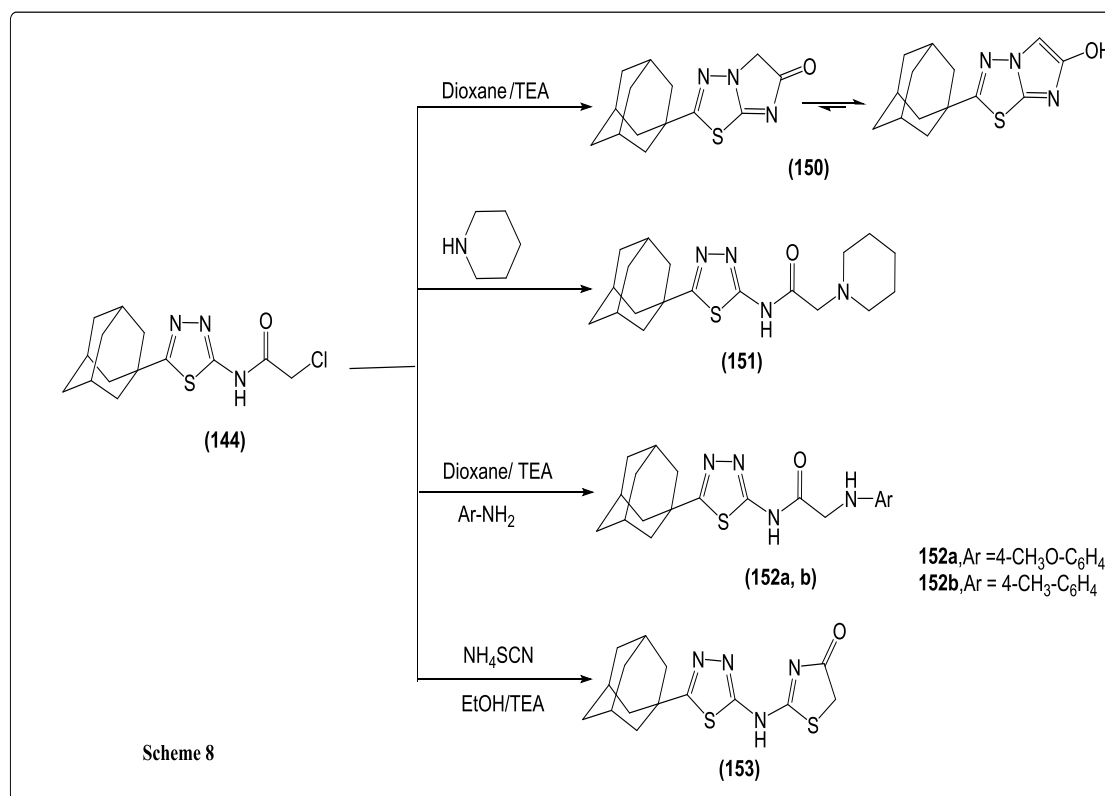
N-(5-(adamantan-1-yl)-1,3,4-thiadiazol-2-yl) benzamide (**146**) was obtained by reaction of 2-aminothiadiazole derivative **143** with benzoyl chloride under reflux condition. Schiff's base (**147**) which contain thiadiazole and indoline moieties was obtained through condensation of compound **143** with isatin in boiling ethanol.

Furthermore, we investigated the reactivity of 2-aminothiadiazole derivative **143** towards some halogenated compounds to prepare imidazo[2,1-*b*] [1,3,4] thiadiazole derivatives. Thus, the reaction of thiadiazole derivative **143** with 3-chloroacetylacetone and ethyl 3-chloroacetoacetate in ethanol containing piperidine as a catalyst for obtaining imidazo-thiadiazole structure (**scheme7**).



Thus, upon refluxing of compound **144** in dioxane containing trimethyl amine as a catalyst caused self-cyclization to furnish the corresponding 2-(adamantan-1-yl)imidazo[2,1-*b*][1,3,4]thiadiazol-6-one (**150**). Amination of compound **144** with piperidine as secondary amine and *p*-anisidine as well as *p*-toluidine as primary amine afforded the corresponding amino derivatives compounds **151** and **152**.

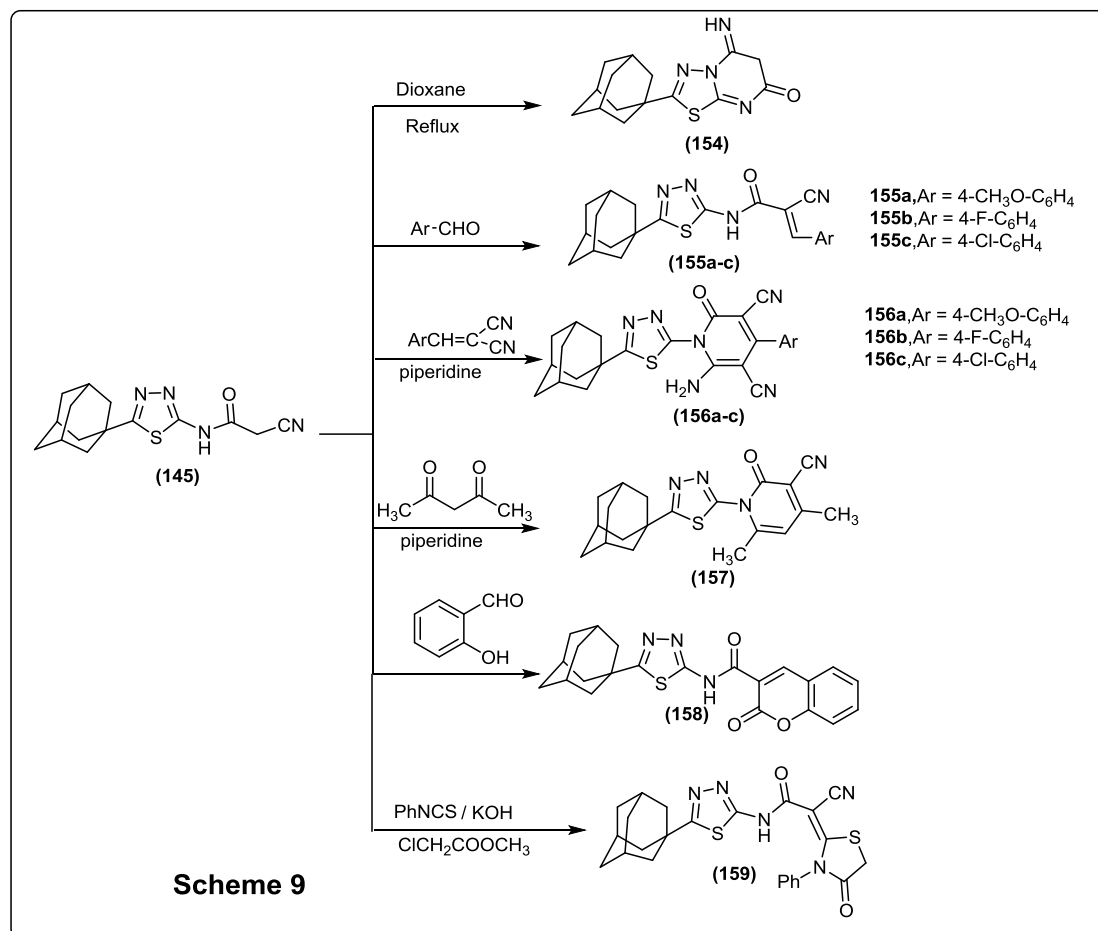
Treatment of 2-chloro acetamide derivative **144** with ammonium thiocyanate in absolute ethanol afford the thiazolidinone derivative **153**.



Furthermore, we also investigated the reactivity of *N*-(5-(adamantan-1-yl)-1,3,4-thiadiazol-2-yl)-2-cyanoacetamide (**145**) towards some selective reagents with the aim of preparing some bioactive derivatives. Thus, compound **145** underwent cyclization when heated under reflux in dioxane to afford the thiadiazolo[3,2-*a*] pyrimidin-7-one derivative **154**. Condensation of cyano-acetanilide thiadiazole derivative **145** with some aromatic aldehydes namely 4-methoxy or 4-chloro or 4-fluoro benzaldehyde afforded the corresponding acrylamide derivatives **155a-c**. On the other hand, the interaction of cyano-acetamide derivative **145** with arylidenemalononitriles in the presence of piperidine affected via cyclization to yield the corresponding pyridine carbonitrile derivatives **156a-c**.

Reactivity of cyano-acetamide derivative with the 1,3-dicarbonyl compound was studied. Thus, compound **145** reacted with acetyl acetone to give the pyridine derivative **157**. Furthermore, cyclo-condensation of

compound **145** with salicylaldehyde in boiling ethanol containing a catalytic amount of piperidine afforded the coumarine derivative **158**. Finally, treatment of cyano-acetanilide thiadiazole derivative **145** with phenyl isothiocyanate in DMF, in alkaline medium followed by treatment with methyl chloroacetate afforded the corresponding thiazolidinone derivative **159**.



A novel series of twenty-one 1,3,4-thiadiazolo-adamantane derivatives were designed and synthesized starting from 5-(adamantan-1-yl)-1,3,4-thiadiazol-2-amine (**143**). The newly synthesized derivatives **144-159** were evaluated *in vitro* for their anti-proliferative activity against the selected three cell lines. The structure of the newly designed compounds was established and confirmed based on its elemental analysis and spectral data. Cytotoxic values showed a broad spectrum of the designed compounds

against three cell lines (MCF-7, HepG-2 and A 549), and seven compounds **147**, **148**, **152a**, **152b**, **156b**, **156c** and **159** with 5-(adamantan-1-yl)-1,3,4-thiadiazole backbone core showed potent cytotoxicity with low micromolar ($<10\ \mu\text{M}$). Moreover, the most potent compounds showed IC_{50} values from 89.75 to 225.7 μM against normal non-cancer cells (WI-38 cells) as well as exhibited chemo suppression/induction cancers cells to apoptosis induction by changes in BCL-2 and BAX gene levels. All the promising compounds investigated EGFR^{WT} inhibitory assay less than 2 μM . Besides, compound **156c** showed the most potent inhibitory activity against EGFR^{L858R-TK} with IC_{50} (37.85 nM) in comparison to Lapatinib as a positive control (IC_{50} = 39.53 nM) and Erlotinib (IC_{50} = 59.56 nM). Both compounds **147** and **159** showed equipotent to the standard drug with IC_{50} values (41.19, 40.58 nM), respectively. Furthermore, the most promising three derivatives **147**, **156c** and **159** against further kinase EGFR^{L858R/T790M} double mutant exhibited IC_{50} values ranged between (0.27-0.78 nM) compared to Lapatinib (0.1823 nM) and Erlotinib (0.218 nM). cell cycle analysis observed that the enaminonitrile pyridine derivative **156c** induced apoptosis and arrested the cell cycle by 74.50 % in both G2/M and PreG1. While the presence of both thiadiazole adamantane derivatives **147** and **159** cause increase the content of DNA in G0-G1 and S phases by nearly 73.36 and 73.71 % respectively. The most potent adamantane derivatives **147**, **156c** and **159** showed an increased sensitivity to the total percentage of apoptosis from 16.59 % to 32.41 % compared to 1.86 % for standard A549 cells. Finally, molecular docking study revealed that the promising compounds deeply bounded inside the active site of pocket as Erlotinib with binding energy between -22.07 to -19.19 Kcal/mol higher than Erlotinib $S = -19.10$ Kcal/mol, as well as the assessment of oral bioavailability (Lipinski's and Veber rules) besides some pharmacokinetics properties.

Introduction



INTRODUCTION

Adamantane whose IUPAC name is tricyclo[3.3.1.1^{3,7}] decane (**1**), Adamantane molecule consists of three connected cyclohexane rings arranged in the "armchair" configuration, This hydrocarbon is the most thermodynamically stable of the numerous possible C₁₀H₁₆ alkane tricyclic isomers ¹, a polycyclic cage molecule with high symmetry and remarkable properties ², is the smallest representative of diamond-like hydrogen-terminated hydrocarbons with a diamond-like structure ^{3,4}

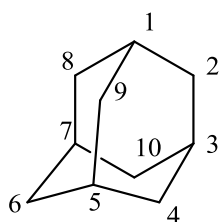


Figure 1 Structure and numbering of adamantane.

It was first isolated in 1933 from crude oil by S. Landa, V. Machacek and M. Mzourek ⁵, and the first synthesis of adamantane was accomplished in 1941 by Prelog and Seiwert via aluminum chloride-catalyzed isomerization of tetrahydrodicyclopentadiene and improved via catalytic hydrogenation of dicyclopentadiene in the presence of aluminum chloride ⁶. However, only after Schleyer discovered the favorable Lewis-acid catalyzed rearrangement procedure leading to the adamantane cage ^{7, 8}, adamantane become a widely available scaffold for numerous transformations ^{9,10}.

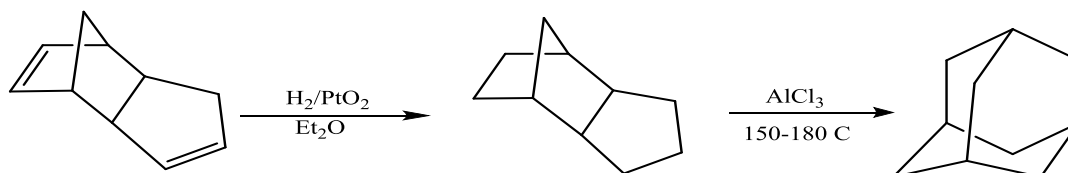


Figure 2 First reported synthesis of adamantane.

Due to the high lipophilicity of adamantane, the incorporation of the adamantyl moiety into several molecules results in compounds with relatively high lipophilicity, which in turn can modify the biological

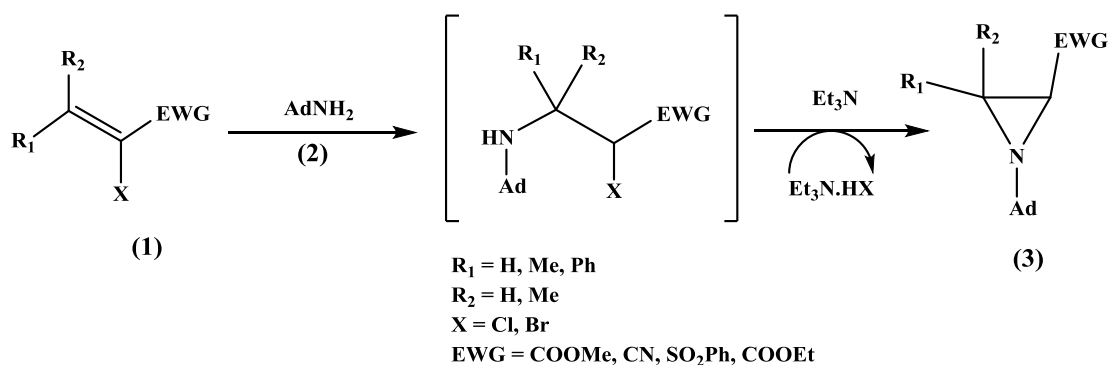
availability of these molecules. Combination of the adamantane structure with heterocyclic compounds modifies their biological activity, often enhancing the effect or imparting a new kind of activity. After the discovery of amantadine in 1960 as antiviral and antiparkinsonian drug, adamantane derivatives attracted the attention of several scientists as potential chemotherapeutic agents. As a result of this intensive search, thousands of adamantane derivatives were synthesized and tested for several biological activities. This resulted in the discovery of several drugs which are now available in market. Among the major biological activities displayed by adamantane derivatives, the antiviral, antibacterial, antifungal, anti-inflammatory, central nervous and 11 β -HSD1 inhibitory activities are the most important ones.

In recent years, adamantane coupled pharmacophoric derivatives have gained importance in medicinal chemistry. It is often viewed as a readily available 'lipophilic bullet' for providing the critical lipophilicity to known pharmacophoric units.

I-Adamantane derivatives containing heterocyclic nuclei with nitrogen atoms:

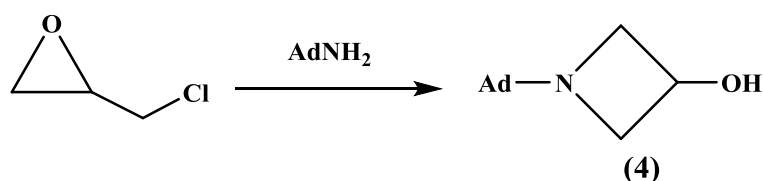
1-Compounds with three Membered heterocycles

Several methods have been proposed for the synthesis of hetero-adamantanes containing residues of three membered nitrogen containing heterocycles. An efficient one-pot synthesis of functionalized adamantyl aziridines (**3**) by aza-Michael initiated ring closure (aza-MIRC) reaction of 1-aminoadamantane (**2**) with α -halogenated Michael acceptors is described. The reaction goes through an aza-Michael intermediate that undergoes an intramolecular nucleophilic substitution.¹¹

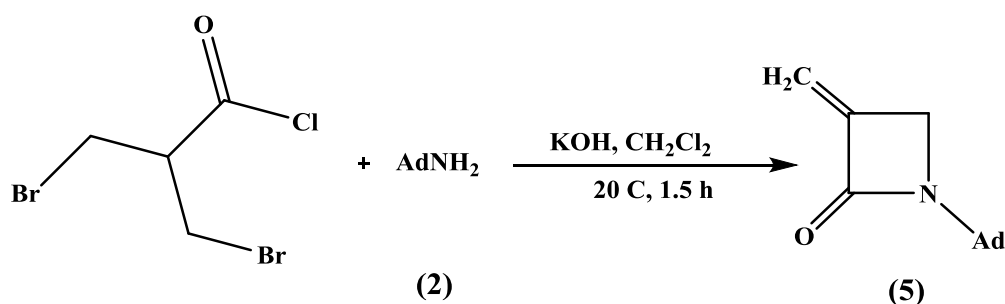


2-Compounds with four Membered heterocycles

The reaction of epichlorohydrin with adamantylamine (2) have been studied, where 1-(adamant-1-yl) azetidin-3-ol (4) was obtained in good yields.¹²



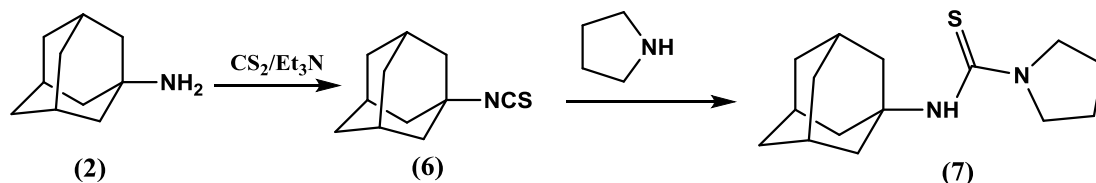
1-(Adamant-1-yl) –3-methyleneazetidin-2-one (5)¹³ was obtained through the cyclization of acid chloride with adamantylamine (2) under the influence of potassium hydroxide.



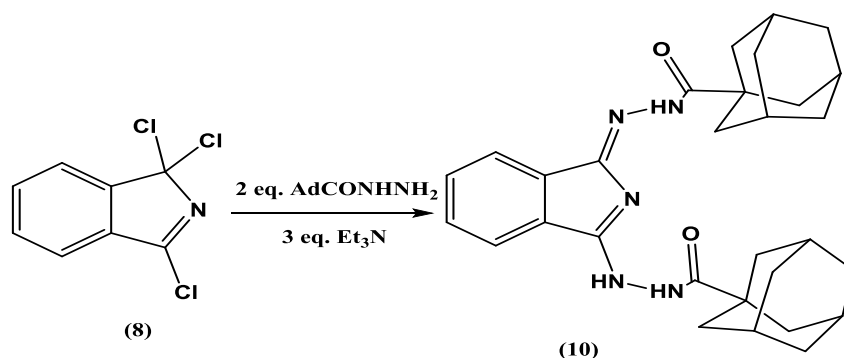
3-Compounds with Five Membered heterocycles

N-(1-Adamantyl) pyrrolidine-1-carbothioamide (7) was obtained via interaction of adamantyl isothiocyanate (6)^{14, 15} as weak electrophiles with

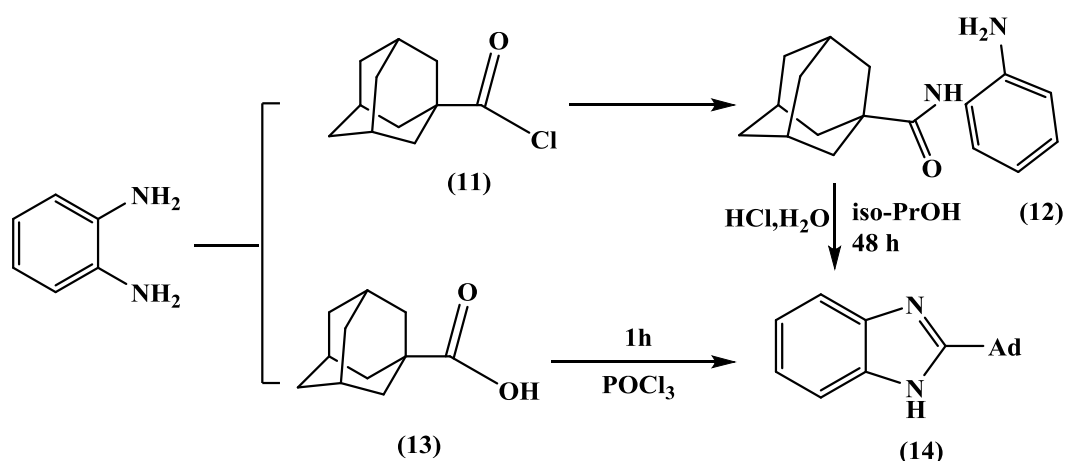
appropriate nucleophilic attack of cyclic secondary amine as pyrrolidine
16.



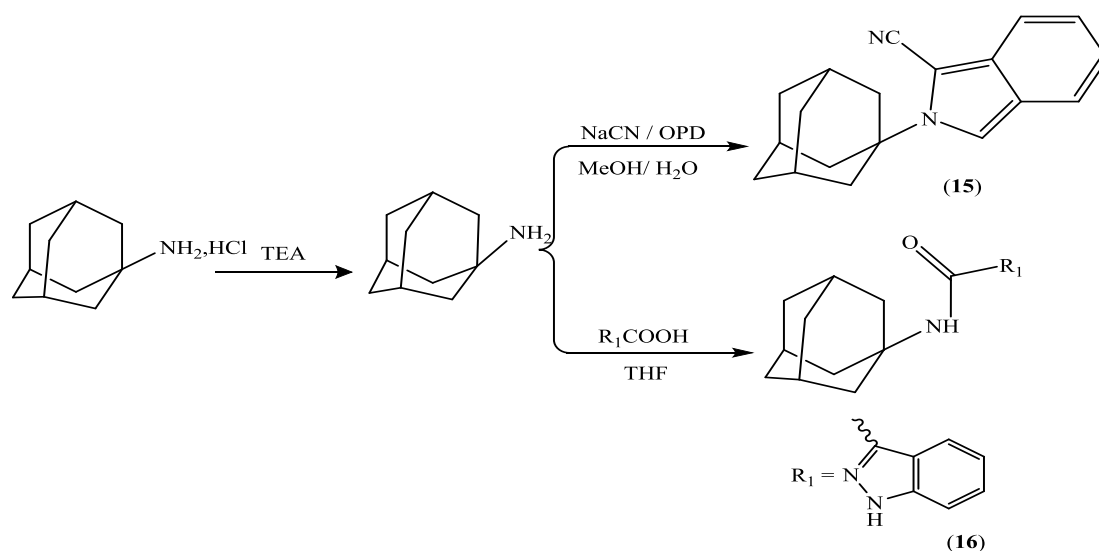
N',N''-1*H*-isoindole-1,3-diylidenedicarbohydrazides (**10**) was prepared by 1, 1, 3-trichloro-1*H*-isoindole (**8**)¹⁷ with adamantyl carbohydrazide (**9**) through nucleophilic substitution reaction in presence Triethylamine which was found to be a good scavenger of the HCl¹⁸.



Condensation of *o*-phenylenediamine with 1-adamantanecarbonyl chloride (**11**) in absolute diethyl ether in the presence of triethylamine (TEA) produced N-(2-aminophenyl) adamantane-1-carboxamide (**12**) in 95% yield¹⁹, which underwent cyclization in the presence of isopropyl alcohol with 35% hydrochloric acid medium to give 2-(1-adamantyl)-1*H*-benzimidazole (**14**) in 96% yield²⁰. This benzimidazole derivative was obtained in one step though the reaction of *o*-phenylenediamine with adamantane carboxylic acid (**13**) in the presence of phosphorus oxychloride

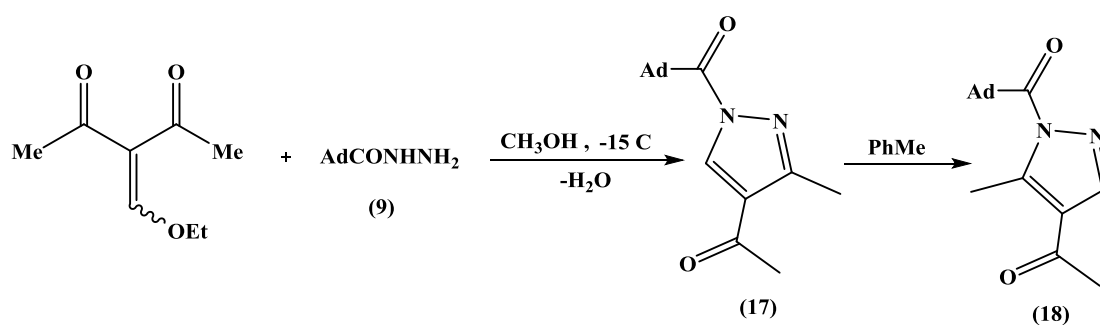


The target fluorescent heterocyclic adamantane amine derivatives (**15**) and (**16**) were synthesized through conjugation of the fluorescent heterocyclic moieties to the adamantane moiety by amidation and amination, the fluorescent isoindole was obtained by reaction between o-phthaldialdehyde (OPD) as good activation amination with adamantine in the presence of sodium cyanide and the second way amidation using N,N-carbonyldiimidazole (CDI) as activation agent and direct amination in reaction between 1-H-indazole-3-carboxylic acid and adamantyl amine.

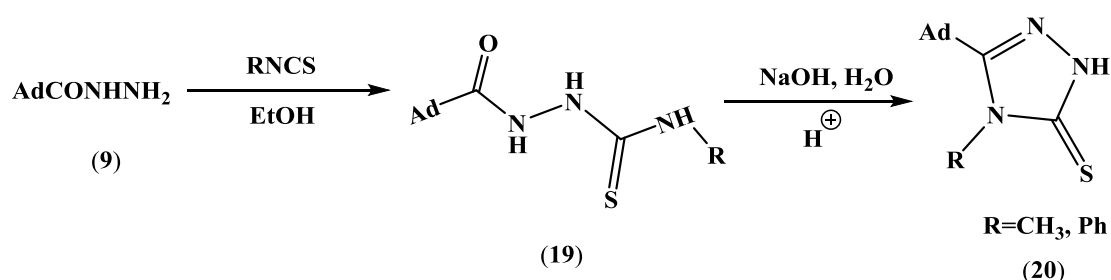


3-(Ethoxymethylidene) pentane-2,4-dione was brought into reaction with adamantyl carbohydrazide (**9**) and 1,4-Diacyl-5-methyl-1H-pyrazoles (**17**)

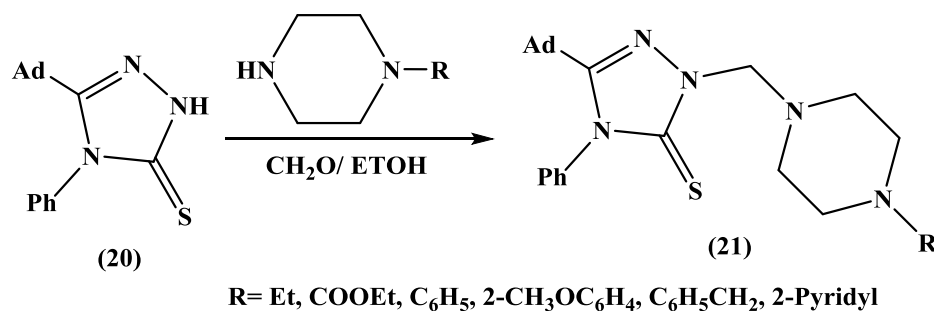
on heating in toluene undergo isomerization to 1,4-diacyl-3- methyl-1H-pyrazoles (**18**) via intermolecular N→N acyl group migration ²¹.



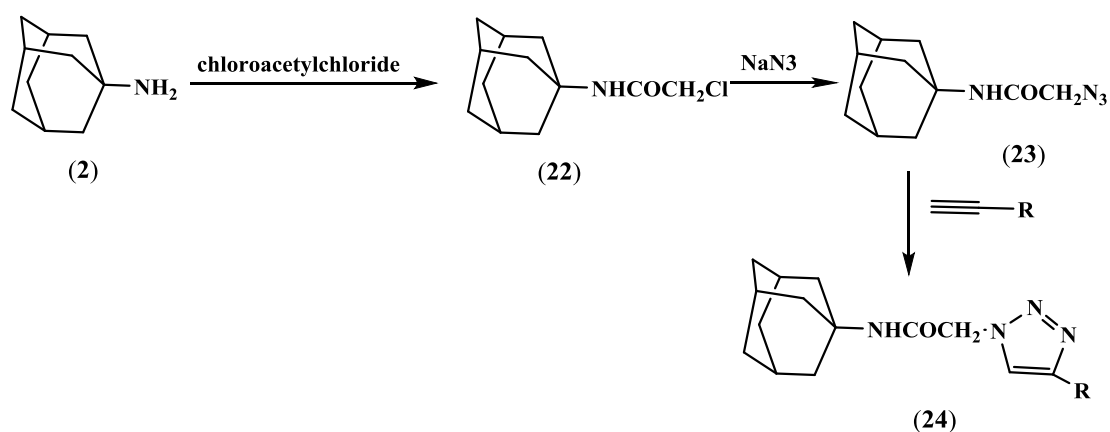
3-(1-adamantyl)-4-substituted-5-mercapto-1,2,4-triazole (**20**) was synthesized by cyclization of 1-(1-adamantylcarbonyl)-4-methyl or phenylthiosemicarbazide (**19**) via heating in 10% aqueous sodium hydroxide ²².



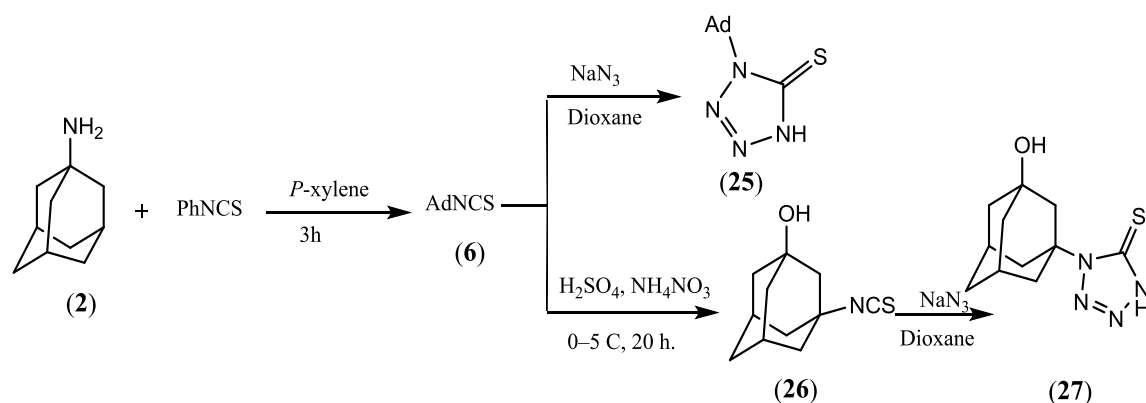
5-(1-Adamantyl)-4-phenyl-1,2,4-triazoline-3-thione (**20**) was reacted with the corresponding 1-substituted piperazine and formaldehyde solution in ethanol to yield the corresponding N-Mannich bases (**21**) in good yields ²².



Reaction of N-(1-adamantyl)-2-chloroacetamide (**22**) (obtained by reacting of 1-adamantylamine (**2**) with chloroacetyl chloride and K_2CO_3) with sodium azide in the presence of tetra-n-butyl ammonium bromide produced, N-(1-adamantyl)-2-azidoacetamide (**23**) in 98.1% yield. The azide undergoes Huisgen's (3+2) cycloaddition reaction. with 1-hexyne in the presence of 20 mol % of $CuSO_4$ catalyst and sodium ascorbate in t-butanol and water (1:1, v/v) gave N-(1-adamantyl)-2-(4-butyl-1H-1,2,3-triazol-1-yl) acetamide (**24**)²³.

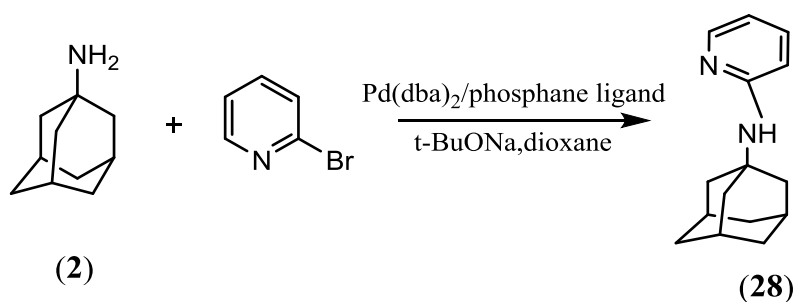


1-(1-Adamantyl) tetrazol-5-thion (**25**) was obtained by cyclo-condensation of 1- adamantyl isothiocyanate (**6**) with sodium azide, instead of direct adamantylation and also oxidation of 1-adamantyl isothiocyanate with ammonium nitrate in sulfuric acid led to 3-isothiocyanatoadamantan-1-ol (**26**) which was then transformed into 1-(3-hydroxy-1- adamantyl) tetrazol-5-thione (**27**)²⁴.

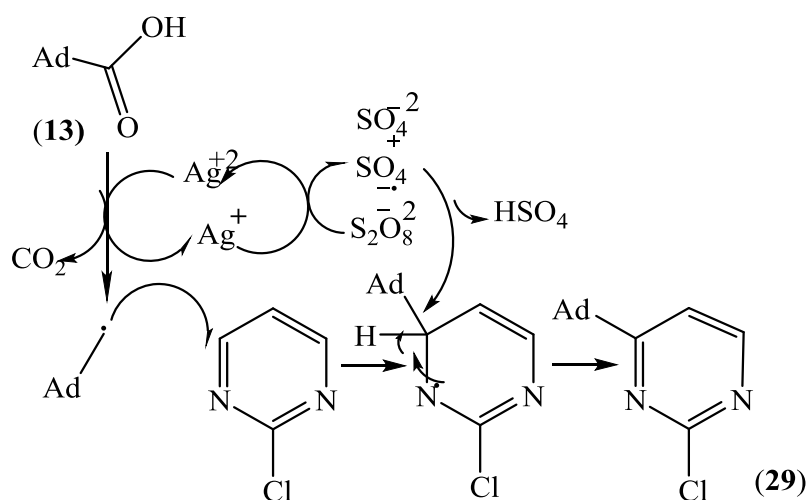


4-Compounds with Six Membered heterocycles

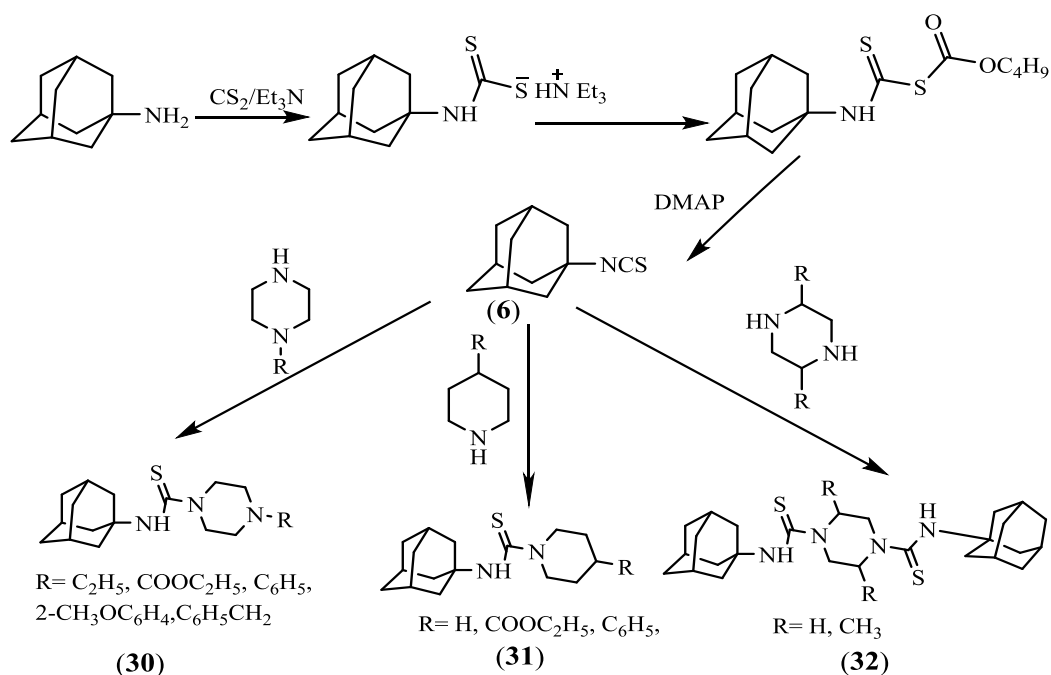
N-(1-Adamantyl) pyridin-2-amine (28) was synthesized by amination of adamantyl amine (2) with 2-bromopyridine under influence of the catalytic system Pd(dba)₂/ BINAP (2–4 mol%) [dba = dibenzylideneacetone; BINAP = 2,2'-bis(diphenyl phosphanyl)-1,1'- binaphthyl] as catalyst ²⁵.



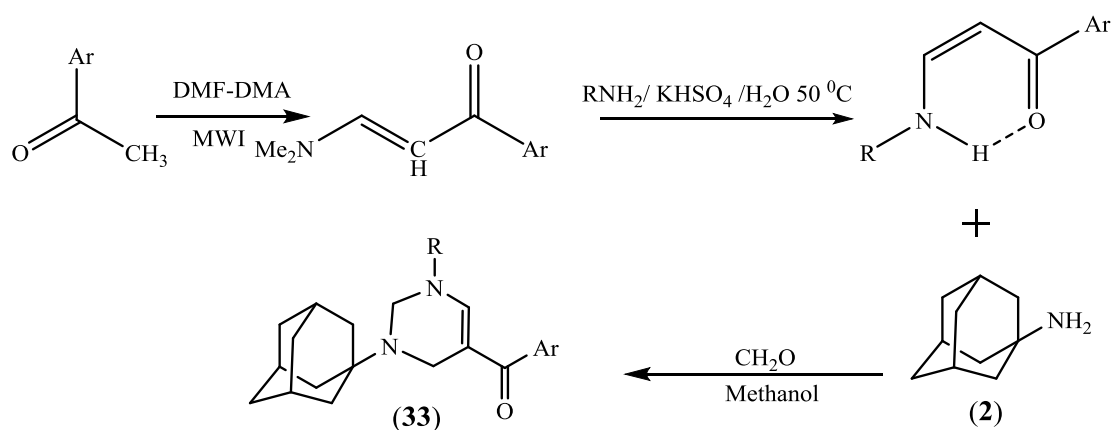
Decarboxylative alkylation and acylation of pyrimidines to afford 4-substituted pyrimidine derivatives (29) via C(sp²)–H functionalization as in reaction of 2-chloropyrimidine and adamantane carboxylic acid (13) in presence of 2.0 equiv. K₂S₂O₈ and 20% AgNO₃ in CH₂Cl₂/H₂O at 45 °C ²⁶.

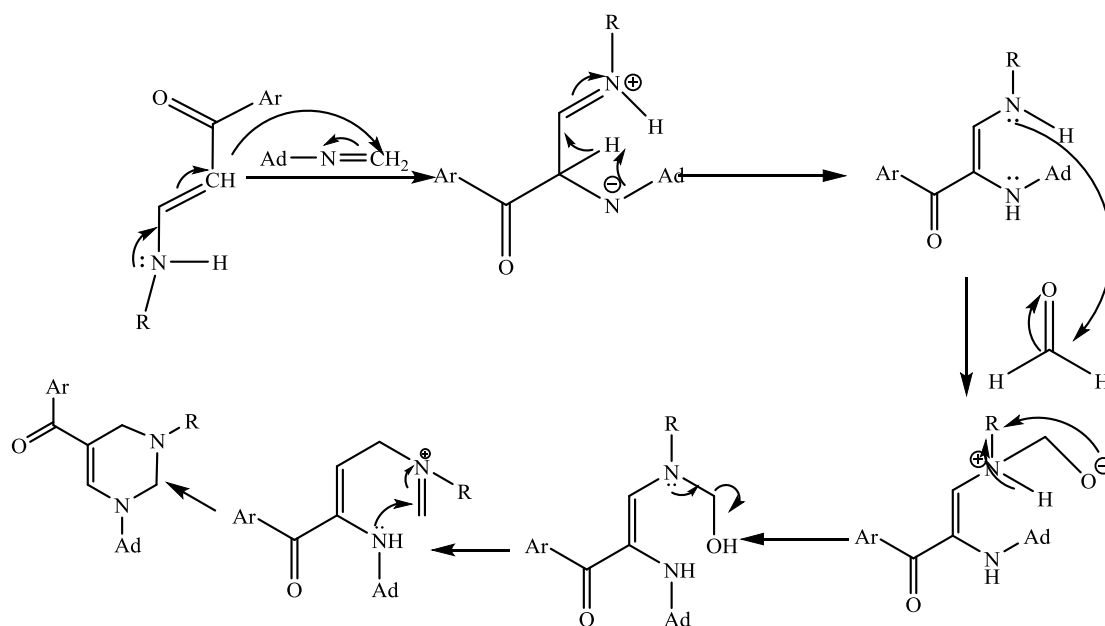


Adamantyl isothiocyanate ^{14, 15} required as starting material, was prepared in good yield via modification of the previously described methods. Thus 1-adamantylamine (2) was reacted with carbon disulfide and trimethylamine in ethanol, to yield the dithiocarbamate salt, followed by addition of di-tert-butyl dicarbonate (Boc_2O) to yield the target adamantyl isothiocyanate (6) which was reacted with the cyclic secondary amines namely, 1-substituted piperazines, 4-substituted piperdines to give N-(1-Adamantyl)-4-substituted piperazine-1-carbothioamides (30) and N-(1-Adamantyl)-4-substituted piperidine-1-carbothioamides (31), 1-Adamantyl isothiocyanate was similarly reacted with piperazine and trans-2,5-dimethylpiperazine in 2:1 molar ratio to give N,N'-bis (1-adamantyl) piperazine-1,4-dicarbothioamide (32) ¹⁷.

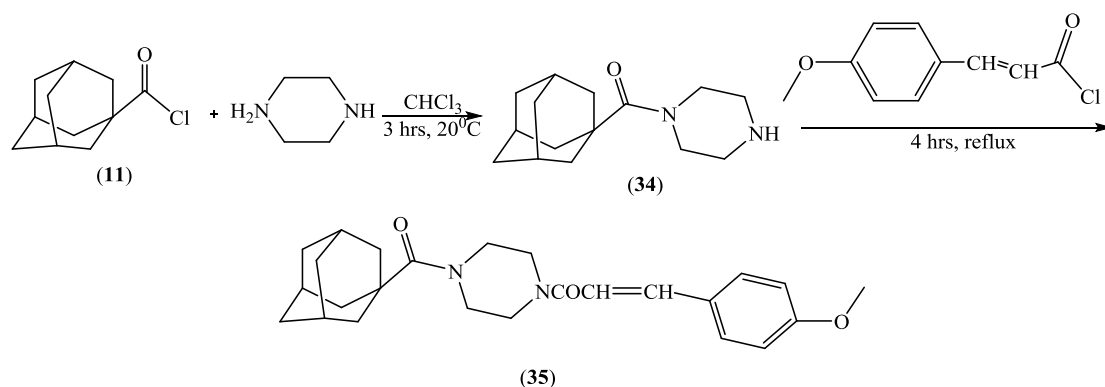


In order to synthesize the desired tetrahydropyrimidine adamantane (33) hybrids, enaminones derived from acetophenone were required. Thus, when a mixture of enaminone, adamantane amine and formaldehyde (1:1:2) in methanol (4 ml) was heated at reflux for 4 hours, work up of the reaction mixture gave in 96% yields ²⁷.



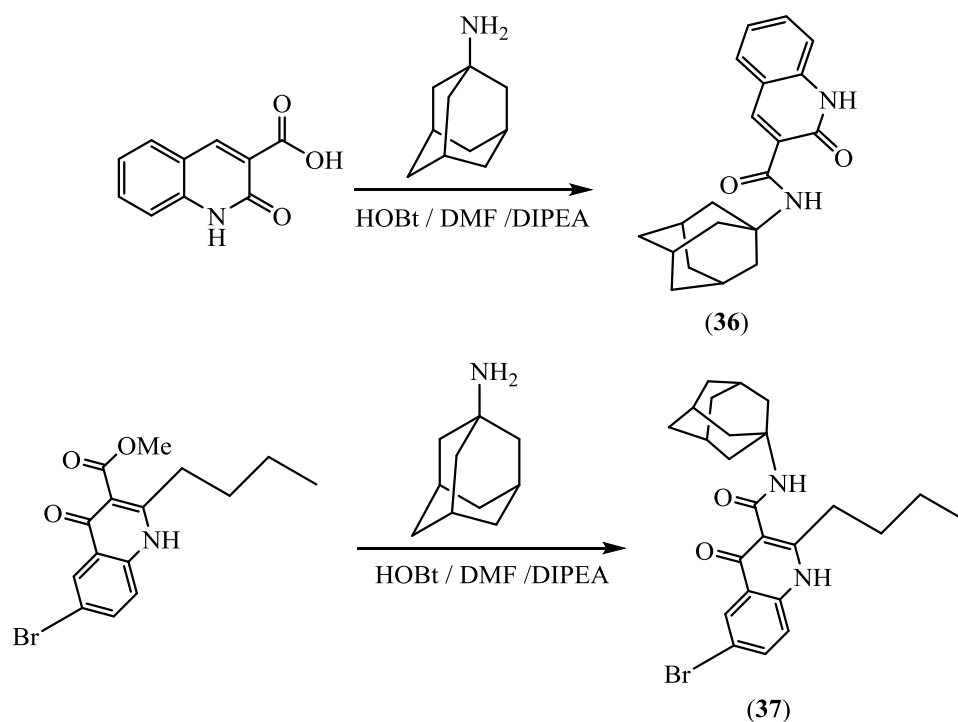
Mechanism:-

It has been reported in a patent that N-(adamant-1-ylcarbonyl) piperazine (**34**) has been synthesised in 40% yield by the acylation of piperazine with adamantyl acid chloride. The product of acylation was converted into the N, N'-diacylpiperazine (**35**) in 90% yield ²⁸.

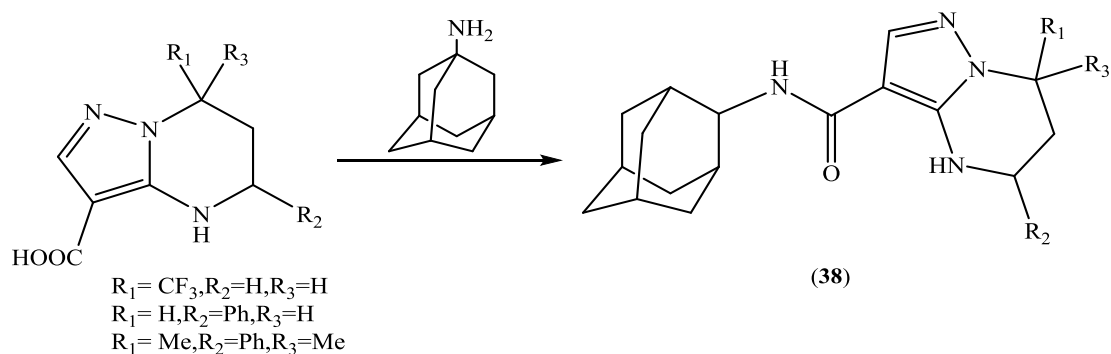


N-(Adamantan-1-yl)-6-bromo-2-butyl-1,4-dihydro-4-oxoquinoline-3-carboxamide (**36**) and N-(adamantan-1-yl)-6-bromo-2-butyl-4-oxo-1,4-dihydroquinoline-3-carboxamide (**37**) were obtained via interaction of adamantyl amine (**2**) by Amidation reaction with 2-oxo-1,2-dihydroquinoline-3-carboxylic acid and Methyl 6-Bromo-2-butyl-1,4-

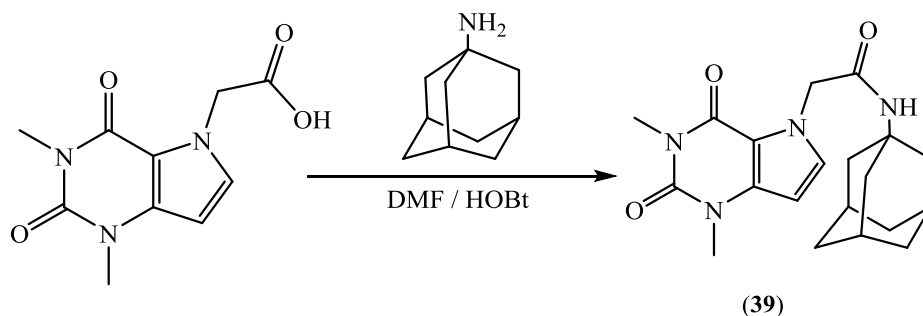
dihydro-4-oxoquinoline-3-carboxylate using diisopropyl ethylamine (DIPEA) as catalyst ²⁹⁻³¹.



N-(1-Adamantyl)-7-trifluoromethyl-4,5,6,7-tetrahydropyrazolo[1,5-a]pyrimidine-3-carboxamide (38) was obtained via interaction of adamantylamine (2) with 7,7-dimethyl-5-phenyl-4,5,6,7-tetrahydropyrazolo[1,5-a]pyrimidine-3-carboxylic acid ³².



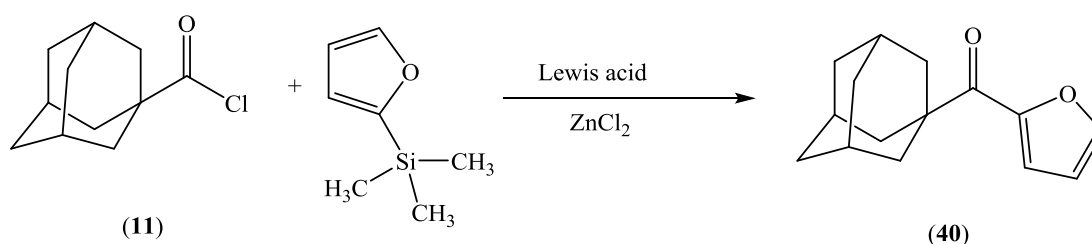
N-Adamantan-1-yl-2-(1,3-dimethyl-2,4-dioxo-1,2,3,4-tetrahydro-pyrrolo[3,2-d] pyrimidin-5-yl)-acetamide (**39**) was obtained by a coupling reaction of adamantylamine (**2**) with acetic acid derivative in presence of N-Ethyl-N'-(3-dimethylaminopropyl) carbodimide ³³⁻³⁵.



Adamantane derivatives containing heterocyclic nuclei with Oxygen atom: -

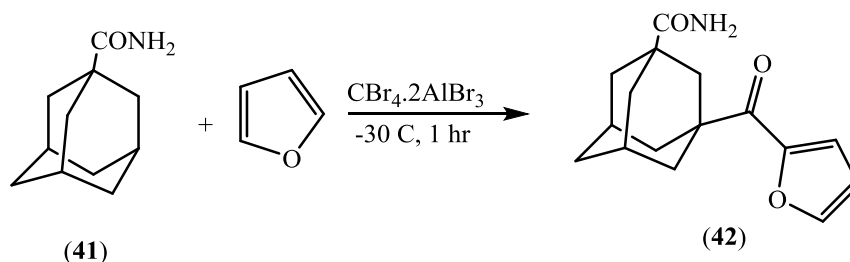
1-Compounds with Five Membered heterocycles

Adamantyl acid chloride (**11**) reacted smoothly with a variety of unsaturated organosilanes at -78 °C in the presence of TiCl_4 or at room temperature in the presence of ZnCl_2 without appreciable decarbonylation. The present success may be due to the enhanced nucleophilicity of silylated olefins as furysilanes to give 1-adamantany-2-furanyl methanone (**40**) ³⁶.

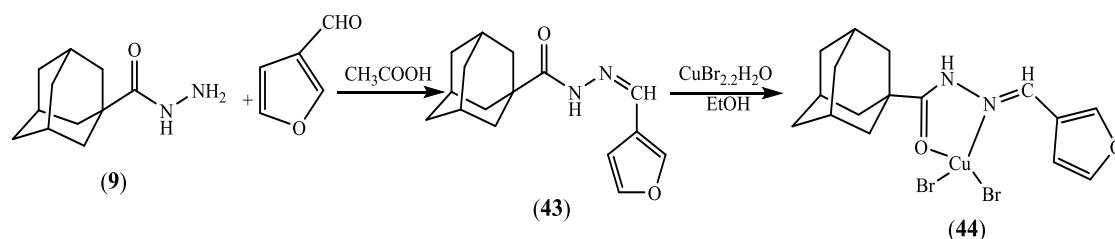


Amide of 1-adamantane carboxylic acid (**41**) contains three relatively reactive CH-bonds in the bridgehead positions which is alkylated with a nucleophile as furan in the presence of super electrophiles $\text{CBr}_4 \cdot 2\text{AlBr}_3$ which can easily generate R^+ carbocations from RH even below room temperature. In the presence of CO , R^+ is transformed into the much more

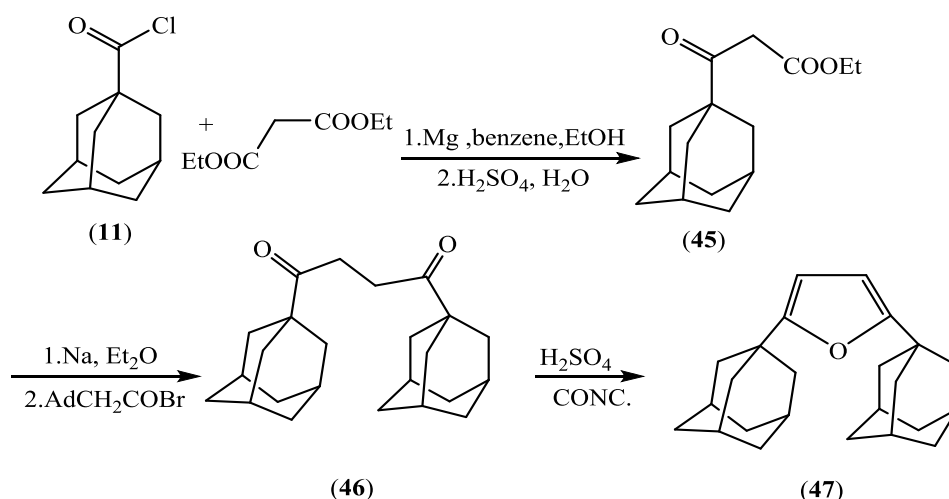
stable acyl cation RCO^+ to give finally 3-(furan-2-carbonyl) adamantane-1-carboxamide (**42**)³⁷.



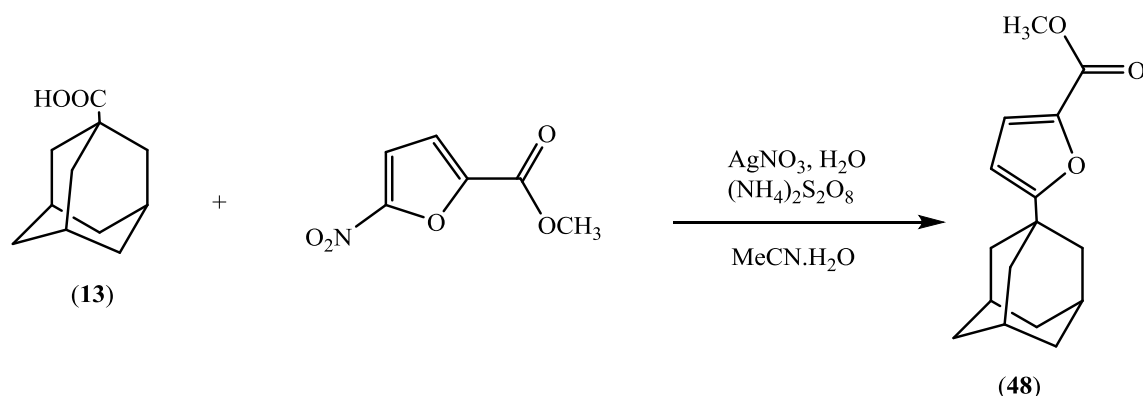
N'-(furan-2-ylmethylene) adamantane-1-carbohydrazide (**43**) has been synthesized by refluxing an equimolar mixture of adamantane-1-carboxylic acid hydrazine (**9**) with furane-2-carbaldehyde in ethanol to produce the desired ligand. The reaction of **L** with copper(II) bromide (CuBr_2) under the solvo-thermal condition results in the formation of Cu(II) complex (**44**)³⁸.



1, 4-di (1-adamantyl) furan (**47**)³⁹ is prepared by acylation between diethyl malonate and 1-adamantoyl chloride (**11**) then, the resulting ethyl 3-(1-adamantyl)-3-oxopropionate (**45**) is alkylated with 1-(1-adamantyl)-2-bromoethane. Subsequent cyclization of 1, 4-di (1-adamantyl) butane-1, 4-dione (**46**) in concentrated sulfuric acid affords the target product in yield of 84%.

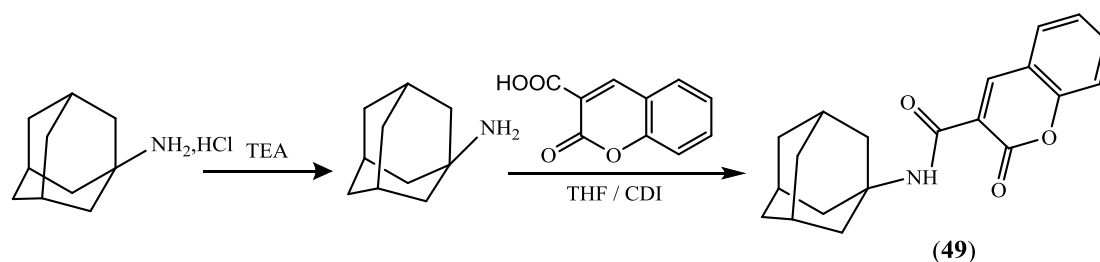


Adamantylated furan (48)³⁹ which includes the radical adamantylation of methyl 5-nitrofuran-2-carboxylic acid or 5-nitrofurfural was described. The adamantyl radical in this method was generated by the Ag (I)-catalyzed oxidative decarboxylation of 1-adamantanecarboxylic acid.

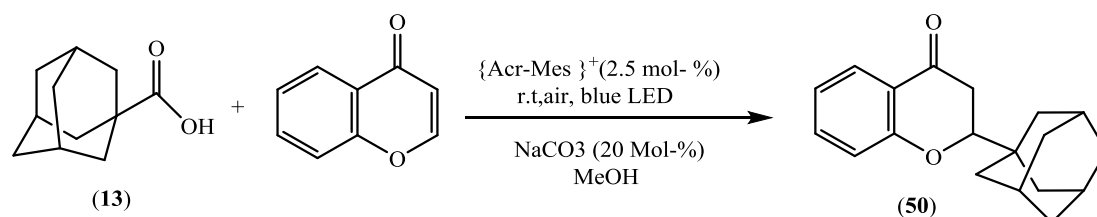


2-Compounds with six Membered heterocycles

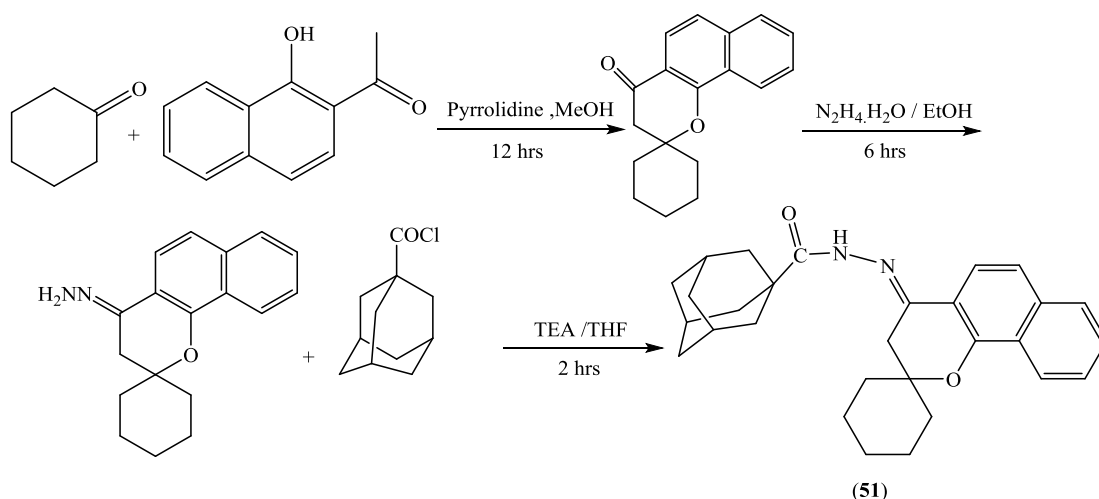
N-(1-adamantyl)-2-oxo-chromene-3-carboxamide (49)⁴⁰ was highly potent antioxidant activity which is synthesized by amidation reaction with coumarin-3-carboxylic acid and adamantyl amine through the intermediate complexes with N, N-carboxyldiimidazole (CDI) as catalyst.



A transition-metal-free method for the decarboxylative generation of radicals from carboxylic acids and their 1, 4-addition to Michael acceptors. The Fukuzumi catalyst (9-mesitylene-10-methylacridinium perchlorate, [Acr-Mes]⁺ ClO₄⁻) enabled this transformation under visible-light irradiation at room temperature with CO₂ as the only by product. The scope and limitations of this protocol were examined by using a range of Michael acceptors as example as 4-chromenone (**50**) and adamantyl carboxylic acid (**13**).



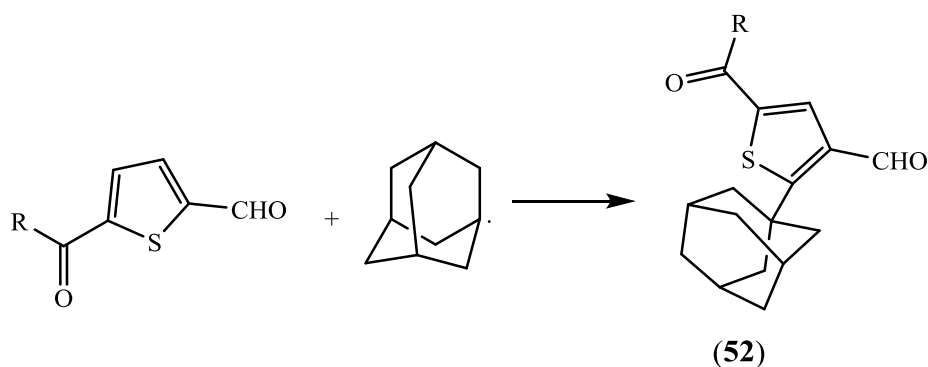
N'-(spiro [benzo[h]chromene-2, 10-cyclohexan]-4(3H)-ylidene) adamantane-1-carbohydrazide (**51**)⁴² was acylated by adamantyl acid chloride (**11**) with Spiro[benzo[h]chromene-2,10-cyclohexan]-4(3H)-ylidenehydrazine which is derived from spirobenzo[h]chromenone starting material was allowed to react with hydrazine hydrate, via a thermal condensation of cyclohexanone, 10-hydroxy-20-acetonaphthone and pyrrolidine in methanol using the reported Kabbe's multi-component reaction⁴³.



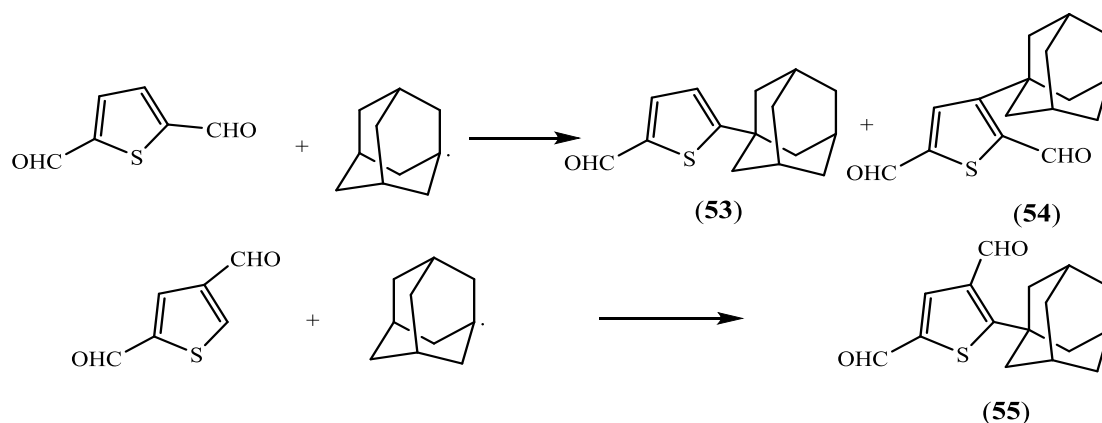
Adamantane derivatives containing heterocyclic nuclei with Sulfur atom: -

1-Compounds with Five Membered heterocycles

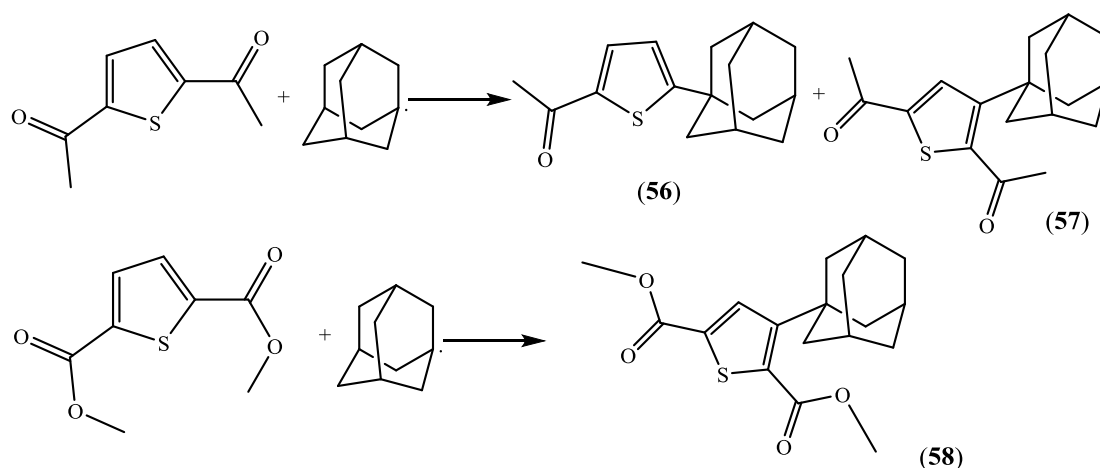
Several examples of the addition of an alkyl or acyl radical to a substituted position of an aromatic substrate to give an ipso-intermediate ; in most cases these radical a-complexes evolve by elimination of the ipso-substituent to give ipso-substitution products, some reactions of adamantyl radical (adamantyl carboxylic acid) which demonstrate that in the thiophen series (**52**) these intermediates can also give rise to rearrangement reactions by migration of an ipso-formyl group to a vicinal position using AgNO_3 and $(\text{NH}_4)_2\text{S}_2\text{O}_8$ dissolved in acetonitrile-water⁴⁴.



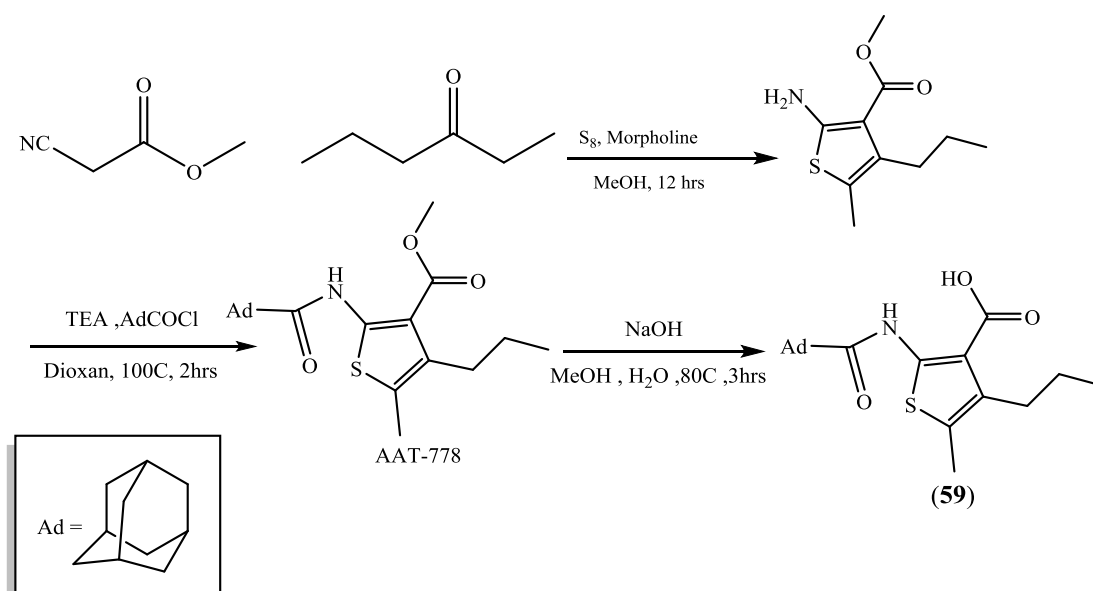
The reaction of 1-adamantyl radical with thiophen- 2,5-dicarbaldehyde ⁴⁴ afforded three products, 5-(1-adamantyl) thiophen-2-carbaldehyde (**53**), 3-(1-adamantyl) thiophen-2,5-dicarbaldehyde (**54**), and 2-(1-adamantyl) thiophen-3,5-dicarbaldehyde (**55**). The structure of the rearrangement 3-(1-adamantyl) thiophen-2, 4-dicarbaldehyd was also confirmed by independent synthesis. 3-(1-adamantyl) thiophen-2, 4-dicarbaldehyd was obtained as the sole product from the radical adamantylation of the thiophen- 2, 4-dicarbaldehyde; it has been shown in previous work that radical substitution occurs selectively at the 2-position of thiophen derivatives bearing electron withdrawing substituent at the 3- and 5-positions.



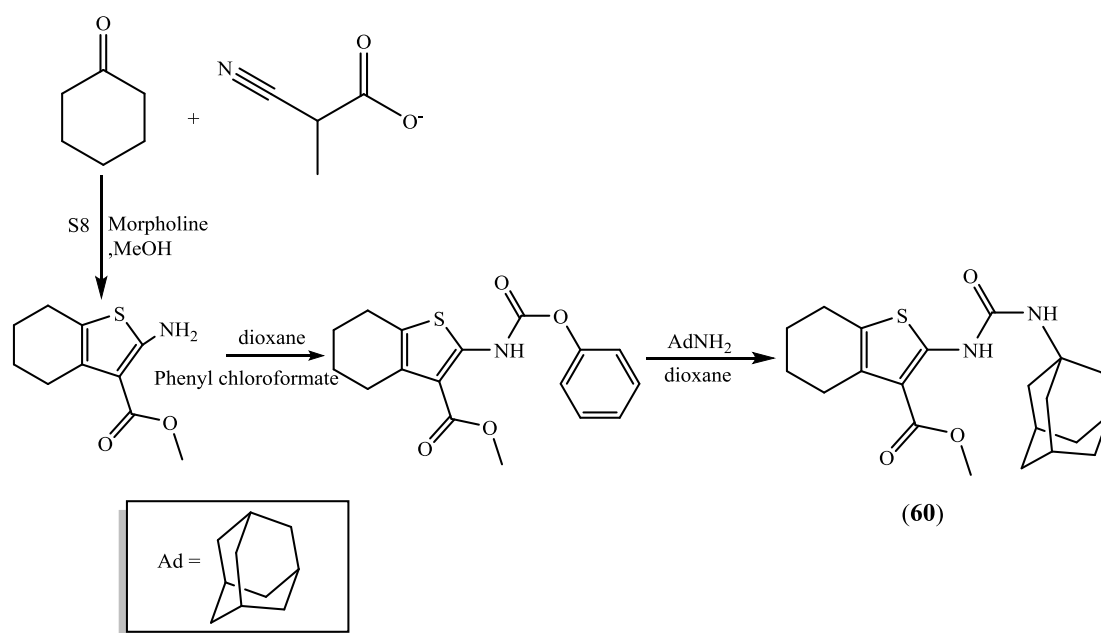
Adamantyl radical with 2, 5-diacetylthiophen afforded only the product of adamantyldeacylation, 2-(1-adamantyl)-5-acetylthiophen (**56**) and the product of substitution at the β -position, 3-(1-adamantyl)- 2,5-diacetylthiophen (**57**). Moreover, from the reaction of Adamantyl radical with 2,5-bismethoxycarbonylthiophen the only product obtained was 3-(1-adamantyl) -2,5-bismethoxycarbonylthiophen (**58**)⁴⁴.



Thiophene-based reference compounds AAT-778 (**59**) was synthesized under the Gewald reaction conditions by condensation between methyl cyanoacetate, hexan-3-one and addition of sulfur to α , β -unsaturated nitrile ring-closure of the ylidenesulfur adduct, the thiophene amine compounds as methyl 2-amino-5-methyl-4-propylthiophene-3-carboxylate⁴⁵ was obtained for coupling with 1-adamantanecarbonyl chloride (**11**).

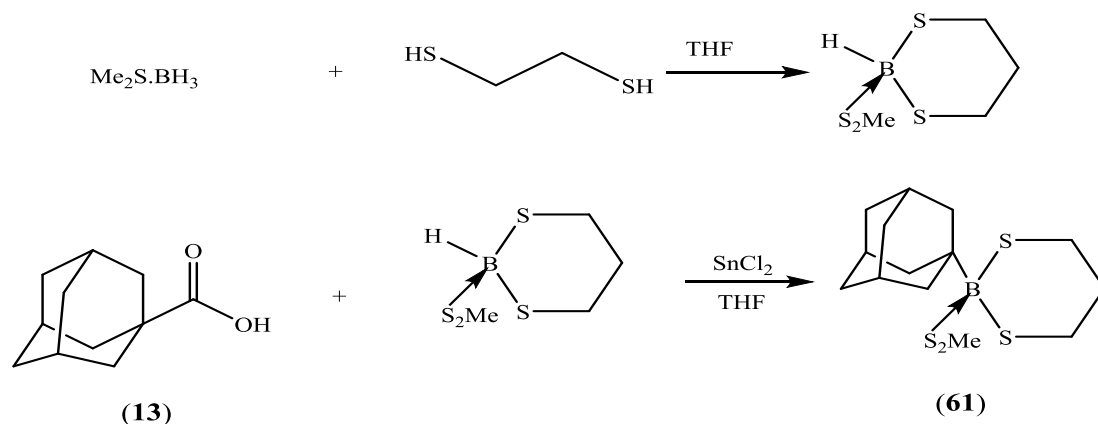


Condensation of methyl cyanoacetate in the presence of sulfur and morpholine with cyclohexanone afforded the bicyclic aminothiophene intermediates which were acylated with phenyl chloroformate to form phenyl carbamate and also the amide functionality is replaced by urea moieties, compound (**60**) was also synthesized in 50-87% yield by reaction of 1-aminoadamantane, morpholine, and piperidine with phenyl carbamate 46.



2-Compounds with six Membered heterocycles

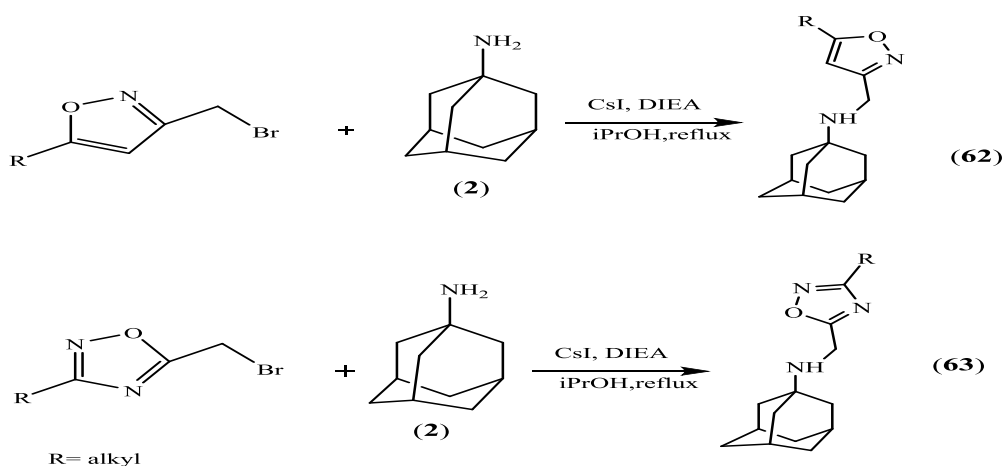
Kresge and co-workers⁴⁷ were suggested that reaction of adamantyl carboxylic acid (**13**) with 1, 3, 2-dithiabornane-dimethyl sulfide in the presence of stannous chloride in tetrahydrofuran affords the corresponding 1, 3-dithianes in high yields (**61**). The reagent of 1, 3, 2-dithiabornane-dimethyl sulfide, is readily prepared by treating borane-dimethyl sulfide complex with 1 equiv of 1, 3-propanedithiol in tetrahydrofuran and subsequent stirring at room temperature for a week.



Adamantane derivatives containing heterocyclic nuclei with Nitrogen and Oxygen atoms: -

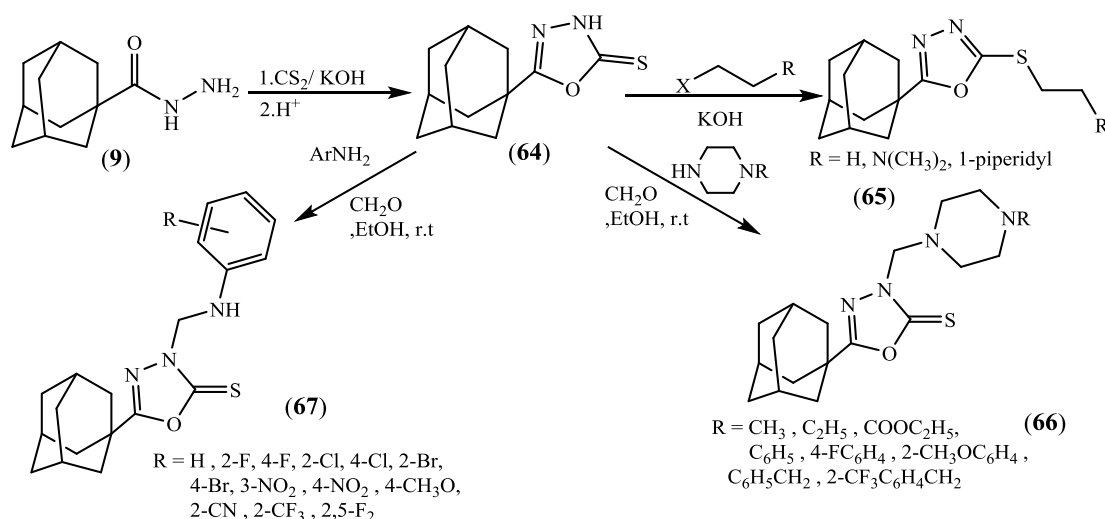
1-Compounds with Five Membered heterocycles

N-alkylation of adamantane amine (**2**) with isoxazole methylene bromide intermediate was performed compound (**62**) under refluxing condition in isopropanol with cesium iodide as the catalyst and triethyl amine and the same reaction occurred in oxadiazole methylene chloride to produce compound (**63**)⁴⁸.

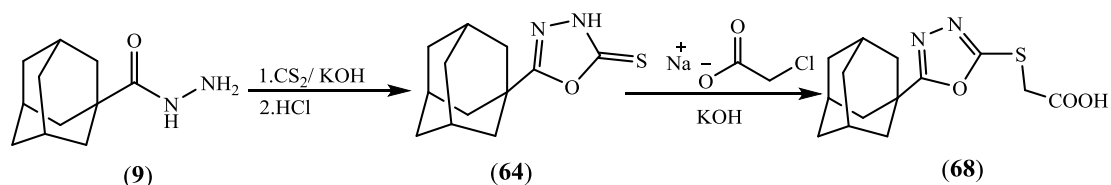


5-(1-adamantyl)-1,3,4-oxadiazoline-2-thione (**64**)⁴⁹ was synthesized by adamantane-1-carbohydrazide (**9**) with carbon disulfide and potassium hydroxide, in ethanol, followed by acidification to yield 81 %, Interaction

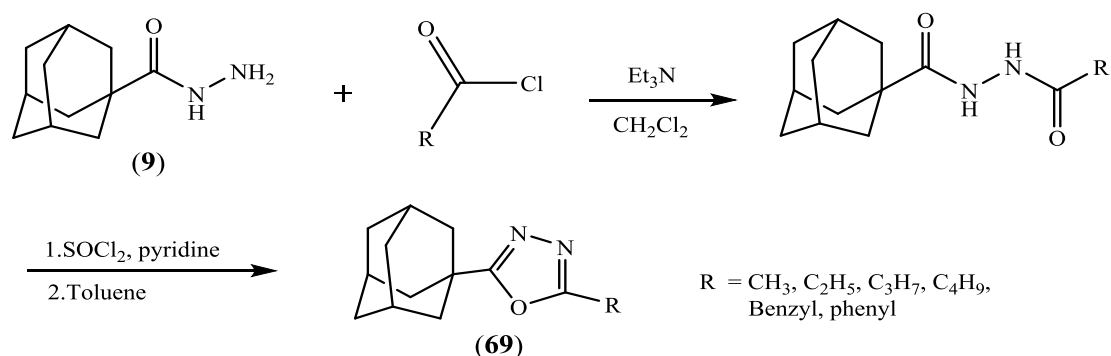
of 5-(1-adamantyl)-1,3,4-oxadiazoline-2-thione (**64**) with iodoethane, 2-dimethylaminoethyl chloride, or 2-(1-piperidyl) ethyl chloride hydrochloride in ethanolic potassium hydroxide yielded the corresponding 5-(1-adamantyl)-2-ethylthio (**65**) or substituted ethylthio-1,3,4-oxadiazoles (**66**). On the other hand, the N-Mannich derivatives 5-(1-adamantyl)-3-arylaminomethyl-1,3,4-oxadiazoline-2-thiones and 5-(1-adamantyl)-3-(4-substituted-1-piperazinylmethyl)-1,3,4-oxadiazoline-2-thiones (**67**) were prepared in high yields via the reaction of 5-(1-adamantyl)-1,3,4-oxadiazoline-2-thione with formaldehyde solution and the corresponding primary aromatic amine or 1-substituted piperazine, in ethanol at room temperature.



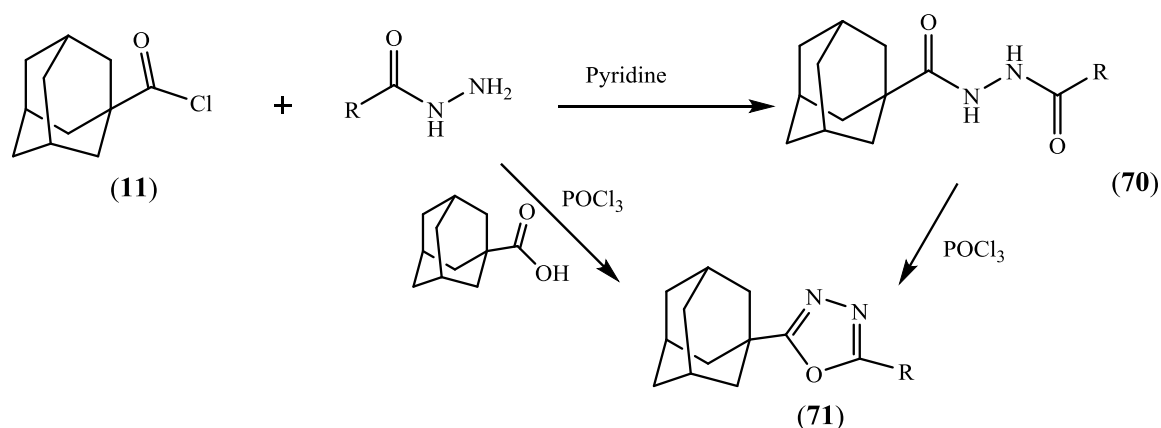
2-(1-Adamantyl)-1,3,4-oxadiazoline-5-thione (**64**)⁴⁹ was obtained in 81% yield via prolonged heating of the hydrazide with carbon disulphide and potassium hydroxide, in ethanol, followed by acidification with hydrochloric acid. the reaction of 2-(1-Adamantyl)-1,3,4-oxadiazoline-5-thione with sodium chloroacetate in ethanol in the presence of sodium hydroxide yielded the S-acetic acid derivative (**68**)⁵⁰.



Adamantane-1-carbohydrazide (**9**) was acylated with an acid chloride in the presence of triethylamine to give an N-acetyl hydrazide. This intermediate was converted to the imidoyl chloride and cyclized to give adamantlyl oxadiazole (**69**)⁵¹.

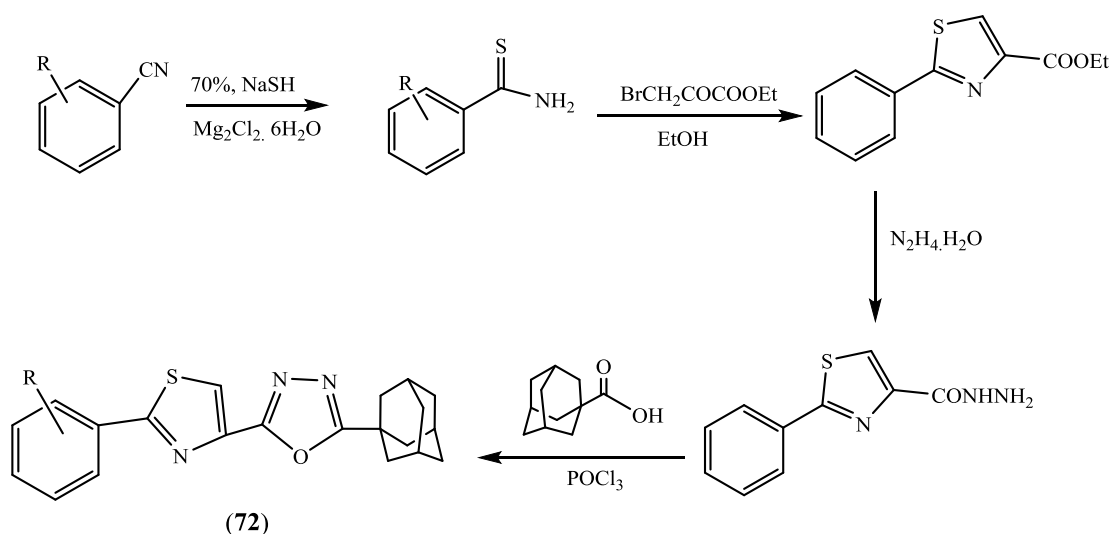


The reaction of 1-adamantanecarbonyl chloride (**11**) with various carboxylic acid hydrazides in pyridine yielded the corresponding N-acyl derivatives (**70**) in high yields. N-acyl derivatives were cyclized by heating with phosphorus oxychloride for 1 h to yield the corresponding 2-(1-adamantyl)-5-substituted-1,3,4-oxadiazoles (**71**). 2-(1-adamantyl)-5-substituted-1,3,4-oxadiazoles were also independently prepared in 85 and 95% yields by the reaction of the carboxylic acid hydrazides with 1-adamantane carboxylic acid in the presence of phosphorus oxychloride⁵².



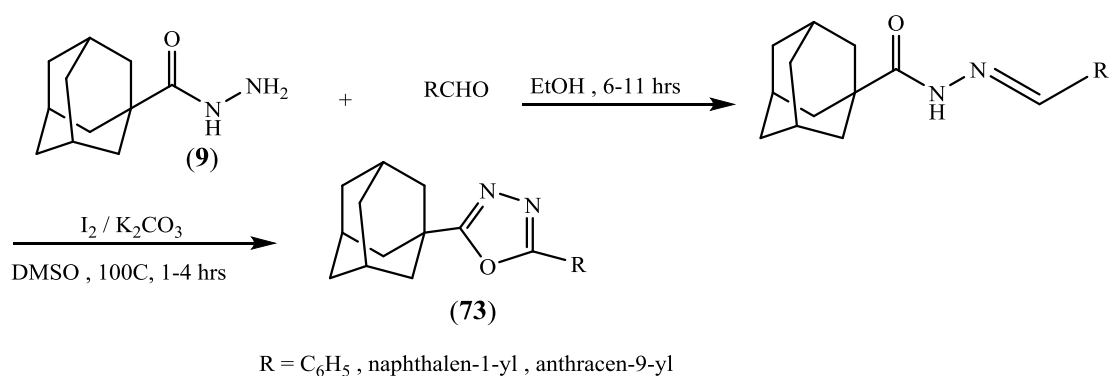
$\text{R} = \text{C}_6\text{H}_5, 4\text{-FC}_6\text{H}_4, 4\text{-ClC}_6\text{H}_4, 4\text{-BrC}_6\text{H}_4, 4\text{-NO}_2\text{C}_6\text{H}_4, 3,5\text{-(NO}_2)_2\text{C}_6\text{H}_3, 3,4\text{-(NO}_2)_2\text{C}_6\text{H}_3, 2\text{-Cl,4-NO}_2\text{C}_6\text{H}_3, 2\text{-thienyl}, 1\text{-adamantyl}$

A series of adamantylmethyl-5-arylthiazolyl-1,3,4-oxadiazole derivatives⁵³ were synthesized from aryl nitriles through a multi-step reaction sequence. Aryl nitriles were converted to aryl thioamide derivatives, which upon cyclization with ethyl bromopyruvate, followed by hydrazinolysis yielded 2-aryl-1,3-thiazole-4-carbohydrazide analogs. Treatment of 2-aryl-1,3-thiazole-4-carbohydrazide analogs with adamantyl-1-carboxylic acid (13) in the presence of POCl_3 afforded adamantylmethyl-5-arylthiazolyl-1,3,4-oxadiazole derivatives (72) (68–81 %).

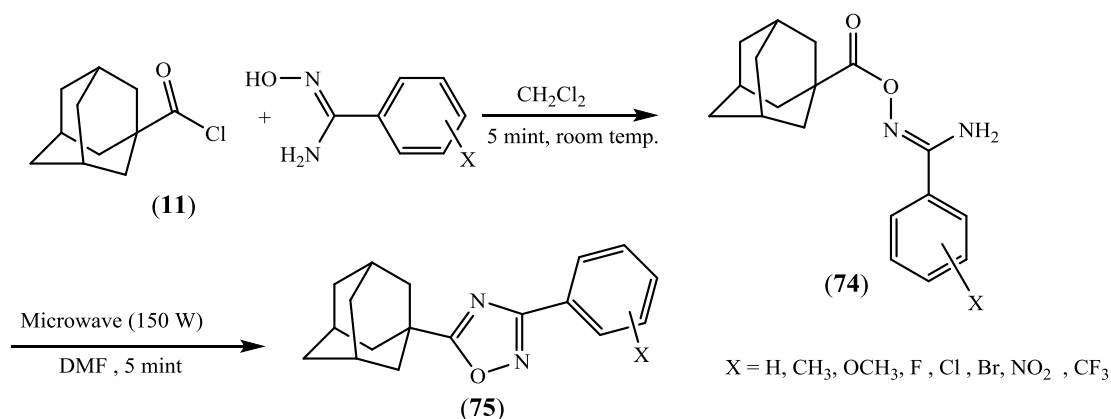


$\text{R} = 2\text{-Me}, 2\text{-Cl}, 2\text{-F}, 2\text{-Br}, 3\text{-Me}, 3\text{-Cl}, 3\text{-F}, 3\text{-Br}, 4\text{-Me}, 4\text{-Cl}, 4\text{-F}, 4\text{-Br}$

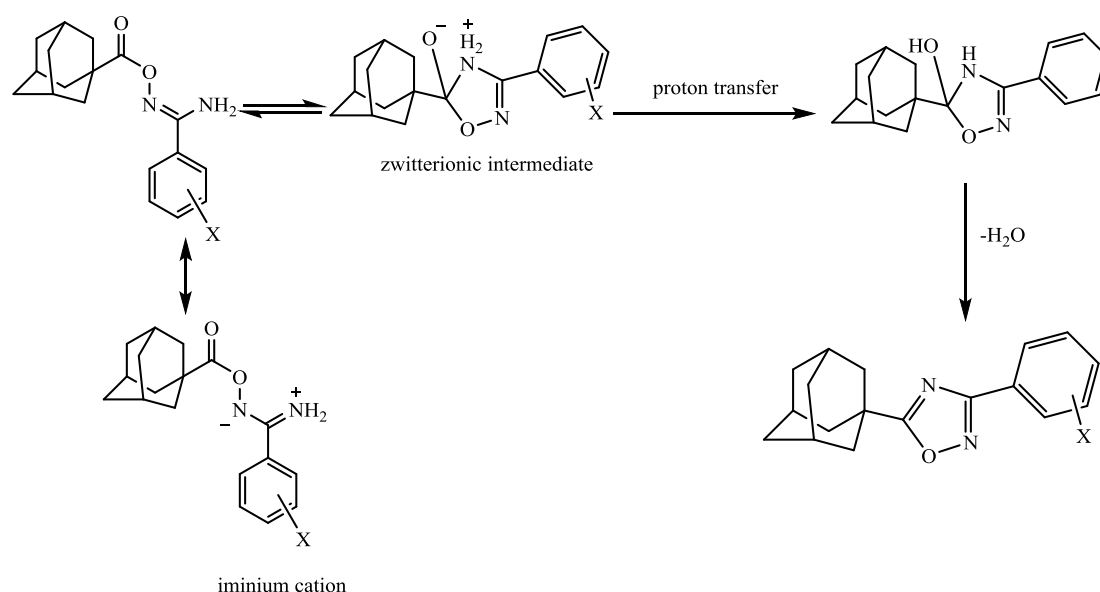
2, 5-Disubstituted 1, 3, 4-oxadiazoles (**73**)⁵⁴ can be obtained by oxidation with molecular iodine of condensation products of aldehydes and carboxylic acid hydrazides. Aldehydes containing both electron-donating and electron-withdrawing substituents and both aromatic and aliphatic carboxylic acid hydrazides can be used as starting compounds(**9**), the cyclization stage with the formation of 1, 3, 4-oxadiazoles is slow and that the presence of excess iodine is necessary for the reaction to occur by optimizing the reaction conditions to obtain target compounds in fairly high yields (84–89) %.



1-adamantanecarbonyl chloride (**11**) was directly reacted with benzamidoxime (1.2 equiv, $X=H$) for 10 min in dichloromethane under reflux, in order to prepare 1, 2, 4-oxadiazole⁵⁵. However, the reaction afforded a mixture of two products that were purified and characterized as an *O*-acyl intermediate (**74**) and the desired 1, 2, 4-oxadiazole (**75**). Based on this observation, our synthetic strategy was designed to develop protocols of arylamidoximes *O*-acylation and subsequent thermal cyclization via intramolecular cyclodehydration dependent on the aromatic ring electron density. Then, the synthesis of the 1,2,4-oxadiazole derivatives was performed with 1-adamantanecarbonyl chloride as starting material and a variety of arylamidoximes in a one-pot two-step reaction.

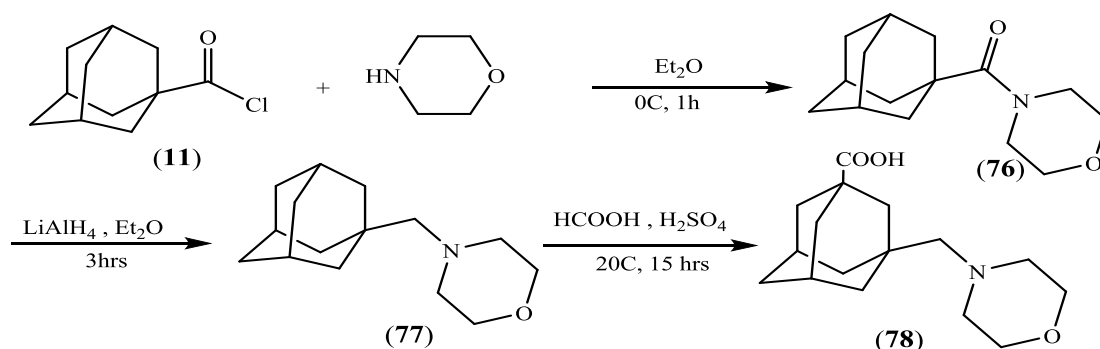


Mechanism: -

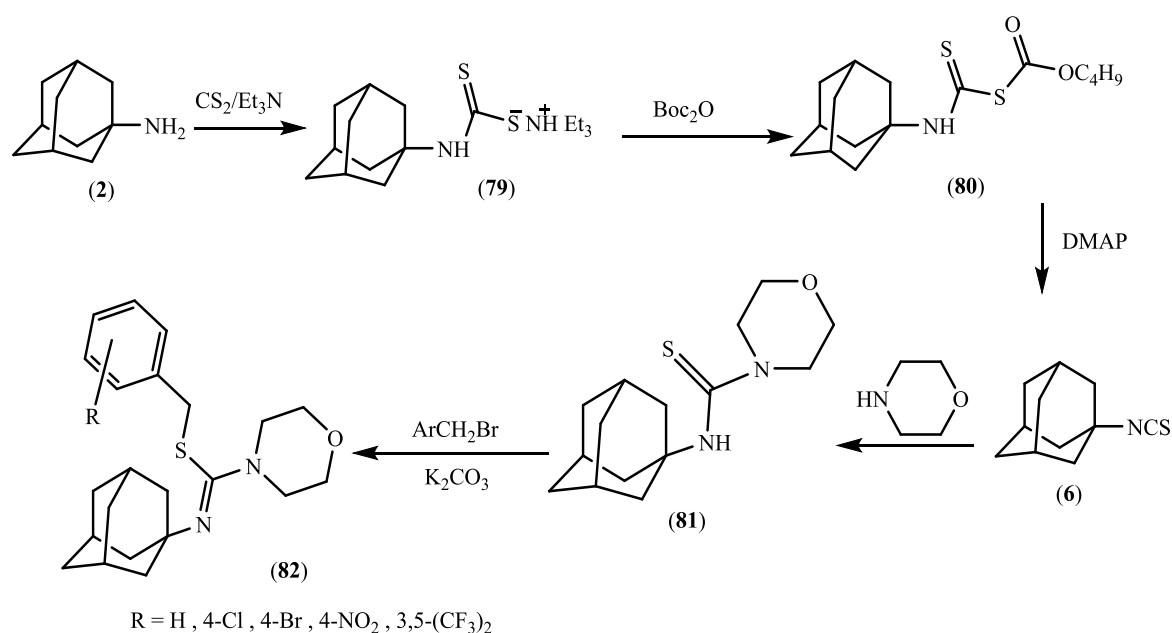


2-Compounds with six Membered heterocycles

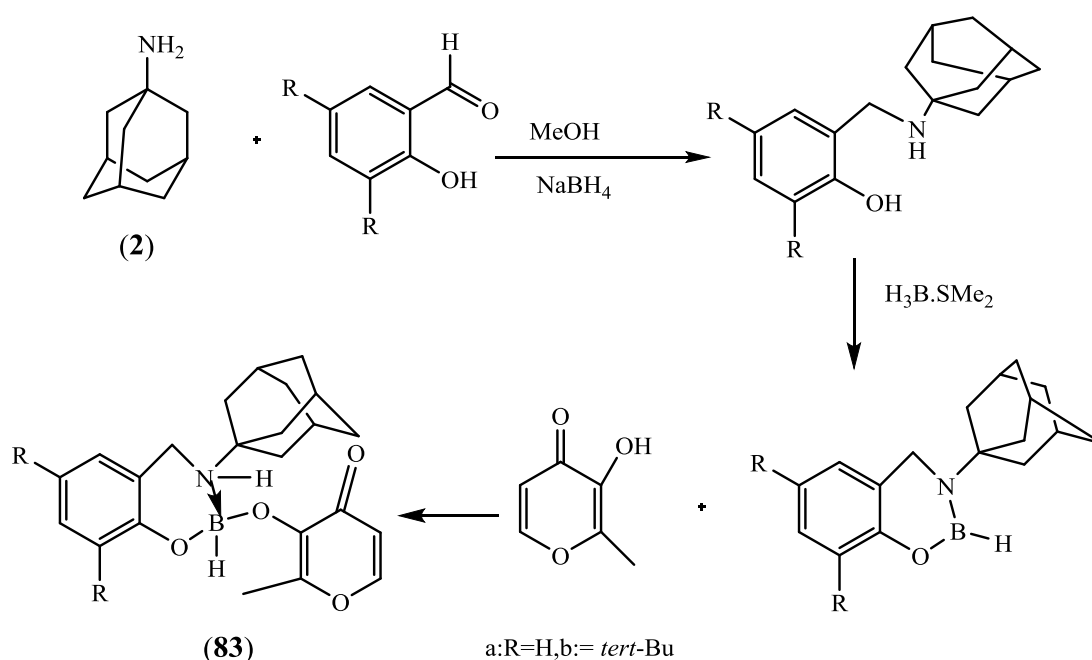
A method for preparing 3-(morpholinomethyl) adamantane-1-carboxylic acid (**78**)⁵⁶ has been proposed. The method includes three stages. The reaction of the chloride adamantyl acid chloride (**11**) with morpholine affords the morpholide of this acid (**76**), which is then reduced with lithium tetrahydroaluminate to 1-(morpholinomethyl) adamantane (**77**). The latter reacts with formic acid in the presence of sulfuric acid to give 3-(morpholinomethyl) adamantane-1-carboxylic acid (**78**).



1-adamantyl isothiocyanate (6) was prepared in good yield via our previously described methods. The reaction of 1-adamantylamine (2) with carbon disulphide and trimethylamine, in ethanol, yielded the dithiocarbamate salt (79), which was reacted with di-*tert*-butyl dicarbonate (Boc_2O) to yield the intermediate (80). The intermediate was stirred with catalytic amount of 4-dimethylaminopyridine (DMAP) to furnish the target product. The reaction of 1-adamantyl isothiocyanate (6) with morpholine in boiling ethanol yielded the corresponding *N*-(adamantan-1-yl) morpholine-4-carbothioamide (81), respectively. The carbothioamides was reacted with benzyl or substituted benzyl bromides, in acetone, in the presence of anhydrous potassium carbonate to yield the corresponding *S*-arylmethyl derivatives (82) ⁵⁷.



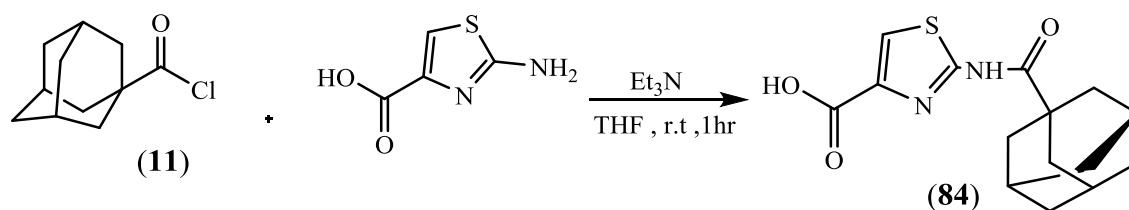
Reductive amination of salicylaldehyde or 3, 5-di-*tert* butyl salicylaldehyde and 1-adamantylamine (**2**) using NaBH_4 gave the corresponding aminoalcohols in high yields. Subsequent addition of one equivalent of $\text{H}_3\text{B}\cdot\text{SMe}_2$ to the aminoalcohols with loss of two equivalents of dehydrogenate resulting in the formation of adamantanyl oxazaborinanes (**83**)⁵⁸.



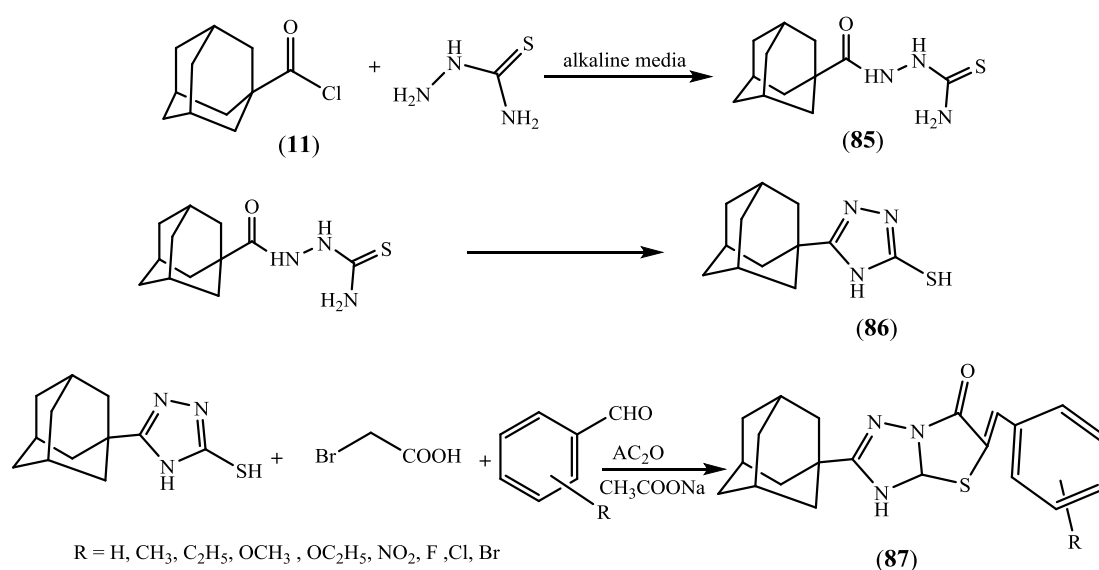
Adamantane derivatives containing heterocyclic nuclei with nitrogen and sulfur atoms: -

Compounds with Five Membered heterocycles

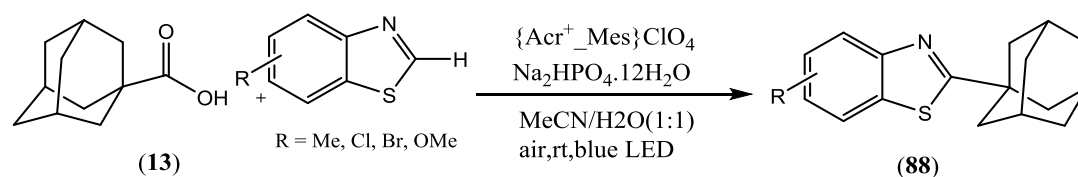
Adamantyl thiazole carboxamide (**84**)⁵⁹ were prepared from acylation adamantyl acid chloride (**11**) with ethyl 2-aminothiazole-4-carboxylate.



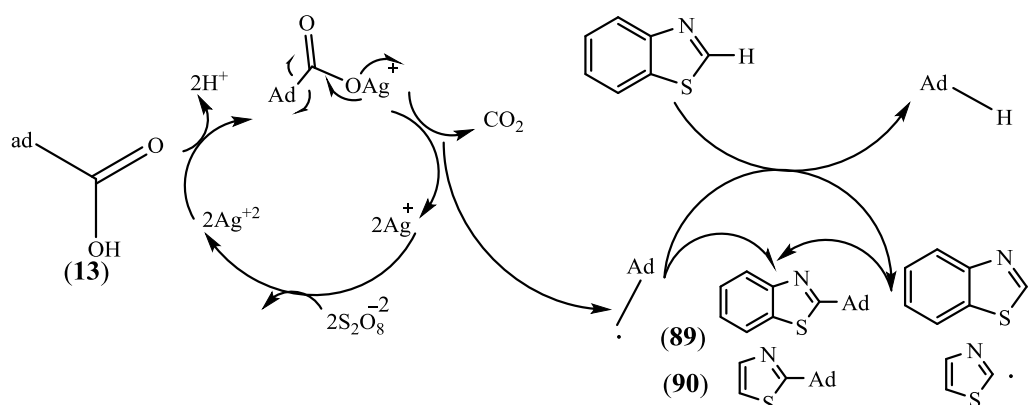
Adamantane thiosemicarbizide (**85**)⁶⁰ was synthesized using a procedure reported earlier starting from adamantane-1-carbonyl chloride (**11**) upon reaction with thiosemicarbazide, followed by cyclization in alkaline solution under reflux to 5-adamantyl-4H-1,2,4-triazol-3-thiole (**86**). The third step includes the one pot condensation of 5-adamantyl-4H-1,2,4-triazol-3-thiole with bromoacetic acid and appropriate substituted benzaldehydes in the presence of sodium acetate and acetic anhydride to produce compound (**87**).



A novel and efficient photoredox induced decarboxylative C2-alkylation of benzothiazoles with adamantane carboxylic acid (**13**) were developed by using a catalytic amount of 9-mesityl-10-methyl acridinium perchlorate (3 mol%) as a photocatalyst and air as an oxidant with the irradiation of a blue LED under transition-metal free conditions at room temperature. A variety of secondary and tertiary alkyl groups could be efficiently incorporated into benzothiazoles (**88**).⁶¹ at the C2-position in good yields.

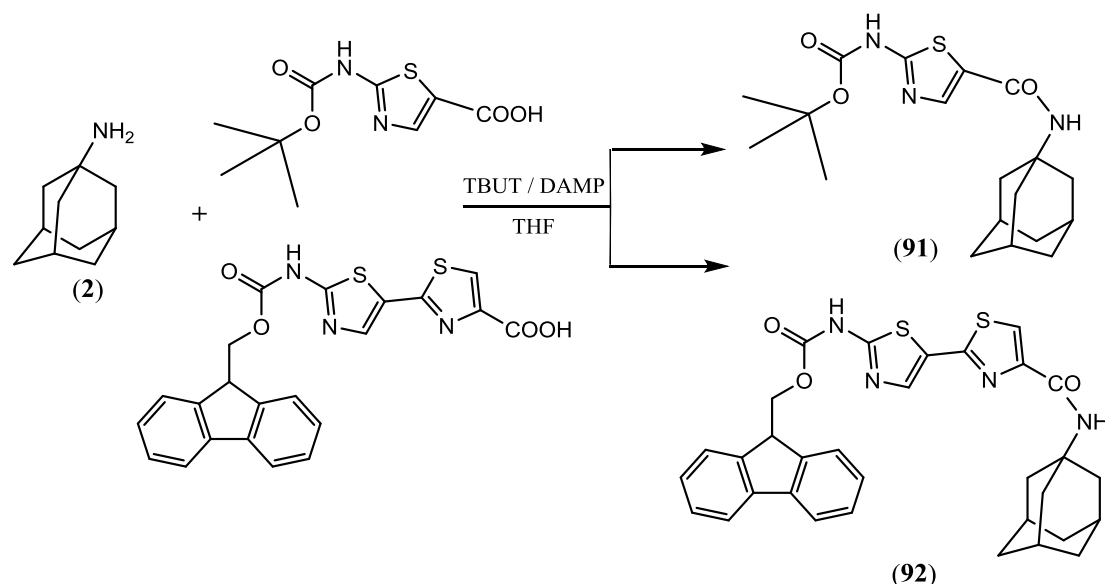


A novel and efficient silver catalyzed decarboxylative direct C2-alkylation of benzothiazoles and thiazoles ⁶² were developed as in the mechanism which an Ag (I) cation is oxidized to an Ag (II) cation by peroxodisulfate. Then, adamantyl carboxylic acid (**13**) reacts with the Ag (II) cation to form cation salt by losing a proton. Further loses one molecule of CO₂ and the Ag (I) cation to form alkyl radical. The obtained free radical subsequently underwent hydrogen atom abstraction from the C2 of thiazole or benzothiazole forming the corresponding thiazole or benzothiazole radical. Subsequently, another alkyl radical couples with thiazole or benzothiazole radical, forming the coupling products (**89,90**). The ease of carboxylic acid decarboxylation seems to be closely related to the stability of the in situ formed adamantyl radical, as the reactivity appears to increase on going from secondary to tertiary radicals.

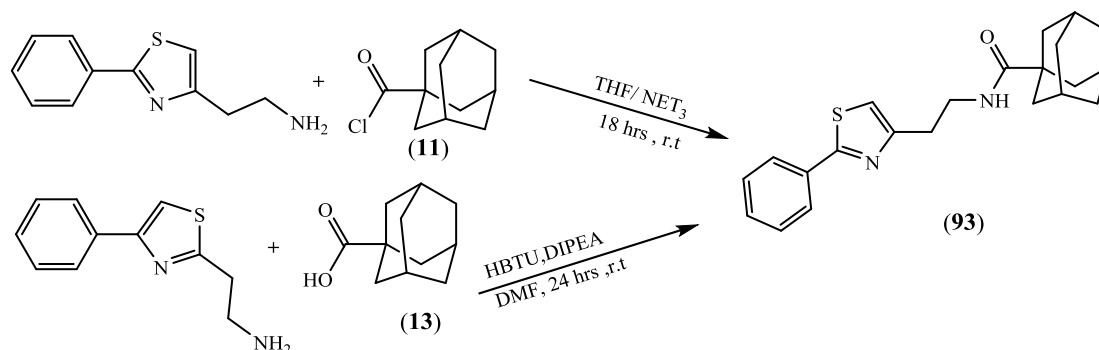


A mixture of amantadine.HCl and TBTU (80 mmol) in tetrahydrofuran (THF) was stirred and a solution of Boc-Gly-Thz-OH or Fmoc-Gly-Thz-Thz-OH (80 mmol) and 4-(*N,N*-dimethylamino)-pyridine (DMAP) (80 mmol) were added to the reaction mixture and stirred for 3 h. Then THF was evaporated in vacuo and the residue was chromatographed on silica gel, using hexane: ethyl acetate (4:5). The compounds containing Boc group was dissolved in 20 mL of TFA and stirred at 0 °C for 1 h to remove the Boc protecting group. Deprotection procedure is followed by

neutralization with aqueous ammonia to obtain the final products Gly-Thz-amantadine (**91,92**)⁶³.

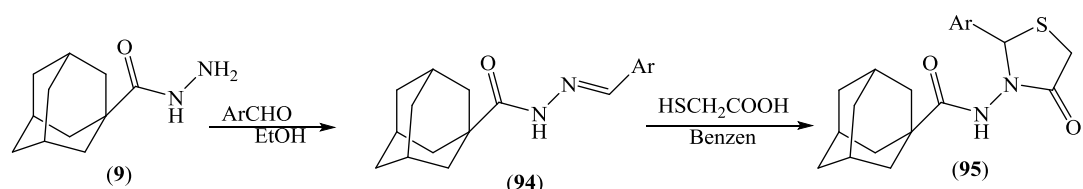


The 1-adamantylcarbonylamide (**93**)⁶⁴ was obtained upon coupling the commercially available 1-adamantylcarbonyl chloride (**11**) with the 2-phenylthiazol-4-ethylamine and the 4-phenylthiazol-2-ethylamine respectively. The acid (**13**) reacted in the presence of the coupling reagent N, N, N', N'-Tetramethyl-O-(1H-benzotriazol-1-yl)uroniumhexafluorophosphate (HBTU), while the chlorides reacted without the aid of any activating reagent.



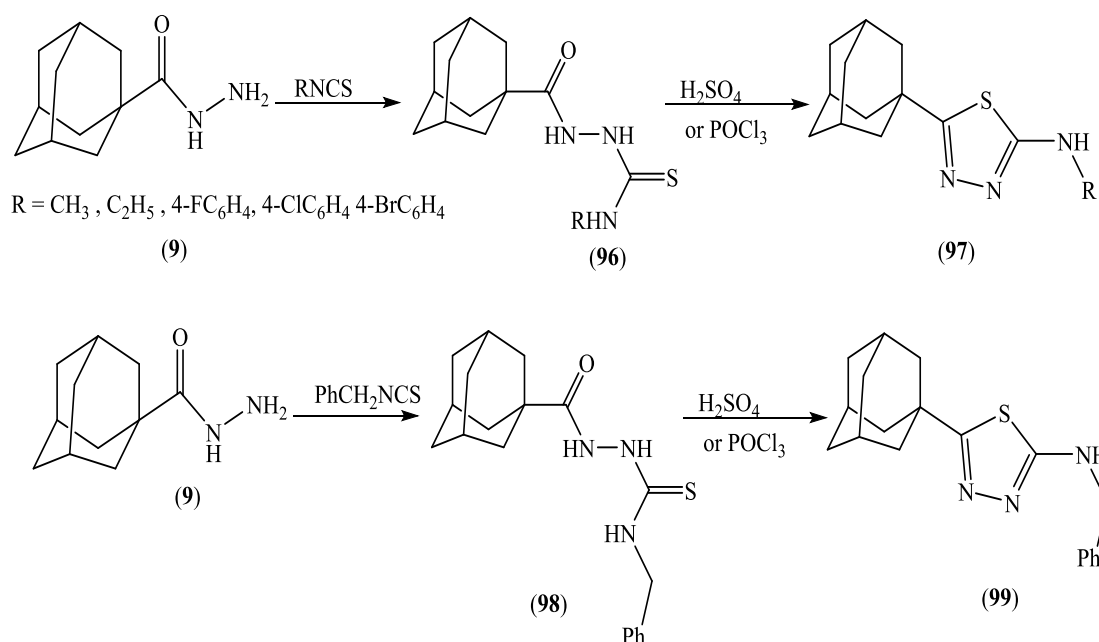
Adamantane-1-carboxylic acid hydrazide (**9**) readily reacts with carbonyl compounds to yield the corresponding anils (Schiff's bases) (**94**). The

reaction is usually carried out in ethanol, acetic acid or in dimethylformamide according to the solubility of the reactants. Accordingly, adamantane-1-carboxylic acid hydrazide was allowed to react with some substituted benzaldehydes, 2-thenaldehyde or 5-nitro-2-thenaldehyde in ethanol for one hour to yield the corresponding N-arylidene-1-adamantylcarboxhydrazides which were reacted with mercaptoacetic acid in benzene to afford the corresponding racemates (\pm) 3-(1-adamantylcarbonylamino)-2-aryl-4-thiazolidinones (**95**)⁶⁵.

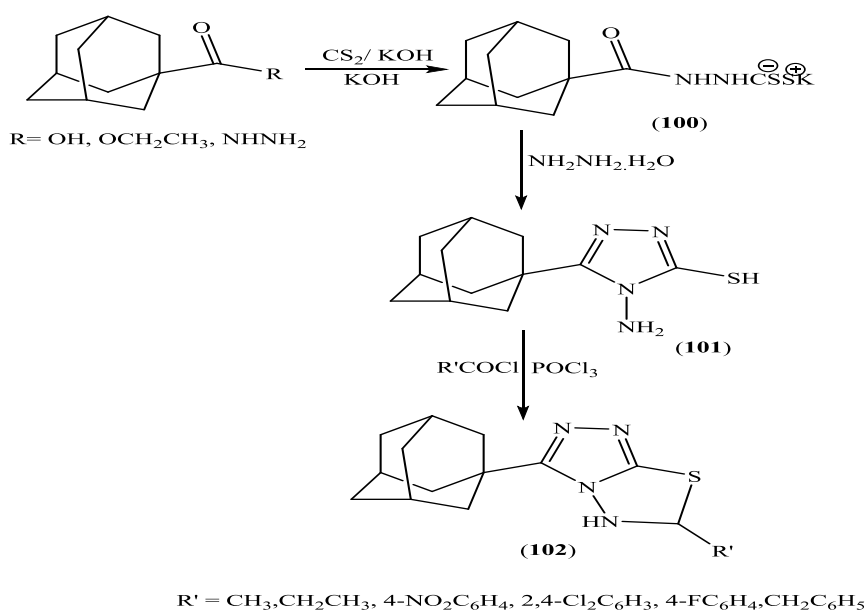


Ar = 4- FC_6H_4 , 4- ClC_6H_4 , 2- ClC_6H_4 , 4- BrC_6H_4 , 4- $\text{CH}_3\text{C}_6\text{H}_4$, 2- $\text{NO}_2\text{C}_6\text{H}_4$, 3- $\text{NO}_2\text{C}_6\text{H}_4$, 2,6- $\text{Cl}_2\text{C}_6\text{H}_3$, 2- Cl , 5- FC_6H_3 , 2- Cl , 5- $\text{NO}_2\text{C}_6\text{H}_3$, 4-(Me_2N) C_6H_4 , 2-Thienyl

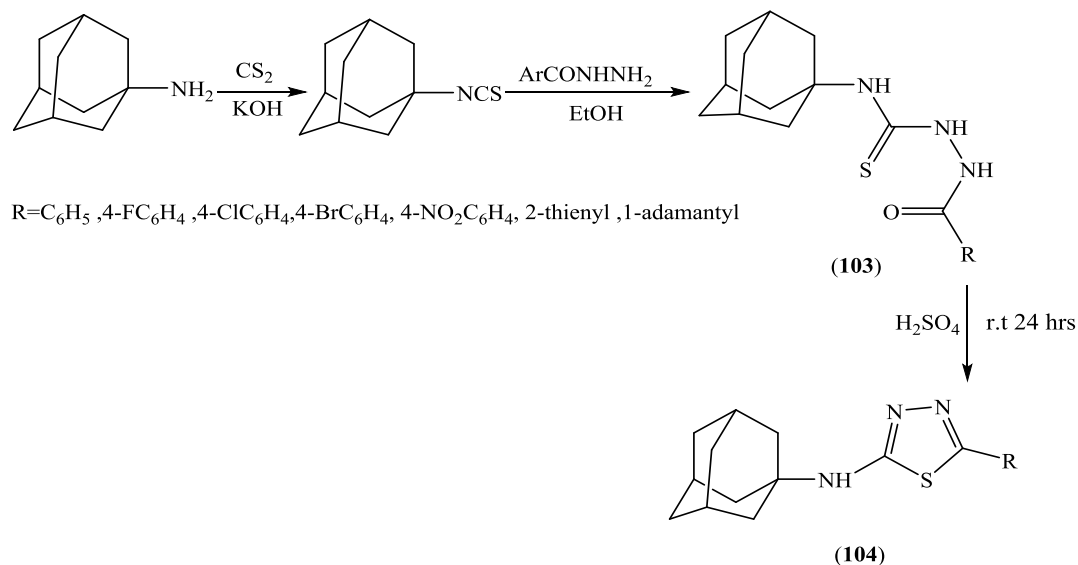
Cyclization of 1-(1-adamantylcarbonyl)-4-substituted thiosemicarbazides (**96**) with dehydrating agent as sulphuric acid at ambient temperature or by heating with phosphorus oxychloride yielded the corresponding 2-(1-adamantyl)-5-amino-1, 3, 4-thiadiazoles (**97**). Cyclization of 1-(1-adamantylcarbonyl)-4-benzylthiosemicarbazide with sulphuric acid gave the debenzylated product 2-(1-adamantyl)-5-amino-1, 3, 4-thiadiazole (**98**). On the other hand, cyclization of 1-(1-adamantylcarbonyl)-4-benzylthiosemicarbazide using phosphorus oxychloride yielded 2-(1-adamantyl)-5-benzylamino-1, 3, 4-thiadiazole (**99**)⁶⁶.



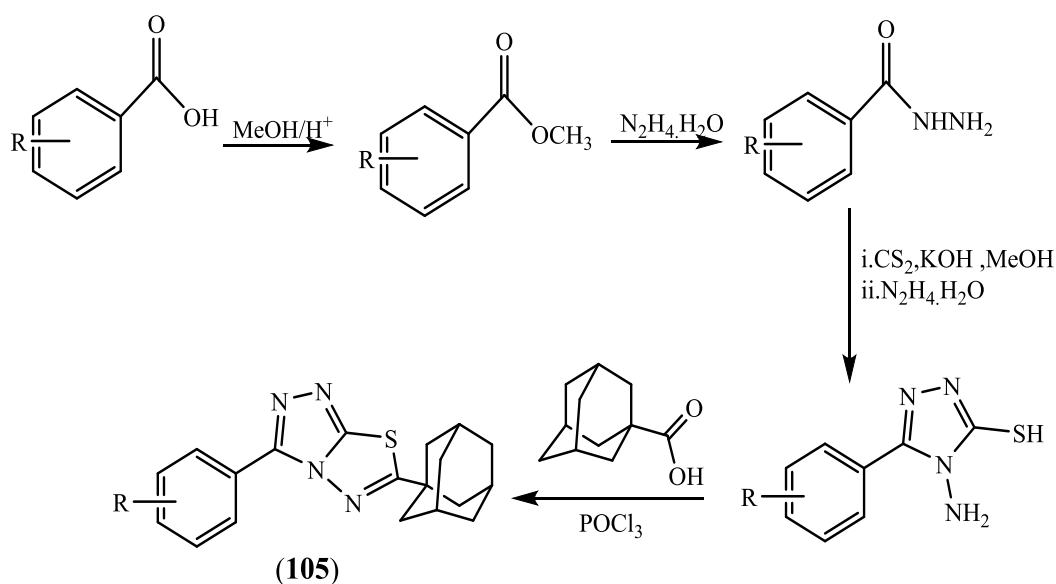
1-Adamantanecarboxylic acid hydrazide was heated with carbon disulfide in the presence of absolute ethanol and potassium hydroxide to afford the intermediate potassium acylhydrazine dithioformate (**100**). This salt underwent ring closure with an excess of 95% hydrazine to give the 3-adamantyl-4-amino-5-mercapto-1,2,4-triazole (**101**). Heating at reflux the triazole with phosphorus oxychloride and the appropriate acyl chloride provided the 3,6-disubstituted 1,2,4-triazolo[3,4-*b*] [1,3,4] thiadiazoles (**102**)⁶⁷.



The reaction of 1-adamantylisothiocyanate with various carboxylic acid hydrazides in ethanol yielded the corresponding 1-acyl-4-(1-adamantyl)-3-thiosemicarbazides (**103**). Cyclization of compounds was achieved by the action of sulphuric acid at room temperature to yield the corresponding 2-(1-adamantylamino)-5-substituted-1, 3, 4-thiadiazole derivatives (**104**)⁶⁸.

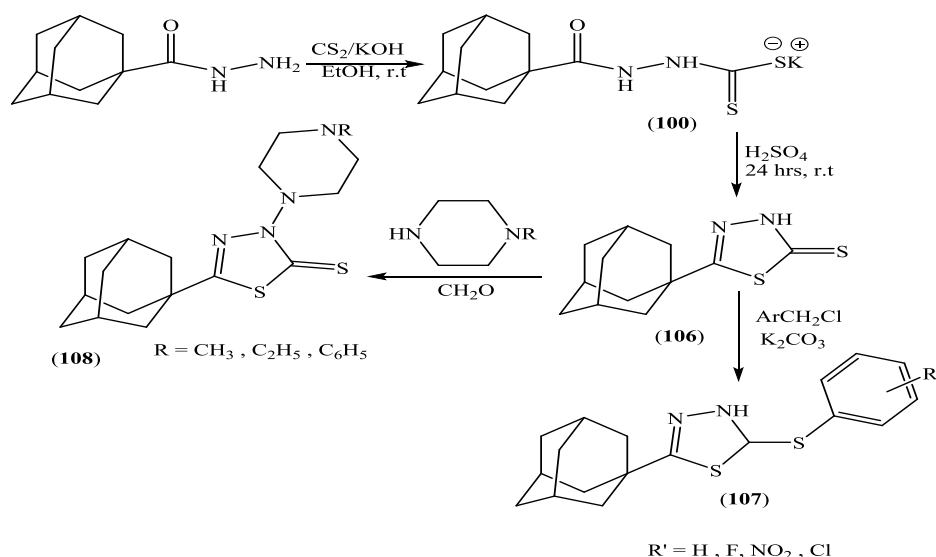


A series of 3,6-disubstituted [1,2,4] triazolo[3,4-*b*] [1,3,4] thiadiazoles (**105**)⁶⁹ bearing an adamantyl moiety were synthesized by condensation of 4-amino-5-aryl-2*H*-1,2,4-triazole-3(4*H*)-thiones with adamantyl-1-carboxylic acid in the presence of POCl₃.

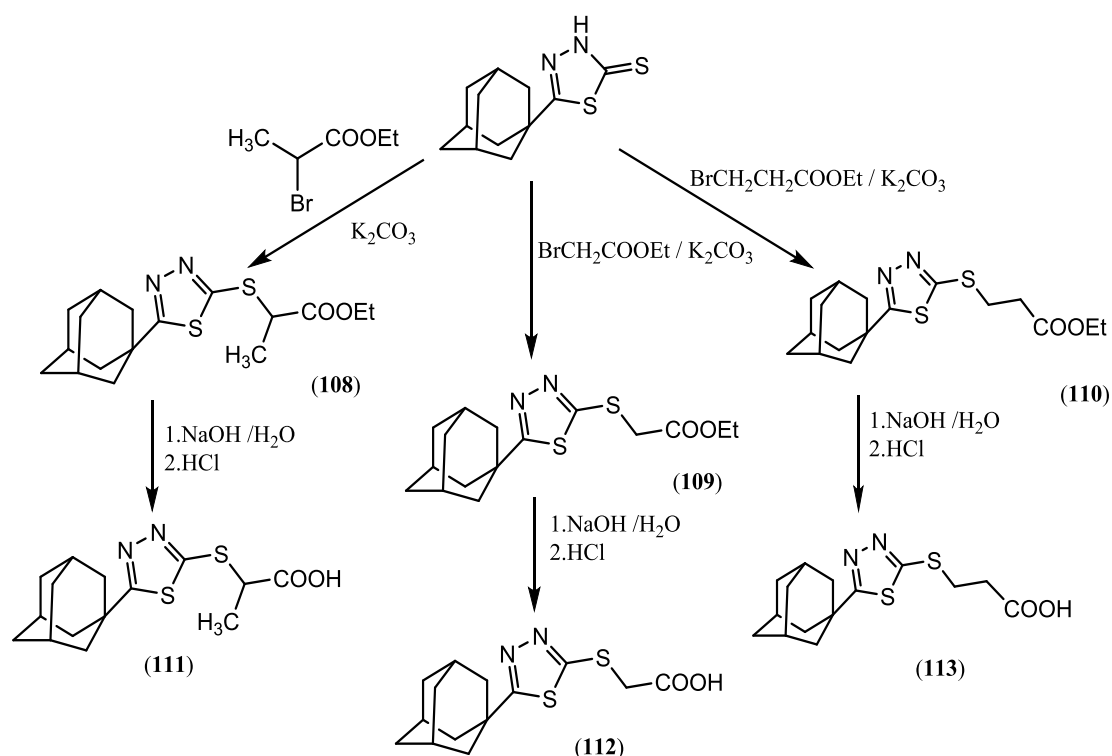


R = 2-CH₃, 3-CH₃, 4-CH₃, 2-F, 3-F, 4-F, 2-Cl, 3-Cl, 4-Cl, 2-Br, 3-Br, 4-Br

5-(1-Adamantyl)-1, 3, 4-thiadiazoline-2-thione was prepared starting from adamantane-1-carboxylic acid hydrazide via treatment with potassium hydroxide and carbon disulphide to afford potassium N'-(1-adamantylcarbonyl) dithiocarbazate (**100**) in almost quantitative yield. Dehydrated cyclization of N'-(1-adamantylcarbonyl) dithiocarbazate using sulphuric acid at room temperature yielded the target 5-(1-Adamantyl)-1, 3, 4-thiadiazoline-2-thione (**106**), which was reacted with benzyl- or 4-substituted benzyl chlorides to yield the corresponding 5-(1-adamantyl)-3-(benzyl- or 4-substituted benzyl)-1, 3, 4-thiadiazoline-2-thiones (**107**). On the other hand, the reaction of 5-(1-Adamantyl)-1, 3, 4-thiadiazoline-2-thione with 1-methyl-, ethyl- or phenyl piperazine and formaldehyde solution in ethanol at room temperature yielded the corresponding 5-(1-adamantyl)-3-(4-substituted-1-piperazinylmethyl)-1,3,4-thiadiazoline-2-thiones (**108**)⁷⁰.



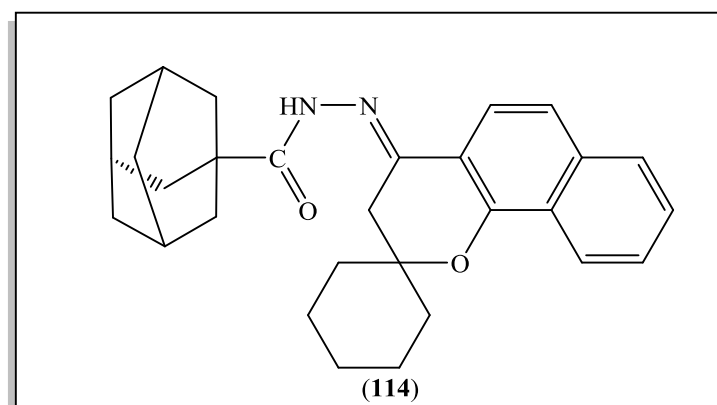
The reaction of 5-(1-Adamantyl)-1,3,4-thiadiazoline-2-thione with ethyl bromoacetate, \pm -ethyl 2-bromopropionate or ethyl 3-bromopropionate, in ethanol, in the presence of anhydrous potassium carbonate yielded the corresponding ethyl esters derivatives (108-110), which were consequently hydrolyzed by heating in 10% aqueous sodium hydroxide solution to afford the corresponding carboxylic acids derivatives (111-113)⁷⁰.



Biological activities

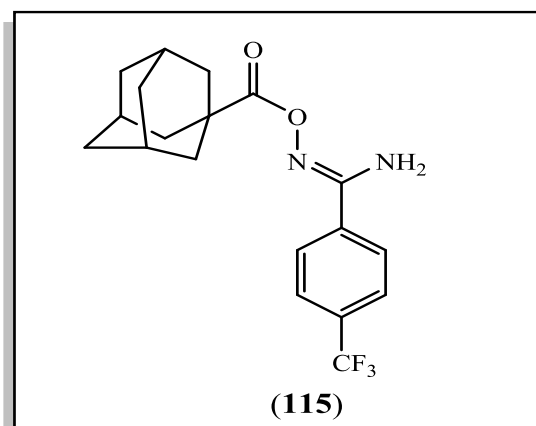
I-Anticancer activities: -

A novel series of N'-(Spiro [benzo[h]chromene-2, 1'-cyclohexan]-4(3H)-ylidene) adamantane-1-carbohydrazide (**114**)⁷¹ was designed, synthesized and evaluated as potential anticancer agents against MCF-7 (human breast carcinoma), HT-29 (human colorectal adenocarcinoma) and A549 (human lung carcinoma) cell lines using MTT assay. It was showed a better anticancer activity than that of sorafenib, the multi-kinase inhibitor with IC₅₀ values 1.78 μ M or erlotinib with IC₅₀ values over 20 μ M. it was selected for further mechanistic investigation via EGFR, B-RAF and tubulin polymerization assays. N'-(Spiro [benzo[h]chromene-2, 1'-cyclohexan]-4(3H)-ylidene) adamantane-1-carbohydrazide was the most potent EGFR inhibitor (IC₅₀ = 1.2 μ M), yet it was displayed moderate tubulin polymerization inhibition effects.

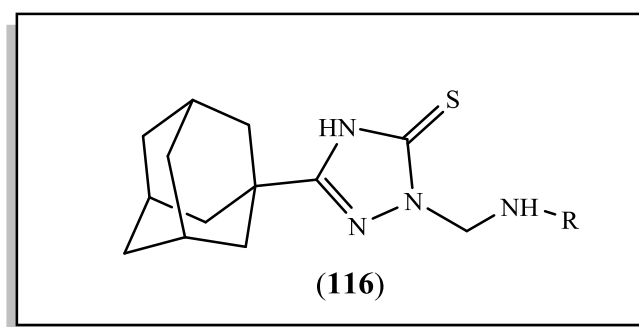


Analysis, and subjected to cytotoxic studies in non-tumoral Vero cells and antiproliferative activity tests in six malignant cell lines. A novel adamantyl O-acylamidoximes presented a concentration-dependent profile for chronic myeloid leukemia (K562) and acute promyelocytic leukemia (HL-60) cell. In addition, (Z)-N'((-adamantane-1-carbonyl) oxy)-4-(trifluoromethyl) benzimidamide (**115**) exhibited the best *in vitro*

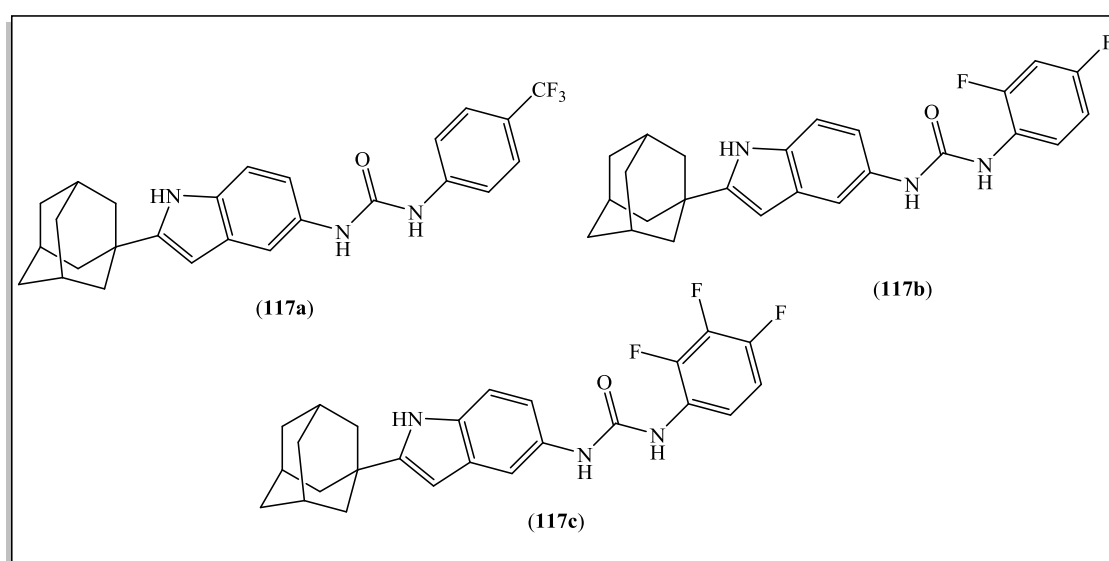
antiproliferative activity against chronic myeloid leukemia (K562) cells (IC_{50} (μM) =19.5).and lower cytotoxicity for Vero cell ⁵⁶.



A series of novel N-Mannich bases derived from 5-adamantyl-1, 2, 4-triazole-3-thiones (**116**)⁷² was synthesized and characterized using NMR spectroscopy and x-ray diffraction technique. All derivatives were evaluated for their anticancer potential against four human cancer cell lines. Several tested compounds exerted good cytotoxic activities on K562 and HL-60 cell lines, along with pronounced selectivity, showing lower cytotoxicity against normal fibroblasts MRC-5 compared to cancer cells. The effects of compounds [R = 2-MeC₆H₄, 2-FC₆H₄, 2-ClC₆H₄] on the cell cycle were investigated by flow cytometric analysis. It's causes the accumulation of cells in the subG1 and G1 phases of the cell cycle and induce caspase-dependent apoptosis, while the antiangiogenic effects of compounds [R = 2-MeC₆H₄, 2-FC₆H₄, 2-ClC₆H₄] have been confirmed in EA. hy926 cells using a tube formation assay. Further, the interaction of Bax protein with compound [R = 2-MeC₆H₄] was investigated by means of mol. modeling, applying the combined mol. docking/mol. dynamics approach.

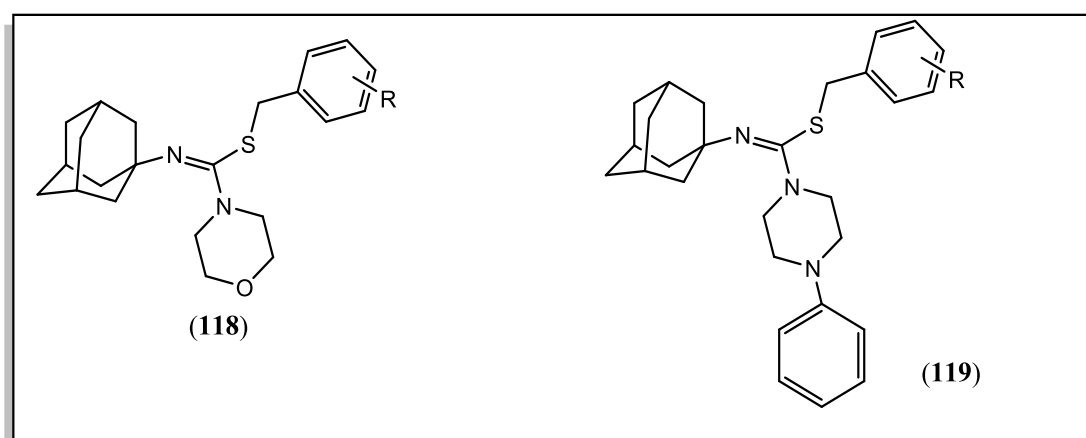


Two new series of 1-(2-(adamantan-1-yl)-1H-indol-5-yl) - 3-substituted urea derivatives (**117a-c**)⁷³ as potential anticancer candidates could modulate the expression and activity of Nur77. The synthesized compounds were initially evaluated for their anti-proliferative activity against H460 lung cancer cells, HepG2 liver cancer cells, and MCF-7 breast cancer cells. Major compounds were found to be active against these tested cancer cell lines. The compounds with IC₅₀ values down to 20 mM exhibited selective cytotoxicity effects on the human lung cancer cell line (H460) and the normal lung cell line (MCR-5). Three compounds were induced Nur77-expression in a time and dose-dependent manner in H460 cells.



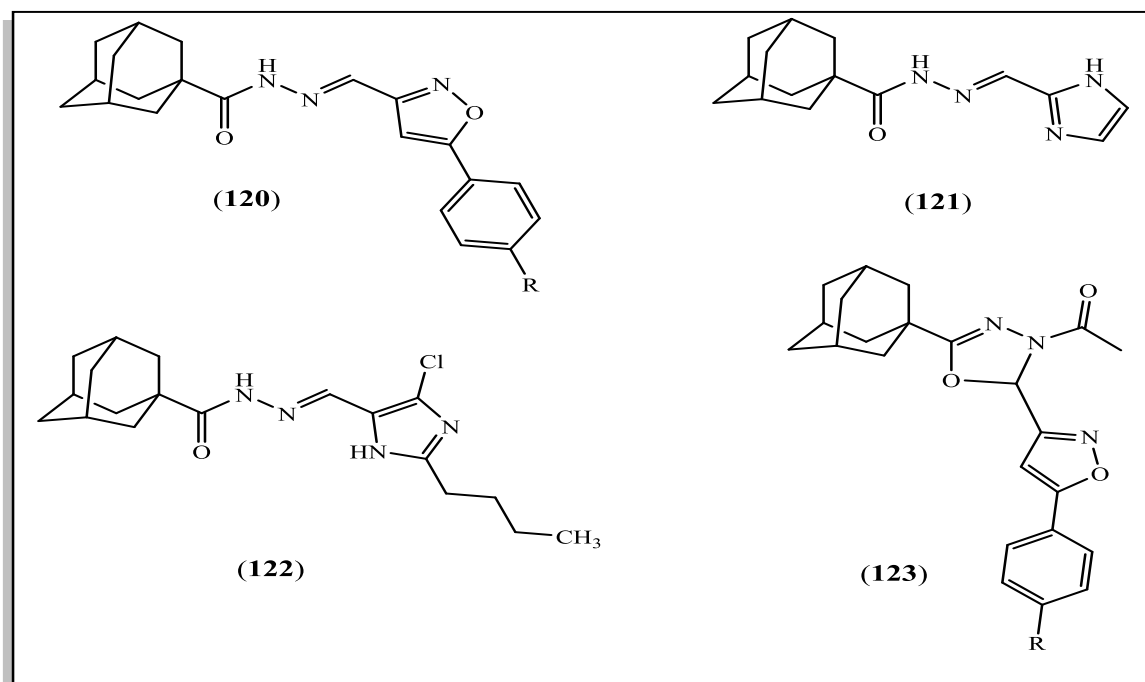
II-Antimicrobial activities: -

4-arylmethyl (Z)-N'-(adamantan-1-yl)-morpholine-4-carbothioimides (**118**) and 4-arylmethyl (Z)-N'-(adamantan-1-yl)-4-phenylpiperazine-1-carbothioimides (**119**)⁵⁷ were displayed potent broad-spectrum antibacterial activity, especially against the tested Gram-positive bacteria. The in vivo oral hypoglycemic activity of the new compounds was carried on streptozotocin (STZ)-induced diabetic rats. Benzyl (Z)-N'-(adamantan-1-yl)-morpholine-4-carbothioimide, Benzyl (Z)-N'-(adamantan-1-yl)-4-phenyl piperazine-1-carbothioimide and 4-Chlorobenzyl (Z)-N'-(adamantan-1-yl)-4-phenyl piperazine-1-carbothioimide were produced potent dose-independent reduction of serum glucose levels, compared to the potent hypoglycemic drug gliclazide.



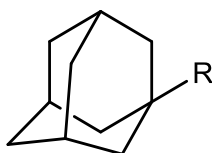
N'-Heteroarylidene-1-adamantylcarbohydrazides (**120**) and 2-(1-Adamantyl)-4-acetyl-5-[5-(4-substituted phenyl-3-isoxazolyl)]-1,3,4-oxadiazolines(**121**)⁷⁴ were tested for in vitro activities against a panel of Gram-positive and Gram-negative bacteria and the yeast-like pathogenic fungus *Candida albicans*. N'-[(1H-Imidazol-2-yl) methylidene] adamantane-1-carbohydrazide (**122**) and N'-[(2-Butyl-4-chloro-1H-imidazol-5-yl) methylidene] adamantane-1-carbohydrazide (**123**) displayed potent broad-spectrum antimicrobial activity, while compounds

N'-Heteroarylidene-1-adamantyl carbohydrazides showed good activity against the Gram-positive bacteria.

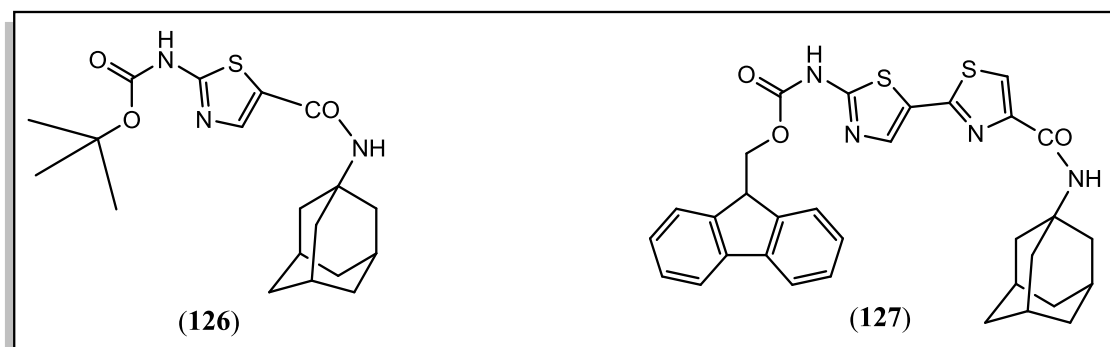


III-Antiviral activities: -

Amantadine (**124**) and rimantadine (**125**)⁷⁵ is an antiviral agent that specifically inhibits influenza A virus replication at a micromolar concentration. This drug is also very effective in the treatment of human Parkinson's disease. Other important clinical applications of this agent have been studied recently, ranging from viral infections, e.g. herpes, herpes zoster neuralgia to granulomatosis and from neuroleptic extrapyramidal movement disease to depression and cocaine dependence and The release of virions from animals cells infected with foot and mouth disease virus (FMDV) was inhibited by amantadine, a viroporin inhibitor⁷⁶. Biological and pharmacological activities of amantadine presented in this paper are focused on the explanation of the mechanism of amantadine antiviral and antiparkinsonian effects and on general use of this agent in medicine .

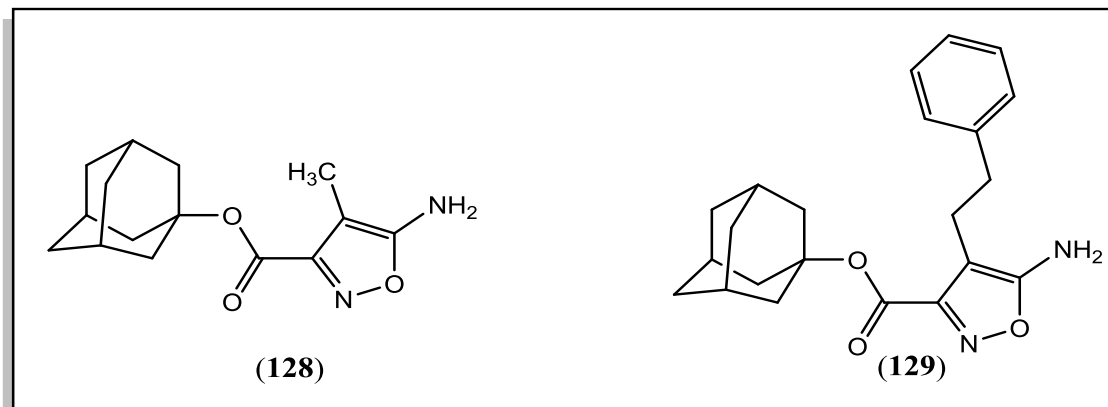
Amantadine (**124**) and rimantadine (**125**) structures

Design and synthesis of series of adamantane derivatives (**126**&**127**) containing modified peptides with thiazol moiety ⁶³. New compounds were synthesized in solution using TBTU (2-(1H-Benzotriazole-1-yl)-1,1,3,3-tetramethylaminium tetrafluoroborate) as coupling agent. All derivatives were obtained with good yields. The antiviral activity of newly synthesized compounds against influenza virus H₁N₁ is studied. Cytotoxicity assay for determination of CC₅₀ were done and IC₅₀ values were calculated. The rimantadine analogue with thiazole ring Gly-Thz-rimantadine showed good activity against influenza virus A/Hongkong/68 with IC₅₀ = 0.11 µg/mL and CC₅₀ = 50 µg/mL.

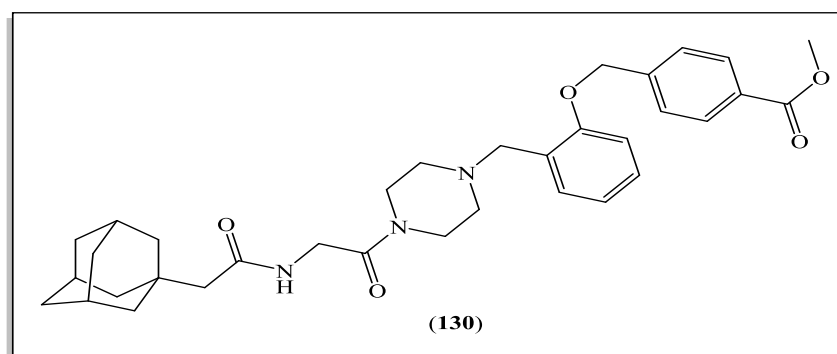


In the present work a large series of novel polyfunctionalized isoxazole derivatives bearing substituents with various steric and electronic effects was obtained by our unique versatile synthetic procedure and their antiviral activity against tick-borne encephalitis, Omsk hemorrhagic fever, and Powassan viruses was studied in vitro. The investigation led to the discovery of two potent and synthetically accessible 5-aminoisoxazole

derivatives containing adamantyl moiety (**128**&**129**), one of them possessing an attractive therapeutic index ⁷⁷.



Previous studies identified an adamantane dipeptide piperazine that inhibits Ebola virus (EBOV) infection by targeting the essential receptor Niemann–Pick C1 (NPC1). The physicochemical properties of an adamantane dipeptide piperazine (**130**) limit its potential for testing in vivo. Optimization by improving potency, reducing hydrophobicity, and replacing labile moieties identified adamantane dipeptide piperazine derivatives with improved in vitro properties that are also highly active against EBOV infection, including when tested in the presence of 50% normal human serum (NHS) ^{78,79}.



DISCUSSION



**SYNTHESIS OF ADAMANTANE PYRAZOLE AND
HYDRAZONE DERIVATIVES AS CARBONIC
ANHYDRASE INHIBITORS**



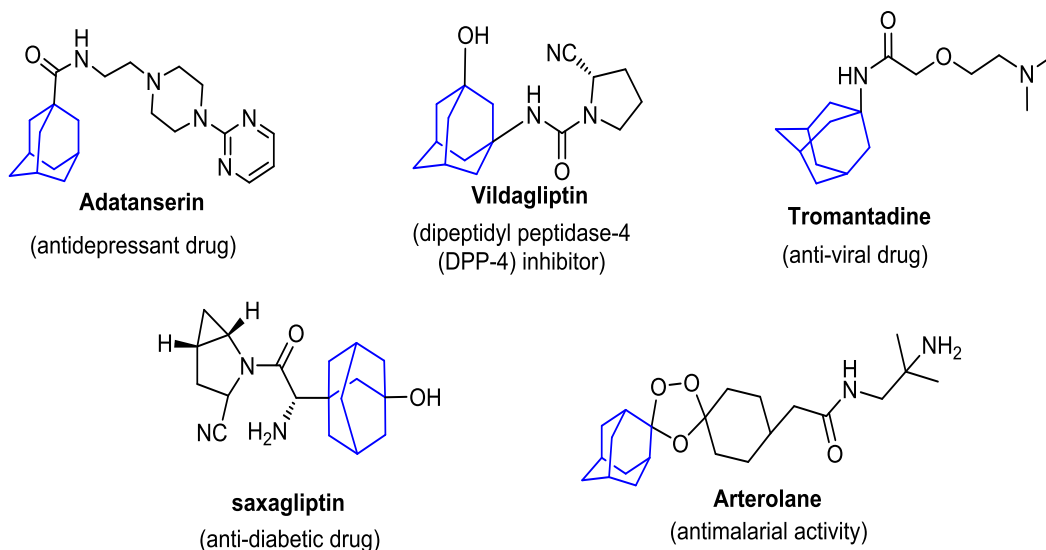
Part I: Novel adamantane-pyrazole and hydrazone hybridized: design, synthesis, characterization, cytotoxic evaluation, SAR study and molecular docking simulation as carbonic anhydrase inhibitors

One of the most significant diseases responsible for worldwide deaths, cancer is a general term used to describe the uncontrolled proliferation of cells resulting from disruptions or dysfunctions of the regulatory signaling pathway.⁸⁰ In other words, cancer is a complex disease caused by genetic and/or epigenetic changes in one cell or a group of cells.⁸¹ At present, it is the major public concerned hotspot across the globe.⁸² Deaths owing to cancer are predicted to continue increasing by 3 million deaths in 2030.⁸³ lung, breast, colon, and melanoma cancers are the most recorded types in developing and underdeveloped countries.⁸⁴

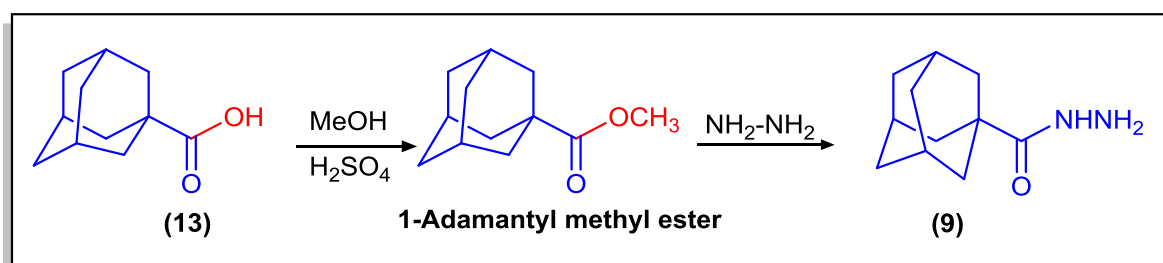
Carbonic anhydrases (CAs) are the most famous enzymes which undergo a physiological reaction that hydrate CO₂ reversibly into a proton and HCO₃.⁸⁵⁻⁸⁸ The human carbonic anhydrase (hCA) is consists of fifteen different isoforms; differ in sequences, mainly for expression tissue, localization and catalytic activity.^{89, 90}

Adamantyl moiety hybrid with several molecules to enhance the biological availability of the designed compounds, and an example of that is **Adapalene** that used as acne vulgaris therapy that containing adamantane in the main skeleton as well as naphthalene derivatives that relatively high lipophilicity⁹¹ (**Fig. 1**). Adamantane nucleus present in many drugs as Vildagliptin (dipeptidyl peptidase-4 (DPP-4) inhibitor),⁹² Adatanserin (antidepressant)⁹³ and Saxagliptin (hypoglycemic drug),⁹⁴ Arterolane (antimalarial activity)⁹⁵ (**Fig. 1**). Furthermore, pyrazoles are an important class of heterocyclic compounds that promising scaffolds in medicinal chemistry.⁹⁶⁻⁹⁸ (**Fig. 1**).

This part of the thesis aimed at the synthesise of a novel pyrazole and hydrazone derivatives bearing adamantane bioactive core as a promising heterocyclic scaffold and screened for anticancer activity and tested the most promising to carbonic anhydrase and therefore the molecular docking simulation and some drug-likeness parameter were evaluated to find potential candidates.

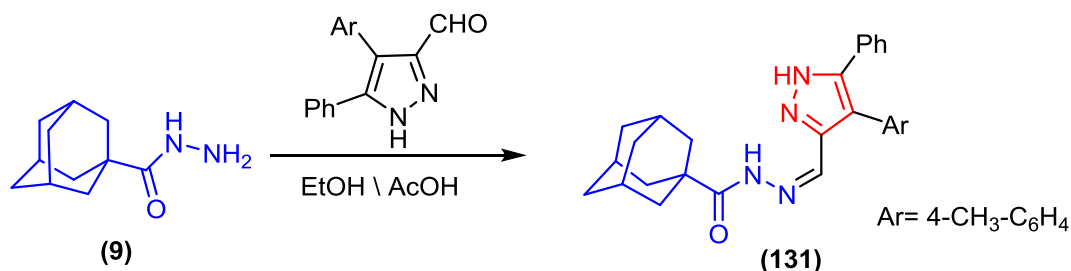


Adamantan-1-carbohyrazide (**9**) that used as key starting material was prepared according to the reported method.⁵¹



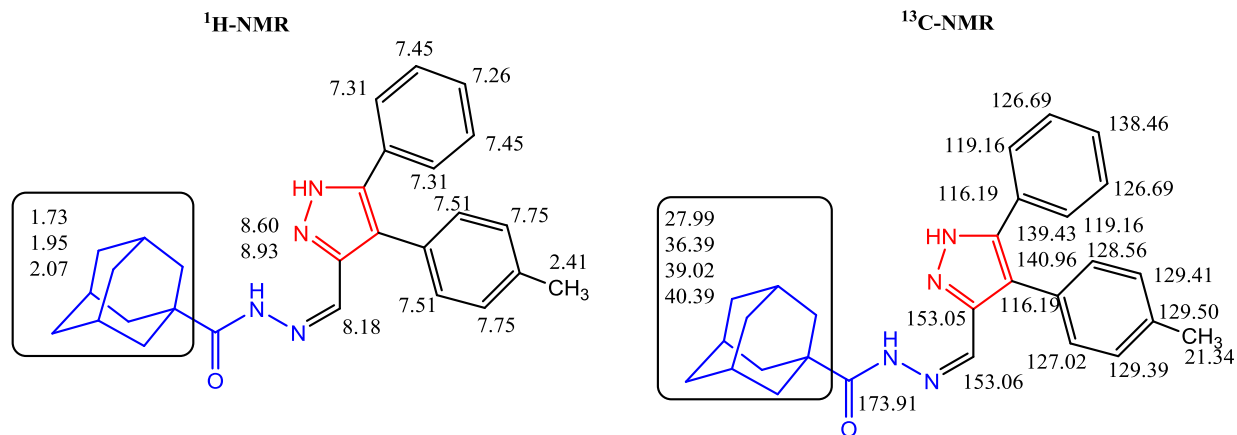
Adamantan-1-carbohyrazide (**9**) was subjected for different reagents for obtaining many pyrazole containing adamantyl moiety with different substituents.

Thus, condensation of the hydrazone derivative (**9**) with 5-phenyl-4-(*p*-tolyl)-1*H*-pyrazole-3-carbaldehyde⁹⁹ afforded the corresponding hydrazone derivative (**131**).

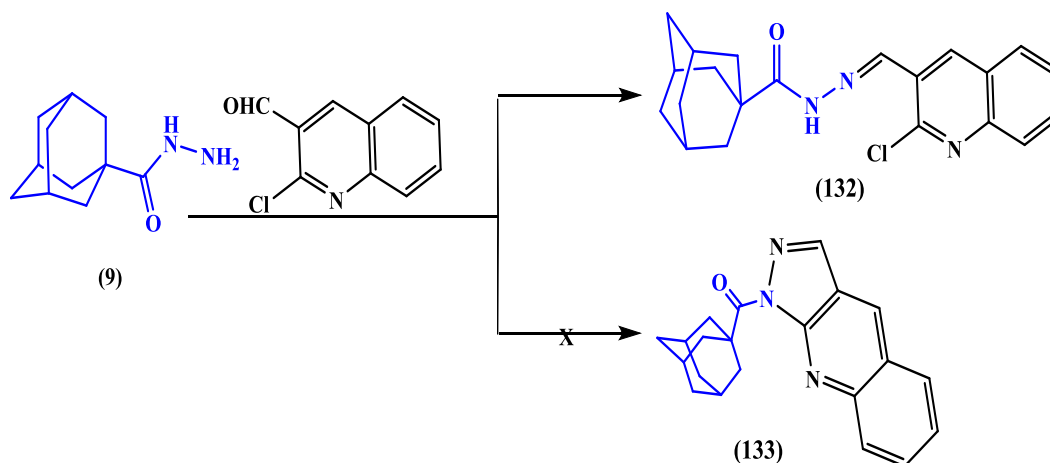


The structure of compound **(131)** was assigned on the basis of IR, ¹HNMR, ¹³C NMR, and mass spectral data. The IR spectra of these compounds showed common characteristic absorption peaks at 3240, 2904, 2850 and 1647 corresponding for NH, CH-aliphatic and C=O respectively. The ¹H-NMR spectra are characterized by the presence of the adamantyl protons (15H) as a doublet or two singlet at δ 1.73 ppm (6H) and two singlets at d 1.97-2.07 ppm for the other nine adamantane protons and two singlets at 2.41 and 8.18 for CH₃ and methine protons respectively. The two NH protons appeared as two singlets at 8.60, 8.93. The ¹³C NMR spectra are characterized by the presence of CH₃ at 21.34 and the adamantyl carbons as four peaks at d 27.99, 36.39, 39.02 and 40.39 ppm. The two ethylenic carbons at 139.43 and 140.96 and two signals at 153.06 and 173.91 corresponding for C=N and C=O respectively. In addition to the aromatic carbons, the detailed are given in the experimental part. Its Mass spectrum showed a molecular ion peak at m/z= 438 with a base peak at m/z=199.

The ¹HNMR and ¹³C-NMR data of compound **(131)** are shown in this figure.

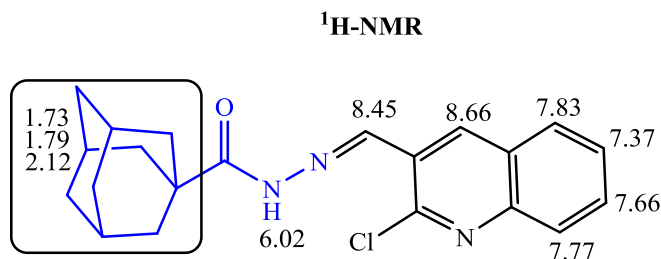


In the same way, interaction of compound (**9**) with 2-chloro-3-formylquinoline¹⁰⁰ for obtaining the pyrazoloquinoline derivative (**133**) but instead of hydrazone derivative (**132**) was obtained.

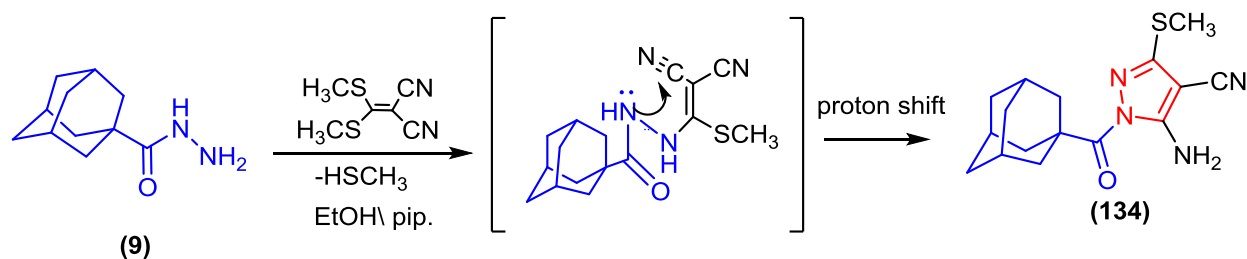


The structure of compound **132** was confirmed on the basis of IR, ¹H NMR. Its IR spectrum of these showed common characteristic absorption peaks at 3261, 1663 for NH and C=O cm⁻¹. The ¹H NMR spectra are characterized by the presence of the 15 adamantyl protons as three singls at 1.73, 1.79 and 2.12 ppm. The NH as singlet at δ 6.02. two singlet signals were showed at 8.45 and 8.66 for the methylenic and quinoline-H4. In addition to the aromatic protons which appeared as two triplets and two doublets at 7.37, 7.66, 7.77 and 7.83.

The ^1H NMR data of compound (**132**) are shown in this figure.



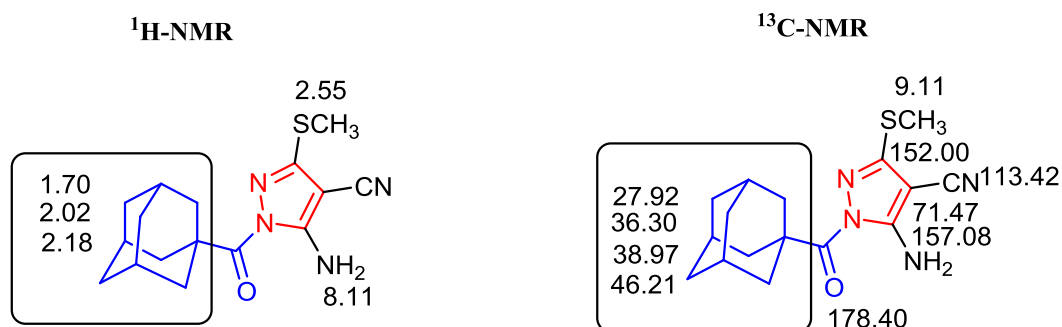
The reaction of adamantane-1-carbohydrazide (**9**) with bis(thiomethyl)methylene malononitrile afforded 2-amino pyrazole derivative (**134**). The reaction proceeds via an addition, elimination mechanism where the amino group of hydrazide derivatives act as nucleophilic that attack the β -carbon of ethylene nitrile derivative followed by elimination of methanethiol (CH_3SH), followed by cyclization (that involve addition and as well as proton shift) to afford the pyrazole enaminonitriles derivatives (**134**).



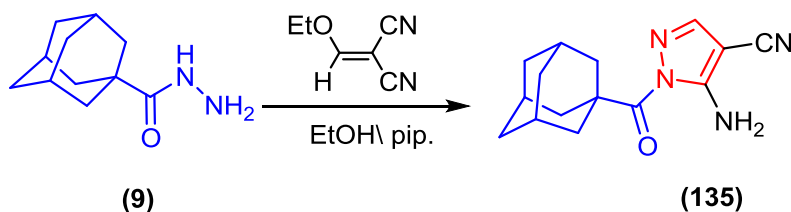
IR spectrum of compound (**134**) showed absorption bands at 3404, 3304 for amino groups besides 2911, 2849, 2215 and 1693 cm^{-1} corresponding to adamantane CH, CN, and carbonyl group respectively. Its ^1H NMR spectrum showed a significant three peaks at δ 1.63-1.70, 2.02 and 2.18 ppm related to protons of adamantyl protons that appear as multiplet and two singlet signals. Furthermore, two-singlet signals

were appearing at δ 2.55 and 8.11 ppm for thiomethyl and the amino group, respectively.

The ^1H NMR and ^{13}C -NMR data of compound (**134**) are shown in this figure.



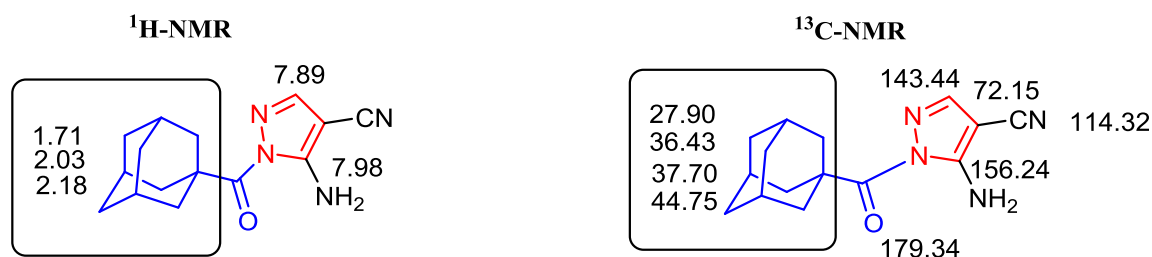
Similarly, interaction of the hydrazide derivative (**9**) with ethoxy methylene malononitrile afforded the corresponding enamionitrile pyrazole derivative (**135**).



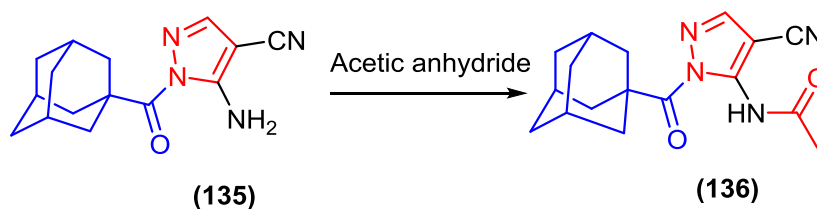
The structures of compound (**135**) was established confirmed on the basis of IR, ^1H NMR, ^{13}C NMR, and mass spectral data. The IR spectrum of these compounds showed common characteristic absorption peaks at 3416, 3229 cm^{-1} corresponding for NH_2 , 2222 for nitrile group and at 1702 for C=O . The ^1H NMR spectra are characterized by the presence of the 15 adamantyl protons as three singlets 1.71, 2.03 and 2.18. in addition to CH-pyrazole as a singlet signal at 7.89 and a single at 7.98 due to NH_2 group, the ^{13}C NMR spectra showed the adamantyl carbons at δ 27.90,

36.43, 37.70, 44.75 (Adamant. Cs), and signals at 114.32, 179.34 attributed to nitrile and carbonyl group respectively.

The ^1H -NMR and ^{13}C -NMR data of compound (**135**) are shown in this figure.

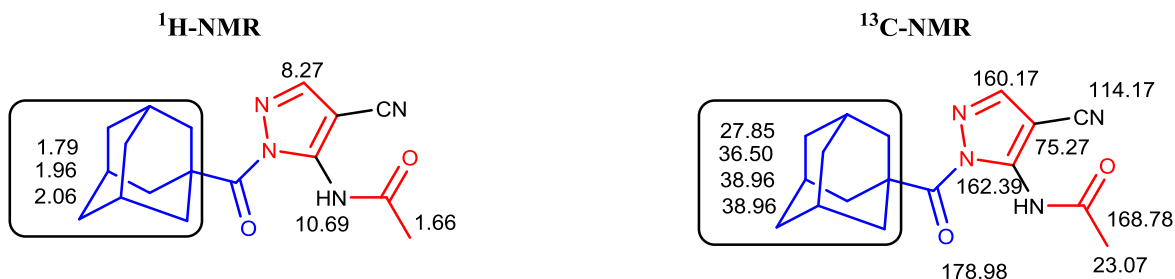


Enaminonitrile derivative (**135**) underwent acetylation when heated with acetic anhydride for one hour under reflux condition to obtain acetamide pyrazole derivative containing adamantane moiety (**136**).

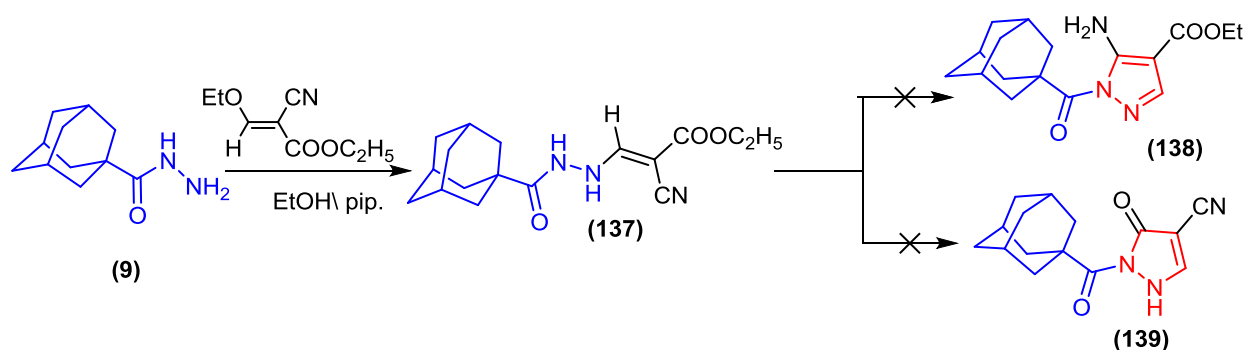


Its IR spectrum showed the presence of nitrile group as absorption peak at 2230 cm^{-1} , and Its ^1H NMR spectrum proved the presence of methyl group as a singlet signal at 1.96. while, its ^{13}C NMR showed the presence of methyl group at 23.07 and nitrile group at 114.17 in addition to two carbonyl groups at 168.78 and 178.98. Its mass spectrum showed a molecular ion peak at m/z 312 corresponding for molecular formula $\text{C}_{17}\text{H}_{20}\text{N}_4\text{O}_2$.

The ^1H -NMR and ^{13}C -NMR data of compound (**136**) are shown in this figure

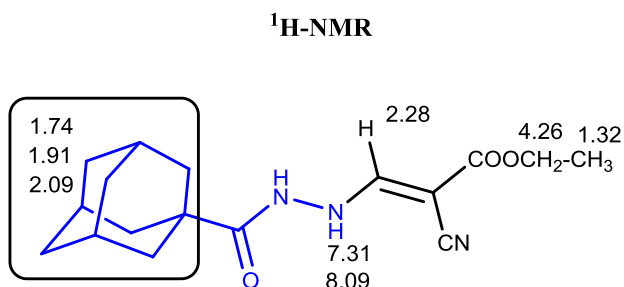


On the other hand, the reaction of hydrazide derivative (**9**) with ethyl ethoxy methylene cyanoacetate not demonstrate pyrazole derivatives as previous compounds (**134**) but the reaction stop at the addition elimination step. and not underwent cyclization to afford the pyrazole derivatives (**138**) or (**139**).

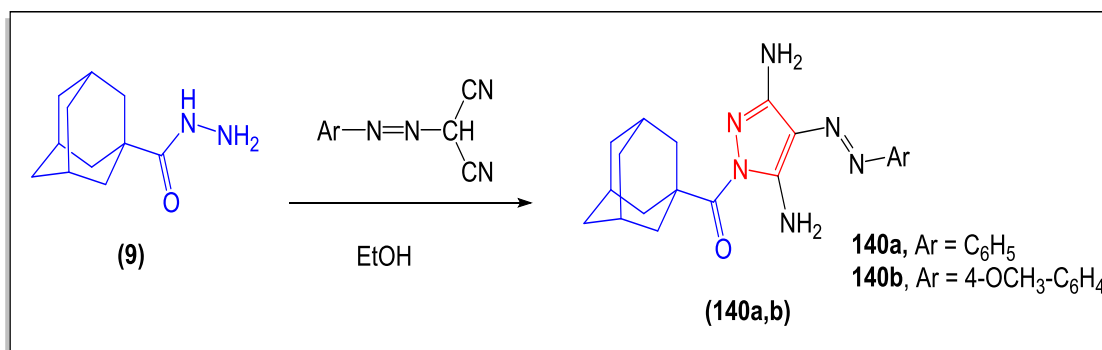


The structure of compound (**137**) was proved on the basis of IR and ¹HNMR spectra. Its IR spectrum showed absorption bands at 3246, 2213, 1710 and 1671 cm^{-1} corresponding to NH, CN and carbonyl group which cancelled structures (**138**) and (**139**). While, ¹H NMR spectrum observed triplet and quartet signals at δ 1.34 and 4.26 with coupling constant ($J = 6.7$ Hz) besides, three singlet signals at δ 2.28, 7.31 and 8.09 ppm for CH-vinylic and 2NH that added three signals at δ 1.74-1.77, 1.91 and 2.09 ppm belonged to adamantane protons.

The ^1H -NMR data of compound (**137**) are shown in this figure



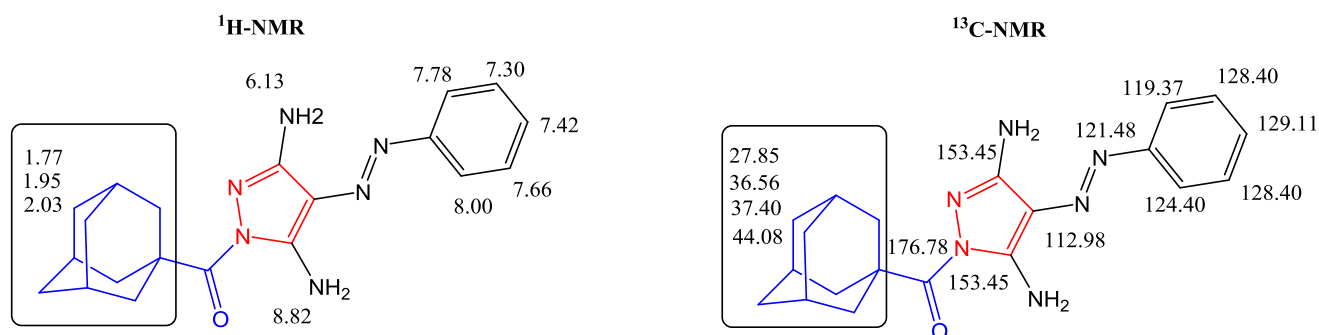
Pyrazole derivatives (**140a, b**) having an azo moiety were synthesized by the reaction of hydrazide derivatives (**9**) with aryl azomalononitrile in ethanol and produced the corresponding pyrazole (**140a, b**).



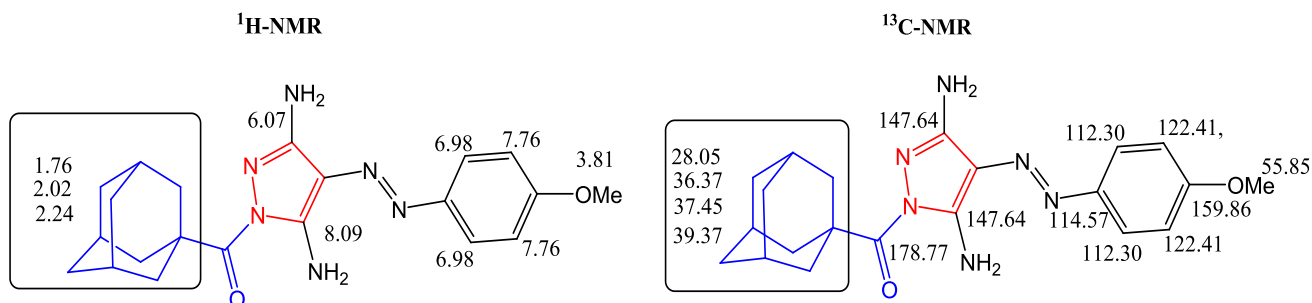
The structure of compounds **140a, b** pyrazole derivatives was confirmed with the help of analytical and spectroscopic data. Thus, the IR spectrum of **140a** exhibited stretching significance absorption bands at 3543, 3480, 3332 and 3281 cm^{-1} for two amino groups and 1663 cm^{-1} for carbonyl group. Its ^1H NMR spectrum of compound **140a** revealed three singlet signals between δ 1.77-2.03 ppm for adamantyl protons, two singlet signals at δ 6.13, 8.82 ppm for two amino groups as well as five aromatic protons between δ 7.27-8.00 ppm. ^{13}C NMR spectrum of **140b** exhibited signals for adamantane ranged between δ 28.05 to 39.37 ppm, in addition to two singlet signals at δ 55.85 and δ 178.77 related to methoxy and carbonyl groups respectively.

Moreover, signals for carbon attached to methoxy and amino groups at δ 159.86 and δ 147.64 as well as aromatic signals between δ 112.30-122.41 ppm.

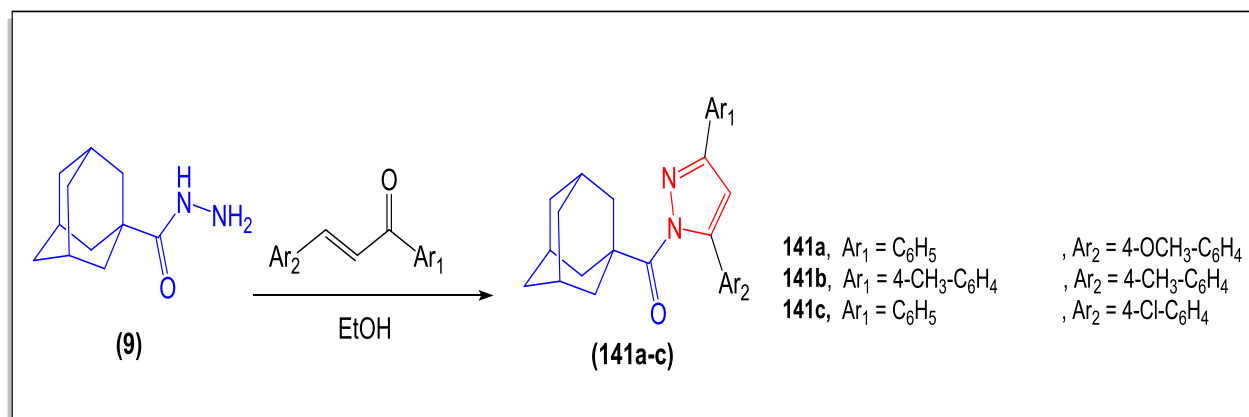
The ^1H -NMR and ^{13}C -NMR data of compound (**140a**) are shown in this figure



The ^1H -NMR and ^{13}C -NMR data of compound (**140b**) are shown in this figure

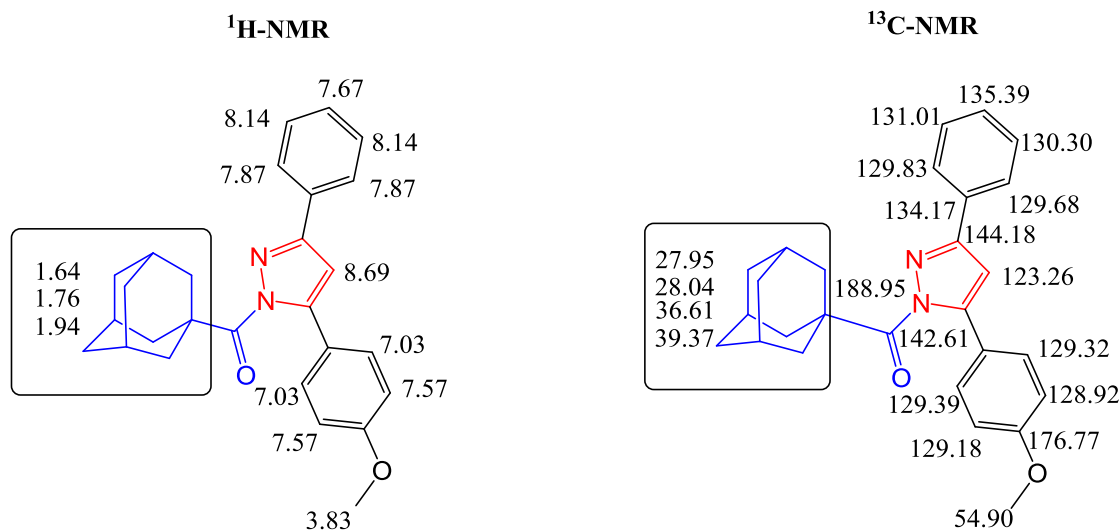


Pyrazole derivatives (**141**) containing two aryl groups at position three and five positions were obtained through the reaction of adamantane-1-carbohydrazide with α , β -unsaturated carbonyl derivatives (chalcones).

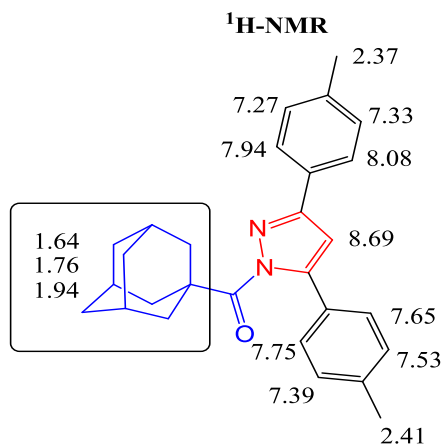


The postulated structures of the newly designed pyrazole derivatives were confirmed on the basis of elemental analysis and spectral data. IR spectrum of compound **141a** showed stretching characteristic bands at 1655 cm⁻¹ for carbonyl group. ¹H-NMR spectrum of compound **141c** demonstrated singlet signal at δ 8.70 ppm for CH-pyrazole proton as well as adamantane and aromatic protons. ¹³C-NMR spectrum of **141c** exhibited signals for adamantane in region δ 25.77-36.60 ppm, aromatic carbon between δ 114.84-143.73 ppm and three singlet signals at δ 144.08, 176.79, 188.91 ppm for C=C, C=N and carbonyl groups respectively.

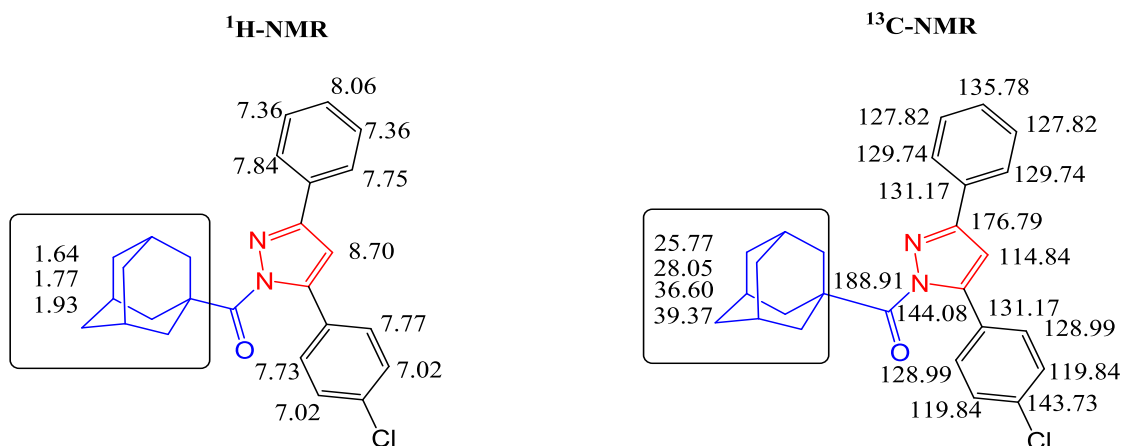
The ¹H-NMR and ¹³C-NMR data of compound (**141a**) are shown in this figure



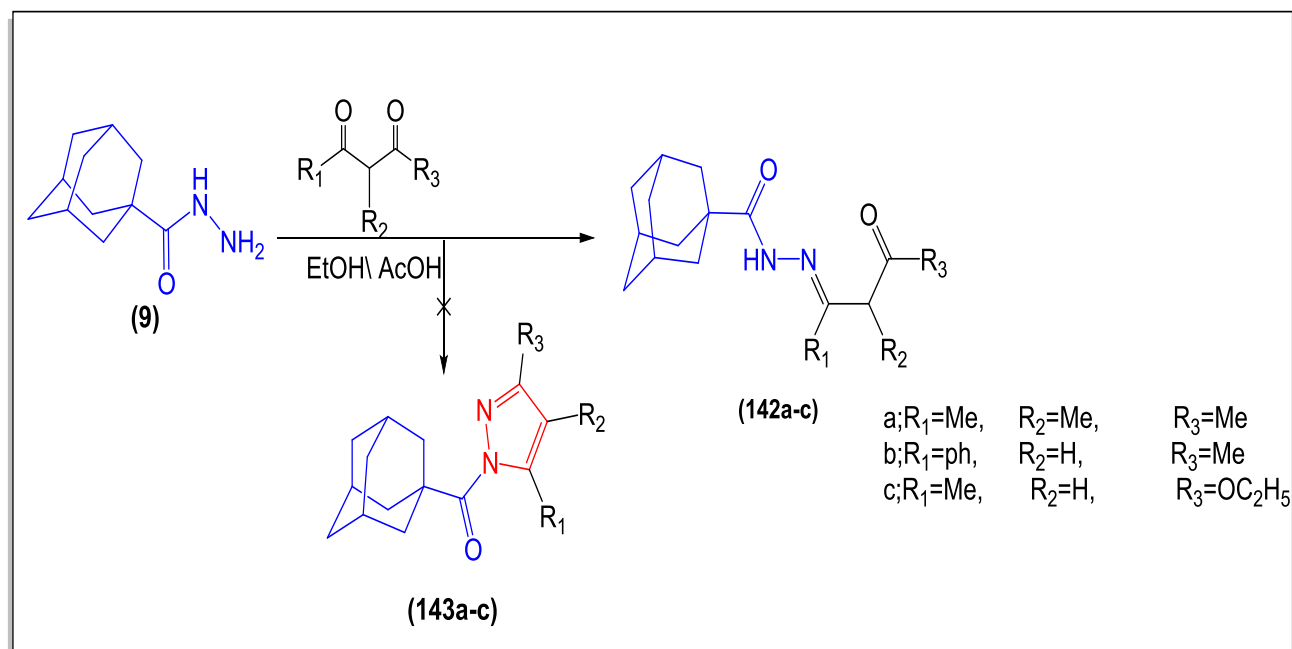
The ^1H -NMR data of compound (**141b**) are shown in this figure



The ^1H -NMR and ^{13}C -NMR data of compound (**141c**) are shown in this figure

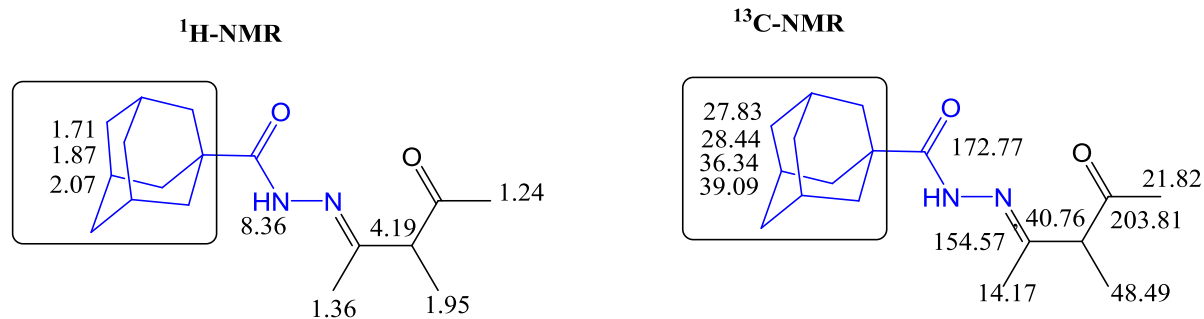


In the same way, the reactivity of hydrazide derivative **9** toward some electrophiles were checked as 1,3-dicarbonyl derivatives don't undergo cyclization and produce acyclic hydrazone derivatives **142a-c**.

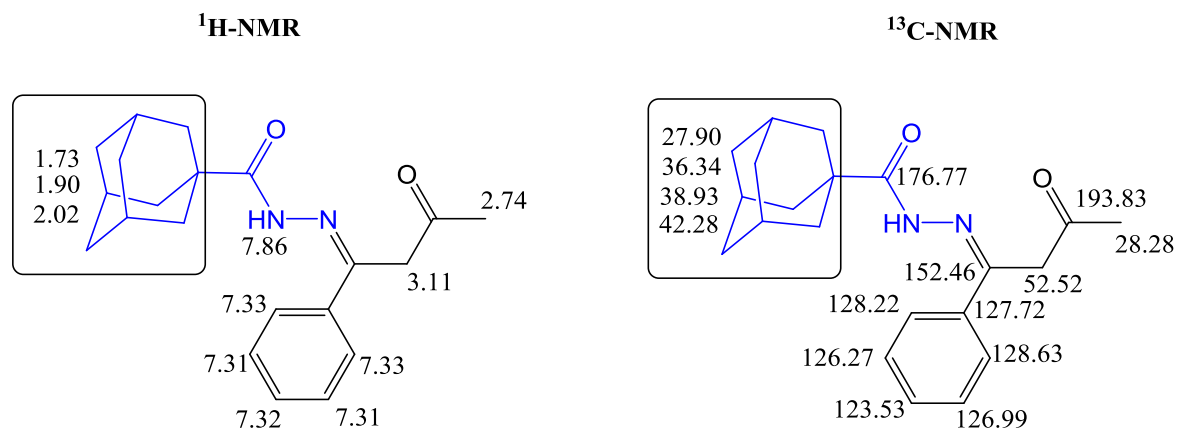


The structure of the obtained products was established on the basis of elemental analysis and spectral data. IR spectrum of compound **142c** revealed stretching signals for NH and two carbonyl groups at 3236, 1678 and 1728 cm^{-1} . ^1H NMR spectrum of the same compound **142c** distinguished triplet and quartet signals, at δ 1.25, 3.70 ppm for ethyl group in addition to, five singlet signals at δ 1.72, 1.90, 1.91, 2.06 and 8.62 ppm related to adamantane protons, methyl and NH proton. ^{13}C NMR spectrum of **142c** displayed signals for adamantane ranged between δ 27.66 to 40.05 ppm. Besides, three singlet signals two of them for the ethoxy group at δ 14.12, 61.53 ppm and the third signal at δ 58.45 ppm for methylene group as well as, three signals at δ 147.17, 165.03 and 173.47 for C=N and two carbonyl groups.

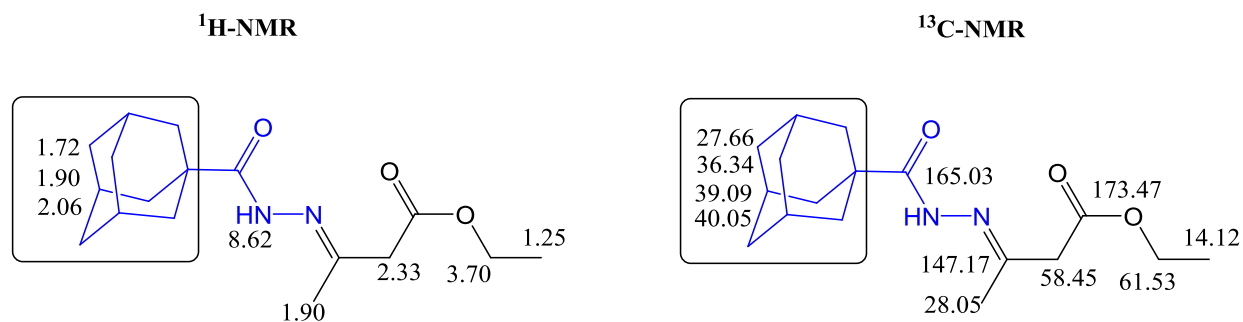
The ^1H -NMR and ^{13}C -NMR data of compound (**142a**) are shown in this figure



The $^1\text{H-NMR}$ and $^{13}\text{C-NMR}$ data of compound **(142b)** are shown in this figure



The $^1\text{H-NMR}$ and $^{13}\text{C-NMR}$ data of compound **(142c)** are shown in this figure



1.1. Biological evaluation

2.2.1. Antiproliferative activity

The *in vitro* cytotoxic activity of the new fourteen compounds that containing adamantane as an important pharmacophore backbone on different three cell lines, namely human breast adenocarcinoma cell line (MCF-7), human hepatocellular carcinoma cell line (HepG-2), as well as human lung adenocarcinoma epithelial cells (A549), were evaluated by using sulforhodamine B (SRB) assay according to reported methods.¹¹⁹ Doxorubicin was used as a positive control and the obtained data represented in **table 1** as IC₅₀ values expressed in μM .

The newly designed compounds in scheme **1** and **2** observed two mainly products as pyrazole derivatives (**131,134, 135, 136, 140a-b** and **141a-c**) and hydrazone derivatives (**132** and **142a-c**) with only one hydrazine derivative compound **137** as well as the main bioactive core adamantane nucleus and most of the designed and synthesized derivatives exhibited moderate to good activity against the tested cancer cell lines. In general, the tested compounds exhibited more sensitive and selectivity to lung cancer cells (A549) with IC₅₀ values ranged between 1.55 ± 0.08 to $15.42 \pm 1.4 \mu\text{M}$, with eight compounds (**131,134, 135, 140a, 141c, 142a, 142b** and **142c**) having IC₅₀ less than or equal ten micromoles, except compound **141a** that showed IC₅₀ ($27.18 \pm 1.95 \mu\text{M}$) in comparison to doxorubicin (IC₅₀ = $2.58 \pm 0.03 \mu\text{M}$) rather than breast cancer (MCF-7) and liver cancer cells (Hep-G2). At the same time, the tested compounds revealed activity against Hep-G2 with IC₅₀ between (2.7 ± 0.15 to $38.12 \pm 2.3 \mu\text{M}$) with five compounds less than $\leq 10 \mu\text{M}$ and (MCF-7) displayed IC₅₀ between (4.68 ± 0.25 to $42.17 \pm 2.58 \mu\text{M}$) with only four compound $\leq 10 \mu\text{M}$ compared to doxorubicin for both cancer cells (11.46 ± 0.95 and $15.29 \pm 1.2 \mu\text{M}$)

respectively. From **table 1**, it's observed that four compounds (**131**, **140a**, **142a** and **142c**) exhibited promising and broad activity to all cell lines.

Table 1: IC₅₀ values expressed in (μM) of the newly designed compounds against three cell lines

Cpd. No.	IC ₅₀ %(μM) ± S.E*		
	MCF-7	HepG-2	A549
131	7.46 ± 0.54	5.11 ± 0.45	3.75 ± 0.26
132	24.19 ± 1.85	22.71 ± 1.74	14.5 ± 1.2
134	12.45 ± 0.97	9.31 ± 0.82	8.4 ± 0.75
135	15.54 ± 1.46	13.89 ± 1.2	10.57 ± 0.86
136	23.45 ± 1.75	18.21 ± 1.61	13.46 ± 1.08
137	35.13 ± 2.45	28.17 ± 1.9	15.42 ± 1.4
140a	4.68 ± 0.25	2.7 ± 0.15	1.55 ± 0.08
140b	13.77 ± 1.1	14.95 ± 1.25	11.5 ± 0.95
141a	42.17 ± 2.58	38.12 ± 2.3	27.18 ± 1.95
141b	17.32 ± 1.5	13.55 ± 1.1	11.73 ± 0.95
141c	15.29 ± 1.2	11.46 ± 0.95	8.52 ± 0.65
142a	8.35 ± 0.74	7.82 ± 0.64	4.39 ± 0.35
142b	20.64 ± 1.8	12.48 ± 1.1	10.78 ± 0.86
142C	11.28 ± 0.92	8.72 ± 0.74	5.06 ± 0.43
Dox.	8.19 ± 0.72	7.46 ± 0.12	3.58 ± 0.03

Each concentration was performed three times.

2.2.2. Structure activity relationship study

The activity of the synthesized compounds varies with respect to substitutions where the presence of pyrazole derivatives containing enaminonitrile as compounds **134** and **135** displayed activity to all cell lines, but the presence of (S-Me) in the ring of pyrazole in compound **134** observed higher activity than its analogue **135** with IC₅₀ (12.45 ± 0.97, 9.31 ± 0.82 and 8.4 ± 0.75 μM) and (15.54 ± 1.46, 13.89 ± 1.2 and 10.57 ± 0.86 μM) against MCF-7, HepG-2 and A549 respectively. Also, acetylation of the amino group in pyrazole enaminonitrile derivatives **135** failed increase

activity with IC_{50} (23.45 ± 1.75 , 18.21 ± 1.61 and 13.46 ± 1.08 μM) compared to other derivatives **134**, **135** and doxorubicin. Replacement enaminonitrile pyrazole derivatives **134-136** with 3,5-diaminopyrazole **140a,b** or 3,5-diarylpyrazole derivatives **141a-c** exhibited that presence of diamino as well as azo derivatives in position four in pyrazole enhance activity against all cell lines and among them azo phenyl derivatives **140a** demonstrated higher activity than azo anisidine derivatives **140b** with IC_{50} values for **140a,b** (4.68 ± 0.25 , 2.7 ± 0.15 , 1.55 ± 0.08 μM) and (13.77 ± 1.1 , 14.95 ± 1.25 , 11.5 ± 0.95 μM) against MCF-7, HepG-2 and A549 and in comparison to doxorubicin (8.19 ± 0.72 , 7.46 ± 0.12 , 3.58 ± 0.03 μM) respectively.

Furthermore, the structure-activity relationships of a series of hydrazone derivatives were designed and tested on the same conditions. Adamantane-1-carbohydrazone derivatives **142a-c** showed that hydrazone of 3-methylacetylacetone **142a** and ethyl acetoacetate derivative **142c** displayed inhibitory activity higher than benzoyl acetone derivative **142b**. Presence of three methyl groups in hydrazone-3-methylpentan-2-one derivatives **142a** explored promising activity than one methyl and one phenyl as **142b** as well as compound **142c** that have one methyl and one ethoxy group and therefor IC_{50} values of hydrazone derivative **142a** (8.35 ± 0.74 , 7.82 ± 0.64 , and 4.39 ± 0.35 μM) closely near to doxorubicin. Additionally, compound **137** that containing hydrazine derivatives with both adamantane as the backbone and acrylate derivatives that poses two functional groups as ethyl ester and cyano groups displayed weak activity with almost IC_{50} values ranged between (15.42 ± 1.4 to 35.13 ± 2.45 μM). Furthermore, introducing the bioactive core as formyl-chloquinoline and formyl-pyrazole derivatives to furnishes the corresponding hydrazone derivatives **131** and **132**. To our delight, hydrazone containing pyrazole moiety (hybridization of two active core), compound **131** exhibited broad activity

with IC₅₀ values (7.46 ± 0.54 , 5.11 ± 0.45 and 3.75 ± 0.26 μM) with IC₅₀ values higher than doxorubicin with 1.1 and 1.45 folds against MCF-7 and HepG-2.

Finally, based on the above analysis of SAR study, we can conclude that presence of pyrazole with diamino, and the azo-phenyl group as compound **140a**, hydrazone derivative by reaction with formyl pyrazole as compound **131** or with 3-methyl acetylacetone **142a** enhance the activity among all the designed compounds. As well as, the most promising synthesis 3,5-diaminopyrazole derivatives **140a** demonstrated IC₅₀ values (4.68 ± 0.25 , 2.7 ± 0.15 , 1.55 ± 0.08 μM) with 1.75, 2.75 and 2.31 folds in comparison to all synthesized compounds and doxorubicin as a positive control.

2.2.3. Carbonic anhydrase inhibitors

Carbonic anhydrase (CA) involved many isoenzymes that distributed to almost all organelle of the human body, and they are necessary for diversities of cellular mechanisms.¹⁰⁴ Inhibition of these isoenzymes is utilized to address an extensive range of disease situations containing glaucoma to cancer.^{105, 106} Both CA IX and CA XII become an important target for lung cancer drugs because it played a vital role in hypoxic condition by controlling intracellular and extracellular pH as well as, they are expressed in a limited number of normal tissues, so inhibition these two isoforms may have interesting clinical implications.¹⁰⁷ The modification of new CA inhibitors has been required to develop as therapeutic agents by introducing several groups as sulfonamide,¹⁰⁸ thiourea derivatives,¹⁰⁹ pyrazole derivatives,¹¹⁰ and bromophenols.¹¹¹

Table 2: Inhibitory activity of adamantane derivatives **131**, **140a** and **142a** on tumor associated carbonic anhydrase CAIX and CAXII

Compound No.	Carbonic anhydrase IC ₅₀ (nM)*	
	CA IX	CA XII
131	272.24 ± 4.2	315.33 ± 5.4
140a	107.20 ± 1.4	180.21 ± 2.5
142a	320.40 ± 3.3	695.84 ± 7.8
Dorzolamide HCl	51.92 ± 0.7	85.95 ± 1.2

*Three independent measurements were performed for each used concentration of the tested compounds.

Depending on the antiproliferative activity results, it found that the most adamantane derivatives exhibited selectivity to lung cancer cell line A549. Among them, we selected the most potent three compounds **131**, **140a** and **142a** (IC₅₀ values less than 5μM) to further evaluation against *in vitro* CA IX and CAXII. The data obtained was represented in **table 2**, by IC₅₀ in (nM) according to 4-nitrophenyl acetate (4-NPA) esterase assay and Dorzolamide HCL used as a standard positive drug.

From the inhibitory activity presented in **table 2**, it was found that the three adamantane derivatives exhibited good inhibitory activity against two isoenzymes CAIX and CA XII by displaying activity in small micromole between (0.107-0.695μM). Firstly, 3,5-diaminoazopyrazole derivative **140a** was the most active derivative and had a significant inhibitory effect against both isoenzymes CAIX and CA XII with IC₅₀ values 107.20 ± 1.4 and 180.21 ± 2.5 (nM), in comparison to Dorzolamide HCL that revealed IC₅₀ values (51.92 ± 0.7 and 85.95 ± 1.2 nM) respectively. Furthermore, the combination between pyrazole and adamantane-1-carbohydrazide to produce hydrazone derivatives with adamantane core showed moderate activity on CAIX with IC₅₀ values 272.24 ± 4.2 (nM) and IC₅₀ value 180.21

± 2.5 (nM) for CAXII and that illustrate that combination of the formyl pyrazole with hydrazine derivative decrease activity. On the other hand, testing of adamantane hydrazone derivative that obtained by incorporation of adamantane hydrazide moiety with 3-methyl acetylacetone without any pyrazole core as adamantane derivative **142a** arose as the weakest CA derivatives in this study with IC_{50} values 320.40 ± 3.3 and 695.84 ± 7.8 (nM) against CAIX and CA XII respectively (**Fig.2**).

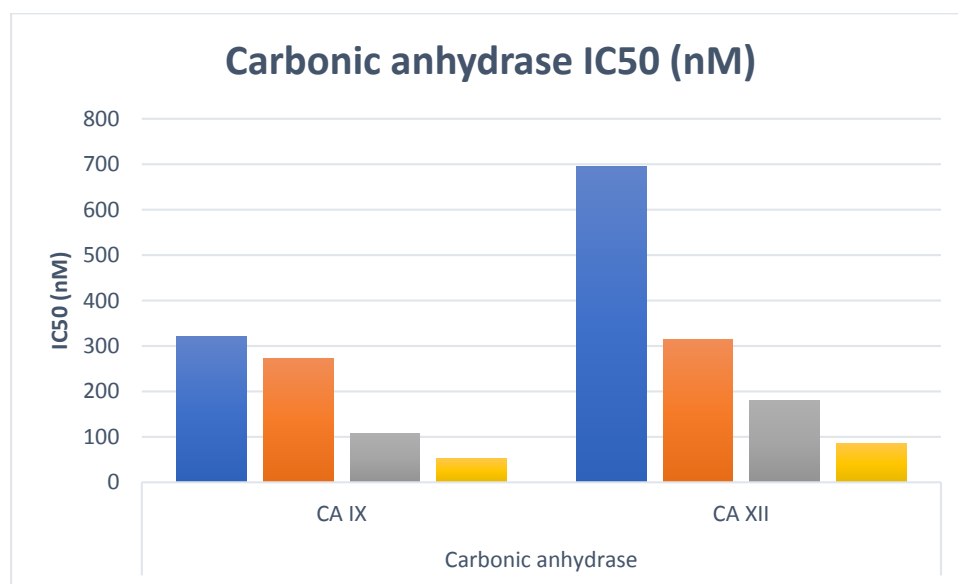


Figure 2: Diagram illustrates the inhibitory activity IC_{50} (nM) of adamantane derivative **131**, **140a** and **142a** and Dorzolamide HCl against transmembrane CA IX and CA XII

Finally, it can conclude that the adamantane derivatives exhibited potency activity to lung adenocarcinoma A549 with IC_{50} values in low micromoles in general, but only adamantane derivatives that were having pyrazole moiety without any hydrazone part in the main skeleton exhibited a good activity to carbonic anhydrase IX and XII, and its noteworthy to mention the order of activity within pyrazole (**140a**) > pyrazole-hydrazone derivative (**131**) > hydrazone derivatives (**142a**) and all containing bioactive adamantane core.

2.2.4. *In silico* Computational studies

2.2.4.1. *Predication of the Drug likeness and physicochemical properties*

Physicochemical properties can be defined as the interaction of a new compound or drug with the physical environment and used to determine both the proper formulation and delivery method of a drug.¹¹² The three adamantane derivative **131**, **140a** and **142a** that tested against CA IX and CA XII were evaluated by using Swiss ADME (<http://swissadme.ch/index.php>) for physicochemical properties and two drug-likeness rule (Lipinski's and Veber rule).¹¹³

The adamantane derivatives that were having hydrazone **142a**, and diaminopyrazole derivative **140a** showed oral bioavailability without any violations for both Lipinski's Rule (involve five rules according to reported methods⁹⁵⁻⁹⁸ discussed in details and summarized in **table 3** and Veber filter¹¹⁴ that include two-parameter that can be known as (i) number of rotatable bonds less than or equal 10 and (ii) topological polar surface area (TPSA) less than or equal 140 Å². Except hydrazone-pyrazole derivative **131** that displayed only one violation MLOGP > 4.15, but all the tested compounds, as well as two standard drugs, meet the criteria of drug-likeness. while the two standard drugs failed in Veber filter where TPSA > 140.

Table 3: *In silico* the physicochemical properties and Lipinski's rule of five and Veber filter for the adamantane derivatives **131**, **140a** and **142a**, Dorzolamide HCl and AZM as a positive control

Cpd. No.	MW	MLog P	nHB A	nHB D	nR B	TPSA	Violations from Lipinski's	Violations from Veber
Rule	<500	≤4.15	≤10	≤5	≤10	≤140 Å ²	Yes; 0 or 1	Yes; 0 violation
131	438.56	4.27	7	2	6	70.14	Yes; 1 violation: MLogP	Yes; 0 violation

140a	364.44	3.50	4	2	4	111.6 5	Yes; 0 violation	Yes; 0 violation
142a	290.40	2.52	3	1	5	58.53	Yes; 0 violation	Yes; 0 violation
Dor. HCl	360.90	-0.05	6	2	3	151.3 3	Yes; 0 violation	No; 1 violation: TPSA>140
AZM	222.25	-2.34	6	2	3	151.6 6	Yes; 0 violation	No; 1 violation: TPSA>140

2.2.4.2. *Molecular docking study*

Molecular docking simulation considered the simplified form of molecular dynamic (MD) simulation that save time and money spent and common component of the drug discovery because traditional experimental methods for drug discovery take a long time.^{115,116} Docking study can also be defined as a computational procedure that studies how ligand and protein fit both energetically and geometrically to give us a complete figure to predict the binding-conformation of small drug-like molecules to target proteins.^{117,118}

To provide a rationale for the cytotoxic activity and carbonic anhydrase values of the newly adamantane derivatives **131**, **140a** and **142a**, the molecular docking simulation was performed using Molecular Operating Environment software 10.2008 (MOE) to predict the possible binding mode as well as the active conformation of these derivatives inside the target enzyme. The three compounds were docked in two proteins that retrieved from protein data bank (<https://www.rcsb.org/>) as **CA IX** (PDB: 3IAI) and **CA XII** (PDB: 1JD0).^{107,119}

Firstly, the promising derivatives **131**, **140a** and **142a** and **Dorzolamide HCl (Dor. HCl)** were docked inside the active site of **CA IX** (PDB: 3IAI). The validation process of these enzymes showed that the original ligand 5-acetamido-1,3,4-thiadiazole-2-sulfonamide (**AZM**) inhibitor fitted deeply inside the active side with (RMDS = 1.02) and different type of binding energy discussed in detail (supplementary information). Due to using Dorzolamide HCl as a reference drug in esterase assay, we replace the **AZM** ligand with **Dor. HCl** that exhibited IC₅₀ value (51.92 ± 0.7 nM) and docking binding energy score $S = -13.23$ Kcal/mol, and three hydrogen bonds that can be described as two with Thr199 that described as one hydrogen side chain bond acceptor with one oxygen of SO₂NH₂ with bond length 2.96 Å (strength = 22%), and another hydrogen bond backbone acceptor with NH of (SO₂NH₂) group with bond length 2.86 Å (59 %). Addition to, that Zn⁺² ion that contact to one oxygen of SO₂ of sulphonamide as well as coordinated to three His 119, 96, 94 and Pro201 contact to water molecule that forms one bond with one nitrogen of ethylamine derivatives. (**Fig. 3**).

Docking of hydrazone-adamantane derivatives showed binding energy $S = -10.96$ Kcal/mol and formed only one hydrogen bond acceptor with His 64 with bond length 2.80 Å (14%). Besides, the carbonyl of hydrazone side chain bound to Zn⁺² ions that surrounded by three coordinated bonds with His 119, 96 and 94 as the original ligand (**AZM**) (**Fig. 4**). By the same way, pyrazolo-hydrazone derivatives **132** (**Fig. 5**) demonstrate one side chain hydrogen bond donor between Gln92 and NH of pyrazole with strength (12%) and bond length (2.95 Å) (See **table 4**). Furthermore, arene-cation interaction between tolyl of pyrazole derivative and His64 added to arene-arene cation interaction between His94 and phenyl ring at position five in pyrazole derivatives and these binding exhibited binding energy $S = -12.63$ Kcal/mol. Compound **140a** with IC₅₀ values against CA IX (107.20 ± 1.4 nM)

advertised binding energy $S = -9.94$ Kcal/mol with one hydrogen bond acceptor through His64 and carbonyl of methanone adamantane derivative with bond length 2.51 Å (40%), beside Zn^{+2} ion form arene-cation interaction with phenyl of the azo-pyrazole derivative. Adamantane moiety in all previous pose showed lipophilic interaction with the carbonic anhydrase binding site.

Table 4: Docking results of the promising adamantane derivatives **131**, **140a** and **142a** and Dorzolamide HCl inside 3IAI and 1JD0 active site

Cpd. No.	(S) (Kcal/mol)	Interacting residues	Type of interaction
For CAIX (3IAI)			
Dor. HCl	-13.23	Thr199, Pro201 and [His94, His96, His119(Zn)*]	H-bond & solvent
131	-12.63	Gln92, His64 and His94	H-bond & aren-cation aren-arene
140a	-9.94	His96	H-bond & aren-cation
142a	-10.96	His64, His96 and [His94, His96, His119 (Zn)*]	H-bond
For CAXII (1JD0)			
Dor. HCl	-14.55	Thr199, Thr200 and [His94, His96, His119(Zn)*]	H-bond& solvent
131	-19.81	Lys 67	H-bond & aren-cation
140a	-13.87	His94, Thr91	H-bond & aren-cation aren-arene
142a	-14.31	His96 and [His94, His96, His119(Zn)*]	H-bond

(*) meaning that Zn ion bind to ligand and the residue amino acid.

Docking of **Dor. HCl** inside the active site of (PDB: 1JD0) displayed two hydrogen bond acceptor with one oxygen and NH of (SO₂NH₂) group with bond length 2.81, 2.66 Å and strength 71, 59 % respectively. Another one H-bond side-chain acceptor occurs between Thr200 and NH of (SO₂NH₂), as well as Zn ions bound to the oxygen of SO₂ and three amino acids (His94, His96 and His119) beside vital water molecule

that contact with the oxygen of 1,1-dioxothiopyrane ring, NH of ethylamine derivatives and residue Thr200 (**Fig. 6**). Furthermore, compound **142a** that have hydrazone derivatives, His96 (hydrogen bond acceptor 3.15Å) and Zn ions bind with oxygen of the carbonyl and the same three histidine amino acid as a ligand with binding energy $S = -14.31\text{Kcal/mol}$ as well as hydrophobic interaction between adamantane moiety and two methyl groups with the active site of pocket (**Fig. 7**). Also, pyrazole derivative **131** with inhibitory activity 0.315μM showed the lowest binding energy $S = -19.81\text{Kcal/mol}$, where His 94 form one hydrogen bond acceptor (2.87 Å) with the carbonyl of the adamantane carbohydrazide derivatives and one arene-cation interaction with tolyl of pyrazole derivatives. Pyrazole derivative **140a** with two amino (in position 3 and 5) and azo-phenyl (position 4) derivative observed a lower docking score energy binding energy $S = -13.87\text{Kcal/mol}$. Moreover, it formed hydrogen bond acceptor (2.57Å and 42%) between the carbonyl of methanone derivative and Thr91 and one arene-arene interaction between phenyl and His94 as well as one arene-cation interaction through the pyrazole ring and Lys 67 (**Fig. 8**). (supplementary data containing all figure).

Finally, the presence of pyrazole derivative enhances binding affinity because it can form many different interactions, as well as the presence of carbonyl at a side chain or tightly direct to pyrazole ring also, increase binding inside the pock in addition, it can bind to Zn ion, and presence of adamantane core (lipophilic properties) exhibited hydrophobic interaction with the active site in a pocket.

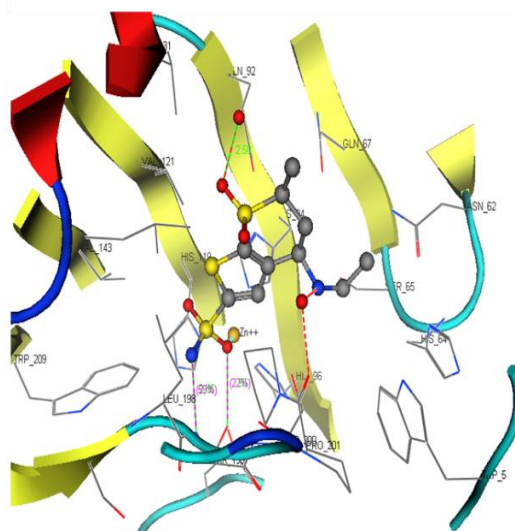
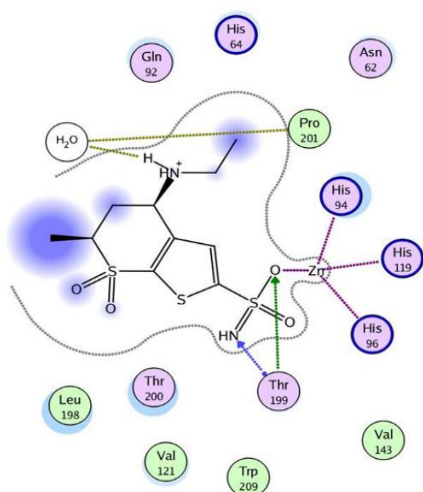


Figure 3: 2D &3D interactions of Dorzolamide HCl (**Dor. HCl**) inhibitor in the active site of 3IaI (CA IX)

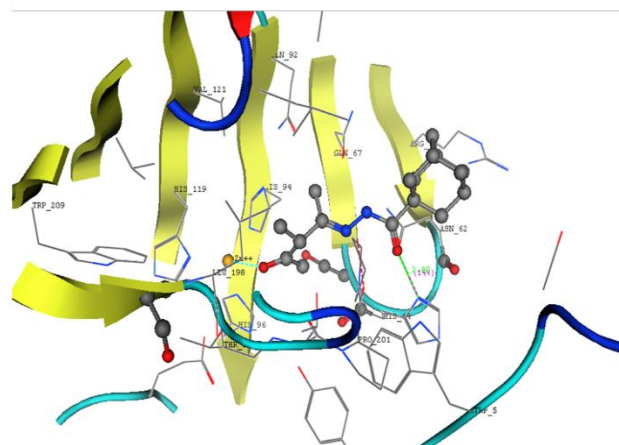
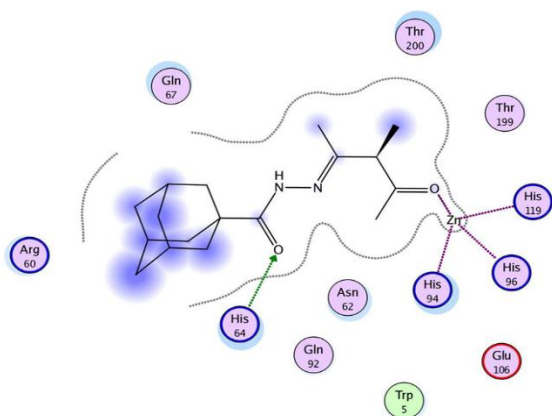


Figure 4: 2D &3D interactions of compound **142a** in the active site of 3IaI (CA IX)

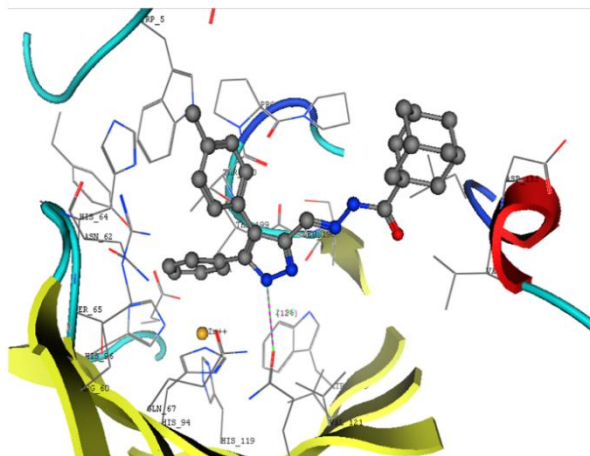
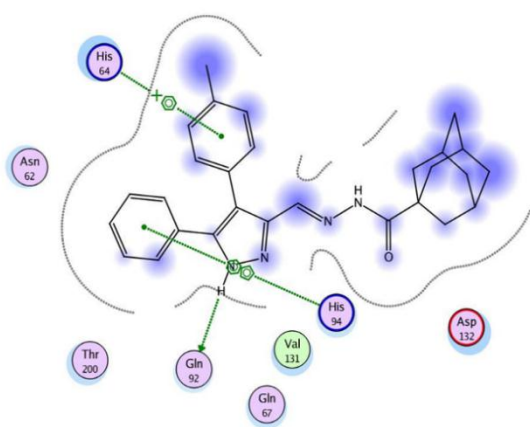


Figure 5: 2D &3D interactions of compound **131** in the active site of 3IaI (CA IX).

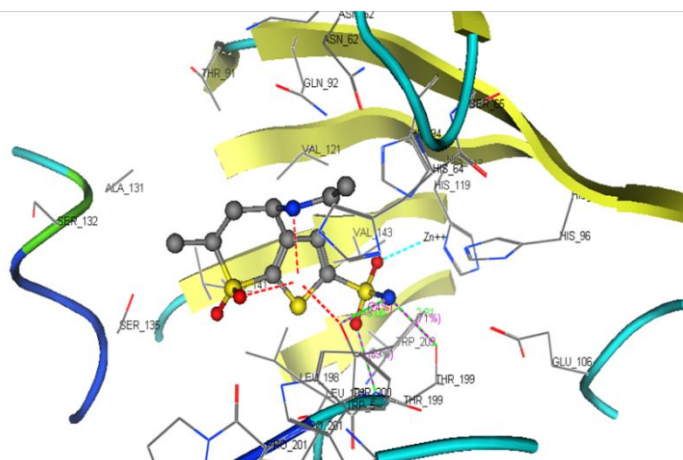
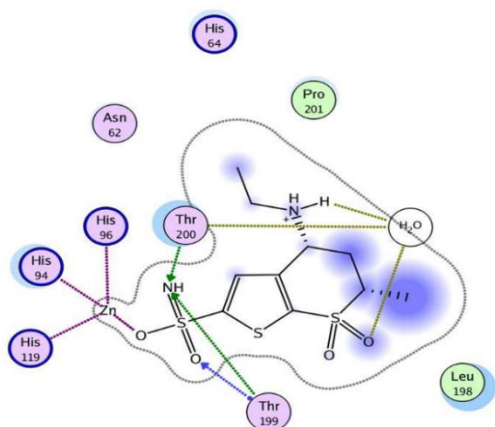


Figure 6: 2D &3D interactions Dorzolamide HCl (**Dor. HCl**)in the active site of 1JD0 (CA XII)

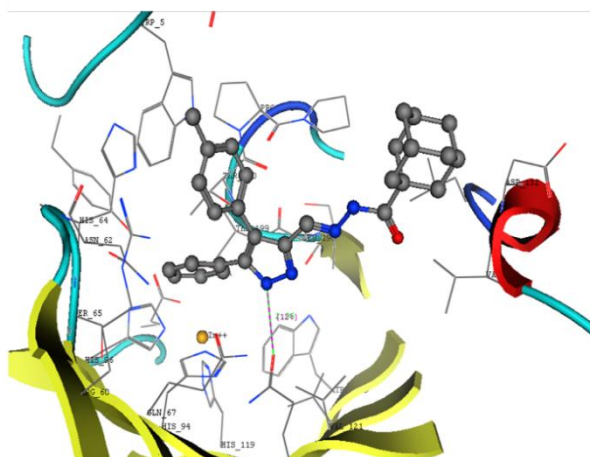
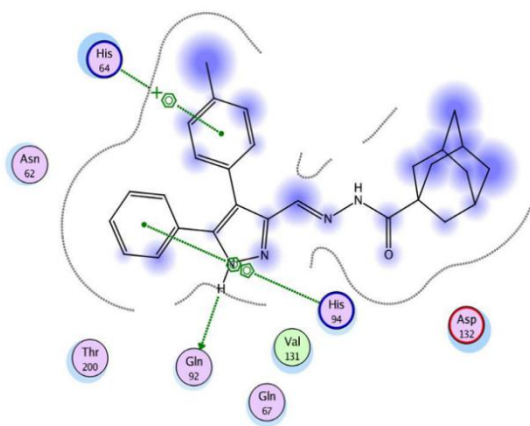


Figure 7: 2D &3D interactions of compound **131** in the active site of 1JD0 (CA XII).

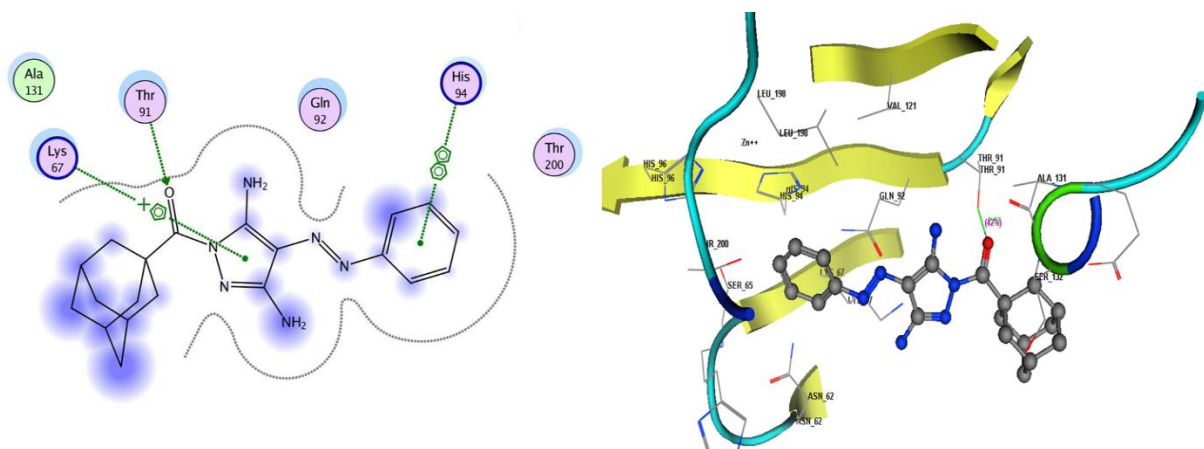


Figure 8: 2D &3D interactions of compound **140a** in the active site of 1JD0 (CA XII)

2. Conclusion

Generally, we successfully designed and synthesized a small library of adamantane nucleus (lipophilic part) bearing pyrazole **131,134, 135, 136, 140, 141**, and hydrazone **137, 142, 132** derivatives at position 1 and all the chemical reaction involve an only one-step reaction to obtain the desired products. The cytotoxic activity against three cell line MCF-7, HepG-2 and A549 were evaluated and displayed good to moderated activity with IC_{50} values (1.55-42.17 μ M). The newly synthesized derivatives revealed sensitive and selectivity to lung cancer cells (A549) with IC_{50} values ranged between 1.55 ± 0.08 to 15.42 ± 1.4 μ M, with eight compounds (**134, 135, 142a, 142b, 142c, 131, 140a** and **141c**) having IC_{50} less than or equal ten micromole except for compound **141a** that showed IC_{50} (27.18 ± 1.95 μ M). The most promising three adamantane derivatives **131, 140a** and **142a** with IC_{50} values less than 5 μ M were elected to evaluate their inhibitory action against isoenzyme hCAIX and hCAXII for the first time. Superiorly, 3,5-diamino-pyrazole core **140a** showed higher IC_{50} values than hydrazo-pyrazole **131** and hydrazone

derivatives **142a** that hybrid with adamantane and exhibited inhibitory effect with submicromolar between (0.107-0.695 μM), in comparison to Dorzolamide HCl (0.052-0.086 μM). Among them, compound **140a** is considered the most promising derivatives with anti-proliferative (A549) ($\text{IC}_{50} = 1.55 \pm 0.08 \mu\text{M}$) and CAIX/XII inhibitors ($\text{IC}_{50} = 0.11$ and $0.18 \mu\text{M}$), respectively. Finally, some drug-likeness model as Lipinski and Verber were predicted. Molecular docking simulation was performed inside the active site of CA IX (PDB: 3IAI) and CA XII (PDB: 1JD0) to evaluate the binding modes of the adamantane derivatives as well as Dorzolamide HCl. Docking score of the promising compounds showed lower values (-9.94 to -19.81 Kcal/mol) in comparison to Dorzolamide HCl (-13.23 to -14.55 Kcal/mol) and different type of interaction as H-bond, arene-arene and arene-cation interaction were present beside in some cases ligand coordinated to Zn ion. Moreover, due to lipophilic characters of adamantane core the hydrophobic interaction appear with both active sites.

2.1. Biological evaluation

2.1.1. Antiproliferative activity

In vitro cytotoxicity of all the newly designed and synthesized adamantane nucleus were tested against three human tumors cell lines including human breast adenocarcinoma cell line (MCF-7), human hepatocellular carcinoma cell line (HepG-2) as well as human lung adenocarcinoma epithelial cells (A549), they were obtained from VACSERA- Cell Culture Unit, Cairo, Egypt, by using colorimetric assay method (SRB) under standard conditions according to our reported methods

101,103.

2.1.2. Carbonic anhydrase assay

Carbonic anhydrase (CA) IX and XII inhibition activity were evaluated using Recombinant Human Carbonic Anhydrase IX / XII Protein, CF Kit, that obtained from R&D Systems (Minneapolis, MN, USA), following the same instructions from the manufacturer protocol that measured by its esterase activity according to reported methods.¹²⁰ Assay procedure involved material as (1) Assay Buffer: 12.5 mM Tris, 75 mM NaCl, pH 7.5, (2) Recombinant Human Carbonic Anhydrase IX/CA9 (rhCA9) (Catalog # 2188-CA) or Carbonic Anhydrase XII/CA12 (rhCA12) (Catalog # 2190-CA), (3) Substrate: 4-Nitrophenyl Acetate (4-NPA) (Sigma, Catalog # N8130), 100 mM stock in acetone. The following steps involving the producer as; firstly, both rhCAIX or rhCAXII was diluted to 20 ng/μL and substrate (4-Nitrophenyl acetate) also diluted to 2 mM by using a buffer. In 96-well Clear Plate (Costar, Catalog # 92592), load 50 μL of 20 ng/μL rhCA12, and start the reaction by adding 50 μL of 2 mM Substrate to wells. Include a Substrate Blank containing 50 μL Assay Buffer and 50 μL of 2 mM 4-Nitrophenyl acetate. Inhibitory effects of three compounds were compared with Dorzolamide HCl were obtained by different inhibitor concentrations where the tested compound and standard dissolved in DMSO (0.1 mM) with dilution from (10 nM) up to (0.01 nM) by using distilled water and all compounds were tested in triplicate at each concentration used to form the enzyme-inhibitor complex. Read absorbance at a wavelength of 400 nm (bottom read) in kinetic mode for 5 minutes. The calculations were performed as per the kit guidelines, where specific activity calculated by the following equation:

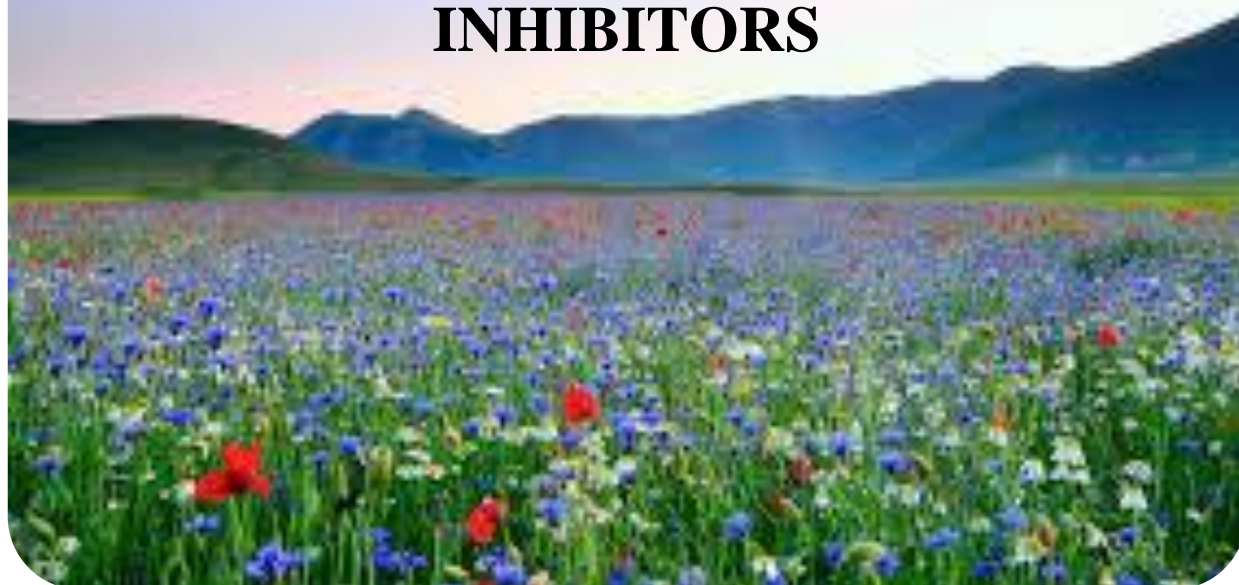
$$\text{Specific Activity (pmol/min/}\mu\text{g)} = \frac{\text{Adjusted Vmax* (OD/min) x Conversion Factor** (pmol/OD)}}{\text{amount of enzyme (}\mu\text{g)}}$$

Control cuvette activity was acknowledged as 100% in the absence of inhibitor, and an activity % – [inhibitor] graph was drawn for each inhibitor.

2.1.3.Molecular docking

Study of molecular docking of the adamantane derivatives and standard drug (Dorzolamide HCl) that used in esterase enzyme assay were performed according to the described reported method under standard protocol and methods¹¹⁹ using Molecular Operating Environment (MOE) software version 2008.10. The X-ray crystallography structure of both CA IX (PDB: 3IAI) and CA XII (PDB: 1JD0) with original ligand 5-acetamido-1,3,4-thiadiazole-2-sulfonamide (**AZM**) inhibitor¹⁰⁷ were downloaded from protein data bank.¹⁰¹ Protein was prepared by protonated 3D and removed the water molecule and ligand that not implicated in the active site. The active site then generated with the default protocol. Trigonal matcher was selected as placement method and London dG as docking score energy using Zn^{+2} ion chelate as a constrain for molecular docking. Docking process was firstly performed by self-docking of original ligand AZM in the active site and the evaluation of the RMSD values for CA IX (PDB: 3IAI) and CA XII (PDB: 1JD0) were 1.02 and 1.06 respectively. (binding of co-crystalized ligand and docking score energy with the figure in supplementary material filed). The newly designed compounds and Dorzolamide HCl was generated from Chemdraw14.0 then protonated and minimized and finally washed the structure and saved as mdb file as ligand atom that then used in docking protocol after replaced the co-crystalized AZM and under the same methods.

**SYNTHESIS OF ADAMANTANE
THIADIAZOLE DERIVATIVES AS EGFR
INHIBITORS**



Part II: Development of adamantane scaffold containing 1,3,4-thiadiazole derivatives: design, synthesis, anti-proliferative activity and molecular docking study targeting EGFR

1,3,4-Thiadiazoles are heterocyclic scaffolds found in several compounds that have various pharmacological activities ^{122,123}. The wide range of pharmaceutically suitable biological activities is due to the existence of the NCS group, a hydrogen-binding domain with two-electron donor systems, as well as sulfur atom, that enhances the lipo-solubility of the molecule ¹²⁴⁻¹²⁸. The lower toxicity and stability of the thiadiazole nucleus *in vivo* is due to its aromatic character ¹²⁹. (**Fig. 1**)

Depending on the biological significance of both adamantane and thiadiazole moieties. It was conceived that binding more than one pharmacophores to design one scaffold using drug design strategy would be of great interest developing highly potent anticancer agents.

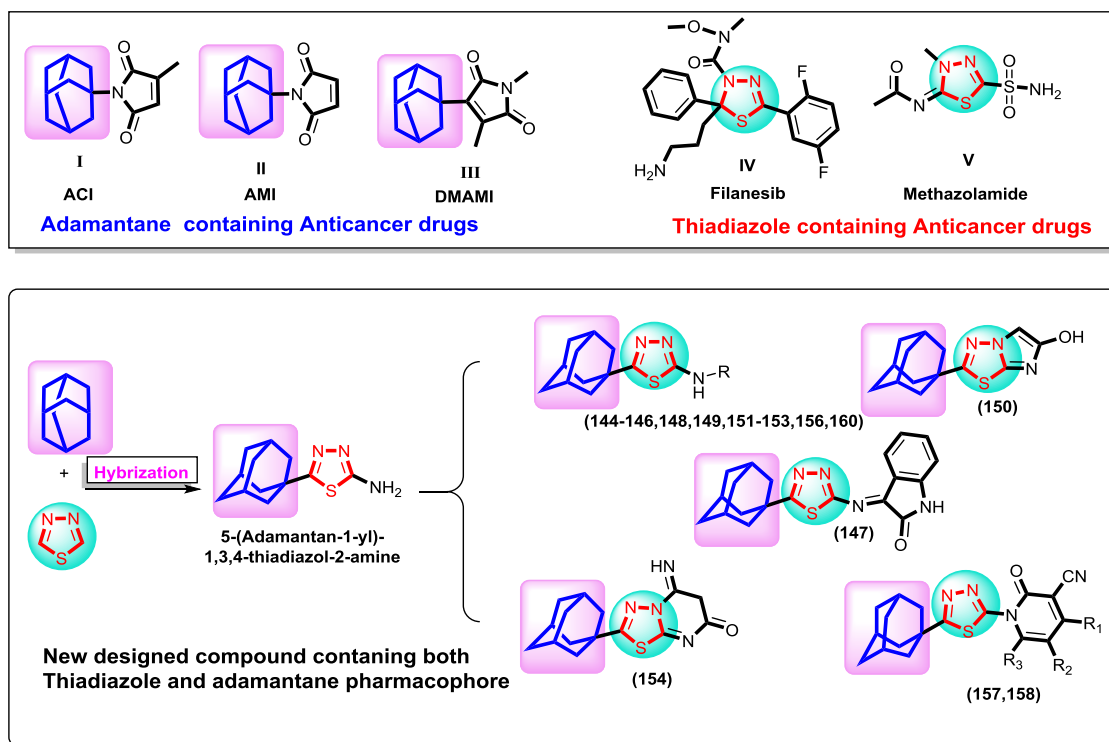
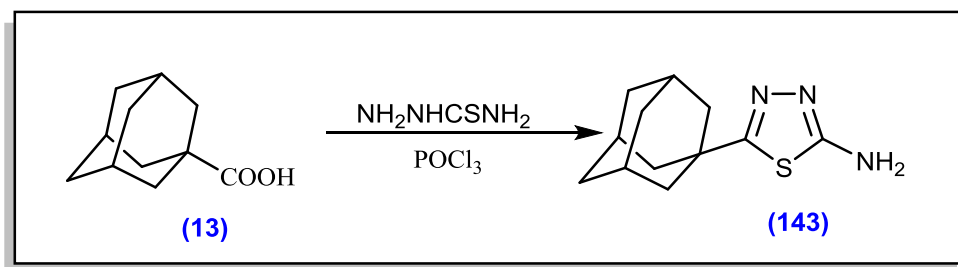


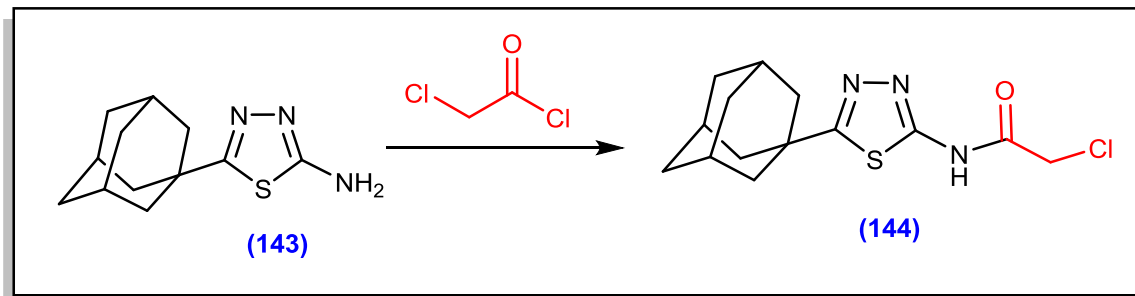
Figure 1: Rationale design for the target molecules

Nowadays, the creation of hybrid molecules is a phenomenon that aims to combine multiple pharmacophore fragments in the same molecule with different biological potentials ¹³⁰⁻¹³⁶. Thus, the rationale for such a study came up from the great importance and synthetic accessibility of adamantly-thiadiazole hybrids in generating potential anticancer molecules. The newly synthesized compounds are structurally similar to other biologically active molecules, with several thiadiazole fragments bearing the adamantly moiety as important pharmacophores and varying degrees of lipophilicity.

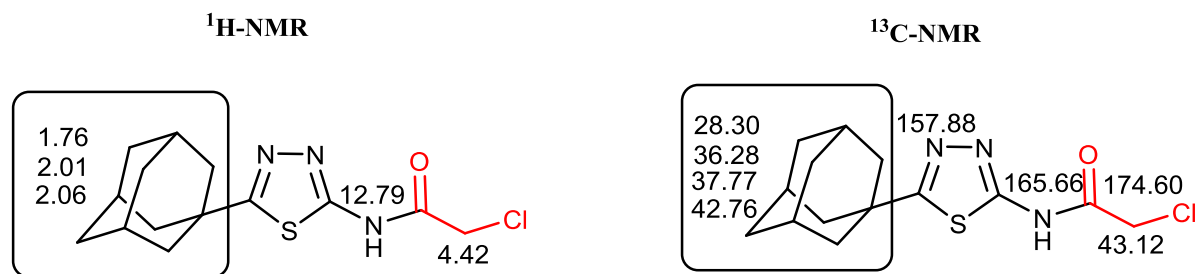
The starting compound, 5-(adamantan-1-yl)-1,3,4-thiadiazol-2-amine (**143**) was prepared according to the previously reported procedure ¹³⁷.



2-Aminothiadiazole derivative **143** was subjected to chloroacetylation through its reaction with chloroacetyl chloride in the presence of trimethylamine as a catalyst to afford the corresponding 2-chloro acetamide derivative **144** ¹³⁸.

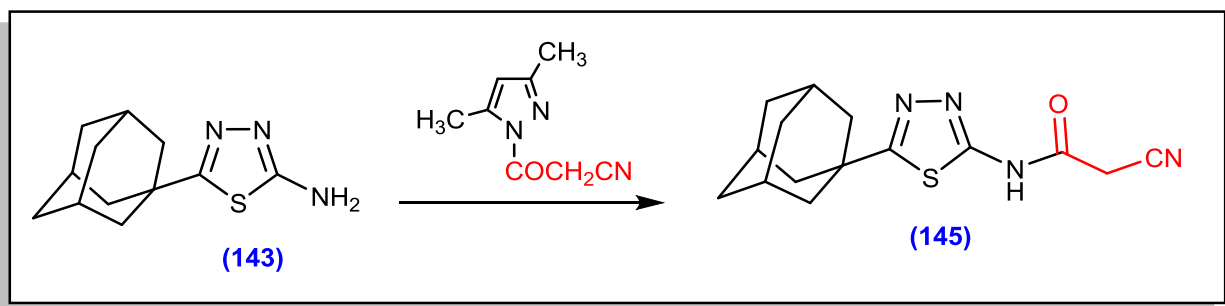


The ^1H -NMR and ^{13}C -NMR data of compound (**144**) are shown in this figure

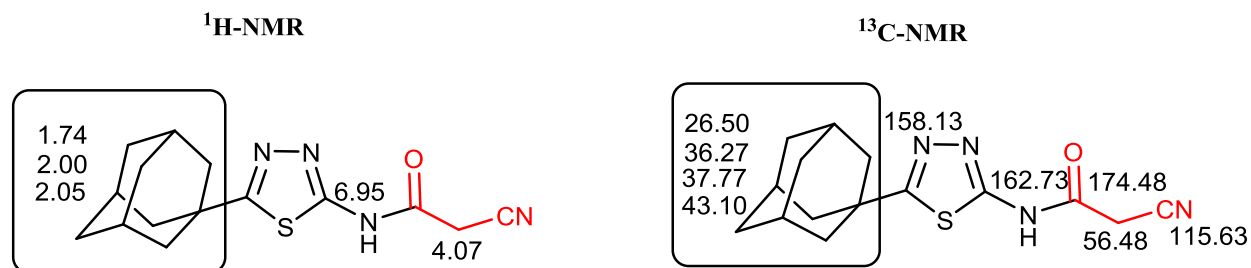


Structure of the latter product was confirmed based on analytical and spectral data. The IR spectrum showed absorption bands at ν 3160, 2905, 2849 and 1714 cm^{-1} due to NH, CH-aliph and C=O groups. Its ^1H NMR spectrum showed two singlet signals at δ 12.79 and 4.42 ppm corresponding to NH and CH₂ groups. The adamantane protons were observed at δ 2.06, 2.01 and 1.76 ppm. ^{13}C NMR for this compound exhibited signals at δ 174.6, 165.66, 157.88 and 43.12 ppm corresponding for C=O, two C=N and CH₂ groups respectively, while the adamantane-C were observed at δ 42.76, 37.77, 36.28 and 28.30 ppm.

In addition, *N*-(5-(adamantan-1-yl)-1,3,4-thiadiazol-2-yl)-2-cyanoacetamide (**145**) was obtained through cyano-acetylation of compound **143** with 3-(3,5-dimethyl-1*H*-pyrazol-1-yl)-3-oxopropane-nitrile in toluene.

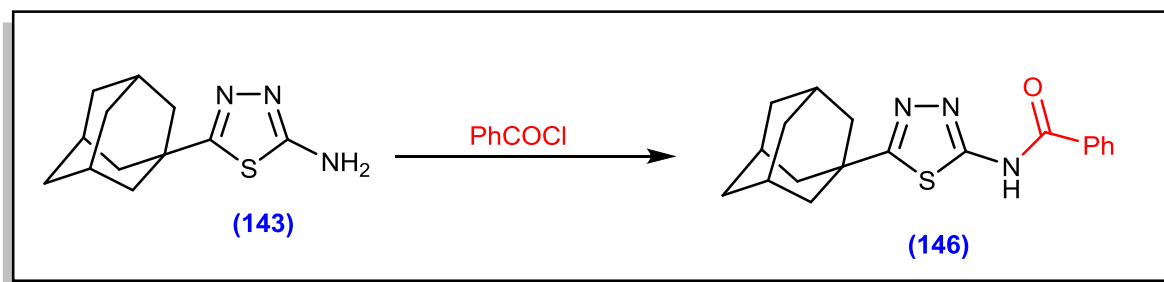


The ^1H -NMR and ^{13}C -NMR data of compound (**145**) are shown in this figure



Elemental analysis, IR, ¹H NMR and ¹³C NMR are in agreement with the proposed structure. Its IR spectrum exhibited two new bands at 2263 and 1720 due to CH₂-CN and C=O respectively. ¹H NMR spectrum displayed a singlet signal at δ 4.07 ppm attributed to CH₂. The ¹³C NMR spectrum characterized signals at δ 174.48, 115.63 and 56.48 ppm assigned to the C=O, CN and CH₂ groups respectively. Its mass spectrum exhibited a molecular ion peak at m/z 302 with a base peak 73.

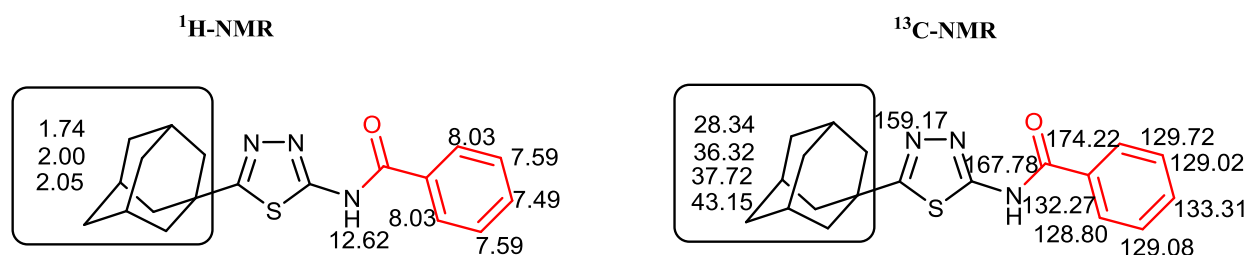
N-(5-(adamantan-1-yl)-1,3,4-thiadiazol-2-yl)benzamide (**146**) was obtained by reaction of 2-aminothiadiazole derivative **143** with benzoyl chloride under reflux condition.



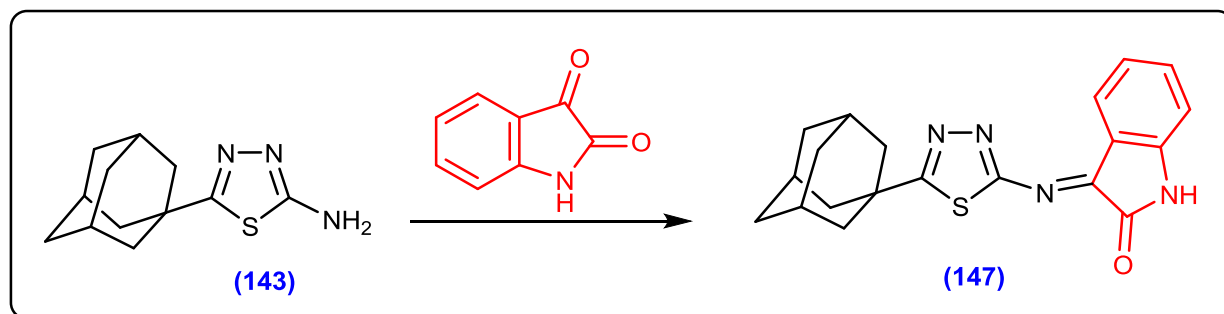
The IR spectrum of compound **146** showed a new absorption band at 1670 cm⁻¹ due to the carbonyl amide group. Its ¹H NMR spectrum revealed a singlet signal at δ 12.62 ppm due to NH proton, in addition to three signals at δ 8.03, 7.59 and 7.49 ppm for aromatic protons. The ¹³C NMR spectrum exhibited signals for carbonyl carbon at δ 174.22 and aromatic at δ 133.31, 132.27, 129.72, 129.08, 129.02 and 128.80 ppm as well as two singlet signals at δ 167.78 and 159.17 ppm for two C=N

groups in thiadiazole moiety in addition to the carbonyl carbon which appeared at 174.22.

The ^1H -NMR and ^{13}C -NMR data of compound (**146**) are shown in this figure

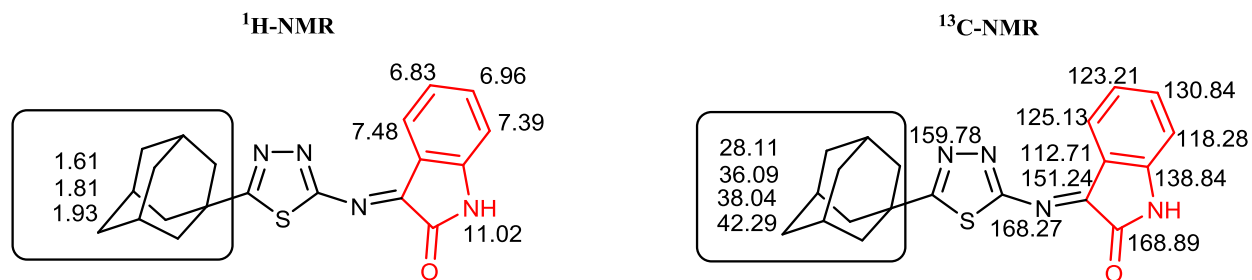


Schiff's base (**147**) which contain thiadiazole and indoline moieties was obtained through condensation of compound **143** with isatin in boiling ethanol.

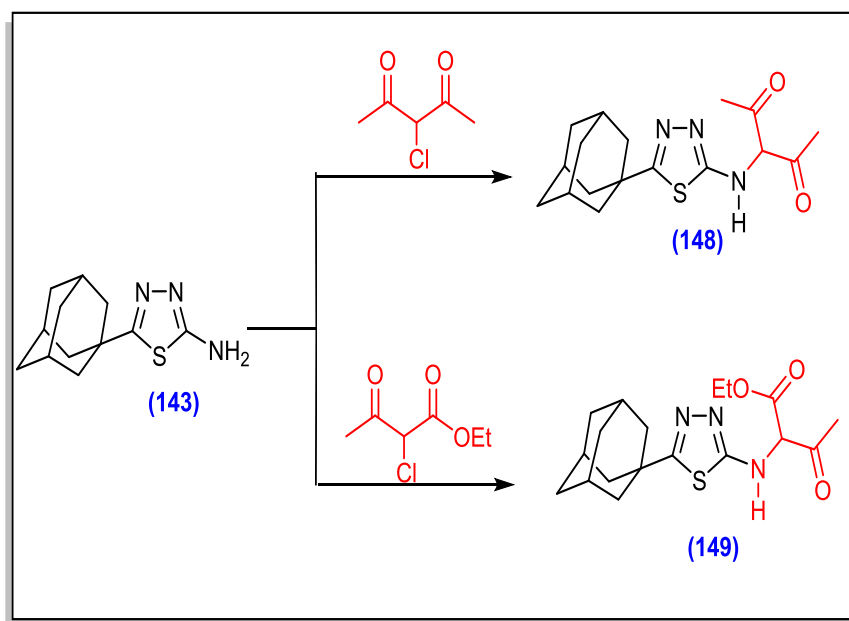


The chemical structure of compound **147** was elucidated based on elemental analysis and spectral data. The IR spectrum indicated the presence of a strong absorption band at 1727 cm^{-1} due to the carbonyl group. ^1H NMR spectrum showed the presence of indolinone part at 11.02, 7.48, 7.39, 6.96 and 6.83 ppm for NH and four aromatic protons respectively. Although, its ^{13}C NMR exhibited signals at 168.89, 168.27, 138.84, 130.84, 125.13, 123.21, 118.28 and 112.71 ppm due to the indolinone core. Its mass spectrum afforded a molecular ion peak at $m/z = 364$ corresponding for the molecular formula $\text{C}_{20}\text{H}_{20}\text{N}_4\text{OS}$ with a base peak at 119.

The ^1H -NMR and ^{13}C -NMR data of compound (**147**) are shown in this figure



Furthermore, we investigated the reactivity of 2-aminothiadiazole derivative **143** towards some halogenated compounds to prepare imidazo[2,1-*b*][1,3,4]thiadiazole derivatives. Thus, the reaction of thiadiazole derivative **143** with 3-chloroacetylacetone and ethyl 3-chloroacetoacetate in ethanol containing piperidine as a catalyst for obtaining imidazothiadiazole structure but acyclic products **148** and **149** were obtained.

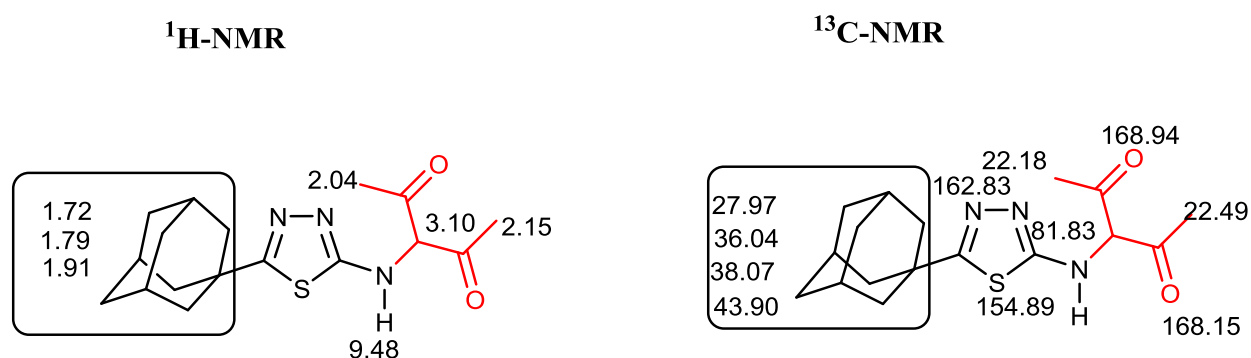


Structure of the latter products was confirmed on the basis of correct elemental analyses and spectral data. The IR spectrum of compound **148** indicated the presence of two strong absorption bands at 1699 and 1676 cm^{-1} due to two carbonyl groups,

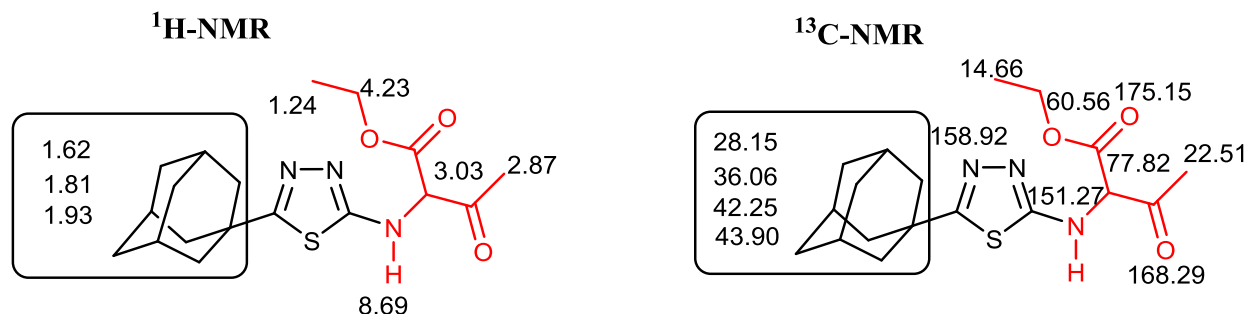
while the carbonyl of ester group in compound **149** was observed at 1698 cm^{-1} . ^1H NMR spectrum of compound **148** showed the presence of NH proton at δ 9.48 and three singlet signals at δ 3.10, 2.15 and 2.04 ppm corresponding for two methyl groups and methine proton in addition to the expected signals for thiadiazole and adamantane moieties.

Compound **149** showed signals at δ 2.87 and 3.03 ppm for methine proton and methyl group in addition to ester group that observed as quartet and triplet at δ 4.23 and 1.45 ppm with coupling constant ($J=6.8\text{ Hz}$). In addition, its ^{13}C NMR exhibited signals at δ 175.15, 168.29, 158.92 and 151.27 ppm for two carbonyls and C=N respectively. Moreover, methine carbon and ethyl group carbons appear at δ 77.82, 60.56 and 14.66 ppm as well as adamantane carbons.

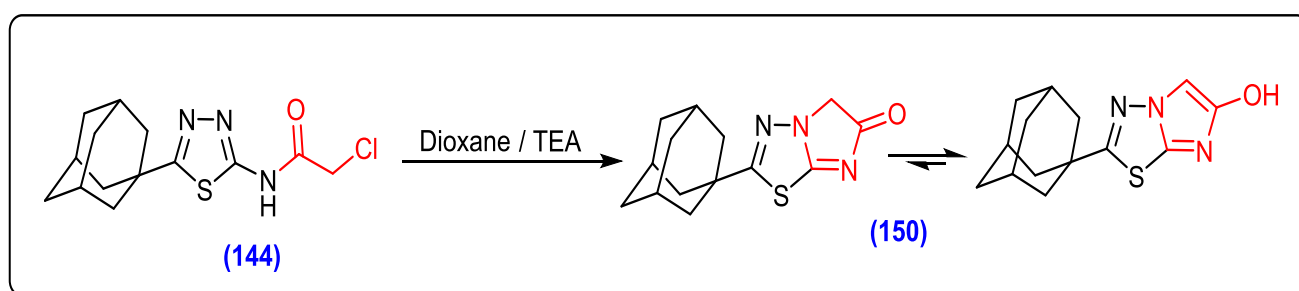
The ^1H -NMR and ^{13}C -NMR data of compound (**148**) are shown in this figure



The ^1H -NMR and ^{13}C -NMR data of compound (**149**) are shown in this figure

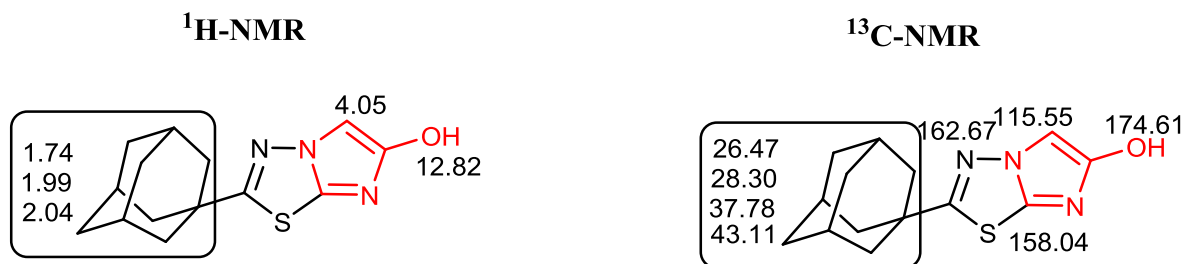


N-(5-(Adamantan-1-yl)-1,3,4-thiadiazol-2-yl)-2-chloroacetamide (**144**) is a versatile reagent and has been extensively used as a synthetic intermediate for the synthesis of thiadiazole derivatives of potential biological activity. It was thus of interest to study the reactivity of compound **144** towards a variety of chemical reagents. Thus, upon refluxing of compound **144** in dioxane containing trimethylamine as a catalyst caused self-cyclization to furnish the corresponding 2-(adamantan-1-yl)imidazo[2,1-*b*][1,3,4]thiadiazol-6-one (**150**).

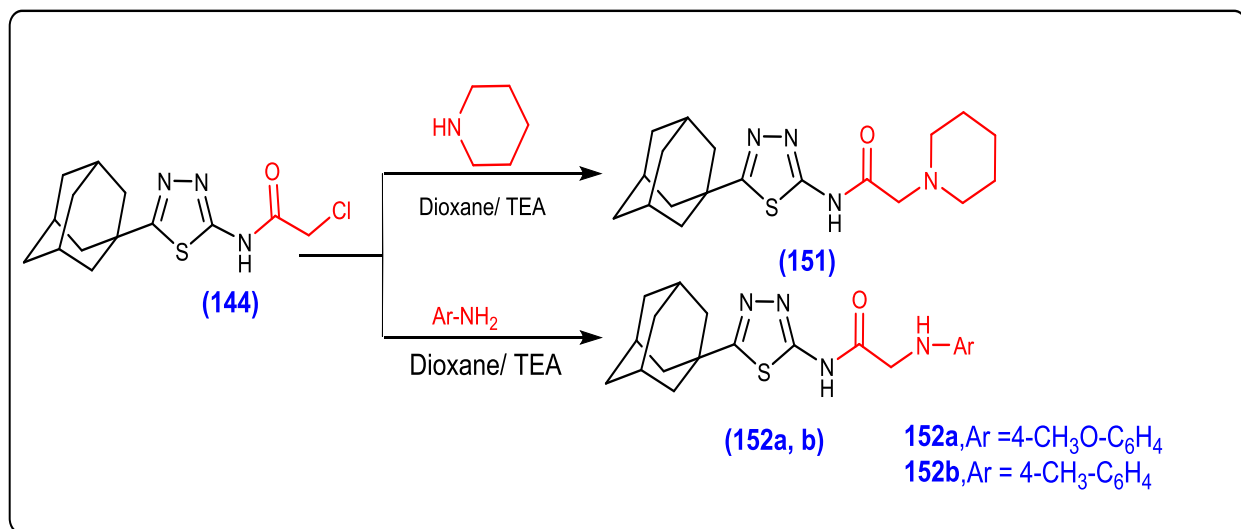


The chemical structure of compound **150** was established on the basis of its elemental analysis and spectral data. Its ^1H NMR spectrum displayed two singlet signals at δ 12.82, and 4.05 ppm for hydroxy and methine proton and its ^{13}C NMR spectrum was characterized by signal at δ 174.61 assigned to the carbon attached to the hydroxyl group.

The ^1H -NMR and ^{13}C -NMR data of compound (**150**) are shown in this figure

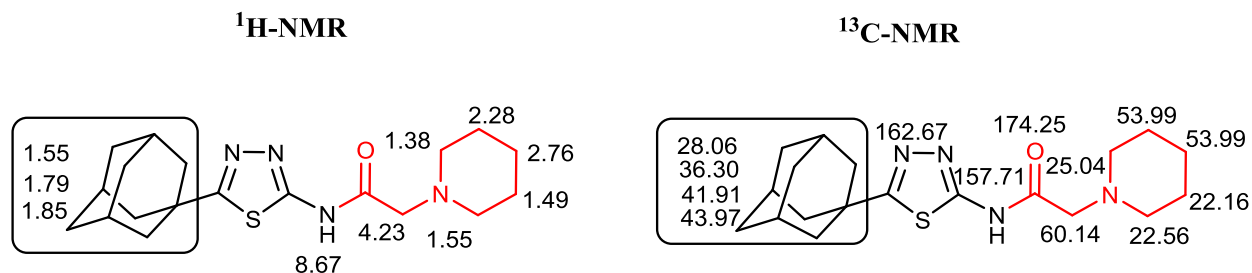


Amination of compound **144** with piperidine as secondary amine and *p*-anisidine as well as *p*-toluidine as primary amine afforded the corresponding amino derivatives compounds **151** and **152**.

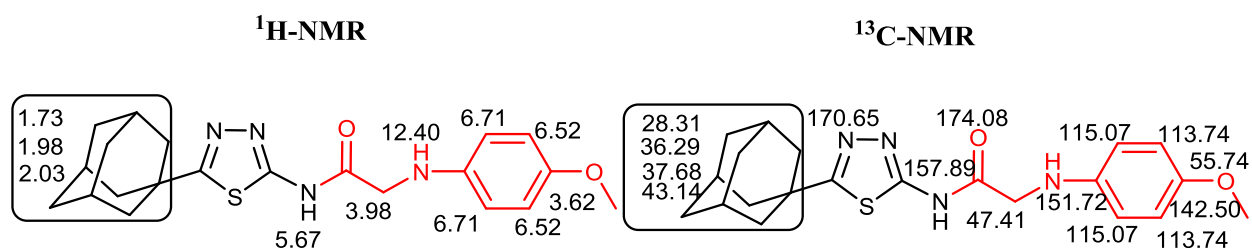


The structure of the amino products **151**, **152** were verified by elemental analyses and spectroscopic methods. For example, ¹H NMR spectrum of compound **151** showed the piperidinyI protons as four multiplet signals at 2.79, 2.31, 1.49, 1.38 corresponding for 10 protons and its ¹³C-NMR the piperidinyI carbons appear in the regions 53.99, 25.04, 22.56, 22.16. While, ¹H NMR of compound **152a** displayed aromatic proton signals appeared as two doublets with coupling constant (*J*=8.8 Hz) at 6.71, 6.52 ppm. In addition to four singlet signals at δ 12.40, 5.67, 3.98, 3.62 ppm characteristic for the 2NH, CH₂, OCH₃ respectively, besides the expected protons of adamantane moiety and its ¹³C NMR showed signals at δ 174.08, 170.65, 157.89, 55.74 and 47.41 ppm corresponding to C=O, 2C=N, OCH₃ and CH₂ groups.

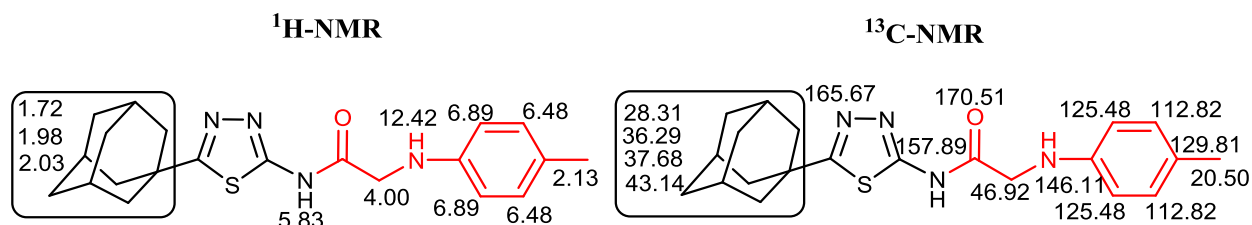
The ¹H-NMR and ¹³C-NMR data of compound (**151**) are shown in this figure



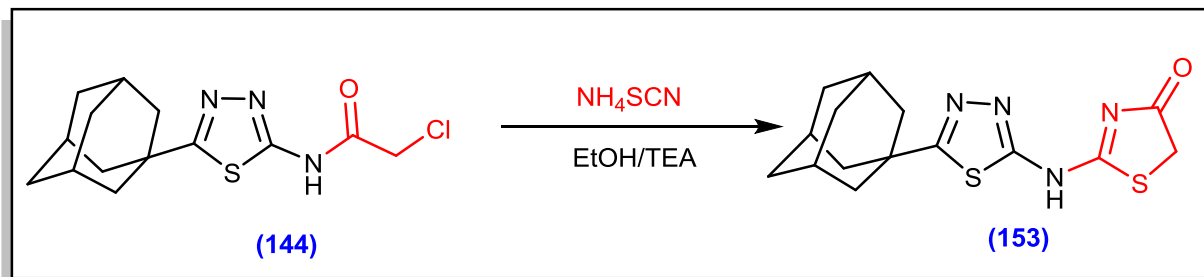
The ¹H-NMR and ¹³C-NMR data of compound (**152a**) are shown in this figure



The ¹H-NMR and ¹³C-NMR data of compound (**152b**) are shown in this figure

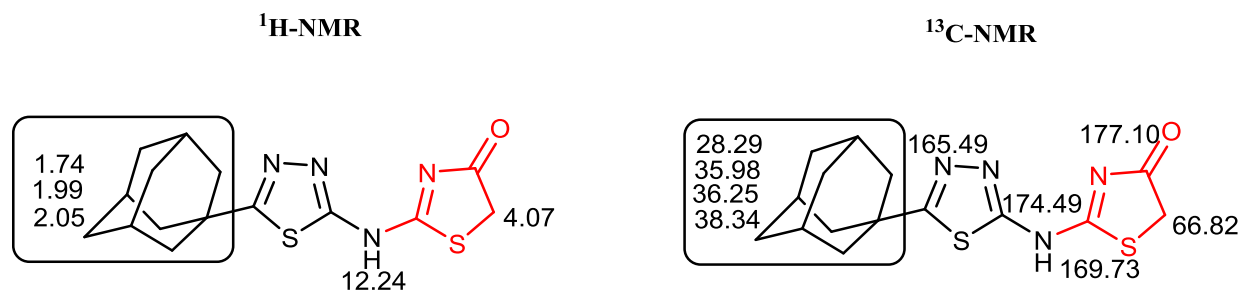


Treatment of 2-chloro acetamide derivative **144** with ammonium thiocyanate in absolute ethanol to afford the thiazolidinone derivative **153**.

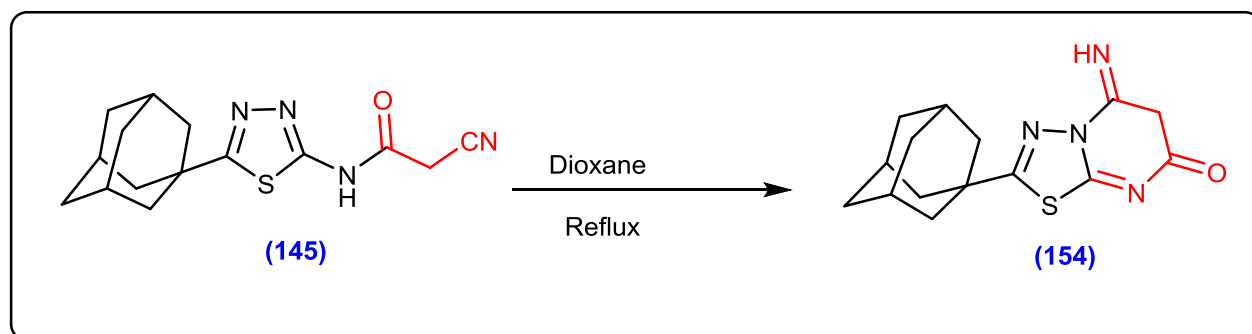


The IR spectrum of compound **153** revealed strong absorption band at 1740 cm^{-1} due to thiazolidine carbonyl function. Its ^1H NMR revealed one proton at δ 12.24 and a singlet signal at δ 4.07 ppm due to CH_2 protons. Moreover, its ^{13}C NMR exhibited signals at δ 177.10, 174.49 and 66.82 ppm for carbonyl group more over endocyclic methylene group of thiazol-4-one derivative.

The ^1H -NMR and ^{13}C -NMR data of compound (**153**) are shown in this figure

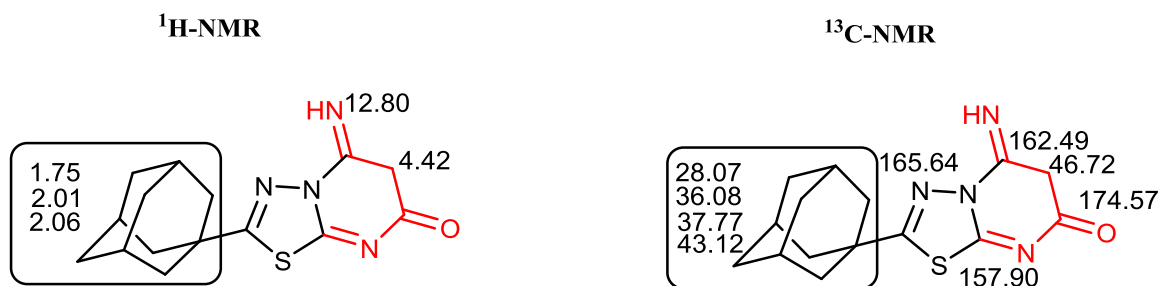


Furthermore, we also investigated the reactivity of *N*-(5-(adamantan-1-yl)-1,3,4-thiadiazol-2-yl)-2-cyanoacetamide (**145**) towards some selective reagents with the aim of preparing some bioactive derivatives. Thus, compound **145** underwent cyclization when heated under reflux in dioxane to afford thiadiazolo[3,2-*a*]pyrimidin-7-one derivative **154**.

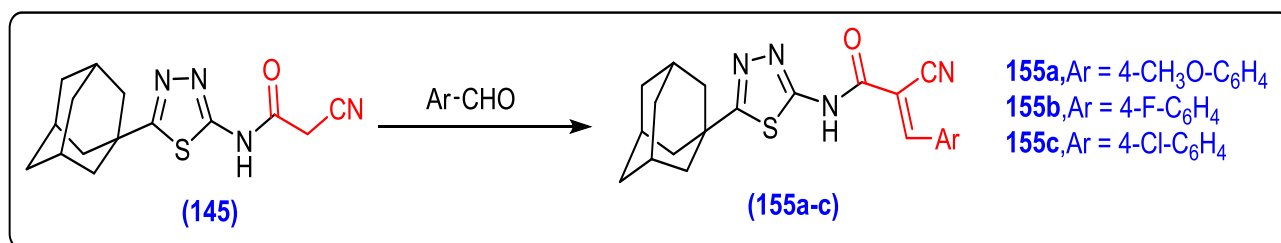


IR spectrum of compound **154** showed absorption bands at 3156 and 1718 cm^{-1} indicating the presence of (NH) and (C=O) groups respectively and absent of the cyano group. Moreover, its ^1H NMR showed two singlets at δ 12.80 and 4.42 ppm due to the presence of NH and CH_2 protons. Furthermore, ^{13}C NMR exhibited the presence of C=O and CH_2 carbons at δ 174.57 and 46.72 ppm respectively in addition to the expected carbons of the thiadiazolo adamantane moiety.

The ^1H -NMR and ^{13}C -NMR data of compound (**154**) are shown in this figure

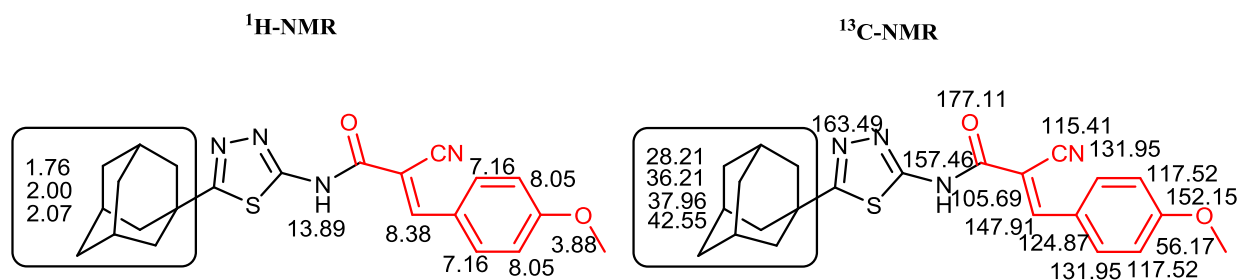


Condensation of cyano-acetamide thiadiazole derivative **145** with some aromatic aldehydes namely 4-methoxy or 4-chloro or 4-fluoro benzaldehyde afforded the corresponding acrylamide derivatives **155a-c**.

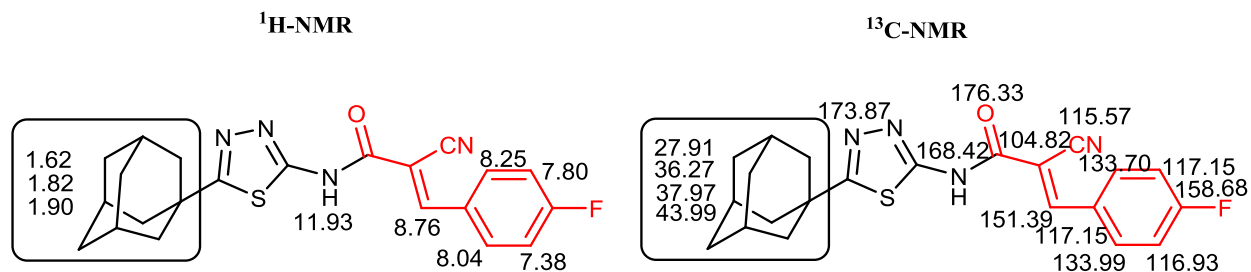


The chemical structure of **155** was assigned on the basis of the spectral and elemental analyses. The IR spectrum of compound **155a** as an example showed absorption bands at 3175 and 1652 cm^{-1} due to NH and amidic carbonyl functions respectively. The ^1H NMR spectrum of compound **155a** revealed the lack of CH_2 signal and the presence of one singlet signal at δ 13.89 ppm due to NH proton, beside a singlet signal at δ 8.38 for =CH methine and two doublets at δ 8.05 and δ 7.16 ppm with coupling constant (J = 8.8 Hz) for aromatic protons and singlet signal at δ 3.88 corresponding for OCH_3 . In addition, ^{13}C NMR of compound **155a** exhibited signals at δ 177.11, 115.41 and 56.17 ppm corresponding for C=O, CN and OCH_3 carbons over the presence of aromatic and adamantane carbons.

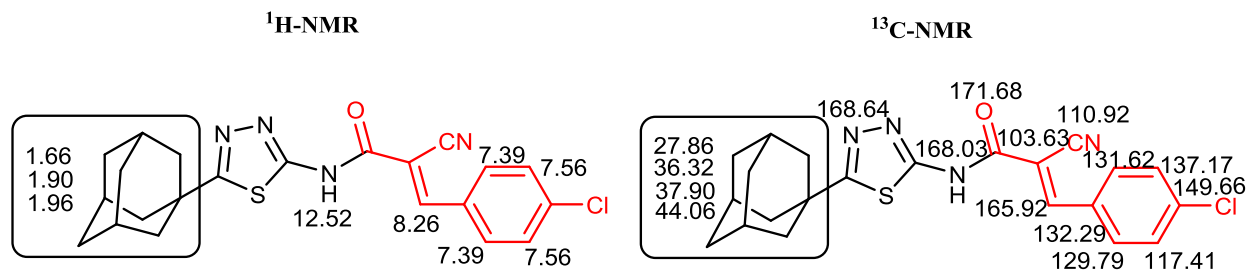
The ^1H -NMR and ^{13}C -NMR data of compound (**155a**) are shown in this figure



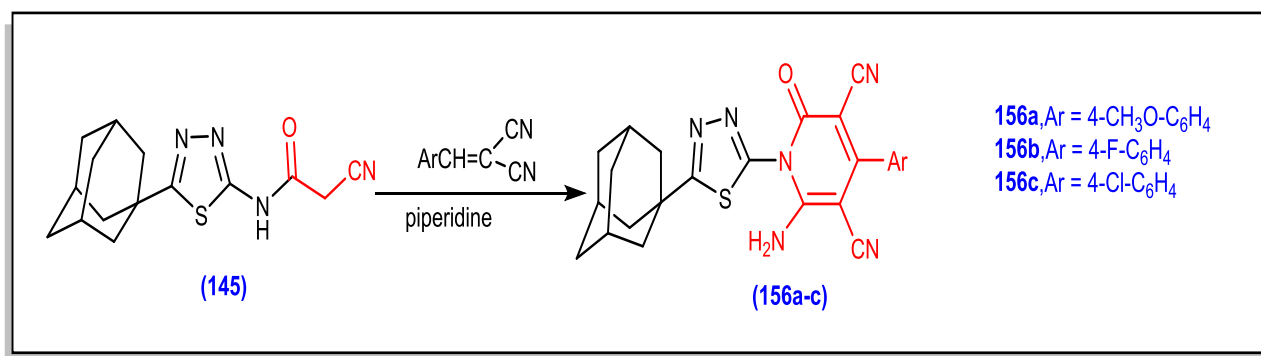
The ^1H -NMR and ^{13}C -NMR data of compound (**155b**) are shown in this figure



The ^1H -NMR and ^{13}C -NMR data of compound (**155c**) are shown in this figure

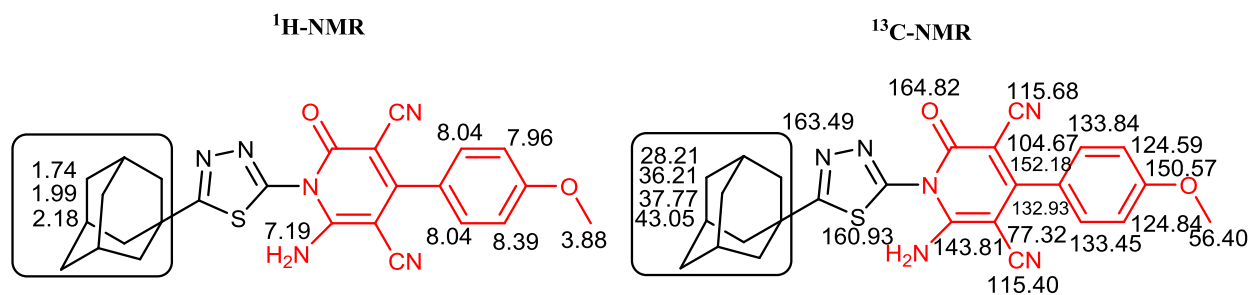


The author planned to synthesize some pyridine derivatives containing thiadiazole and adamantene moieties. Thus, the interaction of cyano-acetamide derivative **145** with arylidenemalononitriles in the presence of piperidine affected cyclization to yield the corresponding pyridine carbonitrile derivatives **156a-c**.

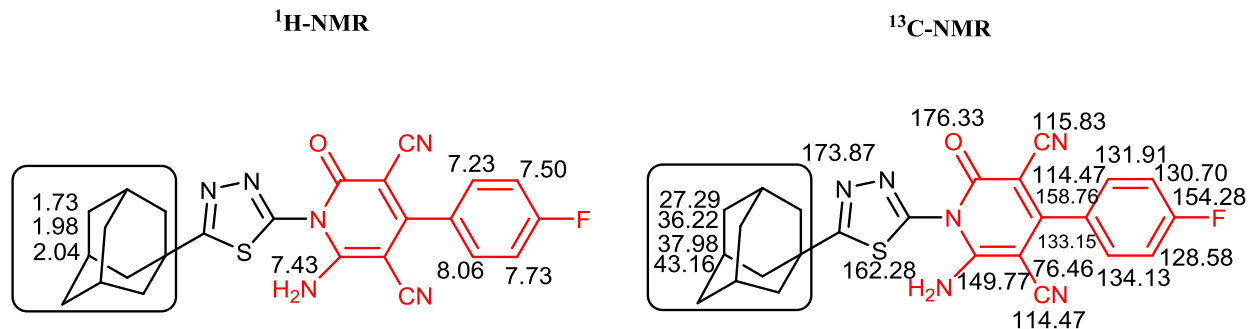


The structure of compound **156** was confirmed on the basis of its elemental analysis and spectral data. The IR spectrum of **156a** as an example showed absorption bands at 3314, 3172, 2223 and 1706 cm⁻¹ indicating the presence of (NH₂), two CN, and (C=O) groups, respectively. The ¹H NMR spectrum revealed the lack of CH₂ signal and the presence of singlet signal at δ 3.88 ppm due to OCH₃ protons beside signals in the region of δ 7.15-8.39 ppm for aromatic and NH₂ protons as well as the expected adamantane protons that appear as three singlet signals at δ 1.74, 1.99 and 2.18 ppm.

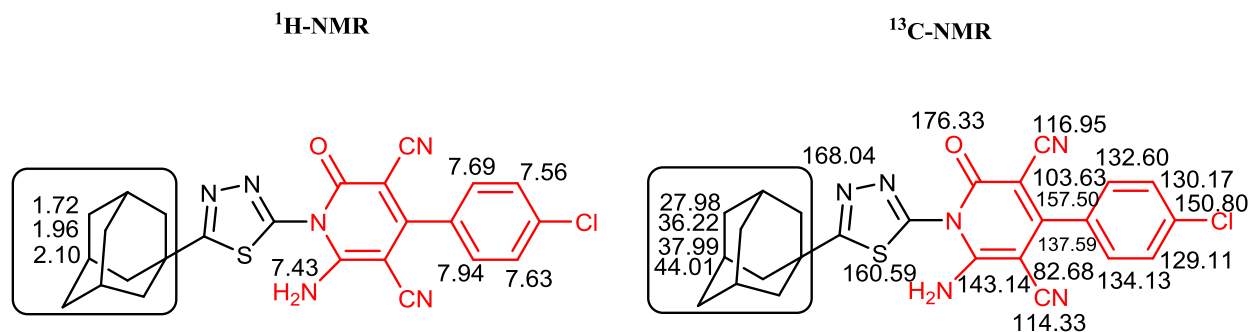
The ¹H-NMR and ¹³C-NMR data of compound (**156a**) are shown in this figure



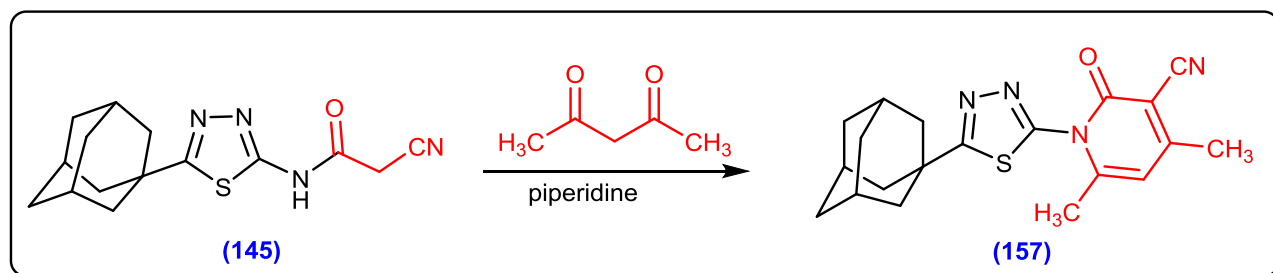
The ¹H-NMR and ¹³C-NMR data of compound (**156b**) are shown in this figure



The ¹H-NMR and ¹³C-NMR data of compound (**156c**) are shown in this figure

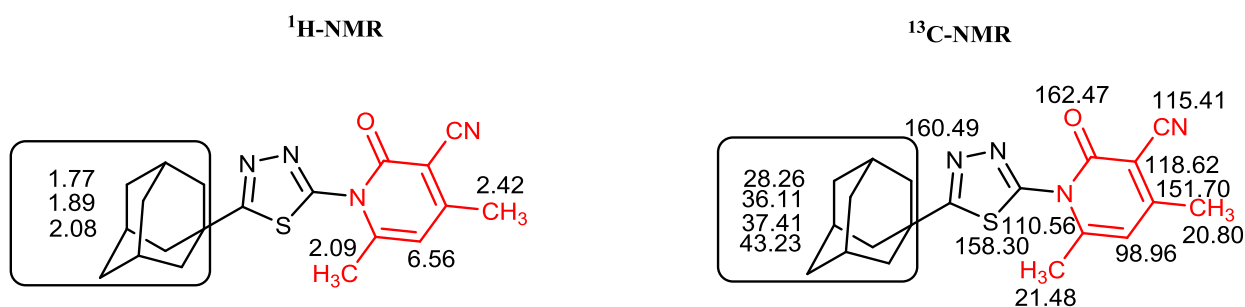


Reactivity of cyano-acetamide derivative with the 1,3-dicarbonyl compound was studied. Thus, compound **145** reacted with acetylacetone to give the pyridine derivative **157**.

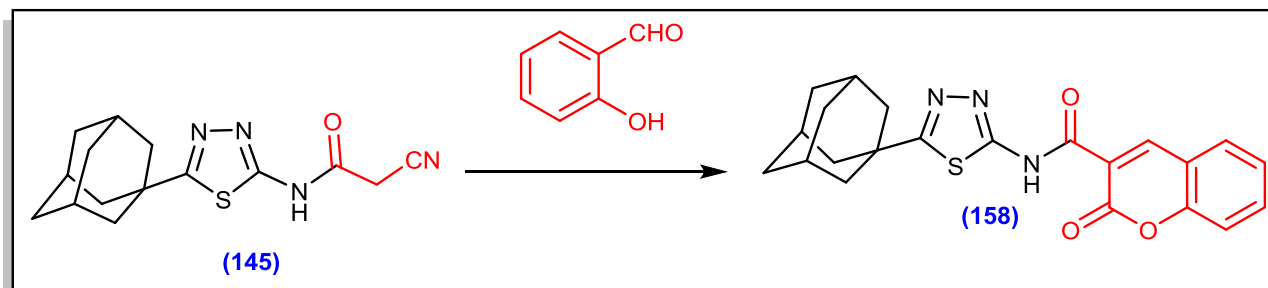


Structure of the latter product was based on analytical and spectral data. The IR spectrum of compound **158** showed the disappearance of NH band and exhibited two absorption bands at 2223 and 1668 cm^{-1} due to CN and C=O groups. While, its ^1H NMR spectrum revealed the appearance of three new singlets at δ 2.09, 2.42 and 6.56 ppm assigned to two methyl protons and the pyridinone *H*-5.

The ^1H -NMR and ^{13}C -NMR data of compound (**157**) are shown in this figure

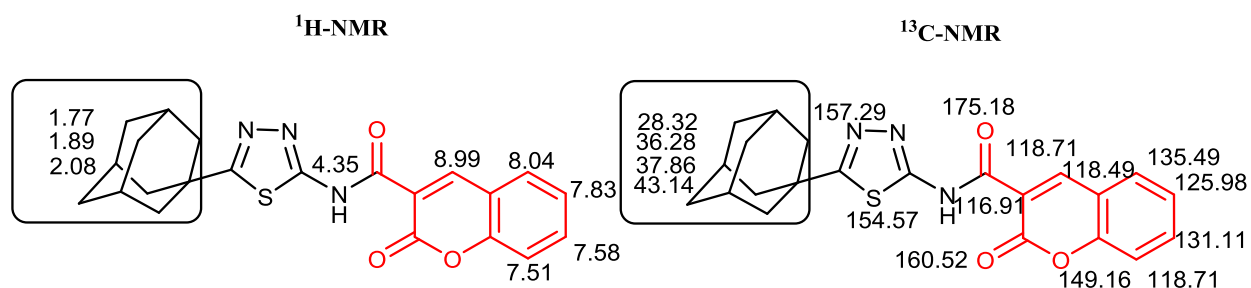


Furthermore, cyclo-condensation of compound **145** with salicylaldehyde in boiling ethanol containing a catalytic amount of piperidine afforded the coumarin derivative **158**.

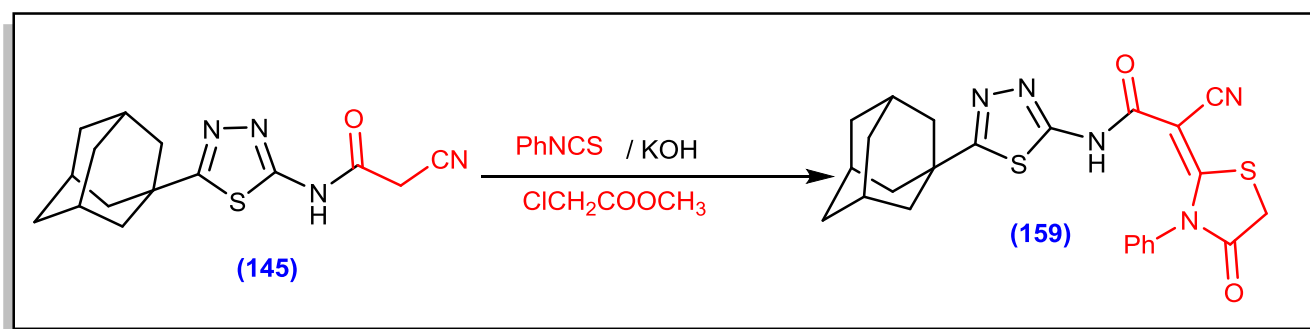


The IR spectrum of compound **158** showed the absence of cyano band that already present in the starting compound and the formed product exhibited the presence of two strong absorption bands at 1712 and 1695 cm^{-1} which prove the formation chromone ring. Its ^1H NMR spectrum revealed the absence of methylene signal and the presence of two singlet signals at δ 8.99 and 4.35 ppm due to chromone *H*-4, NH of amide derivatives. Besides, the presence of aromatic and adamantane protons. Its ^{13}C NMR spectrum is an agreement with the expected structure.

The ^1H -NMR and ^{13}C -NMR data of compound (**158**) are shown in this figure



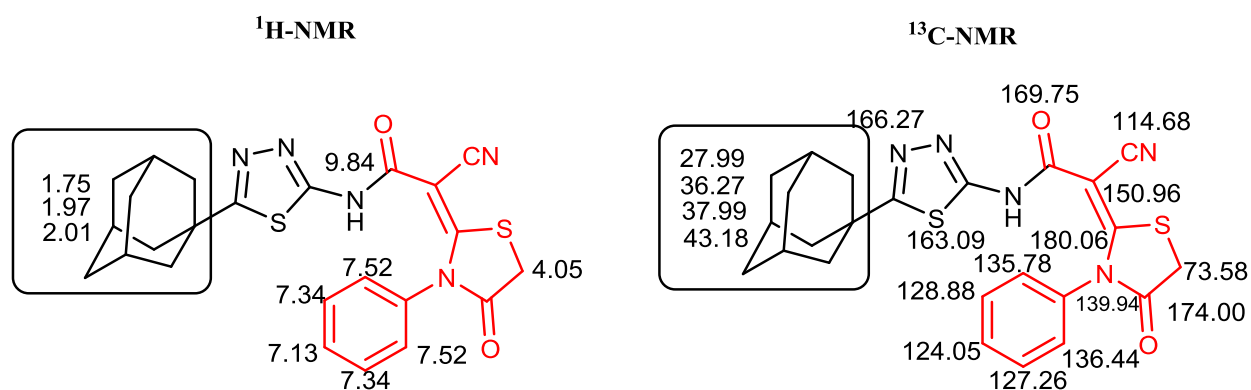
Finally, treatment of cyano-acetamide thiadiazole derivative **145** with phenyl isothiocyanate in DMF, in alkaline medium followed by treatment with methyl chloroacetate afforded the corresponding thiazolidinone derivative **159**.



The structure of thiazolidinone containing thiadiazolo-adamantane **159** was established on the basis of elemental analysis and spectral measurements. Its IR spectrum exhibited a strong absorption band at 1732 cm^{-1} for new carbonyl formed.

This band displayed a strong confirmation for the thiazolidinone nucleus formation. Another evidence for the cyclization occurred is the presence of a singlet signal at δ 4.05 ppm in the ^1H NMR spectrum equivalent to two protons for endocyclic methylene as well as signals at δ 7.13-7.52 ppm related to phenyl group and its ^{13}C NMR spectra aromatic carbons displayed between δ 124.05-136.44 ppm.

The ^1H -NMR and ^{13}C -NMR data of compound (**159**) are shown in this figure



2.2. Biological evaluation

2.2.5. Anti-proliferative activity with SAR study

The *in vitro* anti-proliferative activity of twenty-one 1,3,4-thiadiazole derivatives, **144-159** containing adamantane moiety were evaluated against a panel of three cell lines including mammary gland breast cancer cell line (MCF-7), human hepatocellular carcinoma cell line (HepG-2) as well as human lung adenocarcinoma epithelial cells (A549) by using sulforhodamine B colorimetric (SRB) assay according to reported methods^{138,139}. Doxorubicin (DOX) is one of the commonly used small molecular anti-cancer drugs, was selected to be the reference drug. The *in vitro* cytotoxicity of all the synthesized compounds are summarized in **table 1** and expressed by IC_{50} (μM) that means the concentration of compound or drug required to inhibit the growth of cancer cells by 50%.

The resulting data from **table 1** showed that adamantane-containing 1,3,4-thiadiazole have moderate to potency growth inhibitory effect against tested cell line (MCF-7, HepG-2 and A549) with IC₅₀ values ranged between (5.71 ± 0.37 to 21.47 ± 1.5), (4.28 ± 0.35 to 17.38 ± 1.35) and (4.11 ± 0.28 - 16.31 ± 1.2) μM in comparison to Doxorubicin (8.19 ± 0.72 , 7.46 ± 0.12 and 3.58 ± 0.03) μM respectively. Compounds **144**, **145**, **146**, **151**, **152a** and **152b** that containing thiadiazole having amide derivatives in position two showed that aromatic acetamide **152a**, **152b** revealed the highest active derivatives followed by benzamide, piperidinyl, chloro and cyanoacetamide derivatives (**152a** > **152b** > **146** > **151** > **144** > **145**), and 4-methoxy phenyl acetamide derivatives **152a** more active than 4-methyl derivatives **152b** with IC₅₀ values (6.44 ± 0.52 , 4.92 ± 0.35 and 4.61 ± 0.31 μM) (9.31 ± 0.85 , 7.67 ± 0.64 and 5.74 ± 0.44 μM) respectively. Thiazol-4-one derivatives **153** and **160** obtained from chloro and cyanoacetamide of thiadiazole adamantane derives by reacting with different reagents, and it found that *N*-phenyl thiazol-4-one derivatives **160** exhibited cytotoxic activity higher than its analogue **153** with IC₅₀ values ranged between (4.32 ± 0.25 to 6.51 ± 0.48) μM and in comparison, with Doxorubicin (3.58 ± 0.03 to 8.19 ± 0.72) μM . Amino thiadiazole derivatives with diacetyl derivatives **148** demonstrated a significant activity than 2-aminothiazole **149** with ethyl acetoacetate core where IC₅₀ values (8.41 ± 0.74 , 6.15 ± 0.5 and 5.77 ± 0.4 μM) and (18.22 ± 1.41 , 15.37 ± 1.05 and 13.81 ± 0.98 μM) against tested cell line (MCF-7, HepG-2, and A549), respectively that's due to the presence of ethyl acetate group decrease activity than acetyl group.

2-Cyanoacrylamide 1,3,4-thiadiazolo-adamantane derivatives **155a-c** showed moderate activity and chloro derivatives showed the most active member with IC₅₀ values (10.45 ± 0.93 , 8.22 ± 0.7 and 6.75 ± 0.55) μM for MCF-7, HepG-2 and A549 cell line respectively. *N*-Thiadiazole pyridine derivatives **156** and **157** exhibited

variable activity, and generally, the presence of di-cyanopyridine derivatives **156** exhibited more activity than mono-cyano derivative **156**, as well as the presence of aryl derivatives in compounds **156a-c**. Also, the presence of chloro derivatives causes higher activity than both fluoro and methoxy derivatives in position four in dicyanopyridine derivatives **156**. Simultaneously, it was found that 3-amide-2-oxo-chromene derivatives **158** decrease potency than other adamantane derivatives.

Finally, seven compounds **147**, **148**, **152a**, **152b**, **156b**, **156c** and **159** with 5-(adamantan-1-yl)-1,3,4-thiadiazole backbone core showed potent cytotoxicity with low micromolar ($<10 \mu\text{M}$) and most of these derivatives observed IC_{50} lower than doxorubicin on both MCF-7 and HepG-2 and nearly to reference against A 549 cell line with growth inhibitory ranged between 4.11 to 5.79 μM , besides, compounds **150**, **153**, **155a**, **155c** and **156a** with IC_{50} values between 6.75 to 9.74 μM .

Table 1: Cytotoxic screening of the newly designed compounds **144-159** and Doxorubicin against a three cancer cell lines (IC_{50} values are expressed in $\mu\text{M} \pm \text{S.E.}$).

Compound no.	$\text{IC}_{50} \mu\text{M} \pm \text{S.E.}^*$		
	MCF-7	HepG-2	A 549
144	14.32 ± 1.13	11.46 ± 0.93	10.67 ± 0.84
145	17.44 ± 1.32	15.72 ± 1.1	16.31 ± 1.2
146	12.37 ± 0.97	9.45 ± 0.76	10.18 ± 0.82
147	7.27 ± 0.68	5.83 ± 0.42	4.26 ± 0.35
148	8.41 ± 0.74	6.15 ± 0.5	5.77 ± 0.4
149	18.22 ± 1.41	15.37 ± 1.05	13.81 ± 0.98
150	11.28 ± 0.95	10.17 ± 0.92	9.74 ± 0.86
151	17.55 ± 1.23	13.64 ± 0.97	11.37 ± 0.95
152a	6.44 ± 0.52	4.92 ± 0.35	4.61 ± 0.31
152b	9.31 ± 0.85	7.67 ± 0.64	5.74 ± 0.44
153	14.61 ± 1.1	10.36 ± 0.91	9.38 ± 0.84
154	15.84 ± 1.14	13.49 ± 0.97	10.75 ± 0.85

155a	12.45 ± 0.98	10.77 ± 0.95	8.49 ± 0.75
155b	17.62 ± 1.35	14.92 ± 1.14	15.02 ± 1.16
155c	10.45 ± 0.93	8.22 ± 0.7	6.75 ± 0.55
156a	12.41 ± 1.1	10.37 ± 0.92	9.12 ± 0.76
156b	8.16 ± 0.69	6.75 ± 0.57	5.79 ± 0.41
156c	5.71 ± 0.37	4.28 ± 0.35	4.11 ± 0.28
157	17.39 ± 1.4	14.89 ± 1.1	12.55 ± 0.95
158	21.47 ± 1.5	17.38 ± 1.35	14.62 ± 1.2
159	6.51 ± 0.48	4.47 ± 0.3	4.32 ± 0.25
Dox.	8.19 ± 0.72	7.46 ± 0.12	3.58 ± 0.03

* Three independent experiments were performed for each tested compounds concentration.

2.2.6. Effect on normal cells

The cytotoxic activities of the new promising compounds **147**, **148**, **152a**, **152b**, **156b**, **156c** and **159** were evaluated on normal non-cancer cells (WI-38 cells) to determine the selectivity of the 2-amino-1,3,4-thiadiazole derivatives against cancer cell. The most potent compounds showed IC₅₀ values from 89.75 to 225.7 µM. From **table 2**, the selective index (SI) data indicated that adamantane core that attached to 1,3,4-thiadiazole derivatives exhibits a high degree of cytotoxic selectivity. For instance, compound **148** with pentane-2,3-dione alkyl group attached to the amino of 2-aminothiadiazole adamantane derivatives exhibited the safest compound with IC₅₀ (225.7 µM) and highest SI (26.84, 36.70 and 39.12) respectively. Simultaneously, *N*-1,2,4-thiadiazolo-di-cyanopyridine derivative **156c** with 4-chlorophenyl moiety in position four of pyridine showed IC₅₀ (89.75 µM) with SI (15.72, 20.97 and 21.84) to the tested cell line respectively.

Table 2: Cytotoxicity and selective index of the most promising compounds against the Human WI-38 cell line

Cpd. No.	IC ₅₀ μ M WI-38 Cells	SI*		
		MCF-7	HepG-2	A 549
147	97.55	13.42	16.73	22.90
148	225.7	26.84	36.70	39.12
152a	128.39	19.94	26.10	27.85
152b	178.41	19.16	23.26	31.08
156b	185.9	22.78	27.54	32.11
156c	89.75	15.72	20.97	21.84
159	112.75	17.32	25.22	26.10

*SI: Selectivity index = (IC₅₀ of WI-38)/ (IC₅₀ of cancer cell line).

2.2.7. Study on mitochondrial apoptosis pathway BAX and Bcl-2 proteins

The effect of the new design compound on the induced apoptotic process via mitochondria mediated pathway up-regulation of BAX and down-regulation of Bcl-2 was evaluated and the obtained data represented in **table 3**. Treatment of human lung adenocarcinoma epithelial cells (A549) with the most promising compounds **147,148, 152a, 152b, 156b, 156c**, and **159** expressed high levels of BAX and lower levels of Bcl-2 compared to untreated cells.

From **table 3**, it found that condensation of 2-aminothiadiazole with isatin to produce thiadiazole containing 2-oxoindole **147** exhibited the highest apoptosis induced by (BAX= 415.84 Pg/mL with 8.57 folds) than untreated cells, followed by enaminonitrile containing thiadiazole **156c** (BAX = 411.32 Pg/mL, 8.47 folds), and thiadiazole hybridized with *N*-phenyl thiazole **159** (BAX = 375.19 Pg/mL, 7.73 folds) and the other derivatives induced apoptosis from 6.13 to 7.02 folds higher than control. By the same way, the most promising derivative among the thiadiazole

derivatives that demonstrated the highest value in suppresses of apoptosis against BCL-2 thiadiazole containing enaminonitrile derivatives **156c** with BCL-2 value 1.42 Pg/mL (4.13 folds). Whereas compounds **147**, **148**, **152a**, **152b**, **156b** and **159** showed decrease Bcl-2 values from 3.06-1.75 Pg/mL and that decrease level by 1.92-3.35 folds.

Our study indicated that the promising derivatives **147**, **148**, **152a**, **152b**, **156b** and **159** exhibited chemo suppression/induction cancerous cells to apoptosis induction by changes in BCL-2 and BAX gene levels, depending on the variety of substituents that attached to 1,3,4-thiadiazolo adamantane.

Table 3: Effect of compounds **147**, **148**, **152a**, **152b**, **156b** and **159** on gene expression BAX and BCL-2 as apoptosis markers

Cpd. No	Bax (Pg/mL)	Fold	Bcl ₂ (Pg/mL)	Fold
147	415.84	8.57	1.75	3.35
148	331.75	6.83	2.54	2.31
152a	340.55	7.02	2.19	2.64
152b	329.71	6.79	2.71	2.16
156b	297.46	6.13	3.06	1.92
156c	411.32	8.47	1.42	4.13
159	375.19	7.73	1.88	3.12
A549 cells	48.51	1	5.87	1

2.2.8. EGFR inhibition assay

Epidermal growth factor receptor (EGFR) consider an attractive and clinically validated drug target in cancer therapy because it is important for various biological processes and cancers development and progression, such as cell proliferation, adhesion, migration, differentiation, and survival. EGFR can cause dysregulation by two different mechanisms one of them is the high expression of EGFR that lead to increase receptor signaling output. In contrast, the second mechanism involves the

overexpression of ligand and therefore increase EGFR signaling activity despite normal or even low levels of receptor expression¹⁴⁰⁻¹⁴². Depending on the results of antiproliferative activity, we selected the most promising compounds **147**, **148**, **152a**, **152b**, **156b** and **159** for EGFR enzymatic activity assays using A549 cancer cells to elucidate the mechanism of these active compounds.

From **table 3**, the results of wide type EGFR on A549 cancer cells expressed as the half-maximal inhibitory concentration IC₅₀ (μM). All the promising compound investigated EGFR^{WT} inhibitory assay less than 2 μM. 3,5-Dicyano-pyridine that containing 4-chlorophenyl derivatives as well as backbone core 1,3,4-thiadiazole adamantane **156c** exhibited the most potent derivatives with IC₅₀ values 0.085 μM while the fluoro derivative **156b** showed to be the least inhibitor towards EGFR in comparison to the tested compounds and Lapatinib that used as a positive control EGFR^{WT} IC₅₀ (0.0318 μM). Schiff base derivative **147** of 1,3,4-thiadiazole adamantane with isatin observed 50% inhibition of EGFR^{WT} expression at 0.352 μM. Moreover, compound **159** bearing 2-cyano-2(*N*-phenylthiazolidin-2-ylidene-4-one) acetamide derivatives were found to be active inhibitor (IC₅₀ = 0.715 μM) against overexpression of EGFR^{WT}. Compounds **148**, **152a** and **152b** inhibited the enzymatic activity against EGFR^{WT} with IC₅₀ values (1.32, 0.954 and 1.27) μM.

Table 4: IC₅₀ of the representative anticancer active compounds on different EGFR kinases assay.

Cpd. No.	Enzyme inhibitory activity IC ₅₀ [*]		
	EGFR ^{WT} (μM)	EGFR ^{L858R-TK} (nM)	EGFR L/T ^{**}
147	0.352	41.19	0.788
148	1.32	63.48	-
152a	0.954	52.11	-
152b	1.27	55.28	-
156b	1.96	70.49	-
156c	0.085	37.85	0.467

159	0.715	40.58	0.278
Lapatinib	0.0318	39.53	0.182
Erlotinib	0.0656	59.56	0.218

* data are average of three independent results.

**EGFR L/T= double mutant EGFR L858R/T790M, (-) mean not determined.

Due to the important of EGFR that can define as a member of the membrane-bound receptor tyrosine kinase family and when activated, transduce mitogenic signals¹⁴³. The most promising compounds were selected for further *in vitro* mutant EGFR^{L858R-TK} that expressed by IC₅₀ (nM) to evaluate the activity and selectivity of newly designed compounds. Compound **156c** showed the most potent inhibitory activity against EGFR^{L858R-TK} with IC₅₀ (37.85 nM) in comparison to Lapatinib as a positive control (IC₅₀= 39.53 nM). Both compounds **147** and **159** showed equipotent to a standard drug with IC₅₀ values (41.19, 40.58 nM), respectively compared to Erlotinib (59.56 nM). Chloroacetamide thiadiazole derivatives **144**, when reacted with different aromatic amine (4-methoxy and 4-methyl) to produce acetamide derivative with aromatic core observed activity with 52.11 and 55.28 nM with 30 % less than Lapatinib and still observed inhibitory activity better than Erlotinib 59.56 nM. Surprisingly, compound **156b** that demonstrated the least inhibitor towards EGFR^{WT} observed IC₅₀= 70.49 nM against EGFR^{L858R-TK} with nearly 56% less than the positive control. Most of the tested compounds revealed IC₅₀ values higher than Erlotinib except **148**, **156b** against EGFR^{L858R-TK}.

Our work was extended to study the most promising three derivatives **147**, **156c** and **159** against further kinase EGFR^{L858R/T790M} double mutant with Lapatinib and Erlotinib as reference drugs and as expected they inhibited the enzymatic activity against EGFR^{L858R/T790M} with IC₅₀ values ranged between (0.27-0.78 nM) compared to Lapatinib (0.1823 nM) and Erlotinib (0.218 nM). Thiazolidinone derivative **159** exhibited the highest values with 0.278 nM in comparison to enaminonitrile pyridine

derivative **156c** (0.467 nM) and Schiff bases **147**(0.788 nM), and that may be due to presence of thiazolidinone moiety beside thiadiazolo-adamantane backbone core.

2.2.9. Cell cycle analysis

Depending on the antiproliferative activities, BAX, BCL-2 gene expression as well as single and double mutant EGFR results that obtained previously. The most promising three derivatives **147**, **156c** and **159** were selected and investigated for cell cycle progression and the apoptosis percentage induced by the help of adamantane derivatives on human lung adenocarcinoma epithelial cells (A549) when treated with 5 μ M. The obtained data represented in **table 5** and **fig. 2& 3**.

It is observed that after 24h, the tested compounds exhibited PreG1 apoptosis & cell growth arrest in A549 at G2/M phase. Thiadiazole containing both isatin or thiazole as hybrid molecule derivatives **147**and **159** beside adamantane core causes accumulation of A549 cell at G0-G1 phases by 41.29 and 39.58 percentage respectively as well as, increase G2/M phase percentage by 26.64 and 26.29 % in comparison to untreated cells 14.38 %. While, enaminonitrile pyridine derivatives that are having both *p*-chlorophenyl moiety and adamantyl thiadiazole core revealed cell cycle arrest by 42.09, 29.67 and 28.24 % for G2/M, S and G0-G1 phases respectively. Also, enaminonitrile pyridine derivatives **157c** cause apoptosis and detain the cell cycle in both G2/M and PreG1 by 74.50 percent. Although, both thiadiazole adamantane derivatives **147** and **159** causes increase the content of DNA in G0-G1 and S phases by nearly 73.36 and 73.71 % respectively. Surprisingly, the most promising compounds **147**, **156c** and **159** induced apoptosis at pre-G1 phases by ranged from 16.59 to 32.41 % in comparison to A549 cell by 1.86 %.

Finally, our designed thiadiazolo-adamantane derivatives with different substituent **147**, **156c** and **159** used as inhibitors for cancer cell and induced apoptosis in different phases.

Table 5: Cell cycle analysis by percentage in different phases after treatment the lung cancers cell A549 with 10 μ M of thiadiazolo-adamantane derivatives **147**, **156c** and **159**

Compound No.	Results			
	%G0-G1	%S	%G2/ M	%Pre-G1
147	41.29	32.07	26.64	19.11
156c	28.24	29.67	42.09	32.41
159	39.58	34.13	26.29	16.59
cont. A549	46.93	38.69	14.38	1.86

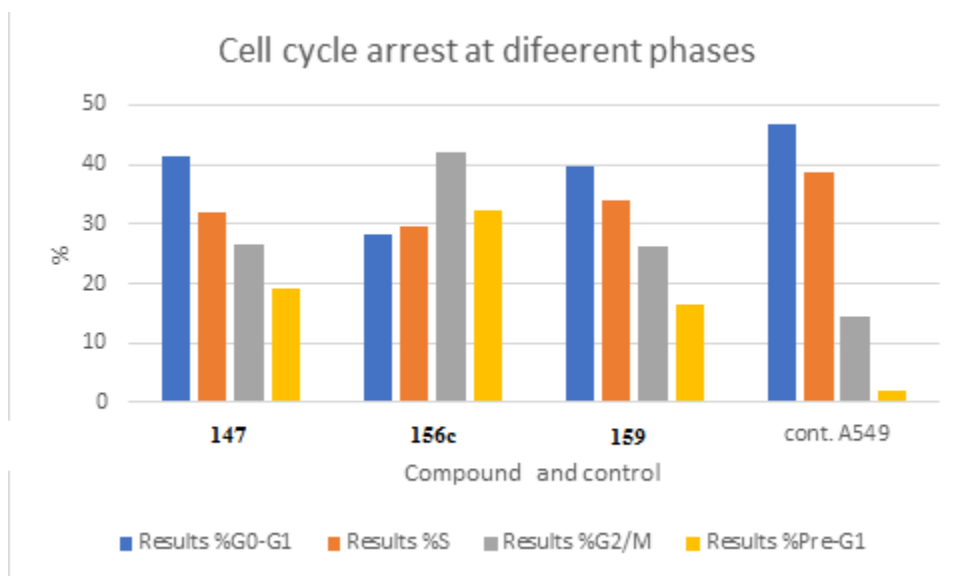
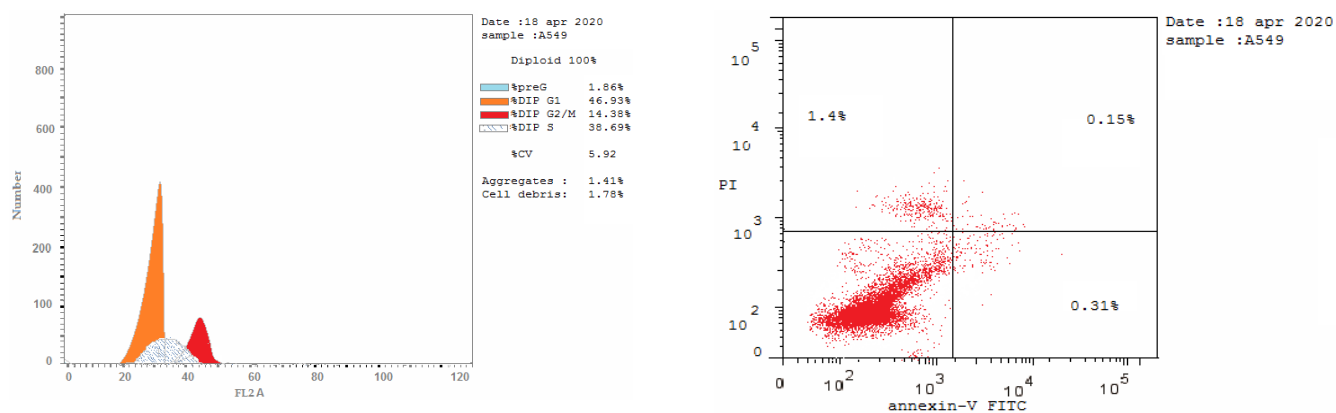
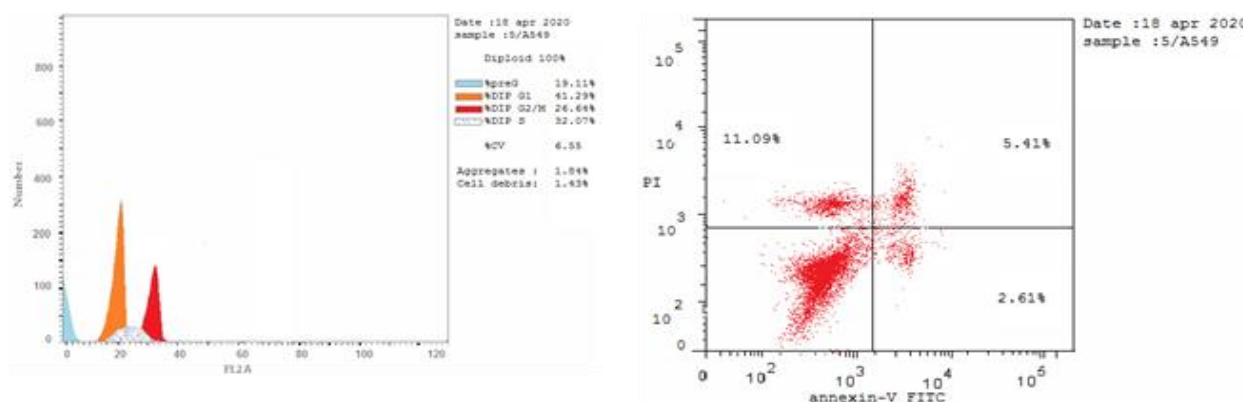


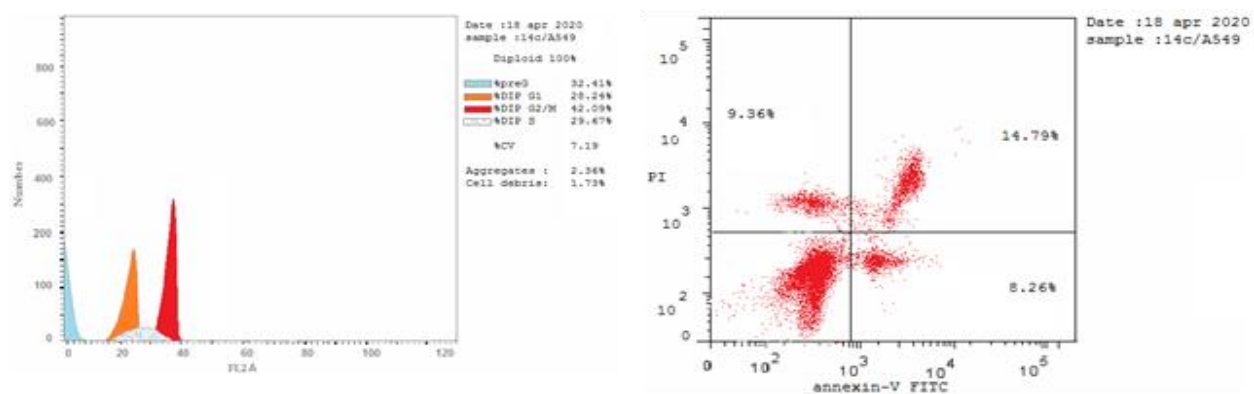
Figure 2: Diagram illustrated cell cycle arrest of the most potency thiadiazole-adamantane derivatives **147**, **156c** and **159** at different phases by percentage



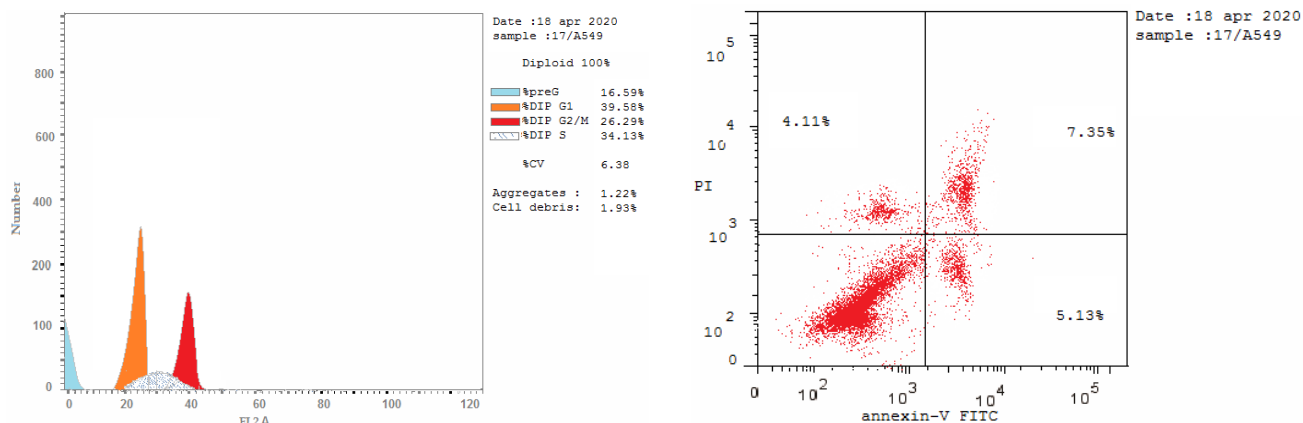
(a) Control A549



(b) 147/ A549



(c) 156c/ A549



(d) 159/ A549

Figure 3: Cell cycle analysis (a) Control A549, (b) 147/A549, (c) 156c/ A549 and (d) 159/ A549.

2.2.10. Apoptotic assay

To determine the mechanism of cell death and apoptosis-inducing effect double staining Annexin V/propidium iodide was used through flow cytometry method^{138,139}, where apoptosis can be defined as an active and regular pathway. At the same time, necrosis is a passive and accident cell death¹⁴⁴. The thiadiazolo-adamantane derivatives **147**, **156c** and **159** were treated with 5 μ M and incubated for 24h on A549 cell, and the obtained data showed in **table 6** and **fig. 4**.

We detected an increase in the total percentage of apoptosis because of the adamantane derivatives that exhibit total apoptosis ranged from 16.59 % to 32.41 % compared to 1.86 % for standard A549 cells. By the same way, it observed that the enaminonitrile pyridine derivative **156c** is the highest induction of total cell apoptosis (32.41 %) by nearly 17.42 folds. Moreover, the percentage in early-stage varies from 2.61, 5.13 and 8.26% for **147**, **156c** and **159** respectively.

Finally, it can conclude that the effect of most promising three derivatives **147**, **156c** and **159** when treatment on A549 leads to an increase in the sensitivity to apoptosis

by different percentage in different stages and therefore increase total apoptosis percentage and these data support the higher values on antiproliferative against A549 ($< 5 \mu\text{M}$).

Table 6: percentage of cell death after treatment with most promising compounds **147**, **156c** and **159**

Cpd. No.	Apoptosis			Necrosis
	Total	Early	Late	
147	19.11	2.61	5.41	11.09
156c	32.41	8.26	14.79	9.36
159	16.59	5.13	7.35	4.11
A549	1.86	0.31	0.15	1.4

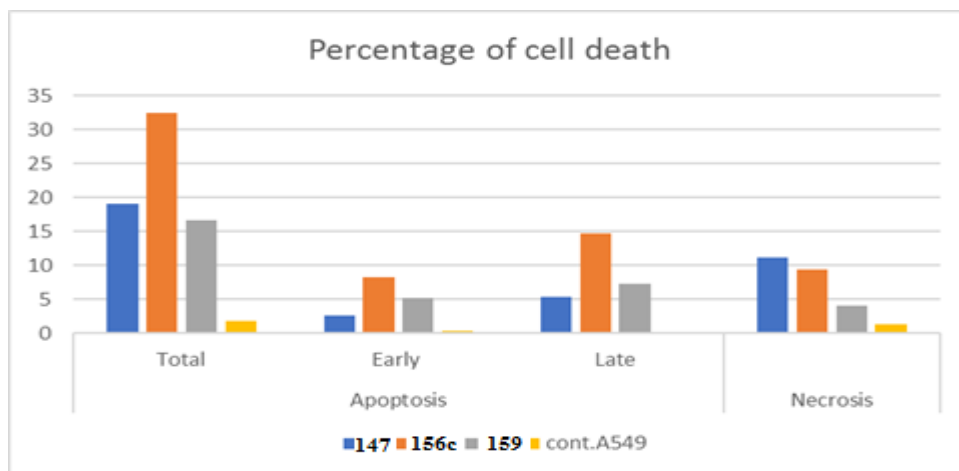


Figure 4: illustrate the different percentage of cell death by thiadiazolo-adamantane derivatives **147**, **156c** and **159**.

2.2.11. In silico studies

2.2.12. Evaluation of physicochemical, and some pharmacokinetic prediction parameters

Physicochemical parameters (oral bioavailability) for both Lipinski's and Veber rules were determined for the most promising compounds as well as Lapatinib and Erlotinib using Swiss ADME: a free web tool ¹⁴⁵. From data in **table 7**, the most promising **147**, **156c** and **159** obey RO5 criteria without no violations from Lipinski's Rule, and both enaminonitrile **156c** and thiazolo-thiadiazole adamantane derivatives **160** failed to pass through Veber rule by Topological polar surface area (TPSA) higher than 140 Å². For two standard drugs, Erlotinib pass in both rule of five and Veber rule while Lapatinib met the RO5 with one violation in MW >500 and passed in Veber rule.

By the same way, some Pharmacokinetics properties were studies depending on Swiss ADME: a free web tool involving Gastrointestinal absorption and blood brain barrier. Compounds **156c** and **159**, as well as Lapatinib, showed low Gastrointestinal absorption with no permeation to blood brain barrier while Schiff's base **147** and Erlotinib exhibited high absorption to Gastrointestinal track. Furthermore, Erlotinib pass through the blood brain barrier but the most promising displayed no promotion.

Finally, our new promising compounds exhibited not only promising activity, but also some oral bioavailability beside pharmacokinetics properties as Lapatinib and Erlotinib.

Table 7: *In silico* the physicochemical and Pharmacokinetics properties of the thiadiazolo-adamantane derivatives **147**, **156c** and **159** as well as standard drugs (as Lapatinib and Erlotinib)

Cpd. No.	Lipinski's Rule				Veber filter		Pharmacokineti	
	MW < 500	MLog P	nHB A	nHBD < 5	nRB < 10	TPSA < 140 Å ²	GI	BBB
147	364.46	3.35	4	1	2	95.48	High	No
156c	488.99	3.26	5	1	3	149.62	Low	No
159	477.60	2.46	5	1	5	152.52	Low	No
Lapatinib	581.06	3.44	8	2	11	114.73	Low	No
Erlotinib	393.44	1.89	6	1	10	74.73	High	yes

* MW; Molecular weight, MLogP; an octanol–water partition coefficient, nHBA; no. of hydrogen bond acceptor, nHBD; no of hydrogen bond donor, nRB; no. of rotatable bond.

2.2.13. Molecular docking study

To explore the possible binding conformation and got deeper insights of the structure activity relationship as well as understanding the potency of the newly designed thiadiazolo-adamantane derivatives **147**, **156c** and **159** molecular docking simulation was performed with the ATP binding pocket of EGFR PDB (1M17)¹⁴⁶. From **table 8**, it was found the co-crystalized ligand 4-anilinoquinazoline inhibitor (Erlotinib) exhibited self-docking process with small RMSD= 1.99 °Å and binding energy S= -19.10 Kcal/mol, through one hydrogen bond backbone acceptor with Met769 with the nitrogen of quinazoline with bond length 3.13 °Å and bound strength 16%. All the tested compound inside the active site revealed binding energy between -22.07 to -19.19 Kcal/mol higher than Erlotinib (**figure 5-8**).

Hydrazone containing 2-oxo-indole as well as thiadiazolo-adamantane derivative demonstrate one hydrogen bond donor from side chain Asp831 with NH of isatin moiety through bond length (2.54 °Å), and displayed binding energy S= -19.19 Kcal/mol. Enaminonitrile pyridine derivative **156c** showed the highest binding

energy score $S = -22.07$ Kcal/mol with one hydrogen bond backbone acceptor between Met769 (the same amino acid binding with Erlotinib) with cyano group in enaminonitrile derivative with bond length 3.18°A (22%). Hybrid structure **159** that containing *N*-phenyl thiazole beside backbone moiety (thiadiazolo-adamantane) displayed binding energy $S = -21.78$ Kcal/mol through two amino acid residue Asp 831 and Lys721 with bond length 2.81°A (45%), 2.60°A (51%) respectively.

Finally, the most promising derivatives investigated binding energy higher than the co-crystallized inhibitor (Erlotinib) as well as adamantane moiety displayed hydrophobic interaction inside the active site of pocket.

Table 8: Docking results of the most promising adamantane derivatives with binding energy and interacting group with specific amino acids in residue inside active side 1M17

Cpd. No.	(S) (Kcal/mol)	Amino acids	Interacting groups	Length ($^\circ\text{A}$)	Strength %
Erlotinib	-19.10	Met769	N of quinazoline	3.13	16
147	-19.19	Asp831	NH of isatin	2.54	49
156c	-22.07	Met769	CN of Enaminonitrile	3.18	22
159	-21.78	Asp831	NH of 2-	2.81	45
		Lys721	aminothiazole	2.60	51
			CN of cyanoacetanilide		

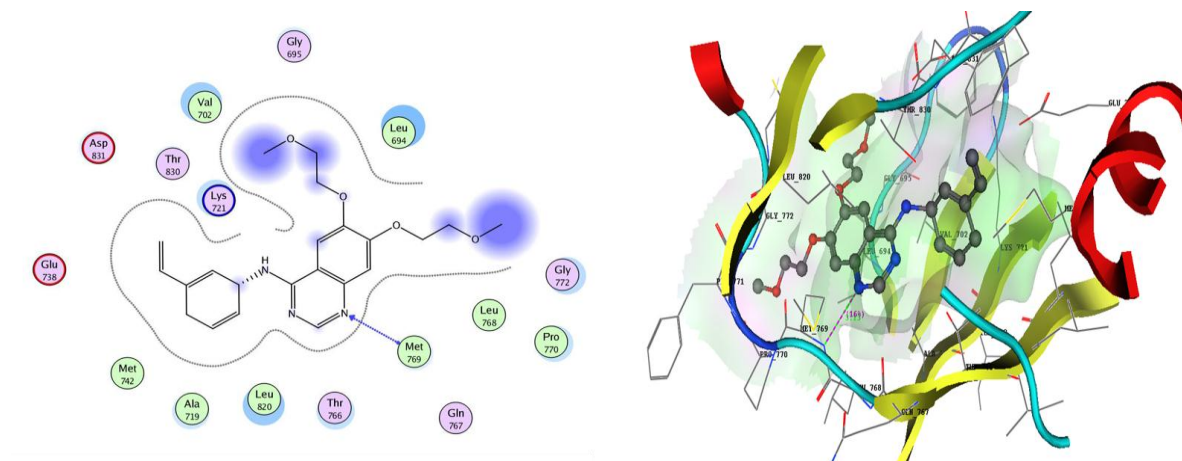


Figure 5: 2D & 3D interaction maps of **Erlotinib** inside 1M17 active site

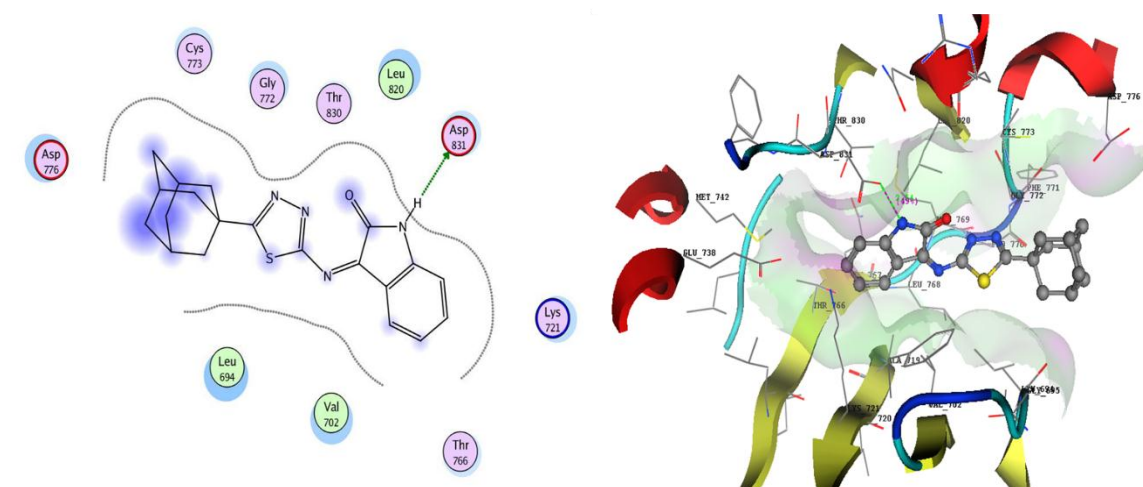


Figure 6: 2D & 3D interaction maps of compound **147** inside 1M17 active site

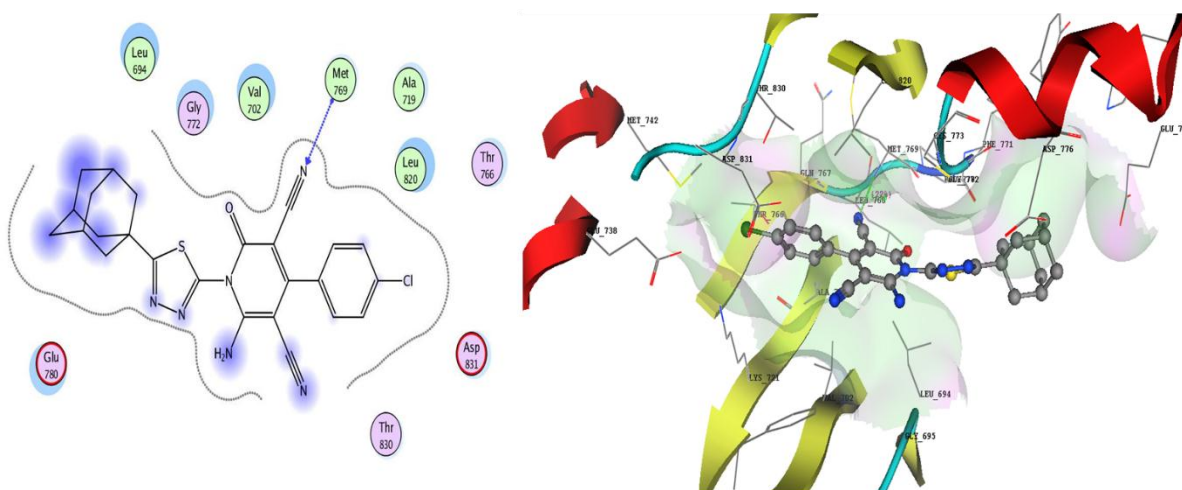


Figure 7: 2D & 3D interaction maps of compound **156c** inside 1M17 active site

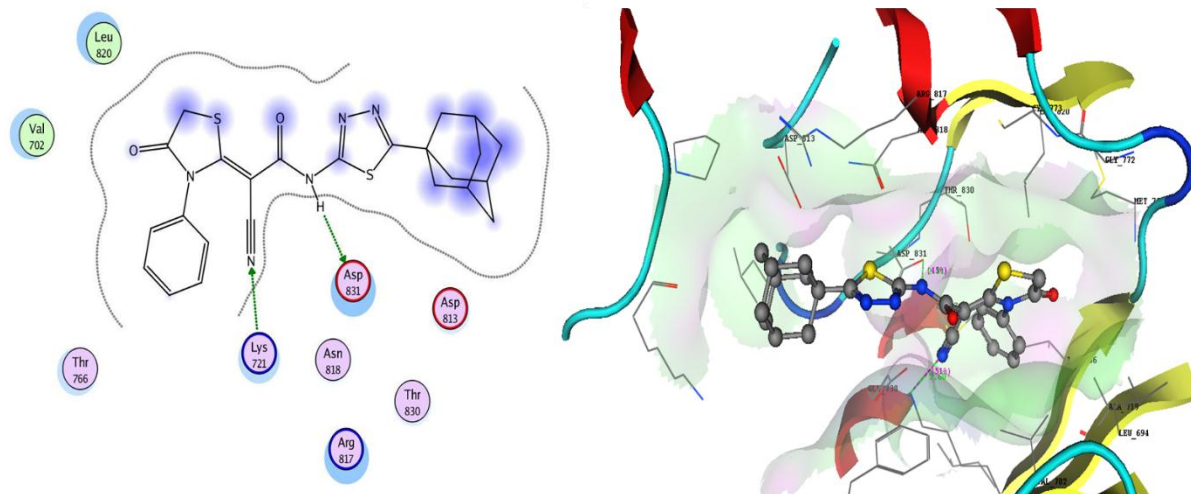


Figure 8: 2D & 3D interaction maps of compound **159** inside 1M17 active site

3. Conclusion

A novel series of twenty-one 1,3,4-thiadiazolo-adamantane derivatives were designed and synthesized starting from 5-(adamantan-1-yl)-1,3,4-thiadiazol-2-amine (**143**). The newly synthesized derivatives **144-159** were evaluated *in vitro* for their anti-proliferative activity against the selected three cell lines. The structure of the new design compounds was established and confirmed based on its elemental analysis and spectral data. Cytotoxic values showed a broad spectrum of the designed compounds against three cell lines (MCF-7, HepG-2 and A 549), and seven compounds **147**, **148**, **152a**, **152b**, **156b**, **156c** and **159** with 5-(adamantan-1-yl)-1,3,4-thiadiazole backbone core showed potent cytotoxicity with low micromolar ($<10\ \mu\text{M}$). Moreover, the most potent compounds showed IC_{50} values from 89.75 to 225.7 μM against normal non-cancer cells (WI-38 cells) as well as exhibited chemo suppression/induction cancers cells to apoptosis induction by changes in BCL-2 and BAX gene levels. All the promising compound investigated EGFR^{WT} inhibitory assay less than 2 μM . Besides, compound **156c** showed the most potent inhibitory activity against $\text{EGFR}^{\text{L858R-TK}}$ with IC_{50} (37.85 nM) in comparison to Lapatinib as a

positive control (IC_{50} = 39.53 nM) and Erlotinib (IC_{50} = 59.56 nM). Both compounds **147** and **159** showed equipotent to the standard drug with IC_{50} values (41.19, 40.58 nM), respectively. Furthermore, the most promising three derivatives **147**, **156c** and **159** against further kinase EGFR ^{L858R/T790M} double mutant exhibited IC_{50} values ranged between (0.27-0.78 nM) compared to Lapatinib (0.1823 nM) and Erlotinib (0.218 nM). Study cell cycle analysis observed that the enamionitrile pyridine derivative **156c** induced apoptosis and arrest the cell cycle by 74.50 % in both G2/M and PreG1. While the presence of both thiadiazole adamantane derivatives **147** and **159** causes increase the content of DNA in G0-G1 and S phases by nearly 73.36 and 73.71 % respectively. The most potent adamantane derivatives **147**, **156c** and **159** showed an increased sensitivity to the total percentage of apoptosis from 16.59 % to 32.41 % compared to 1.86 % for standard A549 cells. Finally, molecular docking study revealed that the promising compounds deeply bounded inside the active site of pocket as Erlotinib with binding energy between -22.07 to -19.19 Kcal/mol higher than Erlotinib S= -19.10 Kcal/mol, as well as the assessment of oral bioavailability (Lipinski's and Veber rules) beside some pharmacokinetics properties.

ANTIVIRAL ACTIVITY



Antiviral activity of Adamantane-Pyrazole and thiadiazole derivatives against Foot and Mouth Disease Virus infection in Vivo and in Vitro with Molecular docking study

Foot-and-mouth disease (FMD) is one of the most economically and publicly devastating diseases that affects cloven-hoof animals including cattle, sheep, swine and goats ¹⁴⁸. Upon infection with the FMD virus (FMDV), following clinical signs include fever, in appetite, lameness, and the appearance of vesicular lesions in the mouth, snout, teats, and feet ¹⁴⁹. The FMDV belongs to the genus Aphthovirus within the family Picornaviridae, and is a small, non-enveloped virus, which has a single-stranded positive sense RNA genome. The virus consists of seven distinct serotypes O, A, C, Asia-1 and Southern African Territories (SAT) 1–3 and as multiple subtypes due to the high mutation rate of the virus ¹⁵⁰. The viral capsid consists 60 copies of four structural proteins (VP1, VP2, VP3, and VP4).

Although FMD vaccines have been accessible since the early 1900s and new novel vaccines are being continuously established, including inactivated whole virus vaccines, new inactivated whole virus marker vaccines and subunit vaccine. These vaccines do not offer early complete clinical protection up to seven days' post-vaccination and also they offer little or no cross-protection against various serotypes and subtypes of FMDV. Therefore, there is a necessity for developing an effective and safe alternative antiviral approaches against FMDV ¹⁵¹. Therefore, finding an effective antiviral agent against FMDV infection is necessary to control incidence of foot and mouth disease virus infection and thus saving some bad economic impact which may occur upon infection.

Adamantane derivatives have found numerous applications indifferent fields of chemistry, but their use in catalysis ¹⁵².and medicinal chemistry ¹⁵³ which has been especially fruitful. With a low molecular weight and highly symmetric structure, adamantane fragments provide a domain with critical lipophilicity with a molecular

diameter of 6.36 Å¹⁵⁴. when inserted in the structure of known pharmacophores, improving pharmacokinetic profiles of the modified drugs¹⁵⁵. Simple amino adamantane (amantadine) have occupied a reliable place in the pharmaceutical market, showing their efficiency for the treatment of viral diseases as influenza A, herpes, hepatitis C and HIV¹⁵⁶.

However, the release of virions from cells infected with FMDV was inhibited by amantadine, a viroporin inhibitor such as amantadine that closes transmembrane pores in host cells via oligomerization.¹⁵⁷, the virus titer decreased as the amantadine concentration increased, which suggests that amantadine inhibited the release of the virus from the cells and that viroporins may be involved in this process.

In this study, we examined the antiviral efficacy of nine adamantane pyrazole and thiadiazole derivatives in vitro and in vivo in comparison with Amantadine against foot and mouth disease virus.

MATERIAL AND METHODS: -

Ethical approval:

The experiment was carried out according to the protocol of the Institutional Animal Ethics Committee, and the authors had permission of the Lab animal isolator.

FMD Virus serotype:

Local Foot and Mouth disease virus serotypes O pan Asia propagated in Baby Hamster Kidney (BHK₂₁) cell line monolayer was supplied by the Department of Foot and Mouth Diseases Research, Veterinary Serum and Vaccine Research Institute. The titer of the serotype was expressed as log₁₀TCID₅₀/ml as calculated by Reed and Muench method¹⁵⁸. Virus stocks were prepared as aliquots of culture medium from BHK-21 cells infected and stored at -70 °C. Working stocks were prepared and titration of the virus by serial dilution in culture medium.

Cell culture:

Baby Hamster kidney cell line (BHK21) was supplied by Veterinary Serum and Vaccine Research Institute, Abbasia, Cairo using Eagle's medium supplemented with

8-10% bovine serum, 60 g/ml Penicillin G and 100 g/ml Streptomycin sulfate maintain at 37 °C. All medium components were obtained from Sigma Chemical Co.,¹⁵⁹.

Suckling baby mice:

Suckling Swiss baby mice, two to four days old, (Charles River Strain, USA) were supplied by Laboratory Animal Department, Veterinary Serum and Vaccine Research Institute (VSVRI), Abbasia, Cairo.

Chemistry of antiviral agent:

Our previous study reported the design and synthesis of novel series adamantane-pyrazole¹⁶⁰ and differed in substituents in three carbon of pyrazole, as showed in **table1**. The pyrazole derivative relationship revealed that pyrazole derivative **134** contains thiomethyl group and enaminonitrile, while compound **135** involves enaminonitrile only and pyrazole **136** involved acetamide derivative beside the cyano group. Pyrazole derivative **140a** showed three substituents as phenyl, tolyl, and methylene Amantadine carbohydrazide derivative. Similarly, diamino-pyrazole derivatives **140a, b** displayed the difference in an azo-aryl group (phenyl **140a**, and *p*-methoxy phenyl **140b**). Finally, di-aryl pyrazoles **141a-c** demonstrated two aryl groups at positions three and five to pyrazole nucleus and also design and synthesis of novel series adamantane-thiadiazole as showed in **table 2**. Compounds **144, 145, 146, 147, 148, 149, 151, 152a** and **152b** that containing thiadiazole having amide derivatives in position two showed that aromatic acetamide, self-cyclization of **144, 145** to furnish the corresponding **150** and **154**, Thiazol-4-one derivatives of **153, 159** obtained from chloro and cyanoacetamide of thiadiazole adamantane derives by reacting with different reagents, Condensation of cyano-acetanilide thiadiazole derivative **145** with some aromatic aldehydes namely (4-methoxy or 4-chloro or 4-fluoro benzaldehyde) afforded the corresponding acrylamide derivatives **155a-c**, *N*-Thiadiazole pyridine derivatives **156** and **157** exhibited variable activity and cyclocondensation of compound **145** with salicylaldehyde afforded the coumarine derivative **158**.

The compound samples were prepared for assay by dissolving 0.01% of DMSO and diluting aliquots into sterile culture media at 0.1 gm/10 mL stock solution of different compounds which it was filtered through a 0.2 μ cellulose acetate membrane (Millipore). The different concentrations of tested compounds (**131, 134, 135, 136, 140a, b, 141a-c, 142a-c, 144,145,146,147,148,149,150,151, 152a, b, 153, 154, 155a-c, 156a-c, 157, 158 and 159**) used as antiviral were 20 to 4000 μ g/mL in triplicates in the wells of microtiter plates.

Determination of Cytotoxic Activity:

Cytotoxicity of different compounds against BHK-21 cells were analyzed based on cellular and morphological changes in a monolayer of cells under light microscope and viable cell count by trypan blue dye exclusion method¹⁶¹. In brief, different concentrations of the compounds were prepared in Glasgow minimum essential medium (GMEM). BHK 21 cells (1x10⁴cells/well) were propagated in 96 well cell culture plates in the presence of diluted compounds (starting from 20 to 4000 ug/ml) by co cultivation method and incubated at 37 °C for 48 hr with appropriate cell control. Cells were observed after 24 h interval for visible morphological changes under inverted microscope and the treated wells were compared with the untreated wells. The total viable cell and viable cell (%) was calculated in comparison to cell control (untreated group) using hemocytometer at different time interval. Highest concentration of the drugs evincing no cellular or morphological alterations and viable cell count C 50% as assessed by trypan blue staining was considered as its respective CC₅₀. Concentrations of drugs exhibiting toxicity to cells were not considered and the concentrations below CC₅₀ were employed to study the antiviral activity.

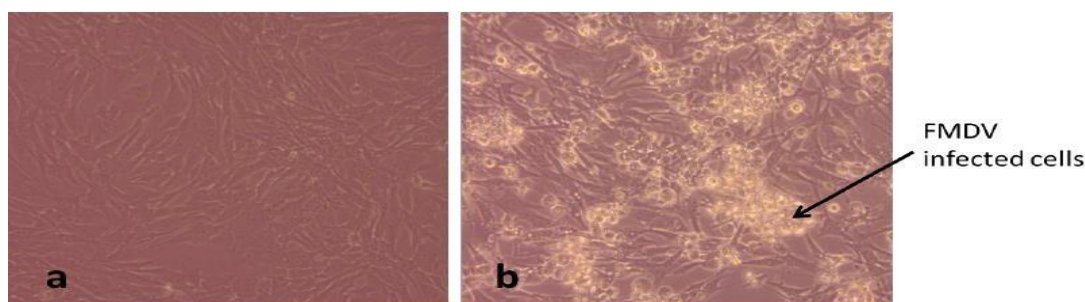


Fig.1: a: Anti-FMDV activity of Compounds (131,134, 135, 136, 140a, b, 141a-c, 144, 145, 146, 147, 148, 149, 150, 151, 152a, b, 153, 154, 155a-c, 156a-c, 157, 158 and 159) detected by disappearance of cytopathic effect of FMDV-infected BHK cells& b: cytopathic effect of FMDV-infected BHK cells.

Antiviral assays:

Virus yield assay in tissue culture:

BHK cells were incubated overnight with dilutions of tested compounds containing supernatants. Supernatants were removed and cells washed with minimal essential medium (MEM; Gibco BRL/Invitrogen). Cells were infected at an MOI of 1 with FMDV O PanAsia for 1 h, and unabsorbed virus was inactivated by washing the cells with 150 mM NaCl, 20 mM morpholine ethane sulfonic acid (MES) (pH 6). MEM was added, and incubation continued for 24 h. Virus was released by one freeze-thaw cycle. As a control, infected cells were frozen and thawed at 1 h p.i. Virus yields were determined by virus titration assay on BHK-21 cells and expressed by subtracting the titers of virus which is expressed as $\text{Log}_{10} \text{TCID}_{50}$ in cells infected for 1 h from then 24-h titers. The reduction (*n*-fold) was calculated by dividing the virus titer in untreated infected cells by the virus titer in treated infected cells. The results are expressed by means from three repetitions ¹⁶².

Antiviral reagent injection, viral challenge, and monitoring in suckling mice

Specific-pathogen-free suckling mice, 3 to 4 days old, (Charles River Strain, USA) were supplied by Laboratory Animal Department, Veterinary Serum and Vaccine Research Institute (VSVRI), Abbasia, Cairo, were used to further investigate the antiviral activity of adamantane-pyrazole derivatives in vivo. The FMDV dose was determined through 10-folds serial dilutions of the virus. The 50% lethal dose (LD_{50})

of FMDV serotype (OPanAsia) was estimated by the Reed-Muench method. Suckling mice were inoculated by intraperitoneal injection with different safe concentration of the di-aryl pyrazole derivatives **141a-c** and pyridine carbonitrile derivatives **156a-c** that ranged between 100, 50, 40, 30, 20 $\mu\text{g/mL}$ while other compounds were not included as there is no antiviral activity evidence on tissue culture. Mice were treated with PBS containing 10% DMSO and 5% Tween-80 in the same volume as controls. Two hours following adamantane-pyrazole and thiadiazole derivatives (**141a**, **141b**, **141c**, **156a**, **156b**, **156c**) injection, the suckling mice were challenged with 100 LD_{50} FMDV serotype (O) in a volume of 100 μL by intraperitoneal injection. The animals were monitored for 5 days. After 48 hours post inoculation, the positive results showed spastic muscular paralysis of hind quarters leading to death due to activity of FMD virus but the action of different safe concentration of compounds were proved in life mice expressed as percentage of number of survival.



Fig.3: Mice showed spastic muscular paralysis of hind quarters leading to death and safe lived mice.

In silico molecular docking simulation: -

The molecular docking modelling studies were carried out by the help of MOE software (Molecular Operating Environment 10.2008 provided with chemical computing group, Canada). The X-ray crystallographic structure of the 3C protease (PDB: 5MH2) were retractive from protein data bank that isolated from Foot-and-mouth disease virus - type SAT 2 and released at 2016-03-02 with resolution: 3.20 Å (<https://www.rcsb.org/structure/5HM2>, last accessed 5 Aug. 2020).

The isolated 3C proteinase consist of five chains and each chain consisted of 209 amino acid. Our study used only one chain. The protein structures for the docking was prepared by added hydrogen atoms to complex structure and electric charge by

Protonate 3D (default settings). The hydrogen atoms were optimized by MMFF94x force field (the heavy atoms were fixed during the optimization and the dummy atoms were disposed in the docking site by Site Finder (default settings). Triangle Matcher placement method and London dG scoring function with retain 50 times were used for docking. The pyrazole and thiadiazole derivatives **141a-c** & **156a-c** as well as the standard drugs Amantadine and Ribavirin were drawn in chem-draw 14.0 and exported to MOE where protonated 3D, minimized energy and render hydrogen were achieved and finally docked inside the active site of the protein.

RESULTS: -

Before checking the antiviral activity of the compounds through observation of cytopathic effect of FMDV on BHK21, the compounds were screened for their cytotoxicity to BHK21 cells which is characterized by change in cell morphology like rounding, increased brightness, and detachment of the cells from the surface¹⁶³. The observed cytotoxic changes in the cells were directly proportional to the concentration of the compound starting from 20 to 4000 ug/mL. The results as shown in **table 1** and **table 2** revealed that the cytotoxicity concentration 50 (CC₅₀) on BHK-21 cells of compounds (**131**, **134**, **135**, **146**, **147**, **150**, **151**, **153**, **154**, **155a-c** and **159**) were 1000 ug/mL, compound (**136**, **144**, **145**, **148**, **149**, **152a,b**, **157** and **158**) were 500 ug/mL, compounds **140a**, **140b** were 2000 ug/mL and compound (**141a**, **141b**, **141c**, **156a**, **156b** and **156c**) were 3000 ug/mL. There is a variety of cytotoxic concentration 50 between the derivatives of adamantane-pyrazole and thiadiazole with pyridine carbonitrile derivatives **156a-c**. The CC₅₀ of compounds **141a**, **141b**, **141c**, **156a**, **156b** and **156c** come in parallel with that obtained for amantadine compound by¹⁶⁴ who showed that the CC₅₀ of amantadine was 3000 ug/ml. As mentioned by Sakar¹⁶³ who stated that the differences in cytotoxic concentration 50 was attributed to intrinsic characteristics of the cell, factors related to the drug.

The results of **table 3-6** showed that the pyrazole derivatives **131**, **134**, **135**, **136**, **140a** and **140b** and thiadiazole derivatives **144**, **145**, **146**, **147**, **148**, **149**, **150**, **151**, **152a, b**, **153**, **154**, **155a-c**, **157**, **158** and **159** did not achieve a comparable degree of inhibition

or mean viral titer fold reduction subsequently, and these compounds did not show any antiviral activity on BHK 21. While pyrazole with di-aryl group **141a-c** and thiadiazole with pyridine carbonitrile derivatives **156a-c** as shown in **table 4** and **table 6** showed a marked antiviral activity on BHK 21 cells as the mean virus titer reduction was achieved from $10^{8.5}$ expressed by $\text{Log}_{10} \text{TCID}_{50}$ on BHK21 till reach its minimum mean virus titer of $10^{1.25} \text{Log}_{10}$. Inhibitory concentration 50 (IC_{50}) was achieved at 100 ug/mL for the pyrazole derivatives **141a-c** and thiadiazole derivatives **156a-c**. Where in case of compound **141a** give mean virus titer 4.2 with 2-folds reduction in virus titer, also compound **141b** give mean virus titer 3.9 with 2.1-folds reduction in virus titer and compound **141c** give mean virus titer 4.2 and with 2.4 folds reduction in virus titer and in case of compound **156a** give mean virus titer 4.3 with 1.9-folds reduction in virus titer, also compound **156b** give mean virus titer 3.9 with 2.1-folds reduction in virus titer and compound **156c** give mean virus titer 4.2 and with 1.8 folds reduction in virus titer. The therapeutic index (TI) was calculated from previous results for diaryl pyrazole derivatives **141a-c**, thiadiazole with pyridine carbonitrile derivatives **156a-c** and displayed 30.

Results of **table 7** showed that 50 ug/mL of pyrazoles **141a**, **141c** and thiadiazole **156a**, **156b** achieve 100 % survival among baby mice while bis-tolyl pyrazole derivatives **141 b** and thiadiazole **156c** gives %100 survival at 40 ug/mL compared with amantadine which give %100 survival at 50 ug/mL.

Generally, the most promising three derivatives **141a-c** exhibited binding energy (S) from -15.41 to -20.0 kcal/mol in comparison to Amantadine (S) = -6.15 kcal/mol, and Ribavirin (S) = -10.77 kcal/mol. The three pyrazole derivatives are only different in substituents in two aryl groups at positions three and five of the pyrazole core. Docking of Amantadine drug inside the active site displayed one hydrogen bond backbone donor with bond length 2.49 °A and 41% strength. At the same time, Ribavirin showed four sidechain hydrogen bond acceptor between Lys 51 and oxygen of carbonyl of the amide group, the nitrogen of triazole, oxygen of furan nucleus and

hydroxy group of methanol derivative with bond length 3.19 (13%), 2.63 (72%), 3.18 (27%) and 2.60 °A (83%) respectively.

By using the docking simulation was carried out using MOE software (Molecular Operating Environment 10.2008 provided with chemical computing group, Canada.) with a standard protocol that previously reported ¹⁶⁵, and the docking process was performed according to the reported methods ¹⁶⁶.

Pyrazole derivatives **141a** showed the highest binding energy (S) = -20.00 kcal/mol with only one sidechain hydrogen bond acceptor between Lys 51 and oxygen of methanone amantadine derivatives with bond length 3.07 °A and strength of the bond (32%) (**Fig. 3**) as showed in **table 8**. Also, compound **141a** interacts through its pyrazole derivatives with three arene-cation interaction between Lys 51 and anisidine group at position five in pyrazole as well as Arg 68 that form two arene-cation with both pyrazole ring and phenyl group at position 3 as well as hydrophobic interaction that appear between active site in pocket and Amantadine part or phenyl group (appear as blue color on the chemical structure in 2D). The pyrazole derivatives with bis-tolyl groups **141b** in position three and five were reveled hydrogen bond acceptor from side chain between Arg 68 and oxygen of methanone derivative with bond length 2.87 °A and strength (14%) (**Fig. 4**). In addition to one arene-cation interaction through the tollyl group at position five and Lys 51 and hydrophobic interaction that arises due to presence of amantadine and *p*-tolyl moiety.

Furthermore, pyrazole derivatives **141c** that containing phenyl and *p*-chlorophenyl as two aryl derivatives observed binding energy S = -18.02 kcal/mol with sidechain hydrogen bond acceptor between Arg 68 and oxygen of carbonyl of the methanone derivative with bond length 2.51 °A and (30%) strength. Besides two arene-cation interaction between Arg 68 with the *p*-chlorophenyl group and Lys 51 with phenyl group at the position three and five in pyrazole core respectively, (**Fig. 5**). Finally, it can conclude that the pyrazole derivatives hybrid with Amantadine core **141a-c** suggested being 3C protease inhibitor and exhibited binding energy higher than the two standard drugs Amantadine (S = 6.15 kcal/mol) and Ribavirin (S = 10.77 kcal/mol)

with different binding mode. All the docked pyrazole derivatives **141a-c** showed favorable binding interactions with hydrophobic interaction and energy scores from -15.41 to -20.0 kcal/mol in comparison to Amantadine (S) = -6.15 kcal/mol, and Ribavirin (S) = -10.77 kcal/mol. These highest binding energy and binding interactions suggest that these compounds may act as 3C protease inhibitors and thus may participate as antiviral drugs.

DISCUSSION: -

In enzootic countries like Egypt, vaccination of susceptible livestock is the method of choice to build herd immunity and ultimate control and eradication of FMD. However, the conventional FMD vaccine induces complete protection after 7 days' post vaccination. Following the acute FMDV infection in ruminants, some proportions of them become carrier to FMDV ¹⁵¹. To overcome these issues, emergency immunization with a high potency vaccine is practiced. The other possible alternatives would be the use of antiviral agents that inhibit FMDV replication.

Adamantane derivatives are known to have a broad spectrum of biological activity including antiviral effects. Adamantane derivatives that are entrenched well into medical practice include the drugs such as amantadine, rimantadine, tromantadine, ladasten, and many others. Compounds with antitumor ¹⁶⁷ and antimalarial ¹⁶⁸ activities; for application as antidiabetic ¹⁶⁹ and antituberculosis ¹⁷⁰ agents, CB1 receptor agonists ^{171,172} and neuroprotective compounds ^{173,174}. and for treatment of Gaucher's disease ¹⁷⁵ and therapy of viral infections ^{176,177} are now undergoing pharmacological testing.

Therefore, the present study aimed to explore the in vitro antiviral efficacy of adamantane-pyrazole derivatives by their inhibition of CPE in BHK21 cell culture system against FMD virus serotype (O) after checking their cytotoxic activity on BHK 21 and also evaluating the antiviral activity of selected compounds of supposed antiviral activity against FMDV in vivo through antiviral reagent injection, viral challenge, and monitoring in suckling baby mice.

With regards to the CC₅₀ results for each compound, the tested concentration used was below the CC₅₀ so as to study its inhibitory effect on FMDV replication. So, it

was selected six concentrations from each compound (concentrations below CC_{50}) to test antiviral activity by virus titration assay on BHK-21 cells which was expressed as $\text{Log}_{10} \text{TCID}_{50}$ for 24 hrs.

The Inhibitory concentration 50% (EC_{50}) was detected for each compound and the fold reduction was calculated according to Mauro¹⁶² through dividing the virus titer in untreated cells by the virus titer in treated cells.

Concerning the *in vivo* evaluation of the selected compounds was achieved through testing the antiviral activity against FMDV challenge in baby mice Clinical signs observed in the treated and control mice: The control mice showed typical clinical signs such as spastic muscular paralysis of hind quarters leading to death. Combination of clinical treatment strategies have been proposed to increase the efficacy of antiviral agents, because of their advantages in overcoming viral mechanisms of resistance to antiviral actions¹⁷⁸.

In agreement with diaryl pyrazole derivatives **141a-c** and thiadiazole with pyridine carbonitrile derivatives **156a-c**, the therapeutic index (TI) which is defined as the relative effectiveness of the investigational product in inhibiting viral replication compared to inducing cell death (FDA., 2006)¹⁷⁹ and according to white and fenner¹⁸⁰ who reported that the effective antiviral was highest therapeutic index preferably more than 10.

This may be contributed to what stated by Moiseev¹⁸¹ that the high lipophilicity and unique geometry of the adamantane skeleton enhances considerably the permeability and adsorption of this type of compounds with respect to cell membranes. This is the reason for the manifestation of the virus-inhibiting action through suppression of early stages of the virus reproductive cycle. Incorporation of an adamantane moiety into molecules of various biologically active compounds modifies significantly their pharmacologic action.

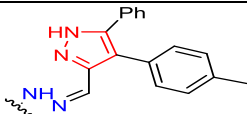
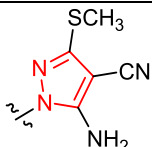
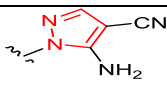
Amantadine is a real inhibitor of viroporins, including the IAV M2 protein¹⁸². the HCV p7 protein¹⁸³.and the C-terminal subunit of the p13 protein (p13-C) of GB virus B(GBV-B)¹⁸⁴. As previously established, viroporins can promote the release of

virions. To investigate the possible mechanism of virion release, the effects of amantadine on FMDV replication were estimated ¹⁸⁵.

Modeling studies are of high importance to obtain a consistent, clearer picture of the biologically active molecules that could be used to design novel therapeutic agents ¹⁸⁶,¹⁸⁷. Our work was extended to investigate the plausible binding pattern and interaction with the vital amino acids inside the active site with the most promising three derivatives **141a-c**. Molecular docking simulation was performed inside the active site of the 3C protease, where the protein that used for this purpose (PDB: 5MH2) downloaded from protein data bank (<https://www.rcsb.org>) .

In conclusion, to the best of author's knowledge, the present study is the first to demonstrate that adamantane pyrazole derivatives can suppress FMDV replication in vitro as well as prolong the survival of mice in vivo, suggesting the potential applications of this drug as an antiviral regiment for FMD treatment. Finally, it is necessary to test the antiviral effect of thiadiazole with pyridine carbonitrile derivatives and pyrazole containing two arylidine groups at position three and five in natural hosts such as swine, cattle, and goats, and against more FMDV strains.

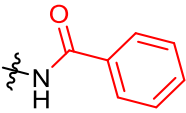
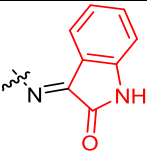
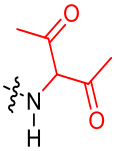
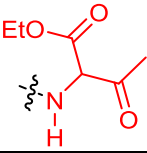
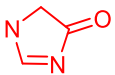
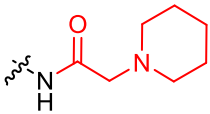
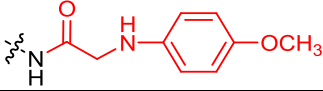
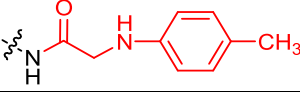
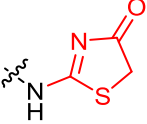

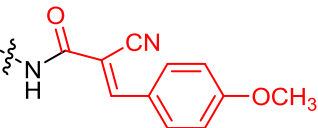
Table 1: The effect of different concentrations of adamantane pyrazole derivatives on normal BHK cells. *CC₅₀: BHK cytotoxic concentration fifty: -

Name of compounds	R	CC ₅₀ (µg /ml)*
131		1000
134		1000
135		1000

136		500
140a		2000
140b		2000
141a		3000
141b		3000
141c		3000

Table 2: The effect of different concentrations of adamantane thiadiazole derivatives on normal BHK cells. *CC₅₀: BHK cytotoxic concentration fifty: -

Name of compounds	R	CC ₅₀ (µg /ml)*
144		500
145		500

146		1000
147		1000
148		500
149		500
150		1000
151		1000
152a		500
152b		500
153		1000
154		1000
155a		1000

155b		1000
155c		1000
156a		3000
156b		3000
156c		3000
157		500
158		500
159		1000

Table 3: Antiviral activity of adamantane pyrazole derivatives no. 131, 134, 135,136,140a and 140b in BHK cell: -

Name of compounds	Concentration of compound ^a	Mean virus titer ^{b,d}	Fold reduction ^c
-	-	8.5	-
131	1000	8.4	1
	500	8.4	1
	200	8.2	1

	100	8.4	1
	50	8.3	1
	20	8.5	0
134	1000	8.3	1
	500	8.5	0
	200	8.2	1
	100	8.5	0
	50	8.4	1
	20	8.5	0
135	1000	8.4	1
	500	8.4	1
	200	8.5	0
	100	8.2	1
	50	8.3	1
	20	8.4	1
136	500	8.4	1
	200	8.3	1
	100	8.3	1
	50	8.5	0
	10	8.5	0
	2	8.5	0
140a	2000	8.5	0
	1000	8.4	1
	500	8.4	1
	100	8.5	0
	50	8.4	1
	20	8.5	0
140b	2000	8.5	0
	1000	8.5	0
	500	8.4	1
	100	8.4	1
	50	8.4	1
	20	8.5	0

^a (ug/ml) ^b expressed by Log₁₀ TCID₅₀ ^c The reduction (*n*-fold) was calculated by dividing the virus titer in untreated cells by the virus titer in treated cells. ^d Results are means from three repetitions

Table 4: Antiviral activity of adamantane pyrazole derivatives no. 141a, 141b and 141c in BHK cell: -

Name of compounds	Concentration of compound ^a	Mean virus titer ^{b,d}	Fold reduction ^c
-	-	8.5	-
141a	3000	1.8	4.7
	1000	2.5	3.4
	500	3.2	2.6
	200	3.8	2.2
	100	4.2	2
	50	6.2	1.37
141b	3000	1	8.5
	1000	1.5	5.3
	500	2.5	3.4
	200	3.9	2.1
	100	4.3	1.9
	50	6.8	1.25
141c	3000	1.5	5.3
	1000	2.3	3.6
	500	3.1	2.6
	200	3.5	2.4
	100	4.2	1.8
	50	5.9	1.4

^a (ug/ml) ^b expressed by Log₁₀ TCID₅₀ ^c The reduction (*n*-fold) was calculated by dividing the virus titer in untreated cells by the virus titer in treated cells. ^d Results are means from three repetitions

Therapeutic index (TI) of amantadine = BHK Cytotoxic concentration fifty (CC₅₀)/ BHK inhibitory concentration fifty (EC₅₀) = 3000/100 = 30

Table 4: Antiviral activity of adamantane thiadiazole derivatives no. 144, 145, 146,147,148,149 and 150 in BHK cell: -

Name of compounds	Concentration of compound ^a	Mean virus titer ^{b,d}	Fold reduction ^c
-	-	8.5	-
144	500	8.4	1
	200	8.4	1
	100	8.2	1
	50	8.3	1
	10	8.5	0
	2	8.5	0
145	500	8.3	1
	200	8.5	0
	100	8.3	1
	50	8.5	0
	10	8.5	0
	2	8.5	0
146	1000	8.4	1
	500	8.4	1
	200	8.5	0
	100	8.3	1
	50	8.2	1
	20	8.4	1
147	1000	8.4	1
	500	8.3	1
	200	8.3	1
	100	8.4	1
	50	8.5	0
	20	8.5	0
148	500	8.5	0
	200	8.4	1
	100	8.4	1
	50	8.5	0
	10	8.5	0
	2	8.5	0
149	500	8.5	0
	200	8.5	0
	100	8.4	1
	50	8.3	1
	10	8.3	1

	2	8.5	0
150	1000	8.4	1
	500	8.3	1
	200	8.3	1
	100	8.4	1
	50	8.5	0
	20	8.5	0

^a (ug/ml) ^b expressed by Log₁₀ TCID₅₀ ^c The reduction (*n*-fold) was calculated by dividing the virus titer in untreated cells by the virus titer in treated cells. ^d Results are means from three repetitions

Therapeutic index (TI) of amantadine = BHK Cytotoxic concentration fifty (CC₅₀)/ BHK inhibitory concentration fifty (EC₅₀) = 3000/100 = 30

Table 5: Antiviral activity of adamantane thiadiazole derivatives no. 151, 152a, 152b, 153,154,155a,155b,155c in BHK cell: -

Name of compounds	Concentration of compound ^a	Mean virus titer ^{b,d}	Fold reduction ^c
-	-	8.5	-
151	1000	8.5	0
	500	8.4	1
	200	8.2	1
	100	8.3	1
	50	8.5	0
	20	8.5	0
152a	500	8.3	1
	200	8.5	0
	100	8.3	1
	50	8.4	1
	10	8.5	0
	2	8.5	0
152b	500	8.4	1
	200	8.4	1
	100	8.5	0
	50	8.3	1
	10	8.2	1
	2	8.4	1

153	1000	8.4	1
	500	8.5	0
	200	8.3	1
	100	8.4	1
	50	8.5	0
	20	8.5	0
154	1000	8.5	0
	500	8.3	1
	200	8.4	1
	100	8.5	0
	50	8.5	0
	20	8.5	0
155a	1000	8.5	0
	500	8.5	0
	200	8.4	1
	100	8.4	1
	50	8.3	1
	20	8.5	0
155b	1000	8.4	1
	500	8.3	1
	200	8.5	0
	100	8.4	1
	50	8.5	0
	20	8.5	0
155b	1000	8.4	1
	500	8.3	1
	200	8.3	1
	100	8.5	0
	50	8.5	0
	10	8.5	0
155c	1000	8.4	1
	500	8.3	1
	200	8.3	1
	100	8.3	1
	50	8.5	0
	10	8.5	0

^a (ug/ml) ^b expressed by Log₁₀ TCID₅₀ ^c The reduction (*n*-fold) was calculated by dividing the virus titer in untreated cells by the virus titer in treated cells. ^d Results are means from three repetitions

Therapeutic index (TI) of amantadine = BHK Cytotoxic concentration fifty (CC₅₀)/ BHK inhibitory concentration fifty (EC₅₀) = 3000/100 = 30

Table 6: Antiviral activity of adamantane thiadiazole derivatives no. 156a, 156b, 156c, 157,158 and 159 in BHK cell: -

Name of compounds	Concentration of compound ^a	Mean virus titer ^{b,d}	Fold reduction ^c
-	-	8.5	-
156a	3000	1.7	5
	1000	2.4	3.5
	500	3.2	2.6
	200	3.8	2.2
	100	4.3	1.9
	50	6.3	1.34
156b	3000	1	8.5
	1000	1.6	5.3
	500	2.5	3.4
	200	3.9	2.1
	100	4.2	2
	50	6.7	1.26
156c	3000	1.5	5.3
	1000	2.3	3.6
	500	3.1	2.6
	200	3.4	2.4
	100	4.2	1.8
	50	5.9	1.4
157	500	8.5	0
	200	8.4	1
	100	8.4	1
	50	8.3	1
	10	8.3	1
	2	8.3	1
158	500	8.4	1
	200	8.4	1
	100	8.5	0
	50	8.5	0
	10	8.4	1
	2	8.5	0
159	1000	8.5	0
	500	8.4	1
	200	8.5	0
	100	8.3	1

	50	8.3	1
	20	8.5	0

^a (ug/ml) ^b expressed by Log₁₀ TCID₅₀ ^c The reduction (*n*-fold) was calculated by dividing the virus titer in untreated cells by the virus titer in treated cells. ^d Results are means from three repetitions

Therapeutic index (TI) of amantadine = BHK Cytotoxic concentration fifty (CC₅₀)/ BHK inhibitory concentration fifty (EC₅₀) = 3000/100 = 30

Table 7: Antiviral activity of adamantane pyrazole and thiadiazole derivatives in Baby mice

Name of compounds	Concentrations	Total number of baby mice	% percentage of survival
141a	100	10	100%
	50	10	100%
	40	10	50%
	30	10	0%
	20	10	0%
141b	100	10	100%
	50	10	100%
	40	10	100%
	30	10	50%
	20	10	0%
141c	100	10	100%
	50	10	100%
	40	10	50%
	30	10	0%
	20	10	0%
156a	100	10	100%
	50	10	100%
	40	10	50%
	30	10	0%
	20	10	0%
156b	100	10	100%
	50	10	100%
	40	10	50%
	30	10	0%
	20	10	0%

156c	100	10	100%
	50	10	100%
	40	10	100%
	30	10	50%
	20	10	0%
Amantadine	50	10	100%
*+ve control	-	10	0%

Table 8: Docking results of the most promising pyrazole derivatives inside active site (5MH2) as well as two reference drugs Amantadine and Ribavirin used in this study:-

Cpd. No.	Energy score (S) (Kcal/mol)	Amino acids	Interacting groups	Length (Å)	Strength (%)
141a	-20.00	Lys 51	O- of carbonyl group	3.07	32
		Lys 51	Anisidine group	-	-
		Arg 68	Pyrazole moiety	-	-
		Arg 68	Phenyl group	-	-
141b	-15.41	Arg 68	O- of carbonyl group	2.87	14
		Lys 51	Tolyl group	-	-
141c	-18.02	Arg 68	O- of carbonyl group	2.51	30
		Arg 68	<i>p</i> -chlorophenyl	-	-
		Lys 51	phenyl group	-	-
Amantidine HCl	-6.15	Val 69	Amino group of amantadine	2.49	41
Ribavirin	-10.77	Lys 51	Carbonyl of amide group	3.19	13
		Lys 51	Nitrogen of triazole	2.63	72
		Lys 51	Oxygen of furan	3.18	27
		Lys 51	derivatives	2.60	83
		Val 69	Hydroxy of methanol derivative	2.77	81
			Hydroxy of furan derivative in position 4		

(-) arene-cation interaction.

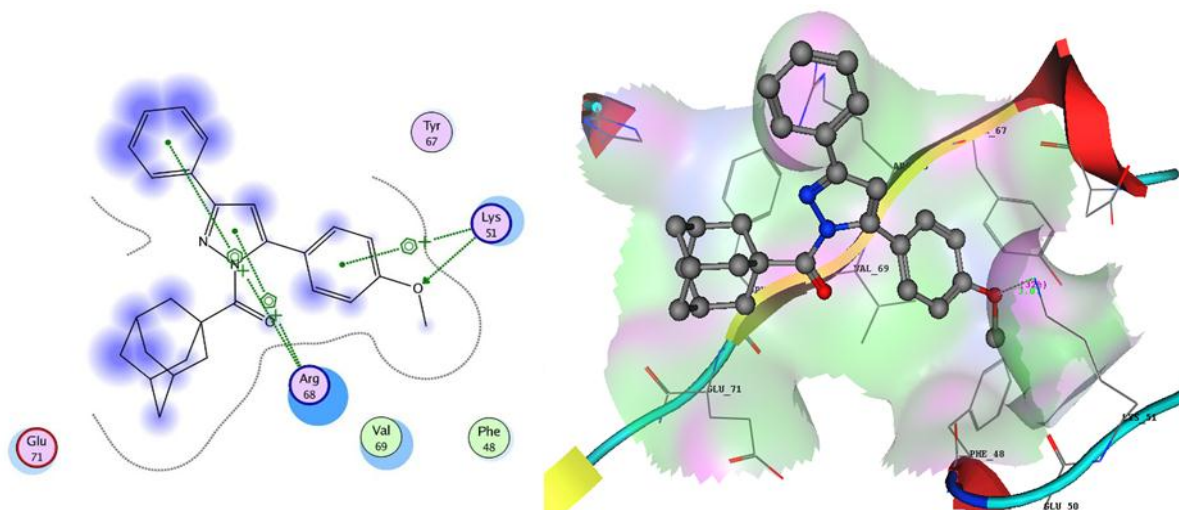


Figure 3: 2D & 3D interactions of pyrazole derivative **141a** in the active site of 5MH2

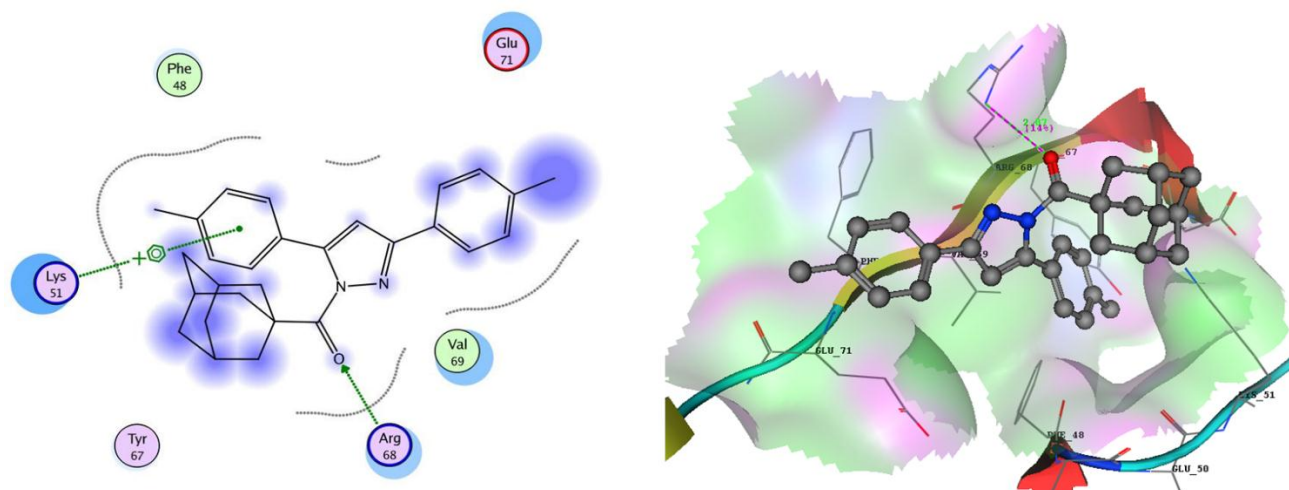


Figure 4: 2D & 3D interactions of pyrazole derivative **141b** in the active site of 5MH2

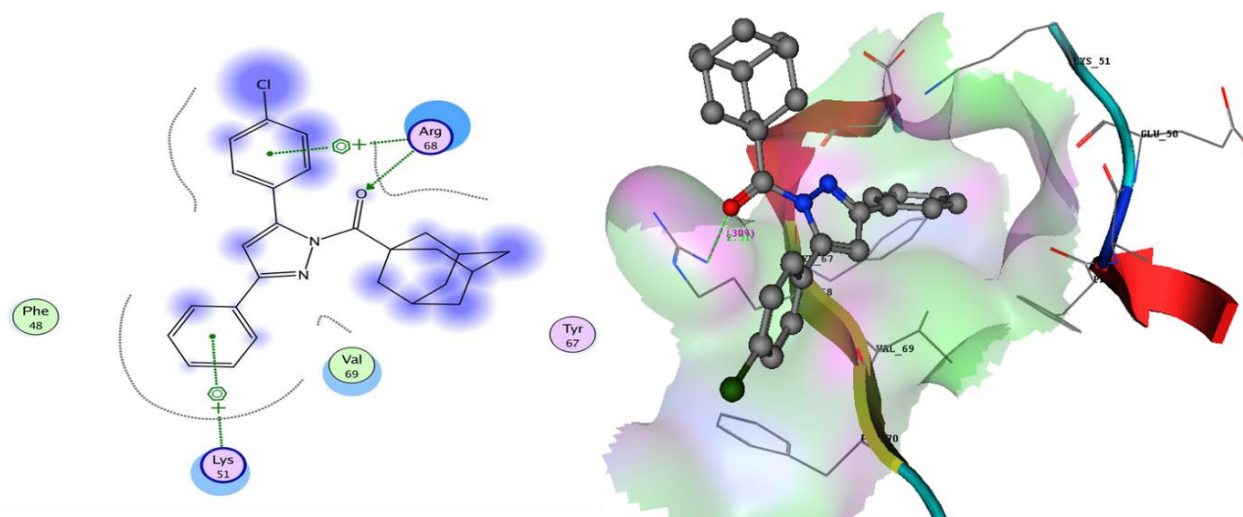
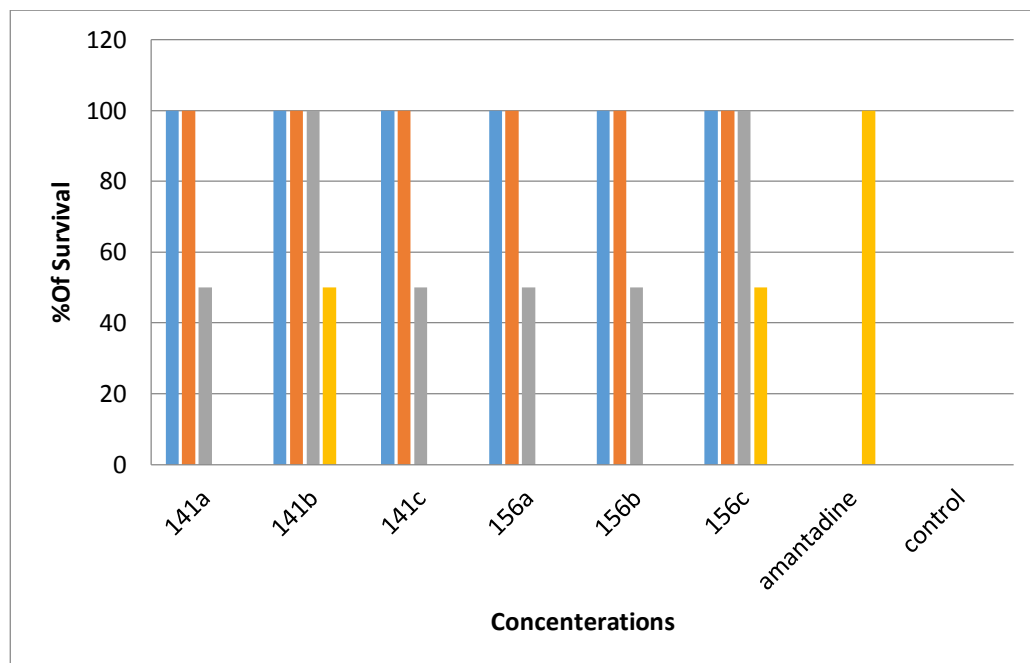
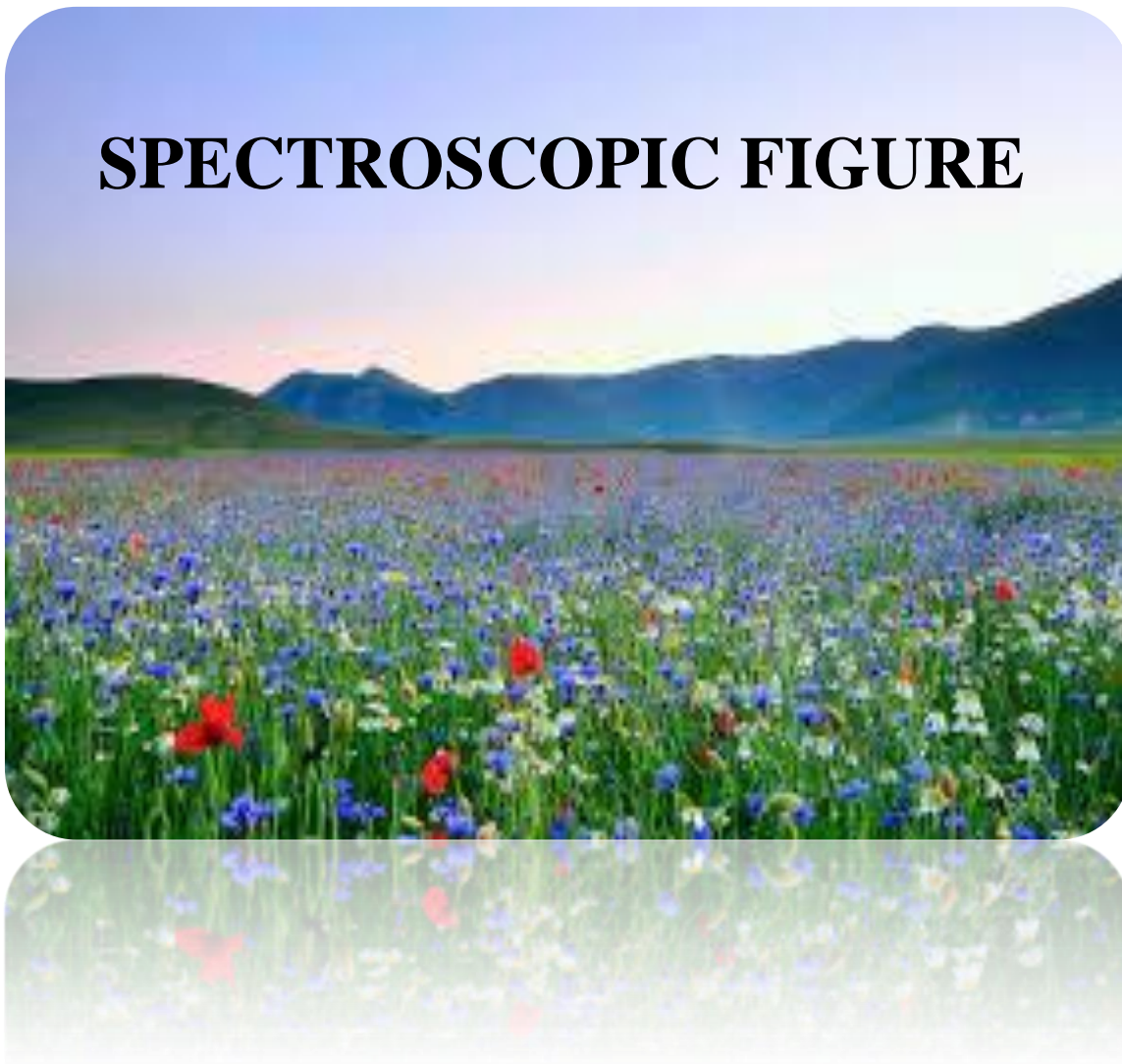


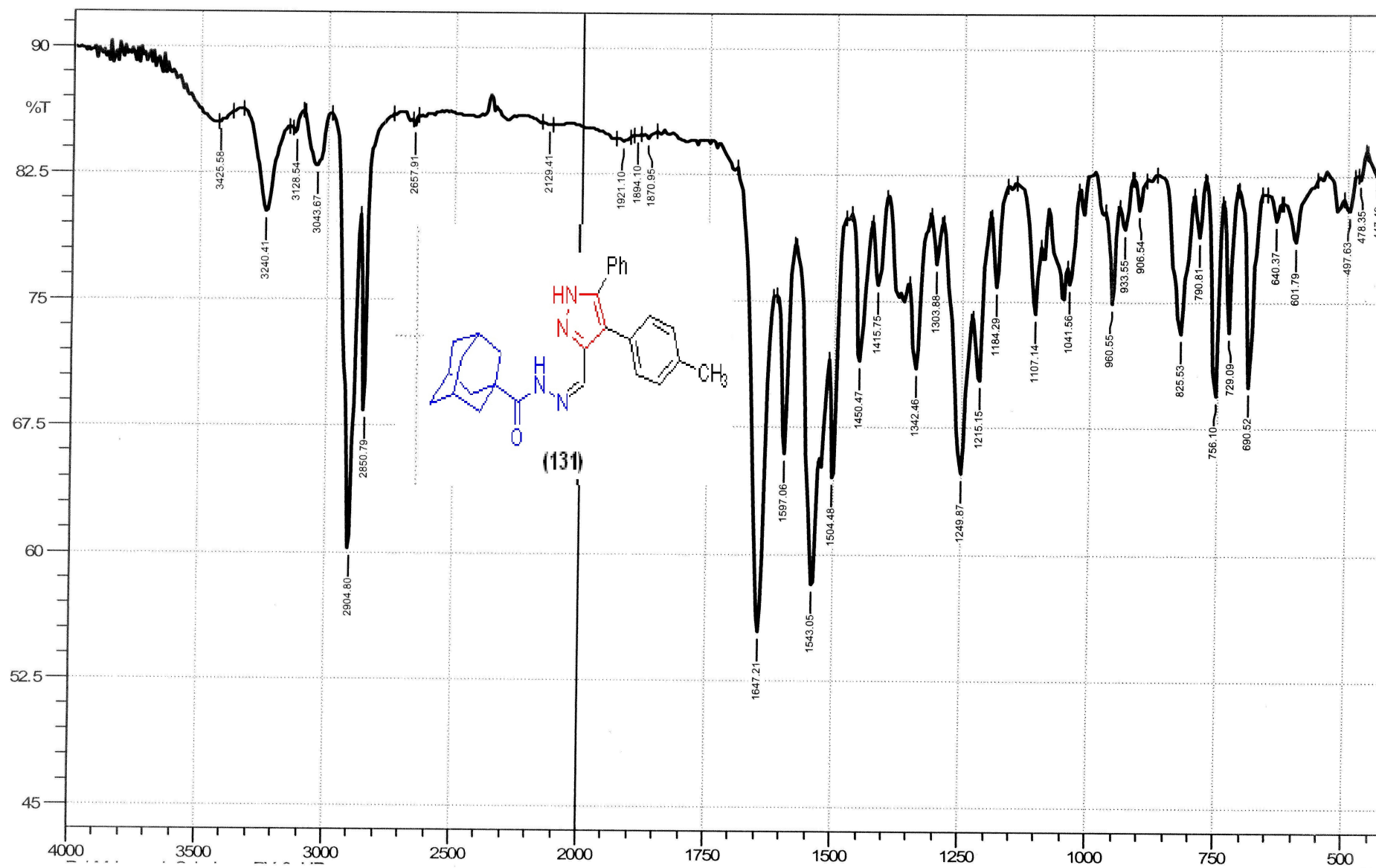
Figure 5: 2D & 3D interactions of pyrazole derivative **141c** in the active site of 5MH2

Figure 6: Antiviral activity of adamantane pyrazole derivatives (141a, 141b,141c) and adamantane thiadiazole derivatives (156a, 156b,156c) in Baby mice

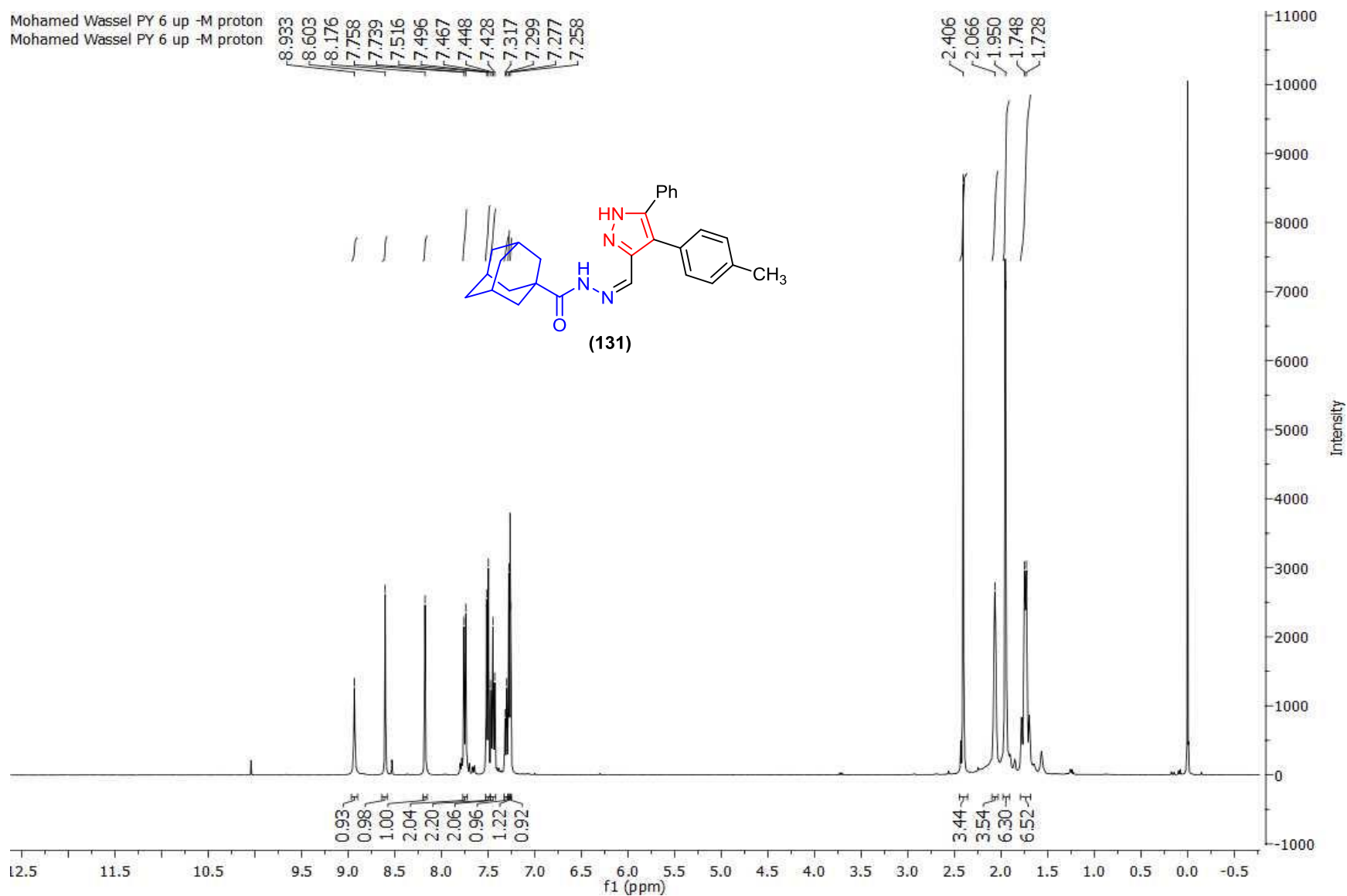


SPECTROSCOPIC FIGURE



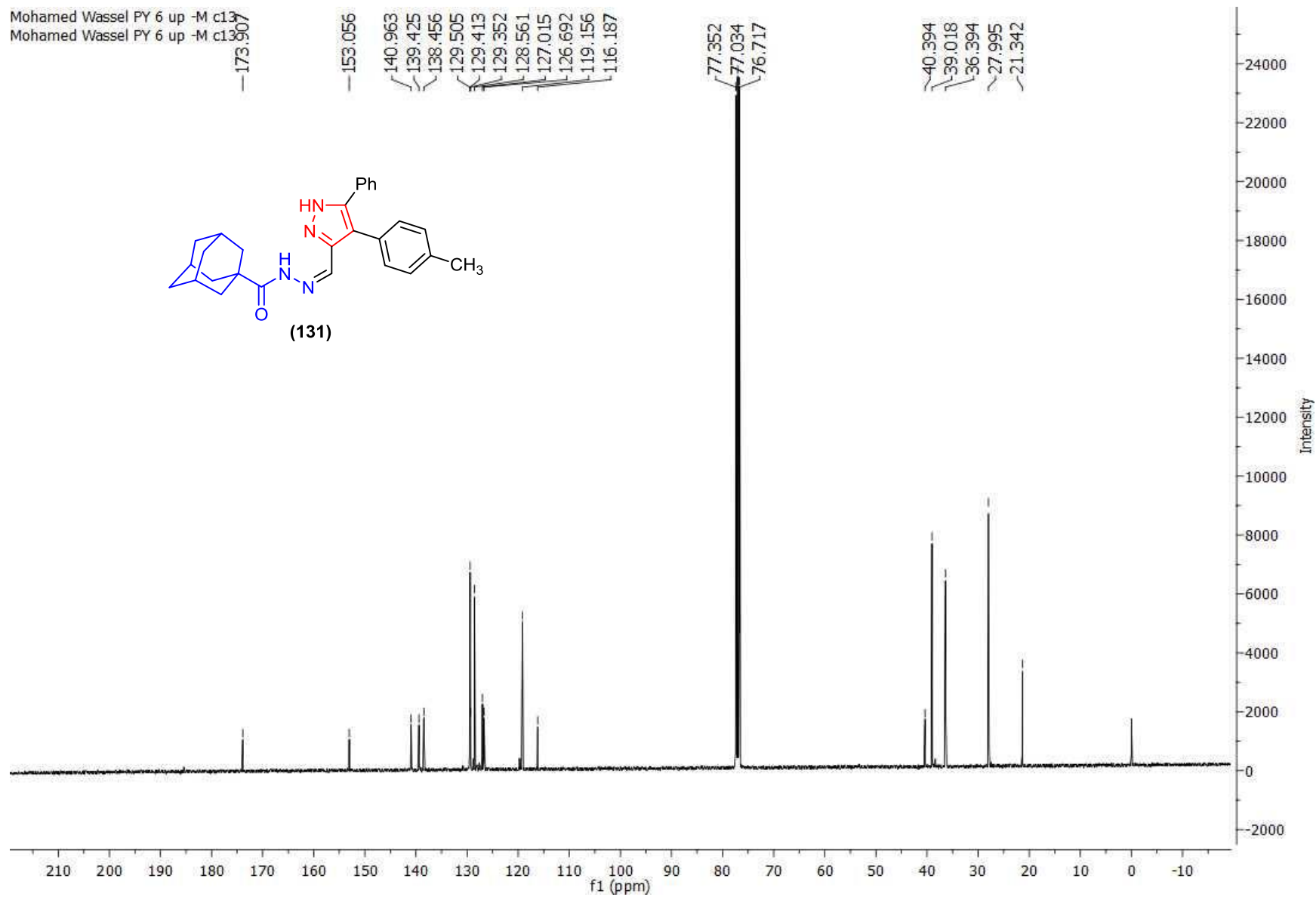


Mohamed Wassef PY 6 up -M proton
Mohamed Wassef PY 6 up -M proton

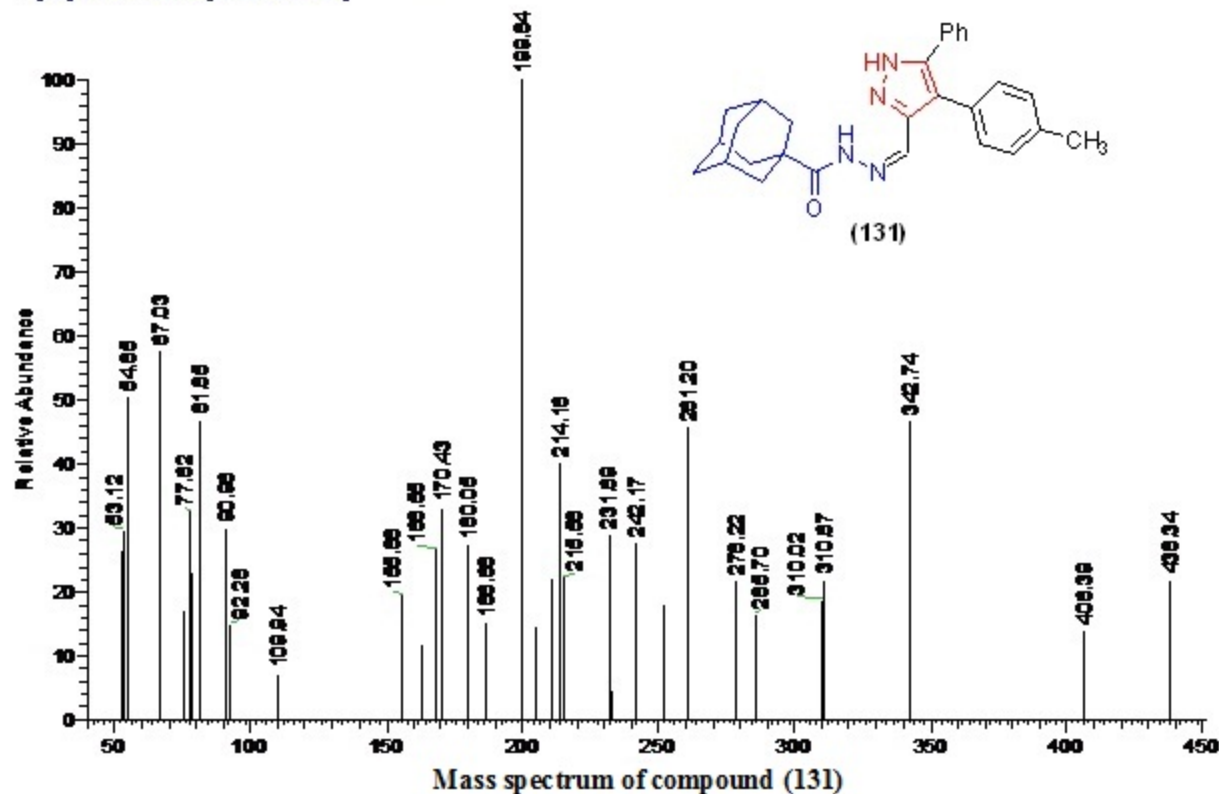


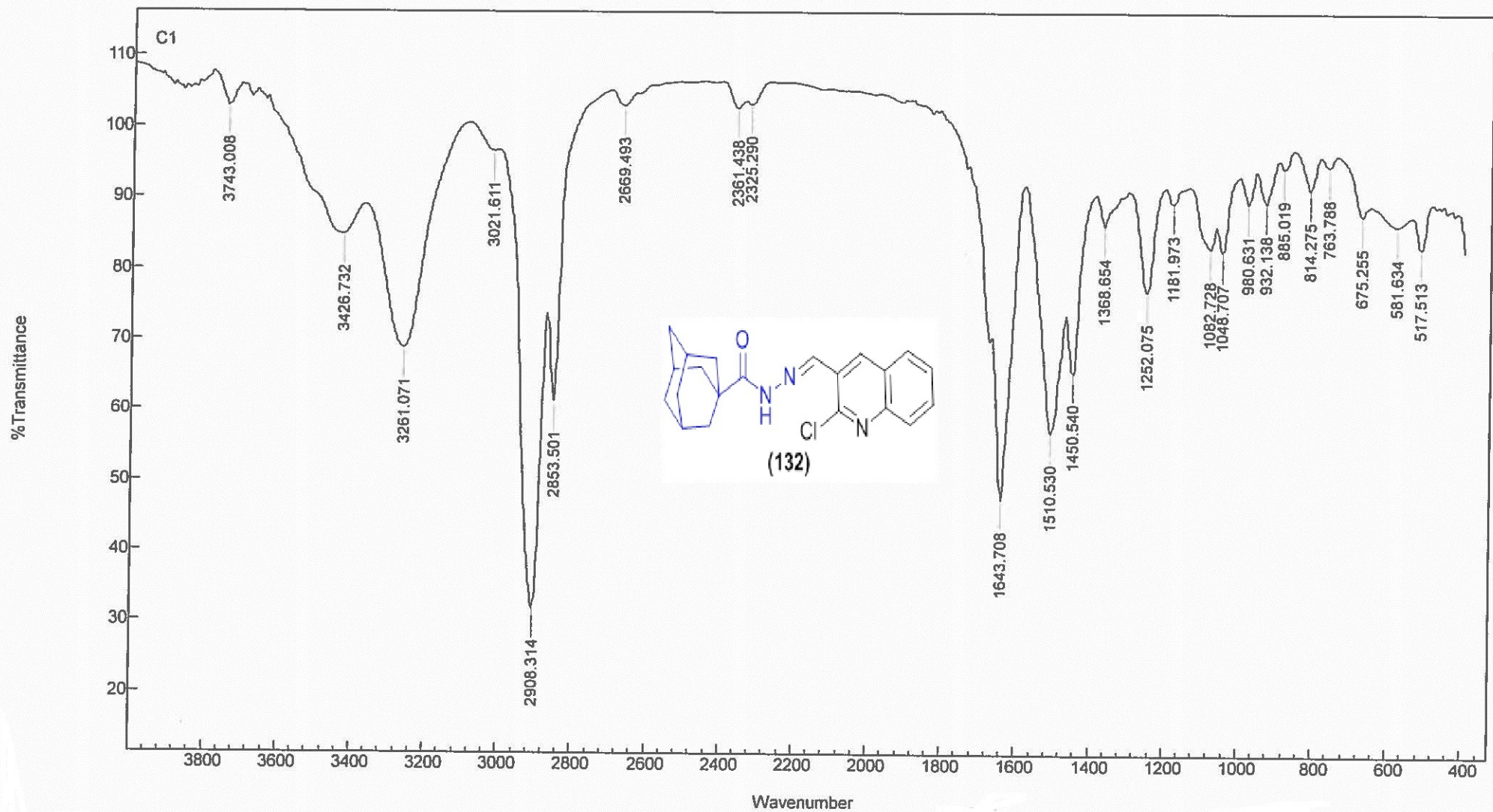
^1H NMR spectrum (CDCl_3-d_6) of compound (131)

Mohamed Wassef PY 6 up -M c13
Mohamed Wassef PY 6 up -M c13



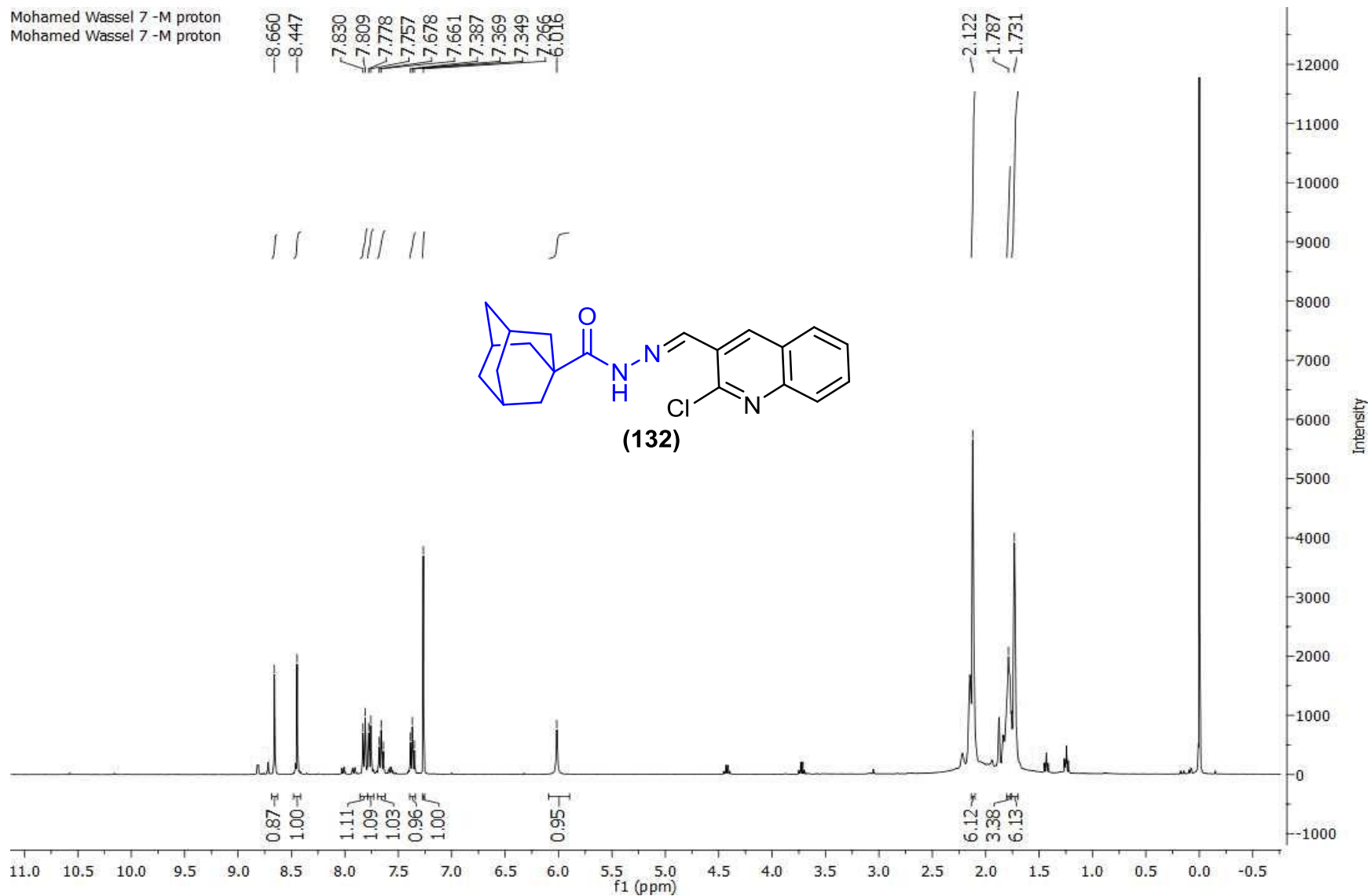
¹³C NMR spectrum (CDCl₃-d₆) of compound (131)



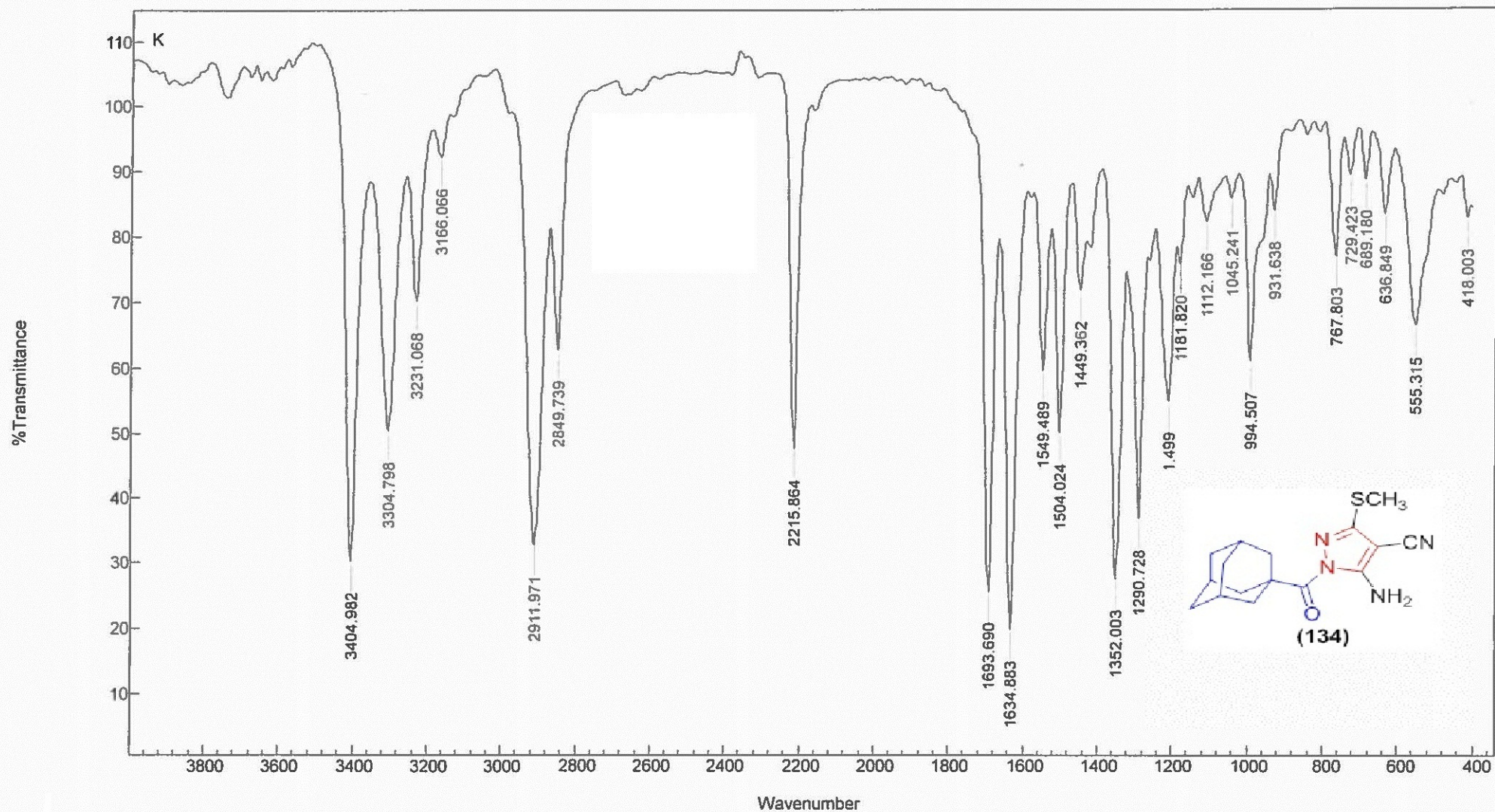


IR spectrum of compound (132)

Mohamed Wassef 7-M proton
 Mohamed Wassef 7-M proton

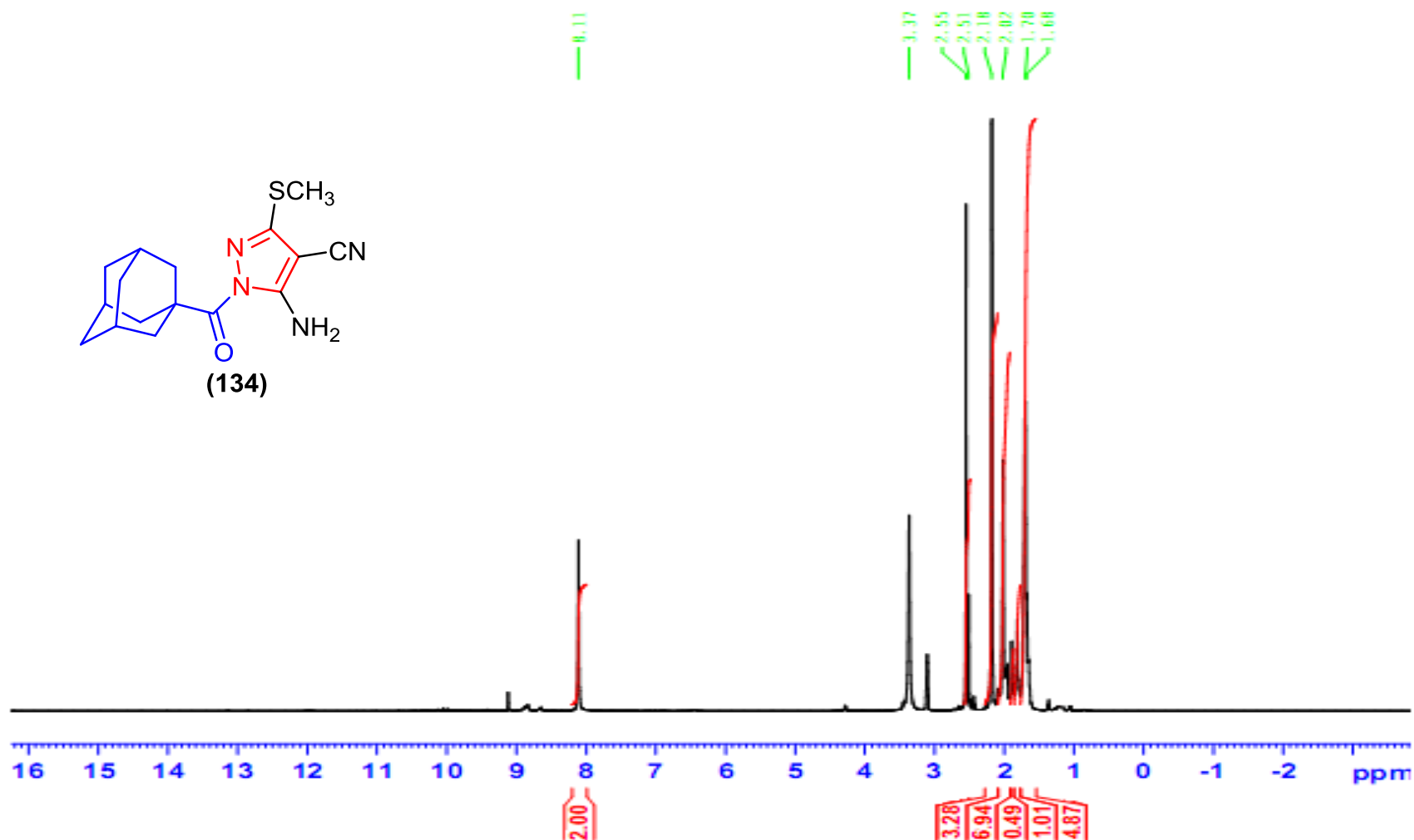


¹H NMR spectrum(CDCl₃-d₆) of compound (132)



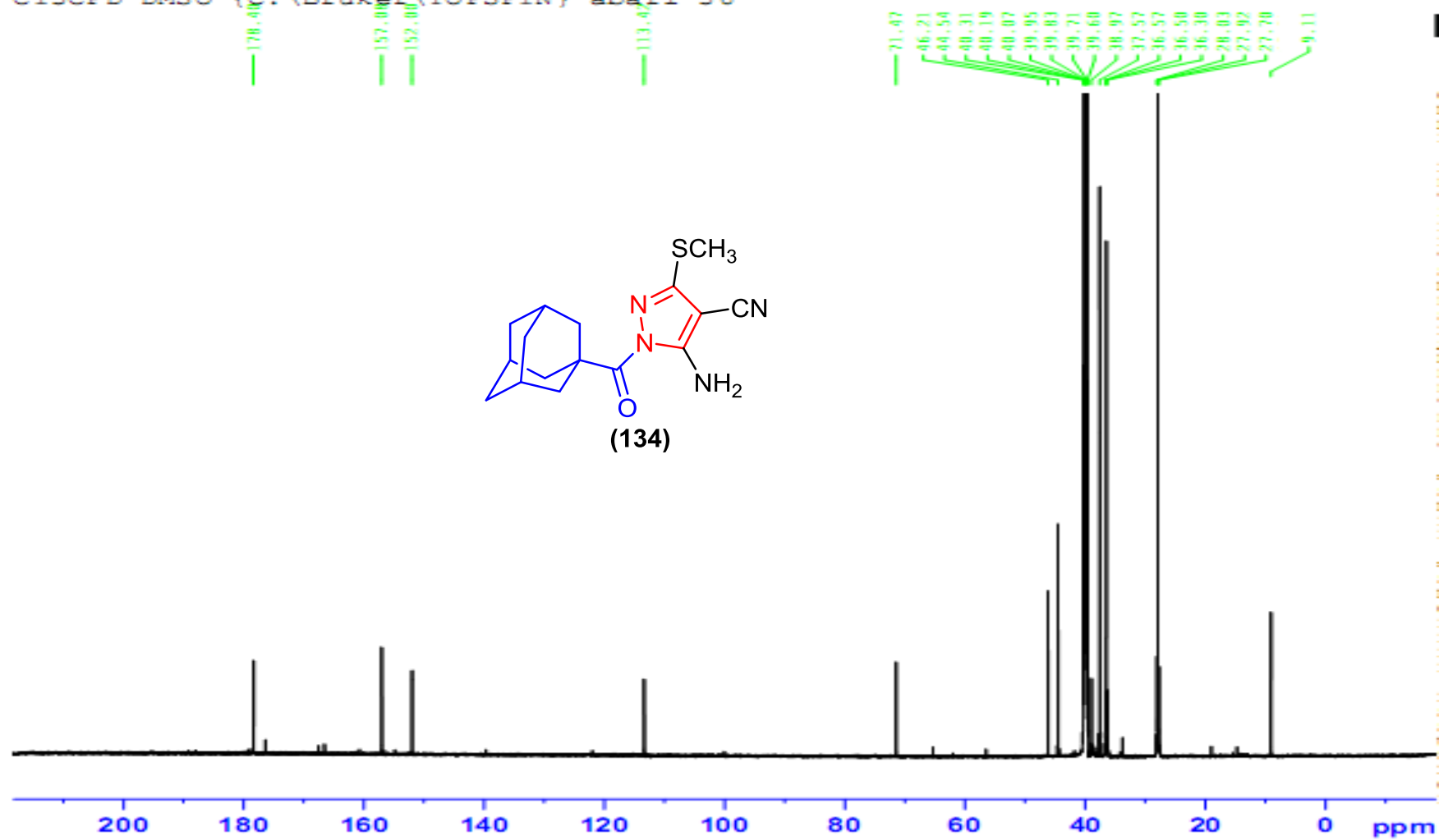
IR spectrum of compound (134)

PROTON DMSO {C:\Bruker\TOPSPIN} abari 36

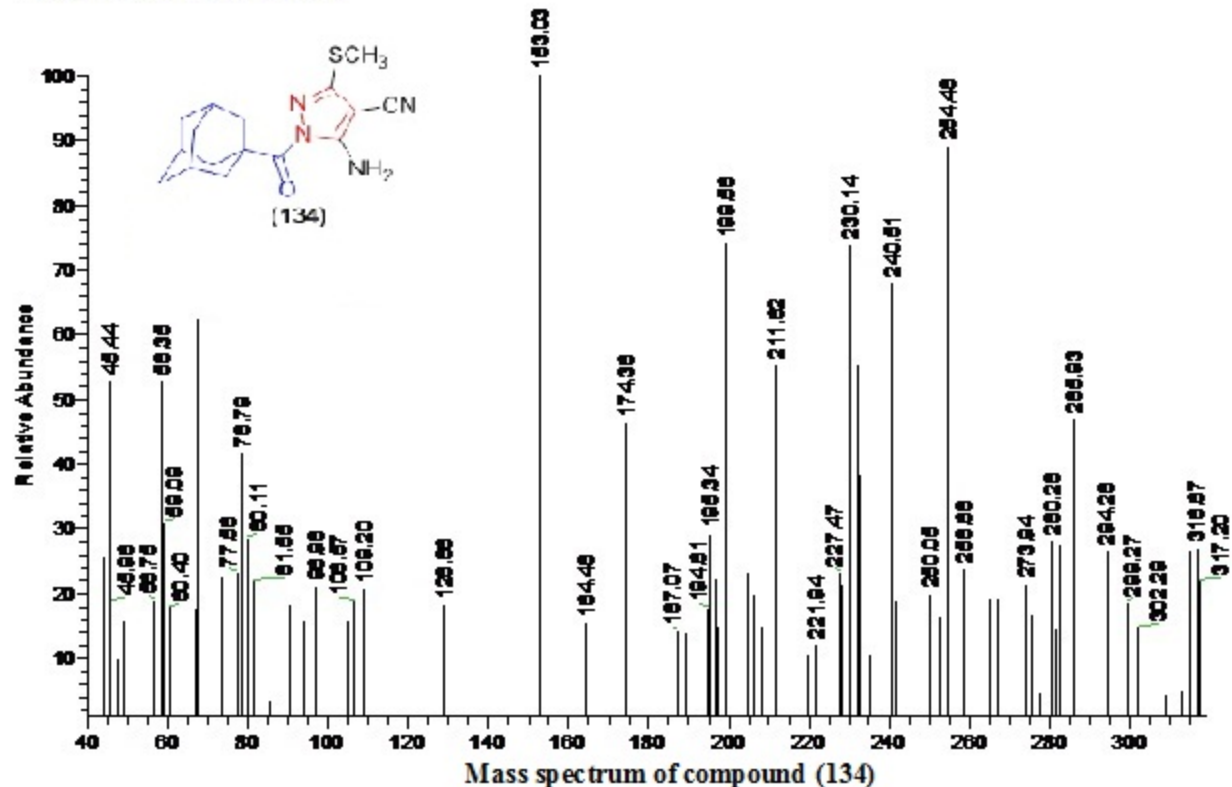
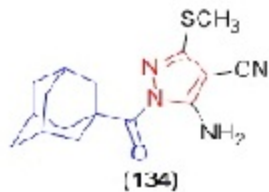


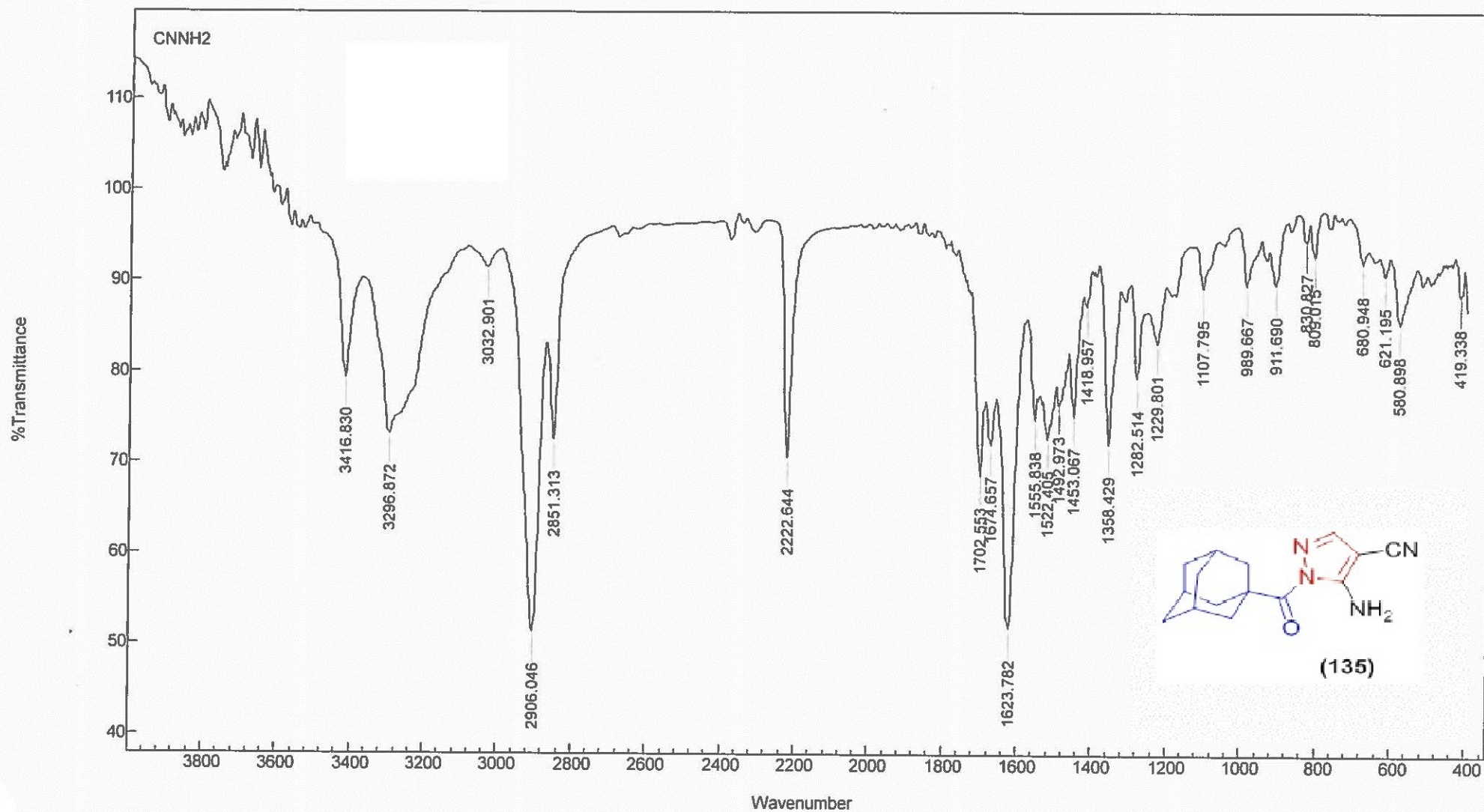
¹H NMR spectrum(DMSO-*d*₆) of compound (134)

C13CPD DMSO {C:\Bruker\TOPSPIN} abari 36



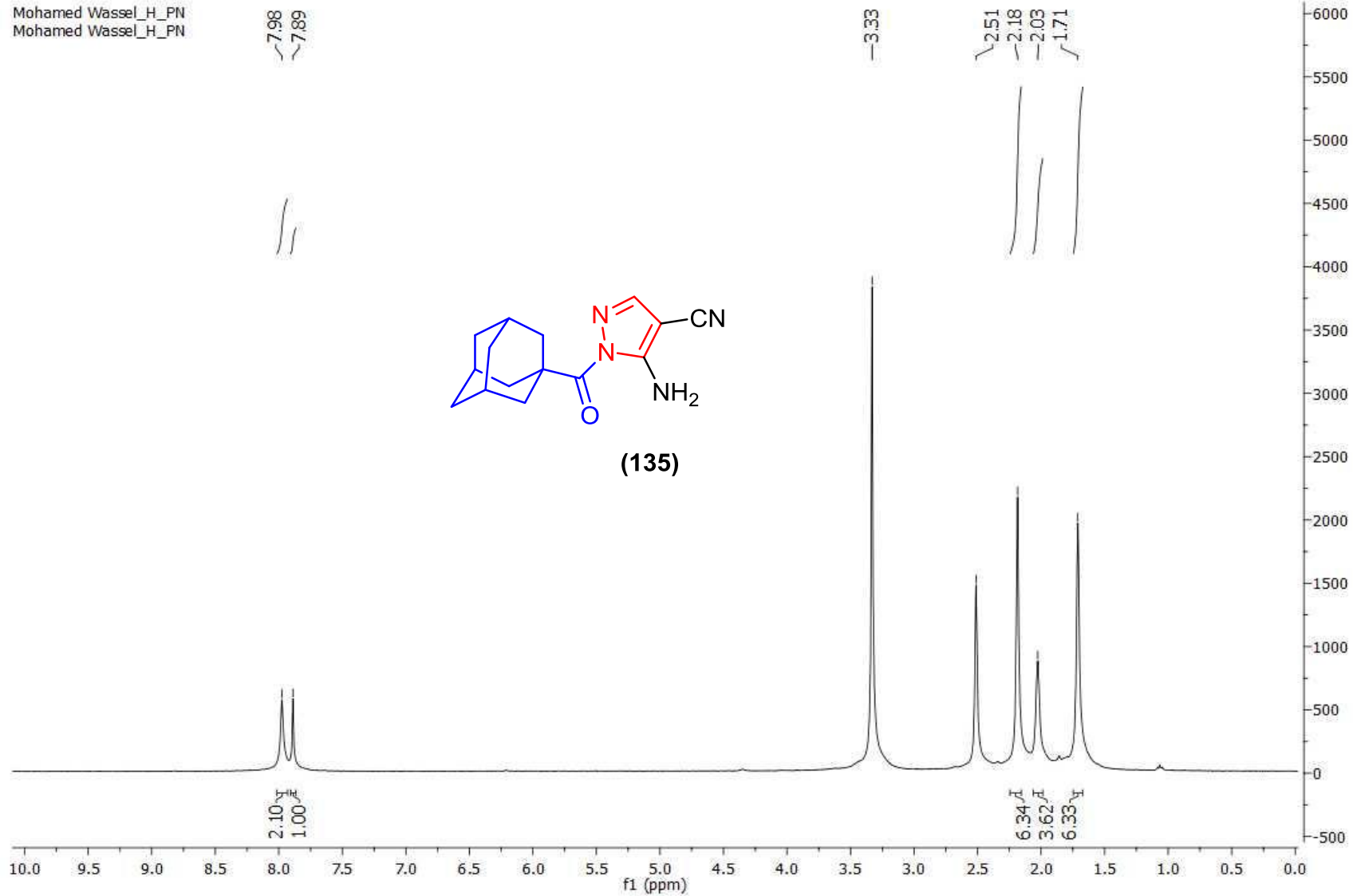
¹³C NMR spectrum of compound (134)





IR spectrum of compound (135)

Mohamed Wassef_H_PN
Mohamed Wassef_H_PN



¹H NMR spectrum(DMSO-*d*₆) of compound (135)